CALX, A SODIUM-CALCIUM EXCHANGER OF *DROSOPHILA MELANOGASTER*

Thesis by

Erich Marquard Schwarz

In Partial Fulfillment of the Requirements

for the Degree of

Doctor of Philosophy

California Institute of Technology

Pasadena, California

1996

(Submitted August 21, 1995)

To my parents

Acknowledgements

I thank Seymour Benzer for his wise and indirect guidance through graduate school. It is not easy to work in a place where one truly has no boundaries but one's own inherent limitations, but that is the sort of laboratory Seymour runs. My experience here would have been remarkable on historical grounds alone, given the probability that such havens of free inquiry are likely to become rarer in coming years. It is more remarkable for having actually been a learning experience, in the good and authentic sense of that phrase.

I thank David Anderson, Elliot Meyerowitz, Mel Simon, and Paul Sternberg for serving on my thesis committee, and for their sparing but incisive criticisms. I thank Elliot and Mel for their seminars on genetics, which have given me much food for thought over the years. I thank Paul for inspiring me to switch to *Caenorhabditis elegans*, and for the hospitality and friendship of his entire research group.

I thank my friends who have made Caltech a place to live as well as work. Special mention must go to: Sasha Kamb, Mani Ramaswami, Matthew Matthew, and Charlie Oh; Kellie Whittaker; Dennis Ballinger, Nancy Bonini, and Billy Leiserson; Gregg Jongeward, Raffi Aroian, Russell Hill, Helen Chamberlin, and Katherine Liu; Suzanne Elsasser; Chris Schoenherr and Benton Yoshida; Gregory Reynard; John DeModena; and Claire Slutter.

I thank my parents for encouraging me to pursue a life in science from my earliest childhood until now.

I thank my wife Kathleen Hubbard for the greatest possible love and support during the interminable endgame of this thesis. Kathleen is, arguably, the most important discovery I made while here.

Abstract

Calcium extrusion is necessary for cellular survival and suspected to modulate cellular activity. *Drosophila* phototransduction is a promising system in which to study calcium export, since it is dominated by calcium activity yet, unlike most calcium-dependent signalling pathways, genetically pliable. The multiple roles of calcium flux in *Drosophila* photoransduction are reviewed in Chapter One.

Calx, a *Drosophila* ortholog of mammalian $3Na^{+}/1Ca^{2+}$ exchangers, was isolated and characterized (Chapter Two). *Calx*'s gene product has ~50% identity to its direct mammalian homologs, with more distant similarities to an exchanger-related superfamily. There exist at least seven alternately spliced adult *Calx* transcripts, with an alternatively spliced miniexon in *Calx*'s protein-coding region. A full-length *Calx* cDNA of 5408 bp has lengthy, elaborate 5' and 3' UTRs. *Calx* transcripts are ubiquitously expressed in embryos and adult heads, with one 5.7 kb transcript expressed in photoreceptors; *Calx* protein is also ubiquitous in adult heads, with a notable presence in photoreceptors and neuropil. Heterologous expression of *Calx* in *Xenopus* oocytes shows that it encodes a bona fide sodium-calcium exchanger; unlike mammalian retinal exchangers, it does not depend on potassium for activity. *Calx* encodes two novel protein motifs, *Calx*-α and *Calx*-β. Both are intragenically duplicated, but they probably have different functions: *Calx*-α is likely to encode residues central to calcium export, while *Calx*-β may mediate intracellular signalling or cytoskeletal anchoring.

Table of Contents

The world globes itself in a drop of dew. The microscope cannot find the animalcule which is less perfect for being little. Eyes, ears, taste, smell, motion, resistance, appetite, and organs of reproduction that take hold on eternity--all find room to consist in the small creature. So do we put our life into every act.

--Ralph Waldo Emerson
Compensation

Calcium in *Drosophila* phototransduction

Erich M. Schwarz and Seymour Benzer
Division of Biology, 156-29, California Institute of Technology, Pasadena, CA, 91125

Summary

Calcium flux in the *Drosophila* photoreceptor is triggered by a relay of signals from rhodopsin, via the heterotrimeric G proteins Dgq and Gβe, to the retina-specific phospholipase C-β4, NorpA. Activated NorpA catalytically releases IP_3; this probably induces an IP_3 receptor (Dip) to release calcium from subrhabdomeric cisternae (SRC) next to the photoreceptive organelle (rhabdomere). This, in turn, activates light-stimulated cation channels (LSCs) in the plasma membrane, which depolarize the photoreceptor (by Na^+ and Ca^{2+} influx) and adapt it to light (by elevating cytoplasmic Ca^{2+}). Two homologous membrane proteins, Trp and Trpl, are respectively known and suspected to be channel components, while a cGMP-gated calcium channel (DmCNGC) might be a third component. LSCs may be activated by cGMP synthesis, elevated cytoplasmic Ca^{2+}, allosteric gating (by activated Dip), or some mixture of these; extant data do not decisively prove any one mechanism. It is clear that, while unknown channel components are sufficient for an initial response to light, calcium influx via Trp is necessary for sustained responses. At the same time, LSCs must be deactivated by an eye-specific protein kinase C (InaC) to prevent photoreceptor exhaustion. Ca^{2+}/calmodulin complexes probably also adjust calcium influx through Trp and Trpl. Elevated cytoplasmic calcium can act backward along the phototransduction pathway: it probably facilitates rhodopsin inactivation, and must dynamically regulate both IP_3 production by NorpA and Dip's response to IP_3. Finally, calcium pumps and sodium-calcium exchangers may influence adaptation to light. A graphic overview is provided in Figure 1 and Table 1.

Introduction

Intracellular fluxes of calcium are known to govern cellular behavior. However, it is often unclear how such fluxes are specifically controlled, what substrates they actually modulate, and what individual effects each modulation has (Clapham, 1995a). *Drosophila* phototransduction affords a context in which these variables can be determined, by isolating and mutating each calcium transporter and ligand. As part of a collaborative effort to characterize visual cDNAs (Palazzollo *et al.*, 1989; Hyde *et al.*, 1990; Lee *et al.*, 1990; Shah and Hyde, 1995), we have identified a *Drosophila* sodium-calcium exchanger that has the appropriate tissue distribution and biochemical activity to comprise a new element of *Drosophila* phototransduction. This review presents the context of our finding. Sodium-calcium exchange has been observed in a number of other tissues besides *Drosophila* photoreceptors--primarily neurons and muscles of various mammals and invertebrates, but also a bewildering array of other cell types (Blaustein *et al.*, 1991; Philipson and Nicoll, 1993). However, in the *Drosophila* retina, most of the partners of sodium-calcium exchangers--signal receptors and amplifiers, internal and external calcium channels, calcium-dependent regulators, and calcium pumps--can be definitely named; many have been cloned and mutated, and the remainder are likely to follow shortly.

This review focuses on calcium flux in *Drosophila* phototransduction (Table 1; Figure 1), taking it to be a model for other situations in which sodium-calcium exchange might be studied. Since some readers will be unfamiliar with the visual anatomy, genetics, and evolution of *Drosophila*, those are reviewed first. Next is described a series of intracellular signals, from photons isomerizing rhodopsin to IP_3 releasing calcium. Known and possible channels and targets of calcium are then discussed at length. Finally, future prospects are briefly considered.

Photoreceptor anatomy

Drosophila has four visual organs: one of them (the compound eye) is known by

anybody who has seen a dipteran; the other three are inconspicuous. The compound eyes are both prominent and highly studied (Horridge, 1975; Pak, 1975; Heisenberg and Wolf, 1984). They consist of ~750 hexagonal facets covering a red compound eye (Wolff and Ready, 1993) and are necessary for acute vision. They undergo modulation: in dim light they are tuned to detect faint signals with relatively low acuity, but can readjust in bright light to work with lower sensitivity and higher resolution (Heisenberg and Buchner, 1977). Three other organs--the ocellus, Bolwig's organ, and extra-ocular photoreceptor--are smaller and less studied. Ocelli have no well-established function, but seem best designed to sense ambient light levels (Pollock and Benzer, 1988; Stark *et al.*, 1989) and cooperate with the compound eyes to confer phototaxis towards very dim light (Miller *et al.*, 1981). Bolwig's organ is needed for larval phototaxis, which in *Drosophila* is generally negative (Bolwig, 1946; Gordesky-Gold *et al.*, 1995). Extra-ocular photoreceptors seem to entrain circadian rhythms (Hofbauer and Buchner, 1989; Hall, 1995; Helrich-Förster, 1995).

The ultrastructure of the adult retina was most recently reviewed by Wolff and Ready (1993). Each facet overlies a single, miniature light-sensing cluster of cells (ommatidium). The facet is the surface of a lens, below which resides a tetrad of cone cells that secrete a transparent medium. Underneath them reside eight photoreceptors at the ommatidial core, surrounded by pigment and bristle cells. Each photoreceptor has a photosensitive lobe, the rhabdomere, projecting into the ommatidial center. The rhabdomere is analogous to the outer segment of a mammalian photoreceptor. The rhabdomere's cylindrical microvilli contain rhodopsin in their lipid membranes and are reinforced by actin filaments in their aqueous cores (Matsumoto *et al.*, 1987; Suzuki *et al.*, 1993). The rhabdomere has a higher refractive index than the cytoplasm or inter-rhabdomeric space, and so acts as a wave guide for light rays focused onto its proximal tip (Snyder, 1975; Heisenberg and Wolf, 1984). This can be modulated by 0.1-μm ommochrome granules in the photoreceptor soma; under strong illumination, the granules move next to the rhabdomere and diminish its light conduction (Franceschini, 1975). An

intracellular region immediately next to the rhabdomeres contains anastomosing elaborations of the endoplasmic reticulum (ER) called subrhabdomeric cisternae (SRC; Matsumoto-Suzuki *et al.*, 1989). These are discussed further below.

Secondary and tertiary pigment cells contain 0.4-μm granules of ommochrome and pteridine (Heisenberg and Wolf, 1984). This optically isolates the ommatidia from UV/blue light, while allowing easy transversal of the retina by orange/red light. The rhodopsins, meanwhile, are tuned to detect UV/blue light, while being regenerated by orange/red light. This is not arbitrary, but an efficient design: were pigments and rhodopsins designed in the opposite way, rhabdomeres would have to be twice as large to detect orange/red light, and the retina would lose 50% of its acuity. Without any isolating pigments, acuity is also lost because rhabdomeres can be stimulated by oblique light (Heisenberg and Wolf, 1984).

Photoreceptor genetics

The most powerful evidence that a given molecule participates in *Drosophila* phototransduction is a mutation of its gene yielding a specific phototransduction defect. Visual mutations have been successfully elicited from mutagenized *Drosophila* by screening for diverse phenotypes.

The least invasive assay is behavioral: failure to respond properly to light can result from (among other things) visual defects. For instance, adult *Drosophila* can be tested for phototaxis: wild-type *Drosophila* strains often show robust positive phototaxis (Benzer, 1967; Pak, 1975). Another test is optomotor: one can place *Drosophila* in a maze, and select them for their ability to follow the motion of a stripe as they pass through a T-intersection (Heisenberg and Götz, 1975). Both tests have successfully identified a number of X-chromosomal visual mutations (Pak, 1975). However, phototactic and optomotor screens are difficult to use for autosomal mutations, due to background modifiers acquired during mutagenesis (Pak, 1979).

A more probing assay relies on the pseudopupil, a visual phenomenon made possible by the regular organization of retinal rhabdomeres: if a light is placed behind an adult fly's head, rays passing through parallel rhabdomeres coalesce to yield a virtual image of seven trapezoidally arrayed rhabdomeres. Since this image entirely depends on retinal organization, an abnormal pseudopupil reveals that the interior of the retina is disordered. Mutations that disorder the rhabdomeres tend to do so through either aberrant development or degeneration of the photoreceptors (Heisenberg and Wolf, 1984); three *r*eceptor *deg*eneration (*rdg*) mutations have proven to impair phototransduction (Steele *et al.*, 1992; Masai *et al.*, 1993; Vihtelic *et al.*, 1993). However, while other photosensory mutations often display photoreceptor degeneration (Chen and Stark, 1983; Meyertholen *et al.*, 1987; Dolph *et al.*, 1993; Colley *et al.*, 1995; Kurada and O'Tousa, 1995; Wu *et al.*, 1995), their degeneration is sometimes much slower to appear than in the *rdg* mutations.

To circumvent both confounding modifiers and laggard degeneration, a more sensitive assay has been used to identify several phototransduction mutations on the autosomes. Adult *Drosophila*, when fitted with corneal and ground electrodes, and stimulated with light, display an electroretinogram (ERG; Pak 1975, 1979). The bulk of the ERG consists of a shift of ~15 mV, reflecting the aggregate depolarization of ~6000 photoreceptors; this response partially weakens during prolonged illumination, due to photoreceptor adapation. Superimposed on this primary response, at its onset and end, are two transient responses (on- and off-transients); these arise from the first visual ganglion (lamina) rather than from the retina (Coombe, 1986). The primary response can be prolonged (in a postdepolarizing afterpotential, or PDA) if the eye is bleached with pure blue light (Cosens and Briscoe, 1972; Stark, 1975). Although screening individual mutant flies with the ERG/PDA is laborious, it is also extremely sensitive, as even subtle defects of the ERG (e.g., quiescence of the lamina) can be detected. Furthermore, the ERG also reveals whether phototaxis or optomotor mutations are due to primary defects within the photoreceptor itself.

Mutant ERG phenotypes fall into several classes (Pak, 1975, 1979; Ranganathan *et al.*, 1991b). The *n*either *i*nactivation *n*or *a*fterpotential (*nina*) mutations fail to be properly bleached by strong blue light, or to maintain a PDA; these invariably have proven to decrease the steady-state level of mature Rh1 in R1-R6 (Pak, 1991). The *i*nactivation *n*o *a*fterpotential (*ina*) mutations can be bleached, but still fail to maintain the PDA; the *r*educed *r*eceptor *p*otential (*rrp*) class displays ERGs that are diminished in magnitude. Both *ina* and *rrp* mutations are thought to block signalling steps downstream of rhodopsin. The *n*o *on* transient (*non*) mutations lack both on- and off-transients, but are otherwise normal; these are thought to block synaptic transmission at the termini of R1-R6, or to prevent reception of R1-R6 signals by L1 cells in the lamina (Pak, 1991; Burg *et al.*, 1993).

Some other mutations confer ERGs unusual enough that they deserve special mention. Severe mutations in the *n*o *o*uter *r*eceptor *p*otential *A* (*norpA*) gene totally shut off phototransduction, yielding a flat ERG (Pak *et al.*, 1970; Pak, 1979). So far, *only* mutations in *norpA* have had this effect. Since even the complete loss of Rh1 opsin in photoreceptors R1-R6 (via *ninaE* null mutations) still allow R7-R8 to produce a dwarf ERG, NorpA protein must be downstream of all opsins in all photoreceptors. Mutant *t*ransient *r*eceptor *p*otential (*trp*) photoreceptors have normal ERGs in dim light, and are able to generate a normal initial response to strong light; however, *trp* photoreceptors cannot maintain a sustained response to strong light, instead decaying to baseline (Cosens and Manning, 1969). There are other mutations with nongeneric ERGs that have yet to be fully studied: a *sl*ow *r*eceptor *p*otential (*slrp*) ERG responds abnormally slowly to light stimuli (Pak, 1975); a *su*per*d*epolarizing receptor *p*otential (*sudp*) ERG responds with abnormally large depolarization (Ranganathan *et al.*, 1991b); and a *h*yperdepolarizing *r*eceptor *p*otential (*hrp*) ERG responds with hyperpolarization instead of depolarization (Ranganathan *et al.*, 1991b).

The highest phenotypic resolution is provided by whole-cell voltage clamp, performed either upon dissociated ommatidia or on photoreceptors in an intact retina. The

former preparation allows much greater control of ionic fluxes, and allows calcium fluxes to be microscopically visualized and quantitated (Hardie 1991; Ranganathan *et al.*, 1991a; Ranganathan *et al.*, 1994). The latter preparation is less harsh to photoreceptors (Hardie *et al.*, 1993b) and prevents them from undergoing catastrophic, irreversible run-down currents (as they do when dissociated; Hardie and Minke, 1994a). Given dissociated photoreceptors, it has become possible to characterize the light-stimulated channels of *Drosophila* photoreceptors for the first time. As will be described in detail below, several mutations involved in calcium transport and signaling perturb these channels' activities.

Despite this plethora of phenotypic assays, the abundance of cloned yet unmutated genes with possible photosensory roles necessitates still more techniques for isolating mutations in specific loci at will. One solution is simply to physically map a clone to a chromosomal locus and compare its position to those of preexisting classical mutations. In some cases (Montell and Rubin, 1988, 1989; Smith *et al.*, 1991b) this approach has shown a clone to overlap a known gene; identity of the two could then be confirmed by transgenic rescue. In other cases (Van Vactor *et al.*, 1988; Dolph *et al.*, 1993, 1994), mutations were generated by screening for loss of a gene-specific antigen in spot-blotted mutant heads (immunoscreening).

Photoreceptor evolution

In some cases, the presence of a function in *Drosophila* phototransduction is solely inferred by assuming identity of *Drosophila* vision to that of various arthropods (*Apis*, *Limulus*) with larger photoreceptors. The justification for this is that phototransduction mechanisms are thought to be conserved within phyla; and that, for electrophysiology, it can be far easier to work with photoreceptors in horseshoe crabs or honeybees than in fruit flies. It should be remembered, however, that *Limulus* does not equal *Drosophila*. While both are arthropods, they represent distinct subphyla that diverged by the Cambrian period (475-550 My ago; Brusca and Brusca, 1991; Raff *et al.*, 1994). By comparison, the split

between *Drosophila* and mammals appears to have been during the Cambrian radiation, 530 My ago (Raff *et al.*, 1994), and *Drosophila* and vertebrates do *not* appear to have equivalent phototransduction pathways (Ranganathan *et al.*, 1991b; Kaupp and Koch, 1992). Even within insects, divergence times can be highly significant: the split between Diptera (e.g., *Drosophila*) and Hymenoptera (e.g., *Apis*) was definitely over 180 My ago (Riek, 1970), and visible diversification of the Neoptera had already occurred by 325 My ago (Kingsolver and Koehl, 1994). At the same time, some evidence for conservatism does exist. Both *Limulus* and *Drosophila* photoreceptors are excited by IP_3 (Brown *et al.*, 1984; Fein *et al.*, 1984; Bloomquist *et al.*, 1988); and both *Limulus* and *Apis* possess IP_3-gated subrhabdomeric stores of calcium (Payne *et al.*, 1988; Baumann and Walz, 1989). Thus, findings in other arthropods can be validly used to fill present gaps in our knowledge, but such comparisons are tentative until rechecked within *Drosophila*.

Molecules that convert a photon to IP_3 release

Rhodopsin. Four *Drosophila* opsins (Rh1-4) have been cloned by positional cloning, or by low-stringency and subtractive hybridization (Zuker *et al.*, 1985, 1987; Cowman *et al.*, 1986; Fryxell and Meyerowitz, 1987; Montell *et al.*, 1987). All four *Drosophila* opsins have 373-383 residues and 25-26% identity to bovine rhodopsin. Phylogenetic analyses indicate that they are true opsins, but that color vision (through opsin gene diversification) arose independently in mammals versus *Drosophila* (Fryxell and Meyerowitz, 1991; Applebury, 1994). All four use covalently bound 3-hydroxyretinal as a cofactor (Vogt and Kirschfeld, 1984), and are most sensitive to blue or UV light.

Rh1 is blue-sensitive (O'Tousa *et al.*, 1985; Zuker *et al.*, 1985; Britt *et al.*, 1993). It is the sole opsin of photoreceptors R1-R6, which comprise most of the compound eye. Accordingly, light responses mediated by Rh1 dominate the ERG/PDA and control most visual behavior (Pak, 1979; Heisenberg and Wolf, 1984). All known phototransduction genes act downstream of Rh1, and one visual mutation (*ninaE*) actually ablates Rh1's

structural gene. No mutations of other opsins have yet been isolated; they are expressed in the R7 photoreceptors (Rh3 and Rh4: Fortini and Rubin, 1990), the ocelli (Rh2 alone: Mismer *et al.*, 1988; Pollock and Benzer, 1988) or Bolwig's organ (Rh1, Rh3, and Rh4: Pollock and Benzer, 1988). A preliminary report describes an Rh5 in R8 cells (Britt and Hall, 1995). These opsins vary in spectral sensitivities and required chaperonins, and have accordingly been used in transgenic *Drosophila* to probe determinants of opsin specificity (Stamnes *et al.*, 1991; Britt *et al.*, 1994).

All *Drosophila* opsins are thought to activate a G protein while in a light-activated conformation (metarhodopsin; Pak, 1979). *Drosophila* metarhodopsin, unlike that of mammals, is thermostable; to prevent it from bleaching the photoreceptor, metarhodopsin is rapidly quenched by arrestin-binding (Byk *et al.*, 1993; Plangger *et al.*, 1994; Ranganathan and Stevens, 1995) and phosphorylation (Doza *et al.*, 1992), isomerized by absorbing a red/orange photon, freed of arrestin, and restored to active rhodopsin by dephosphorylation (Steele *et al.*, 1992; Byk *et al.*, 1993). Biosynthesis of Rh1 requires the retina-specific proline isomerase NinaA, which acts as an Rh1 chaperone in vivo; *ninaA* mutations cause the endoplasmic reticulum to swell with immature Rh1 (Baker *et al.*, 1994).

Heterotrimeric G proteins: Dgq/Gβe. *dgq* was cloned as one of 20 novel genes expressed in the visual system (Hyde *et al.*, 1990). It proved to encode an ortholog of mammalian $G_{q\alpha}$ specifically expressed in adult retinas and ocelli (Lee *et al.*, 1990, 1994). Two isoforms with 360 and 325 residues (Dgq1 and Dgq2) arise from alternately spliced *dgq* transcripts. Dgq1-2 are 76% identical to mammalian $G_{q\alpha}$ subunits but only 40-53% identical to other classes of G_{α} (Lee *et al.*, 1994b). Immunoelectron microscopy demonstrates that, in adult retinas, Dgq protein is localized to rhabdomeres; by light microscopy, some Dgq can also be seen in axonal termini in the lamina (Lee *et al.*, 1994b). Protein blotting shows that Dgq1 is present in both retina and ocellus, but that Dgq2 is retina-specific (Lee *et al.*, 1994b). No loss-of-function *dgq* mutations have yet been reported. Accordingly, dominant mutations of Dgq1 and Dgq2 were created in vitro (by

crippling their GTPase activities), and then expressed transgenically in vivo (Lee *et al.*, 1994b). Mutant *dgq1* and *dgq2* transgenes are both expressed effectively, since each confers a light-independent GTPase activity upon head membranes extracted from transgenic adults. Nevertheless, *dgq2* mutant adults show no noticeable defects in phototransduction. In contrast, the retinas of *dgq1* mutants display multiple defects: they require 400-fold more light than normal to elicit a 1 mV depolarization in an ERG; when stimulated by light, they depolarize 2.5 times more slowly than normal; and, after stimulation ends, they repolarize 5.0 times more slowly. Furthermore, *dgq1 rdgB* mutants undergo retinal degeneration even when in total darkness, despite the normal light-dependence of *rdgB* degeneration; this *dgq1 rdgB* phenotype is suppressed by *norpA* mutations (Lee *et al.*, 1994b). These data indicate that Dgq1 is the sole conduit between rhodopsin and NorpA activity. If Dgq2 has a function, it might be to titrate excess Gβe.

The retina-specific G_β-subunit Gβe was isolated by antigenic cross-reaction with a brain-specific β-subunit (Gβb; Yarfitz *et al.*, 1991). As with Dgq, Gβe is the only retinal member of its class in *Drosophila*, and resides in rhabdomeres (Yarfitz *et al.*, 1994). It comprises 346 residues, with 40-45% identity to mammalian $G_{\beta 1}$-$G_{\beta 3}$ proteins. In contrast, while Gβb has 80% identity to mammalian G_β proteins, it only has 43% identity to Gβe (Yarfitz *et al.*, 1991). Two *Gβe* loss-of-function mutations (*Gβe*^{1} and *Gβe*^{2}; Dolph *et al.*, 1994) have been isolated by immunoscreening (Van Vactor *et al.*, 1988). *Gβe*^{1} lowers Gβe protein levels to ~0.5% wild-type; *Gβe*^{2} has ~5% wild-type (Dolph *et al.*, 1994; Yarfitz *et al.*, 1994). The *Gβe*^{1} mutation blocks phototransduction: 100-fold more light is required to evoke a minimal current from *Gβe*^{1} than wild-type photoreceptors. *Gβe*^{1} photoreceptors are also sluggish: they start light-induced depolarization 1.7-fold more slowly than normal; they reach peak response 3.8-fold more slowly; and, after light ends, they inactivate 4.7-fold more slowly. Surprisingly, *Gβe* ^{2} is normal in its light-sensitivity and in its response times to an onset of light; yet *Gβe*^{2} photoreceptors still take 1.9 times as long as normal photoreceptors to shut off after a light-stimulus ends. These findings imply

that Gβe protein has two roles: a catalytic role in primary phototransduction (most likely, presenting Dgq1 to rhodopsin); and a second, structural role in adaptation. The latter role may be to inhibit calcium influx by activating InaC, a retinal protein kinase C; this will be discussed further below.

Because mammalian retina uses transducin ($G_{t\alpha}$) rather than $G_{q\alpha}$ for phototransduction, it is important to know if another G_{α} acts in the *Drosophila* retina. *Drosophila* $G_{o\alpha}$, $G_{s\alpha}$, and $G_{i\alpha}$ homologs have been histochemically localized by antibodies against highly conserved mammalian G_{α} peptides. In retinal photoreceptors, none of these homologs are expressed in rhabdomeres or cytoplasms (although $G_{i\alpha}$ exists at axonal termini, and $G_{o\alpha}$ in nuclei; Wolfgang *et al.*, 1990). Furthermore, transgenic pertussis-toxin--expected to block $G_{o\alpha}$,$G_{i\alpha}$, and $G_{t\alpha}$ proteins--has no effect upon photoreceptors when its expression is induced in adult flies, although it does block ERG on- and off-transients in the lamina (Fitch *et al.*, 1993). *Drosophila* photoreceptors are thus unlikely to employ $G_{t\alpha}$ in phototransduction.

Phospholipase C-β4. As noted, *norpA* is the only *Drosophila* gene known that can be mutated to block phototransduction completely (Hotta and Benzer, 1970; Pak *et al.*, 1970). However, *norpA* mutations do not abolish the elementary machinery required for photoreceptor depolarization: miniature depolarizations (quantum bumps; Pak, 1979) occur in *norpA* photoreceptors, and are themselves normal. *norpA* was cloned by genomic walking and verified by protein sequencing and transgenic rescue (Bloomquist *et al.*, 1987; Toyoshima *et al.*, 1990; McKay *et al.*, 1995). The NorpA protein is a peripheral membrane enzyme (McKay *et al.*, 1994) with 1095 residues; it is orthologous to mammalian phospholipase C-β4, with 70% identity over 559 aligned residues (Ferreira *et al.*, 1993; Lee *et al.*, 1993). NorpA contains extremely conserved sequences (boxes X and Y) that probably comprise its active site, interspersed with GTPase motifs (Ferreira *et al.*, 1993). NorpA's N-terminus contains a pleckstrin homology (PH) domain (Parker *et al.*, 1994; Cohen *et al.*, 1995) of controversial function: the PH domain may enable NorpA to

bind Gβe as a βγ heterodimer (Touhara *et al.*, 1994); or it may instead bind PIP_2 (Harlan *et al.*, 1994). Since mammalian PLC-β4 is stimulated solely by $G_{q\alpha}$ and not by βγ heterodimers (Lee *et al.*, 1994a), the latter function is more credible. By analogy with mammalian PLC-β1, NorpA may quench Dgq1 by activating Dgq1's intrinsic GTPase activity (Berstein *et al.*, 1992). Conceivably the GTPase motifs of NorpA itself enable this (Ferreira *et al.*, 1993).

NorpA hydrolyses both PIP_2 and PI in vitro, indicating that it must be physically sequestered from PIP_2 precursors in some way (Toyoshima *et al.*, 1990). NorpA, like Dgq and Gβe, localizes to photoreceptor rhabdomeres (Schneuwly *et al.*, 1991); however, it also exists in male abdomens and neural cortices (Zhu *et al.*, 1993). This expression pattern is biochemically reasonable, since PIP_2 is thought to be synthesized outside of the rhabdomeres (Vihtelic *et al.*, 1993); it also parallels the expression pattern of mammalian PLC-β4 (Ferreira *et al.*, 1993, 1994). NorpA hydrolyzes PIP_2 most effectively with 1 μM Ca^{2+} present; either lower or higher Ca^{2+} levels decrease NorpA's efficiency (Toyoshima *et al.*, 1990; Running Deer *et al.*, 1995).

An IP_3 receptor probably releases Ca^{2+} from the photoreceptor SRC

Both *Apis* and *Drosophila* photoreceptors have a specialized extension of the endoplasmic reticulum (subrhabdomeric cisternae, or SRC) lining the intracellular surface of their rhabdomeres. The *Drosophila* SRC spreads thoroughly over the roots of the rhabdomeres, while remaining closely apposed to them (20 nm away in *Drosophila*; Matsumoto-Suzuki *et al.*, 1989), forming a tight layer (30 nm thick). The activity of *Drosophila* SRC has not yet been studied directly; but, from the larger *Apis* cells, the SRC can be dissected, washed with saponin, and observed by polarized-light microscopy for Ca^{2+} uptake into oxalate crystals (Baumann and Walz, 1989a, 1989b). In vitro, *Apis* SRC takes up calcium in an ATP-dependent manner (Baumann and Walz, 1989a), consistent with its using an ATP-driven Ca^{2+} pump (Clapham, 1995a). Calcium uptake is

sigmoidally dependent on log[Ca^{2+}], with half-maximal uptake at 0.6 μM (Baumann and Walz, 1989b). This uptake can be depressed or halted by added IP_3, demonstrating the presence of an IP_3 receptor in the SRC. In the presence of 0.28 μM Ca^{2+}, uptake by SRC shows a sigmoidal dependence on log[IP_3], with half-maximal inactivation at 0.2 μM IP_3. At the same time, the half-maximal affinity for IP_3 itself is dependent on [Ca^{2+}], rising from 0.2 μM IP_3 to >0.5 μM IP_3 as [Ca^{2+}] either decreases or increases from 0.28 μM Ca^{2+}; indeed, at 32 nM Ca^{2+}, the SRC is unaffected by IP_3. This biphasic regulation of IP_3 affinity by [Ca^{2+}] is a general feature of IP_3 receptors (Payne *et al.*, 1990; Bezprozvanny *et al.*, 1991; Finch *et al.*, 1991). Because *Drosophila* SRC anatomically resembles *Apis* SRC, and because both *Apis* and *Limulus* photoreceptors have IP_3-gated, ATP-dependent calcium stores, *Drosophila* SRC presumably has IP_3 receptors and Ca^{2+}-pumps.

IP_3 receptors are homotetrameric Ca^{2+}-channels (monomeric mass, ~310 kD) known to mediate IP_3-triggered calcium release from the endoplasmic reticulum in diverse cell types (Berridge, 1993; Clapham, 1995a). The *Drosophila* IP_3 receptor gene (*dip*) was cloned by low-stringency hybridization (Hasan and Rosbash, 1992; Yoshikawa *et al.*, 1992). Dip has 2833 residues, with 57% identity to mammalian IP_3 receptors; like them, it has a massive (~2300-residue) N-terminal cytoplasmic domain, and 6-8 predicted transmembrane sequences in its C-terminal region. Two regions of Dip have detectable similarity to ryanodine receptors: the N-terminal 677 residues, thought to be the IP_3 binding site; and transmembrane sequences M5-M6, which may line the Dip channel (Yoshikawa *et al.*, 1992). These and other data support the hypothesis that IP_3 receptors and ryanodine receptors diverged evolutionarily from one another before the last common ancestor of mammals and arthropods (Takeshima *et al.*, 1994). Dip protein has not yet been localized immunohistochemically. However, *dip* transcripts have been detected by PCR of reverse-transcribed RNA (RT-PCR) from dissected adult retina, and weakly visualized by in situ hybridization to sectioned adult retina (Hasan and Rosbash, 1992).

Furthermore, neither of the two groups cloning *dip* found evidence for other IP_3 receptor genes in *Drosophila*. Accordingly, Dip probably resides in the *Drosophila* SRC and is the direct target of NorpA activity. Testing this hypothesis will eventually require either Dip-specific antibodies, or retina-specific *dip* hypomorphic mutations, or both.

Ryanodine receptors resemble IP_3 receptors in being homotetrameric Ca^{2+}-channels (monomeric mass, ~560 kD) that release Ca^{2+} from the endoplasmic reticulum; they differ from IP_3 receptors in being triggered by Ca_o^{2+} influx instead of by IP_3 (Berridge, 1993; Clapham, 1995a). The *Drosophila* ryanodine receptor gene (*dry*) encodes polypeptides of 5112 or 5216 residues with 45-47% identity to mammalian ryanodine receptors (Takeshima *et al.*, 1994). Each Dry isoform has an exceedingly large (~4500-residue) N-terminal cytoplasmic "foot", followed by 4 transmembrane sequences. Like *dip* transcripts, *dry* transcripts have been detected in the adult retina with RT-PCR (Hasan and Rosbash, 1992). Although Dry has not been histochemically localized within *Drosophila* photoreceptors, treatment of the *Apis* SRC with caffeine (a ryanodine receptor agonist) causes IP_3-independent Ca^{2+} release (Walz *et al.*, 1995). Dry may thus act after Dip to prolong and augment Ca^{2+} release from the *Drosophila* SRC.

Because NorpA is necessary for *Drosophila* phototransduction, one might assume that Dip's necessity was a purely academic issue. It is not, because gating IP_3 receptors is not the only possible use for NorpA activity. NorpA might instead be solely needed to produce diacylglycerol, in order to activate a phorbol-ester receptor (such as UNC-13 in *Caenorhabditis elegans*; Ahmed *et al.*, 1992). Or it might produce IP_3, only to have it immediately converted to IP_4 by an inositol-3-kinase (Majerus, 1992), which in turn might activate a distinct IP_4 receptor (Berridge, 1993). Until such possibilities are experimentally eliminated, Dip is plausibly but not inexorably downstream of NorpA.

In any case, activation of Dip alone cannot be enough to depolarize the photoreceptor; a light-stimulated photoreceptor must actually depolarize by opening light-stimulated channels (LSCs) in its plasma membrane. How this happens is presently

unresolved in two major ways: first, we do not presently know what all of the protein components of LSCs are; moreover, we do not have any firm idea about what may actually connect Dip activation to LSC activation. Nevertheless, many data exist that suggest solutions to both problems: electrical recordings of LSCs in photoreceptors; genetic and molecular properties of *trp*, which encodes a LSC component; and two other genes (*trpl*, *DmCNGC*) encoding possible LSC components. After these are reviewed, three proposed LSC activators will be evaluated: elevated cGMP, elevated Ca^{2+}, and mechanical opening by Dip.

Light-stimulated channels (LSCs)

The first studies of LSCs employed intracellular recording from photoreceptors (Minke *et al.*, 1975; Wu and Pak, 1975). This demonstrated that *Drosophila* photoreceptors can respond to very dim light with small (1.0 ± 0.4 mV; Johnson and Pak, 1986) and fleeting (25-30 ms; Wu and Pak, 1978) depolarizations from their resting membrane potential (about -55 mV; Hardie, 1991); each depolarization reveals a group of LSCs being activated by a single photon. Such "quantum bumps" have been observed in both vertebrate and invertebrate photoreceptors (reviewed in Wu and Pak, 1975; Johnson and Pak, 1986). *Drosophila* quantum bumps display no size heterogeneity (Wu and Pak, 1975), do not require cooperative interactions between rhodopsin molecules (Johnson and Pak, 1986), and do not vary in duration over a 10^3-fold range of light intensities (Wu and Pak, 1978). They do, however, shrink in size 10^2-fold over a 10^4-fold range of increasing light intensity; the rate of bump production varies linearly with intensity over a 10^3-fold range (Wu and Pak, 1978).

Intracellular recording can probe LSCs through observing the effects of mutations on quantum bumps, or more sustained light-induced currents (described below; Minke *et al.*, 1975; Hardie *et al.*, 1993b; Peretz *et al.*, 1994b). However, much progress in observing LSCs has come from new techniques for whole-cell voltage-clamping

photoreceptors in dissociated ommatidia (Hardie, 1991; Ranganathan *et al.*, 1991a) which allow the extracellular medium to be varied and the cytosol to be viewed directly. This newer approach has some limits: the LSCs themselves remain buried within the ommatidium, and thus cannot be patch-clamped (Ranganathan *et al.*, 1994; Pollock *et al.*, 1995); and LSCs spontaneously and irreversibly open ≤20 min after the whole-cell voltage clamp is established (Hardie and Minke, 1994a, 1994b). Nevertheless both methods, combined, have generated many findings.

LSCs are cation channels, and at least a subset of them have large pores: they show no variation in reversal potential when extracellular chloride is replaced by gluconate, while showing some permeability even to bulky organic cations such as $Tris^+$ and TEA^+ (Ranganathan *et al.*, 1991a). More importantly, LSCs are predominantly Ca^{2+}-channels. Their permeabilities were qualitatively ranked by Ranganathan *et al.* (1991a) as $Ca^{2+} > Cs^+ > Na^+ \approx K^+ > Tris^+ > TEA^+$ (Ranganathan *et al.*, 1991a). For $Ca^{2+} : Mg^{2+} : Cs^+ : Na^+$ they were quantitatively ranked as 40 : 8 : 1 : 1 by Hardie and Minke (1992). Because of their cation-specificity and reversal potential (~+10 mV; Hardie and Minke, 1992; Ranganathan *et al.*, 1991a), light-induced currents are inward in vivo; 35-40% of such inward currents should consist of Ca^{2+} ions (Peretz *et al.*, 1994a).

In a functioning photoreceptor, LSCs are activated in tightly regulated temporal patterns visible as stereotypical waveforms of current. The waveform shape and magnitude depends on the intensity of light with which they are activated, the duration of their light stimulus, the voltage at which they are clamped, and the levels of both extracellular and intracellular calcium present.

In dark-adapted cells at resting potential, steady dim illumination evokes quantum bumps 4-10 pA in amplitude and 30 ms in duration; the smallest voltage steps seen within them are about 1.3 pA, and could represent the opening or closing of a single ~20 pS channel (Hardie, 1991; Hardie *et al.*, 1993b). Increasing such illumination induces a linearly proportionate response in the photoreceptor up to at least 100

photons/photoreceptor (Hardie, 1991). This response is most easily observed if potassium channels, normally used by the photoreceptor to sharpen its action potential in vivo (Hevers and Hardie, 1995), are blocked by mutation or intracellular cesium. As light intensity increases, such linearity eventually yields a square wave of photoreceptor depolarization in response to lengthy (~1 sec) stimuli of medium intensity (Hardie and Minke, 1992). Stronger pulses produce a more complex pattern (Ranganathan *et al.*, 1991a; Hardie and Minke, 1992): the photoreceptor fails to respond for ~≤6 ms, strongly depolarizes to a transient peak in ~15 msec, remains there for ~250 ms, largely repolarizes over ~200 ms to a lesser plateau, and then very slowly (over ~1 s) increases this plateau until the stimulus ends (Peretz *et al.* 1994b). In other words, strong light pulses evoke a miniature, single-celled version of the primary component of the ERG. Brief (30 ms) flashes of light evoke simple, sinusoidal inward currents reaching a peak of 20 nA in ~40 ms at maximum intensity (Ranganathan *et al.*, 1991a); over a 100-fold range of stimulus intensities, the currents are identical in shape if normalized to a single amplitude (Hardie, 1991).

Both the modulation of quantum bumps by background light (Wu and Pak, 1978) and the dynamic response of LSCs to sustained illumination demonstrate that LSCs are not merely light-stimulated, but somehow light-regulated. That this is not a simple matter of partial inhibition is proven by two independent facts. First, if a dark-adapted photoreceptor is stimulated with an initial adapting flash, and then with a second test flash, its second response is not merely weaker than the first (as might be guessed) but also *faster*: the time needed for the second response to reach its peak (latency) is shortened (Hardie *et al.*, 1993b). Thus, adaptation does not merely inhibit but also speeds LSC opening. Second, *Drosophila* photoreceptors, over many orders of light intensity, manifest a linear relationship between the peak amplitude of their light-induced depolarization (V_{max}) and the logarithm of their stimulus (log I). This V_{max}/log[I] line is positively displaced along the log[I] axis, if photoreceptors are first treated with logarithmically increasing intensities of background adapting light (Minke, 1982; Hardie *et al.*, 1993b). An alternative quantitation

is that, at any level of background light, the additional light intensity needed to evoke a current of $V_{max}/2$ from a photoreceptor (σ) increases *logarithmically* as V_{max} itself (lowered by background light) decreases *linearly* (Hardie *et al.*, 1993b); $V_{max}/\log[\sigma]$ has a negative linear slope. Thus, LSCs are not merely *inhibited* by sustained light: their activity is somehow *adjusted* so that they can convey information about 10^4-fold variations of light, despite background light intensities varying 10^3-fold (Minke and Armon, 1980; Hardie *et al.*, 1993b).

Given the high permeability of LSCs to calcium, and the precedent of vertebrate phototransduction (Kaupp and Koch, 1992), it is a straightforward inference that *Drosophila* photoreceptors use varying levels of cytosolic calcium to regulate LSCs. The effects of perturbing either calcium or voltage levels in the *Drosophila* photoresponse strongly support this inference. The simplest such perturbation is simply to remove calcium from the buffer around an isolated photoreceptor, lowering it from a physiologically correct level (1.4 mM; Peretz *et al.*, 1994a) to trace levels (with EGTA or nominally Ca^{2+}-free buffer). This causes the inward currents evoked by brief flashes to malfunction grossly. Their waveform changes from tight sinusoidal pulses of current, closely following the flash, to sluggish, extended sine waves that do not reach peak intensity until well after the flash itself (Ranganathan *et al.*, 1991a; Hardie and Minke, 1992). Moreover, calcium-deprived photoreceptors also show an aberrant response to sustained light stimuli, completely losing their normally complex waveforms (Ranganathan *et al.*, 1991a). This requirement for calcium is chemically specific; extracellular 8 mM Mg^{2+} does not restore normal regulation (Hardie and Minke, 1992). The misregulation is not all-or-none; unusually dilute, but nonzero calcium buffers cause fuzzy light responses, with blurred but visible peaks and plateaus (Ranganathan *et al.*, 1991). Conversely, pipetting a wave of abnormally concentrated calcium (10 mM) onto photoreceptors during a flash response causes the photoreceptor to increase its current flow abruptly, reach a larger magnitude of peak current than normal, and then inactivate itself unusually quickly (Hardie,

1991). More generally, the time to peak current after a flash decreases as extracellular calcium (Ca_o^{2+}) is increased (Hardie, 1991; Ranganathan *et al.*, 1991a).

In contrast to direct changes of Ca_o^{2+}, voltage changes seem to have no effect on the LSCs, other than to govern the rate at which calcium can enter the photoreceptor. In moderate (0.5-1.5 mM) levels of Ca_o^{2+}, photoreceptors stimulated by strong sustained light pulses display asymmetric waveforms when clamped at highly negative (e.g., -80 mV) versus highly positive (e.g., +60 mV) potentials: negative polarization yields inward currents with the transient peak and diminished plateau currents described above, while positive polarization causes outward currents which neither diminish in sustained light nor shut off promptly after light ends (Ranganathan *et al.*, 1991a). Likewise, positively polarized photoreceptors do manifest outward currents upon a brief flash, but they tend to peak and inactivate more sluggishly than their reverse (Hardie, 1991; Ranganathan *et al.*, 1991a). In fact, the pulse- and flash-evoked *outward* currents seen with normal Ca_o^{2+} look very much like the poorly regulated *inward* currents seen with deficient Ca_o^{2+}. This resemblance is made more compelling by the effects of raising Ca_o^{2+} to nonphysiologically high levels (3.5-10 mM) on voltage-dependent currents: both flash- and pulse-evoked inward versus outward currents become symmetrical in waveform, or nearly so (Hardie, 1991; Hardie and Minke, 1992). Moreover, the LSCs display a different relationship of voltage to current flow at varying levels of Ca_o^{2+}. At moderate Ca_o^{2+} levels (0.5-2.0 mM) LSCs are inwardly rectifying below their reversal potential (~+10 mV) but outwardly rectifying above it (Hardie, 1991; Hardie and Minke, 1992); the most direct interpretation of this is that LSC open times become greater as voltages diverge from reversal potential (Hille, 1992). If Ca_o^{2+} is raised to 10 mM, on the other hand, the I/V relationship of LSCs becomes linear. The calcium-dependence of both asymmetrical waveforms and rectifying conductances implies that voltage regulates LSCs by governing the rate at which Ca_o^{2+} enters the photoreceptor. Furthermore, the speed (3 ms) with which LSCs can alter their conductivity in response to a voltage jump during the light response suggests that calcium

regulates LSCs directly (Hardie, 1991).

The relationship between calcium influx and light-induced current flow can be directly examined in dissociated, voltage-clamped photoreceptors that have been loaded with a calcium-sensitive fluorescent dye. Peretz *et al.* (1994b) found that, in physiological levels of Ca_o^{2+}, a 5-s light pulse induces LSC opening (observed by current flow) which initially parallels an approximate doubling of the average intracellular calcium Ca_i^{2+}; but that, as the pulse continues, LSCs are largely inactivated while Ca_i^{2+} remains high. *norpA* photoreceptors have resting Ca_i^{2+} levels indistinguishable from wild-type, but completely lack both inward current and elevated Ca_i^{2+} upon illumination; this shows both phenomena to be triggered by IP_3 production. All observable rises in Ca_i^{2+} represented an influx of Ca_o^{2+} instead of Ca^{2+} release from the SRC, since bathing photoreceptors in EGTA before stimulation totally prevents Ca_i^{2+} elevation (Peretz *et al.*, 1994b). Furthermore, in an intact retina, light stimuli induce a directly measurable reduction of Ca_o^{2+} next to photoreceptors (measurable by Ca^{2+}-selective electrodes) that closely resembles its inward charge current (Peretz *et al.*, 1994a).

Photoreceptors with diminished sensitivity (*ninaE*^{P322}) expel Ca_i^{2+} during 20 s of dark following an adapting pulse; a second pulse then induces them to display both reduced currents and diminished increases of Ca_i^{2+} (Peretz *et al.*, 1994b). Thus Ca_o^{2+} influx, like currrent influx, is subject to light adaptation. Furthermore, adaptation was shown by Peretz *et al.* (1994b) to have complex responses to influx from varying calcium buffers: 200 μM EGTA allows a slightly diminished excitation of LSCs (86% normal), followed by their slow inactivation; ~4 μM Ca_o^{2+} increases LSC activation while paradoxically preventing LSC inactivation; 200 mM Ca_o^{2+} shows sluggish inactivation, while 400 mM Ca_o^{2+} showed a normal pattern of LSC activation and adaptation. One implication is that Ca_o^{2+} influx is not itself needed to activate LSCs, since sizable light-activated currents can be seen even in extracellular EGTA. Another implication, further discussed below, is that multiple LSC components may exist which are differently regulated by Ca_o^{2+} influx.

Where Peretz *et al.* (1994a,1994b) observed Ca_o^{2+} influx during pulse stimuli, Ranganathan *et al.* (1994) observed it during flash stimuli. They achieved this by studying ommatidia from flies whose endogenous Rh1 opsin had been transgenically replaced with purely UV-sensitive Rh4 opsin. As in Peretz *et al.* (1994a,1994b), dissociated ommatidia were loaded with calcium-sensitive fluorescent dye before being stimulated. With such transgenic ommatidia, the stimulating light (λ = 351-364 nm) and the dye-exciting light (λ = 543.5 nm) have entirely separate wavelengths, so that the effects of a single stimulating flash stimulus on calcium flux can be continuously monitored by nonstimulating light. As do pulses, flashes induce rapid Ca_i^{2+} elevations that parallel inward current, followed by slow Ca_i^{2+} decreases that take much longer (seconds) than current inactivation (milliseconds). Persistent post-flash Ca_i^{2+} elevation coincides with a visible reduction in background current noise, which implies that quantum bumps shrink in size (light-adapt) as Ca_i^{2+} increases. Both Ca_i^{2+} elevation and bump shrinkage are abolished if photoreceptors are placed in ~0 mM Ca_o^{2+} before a light flash. Conversely, the resensitization of a photoreceptor after an adapting flash quantitatively matches the decrease of Ca_i^{2+} after that flash.

When observed by high-resolution confocal microscopy, light-induced Ca_o^{2+} influx does not appear to occur uniformly over the photoreceptor surface (Ranganathan *et al.*, 1994). Instead, the first traces of Ca_i^{2+} elevation arise ~70 ms after a light flash, at the junction of the photoreceptor's cell body with its rhabdomere. As the photoresponse proceeds, Ca_i^{2+} rises throughout the photoreceptor, but predominantly continues growing at the rhabdomere junction, and in the rhabdomere itself. Ca_i^{2+} elevation at the rhabdomere junction is particularly important because this site is physically near the SRC (20 nm away), suggesting that Dip may activate the LSCs by mechanisms that are local in nature (Matsumoto-Suzuki *et al.*, 1989).

In summary: wild-type LSCs are primarily Ca^{2+}-channels, but with some ability to admit virtually any small cation. In vivo, LSCs open and shut in small groups activated by

single photons, yielding quantum bumps of current. These currents consist of ~65% Na^+ and ~35% Ca^{2+} ions. Changes in the size of light-induced current are brought about by accelerating bump rate and diminishing bump size with increasing light, which in turn depends on ingress of Ca_o^{2+} to the cytosol via LSCs themselves. Nevertheless, EGTA-challenged LSCs can conduct inward currents without Ca_o^{2+}; calcium influx is not needed to initiate LSC activity. The speed of LSC responses to changing Ca^{2+}, and the dependence of LSC rectification on moderate Ca^{2+}, implies that Ca_i^{2+} acts directly on LSC components. LSCs may be localized to a limited region of the photoreceptor near the SRC. Further analysis of LSC composition and regulation requires genetics.

trp encodes a Ca^{2+}-selective light-stimulated channel component

Only one gene actually encoding a LSC component, *trp*, has been well studied. The first *trp* mutation arose spontaneously (Cosens and Manning, 1969); later alleles were isolated in a screen for autosomal mutations conferring a defective PDA (Pak, 1979). The most obvious phenotype of *trp* flies is that they behave as if they are blind in strong light, but normally sighted in dim light (Cosens and Manning, 1969). In an ERG, *trp* retinas decay from full polarization to the resting baseline voltage, even while the stimulus remains; the decay time depends on light intensity, but can range from 1-15 s. After a stimulus, *trp* retinas require 30-50 s in the dark to recover their sensitivity gradually, while wild-type retinas have fully recovered in 10 s (Cosens and Manning, 1969; Minke, 1982). Yet, when recorded during pulses of dim light, *trp* photoreceptors generate square-wave responses like those in wild-type (Minke, 1982) and have normal quantum bumps (Minke *et al.*, 1975).

One explanation for this selective defect might be that trp^+ is needed to limit light adaptation properly, so that *trp* mutations cause *hyper*adaptation that silences rather than mutes the photoreceptor. But several data indicate otherwise. Quantum bumps in *trp* fail to diminish 10^2-fold, as do wild-type bumps, with strong light; in fact, they do not shrink at

all (Minke *et al.*, 1975). Since the *trp* ERG collapses to resting voltage levels, *trp* photoreceptors must grossly reduce their quantum bump frequency in strong, sustained light (whereas wild-type bump frequency scales linearly with light intensity). Because stimuli that blind *trp* photoreceptors only isomerize 1-3% of their rhodopsin (Minke *et al.*, 1975), and because *trp* rhodopsin levels are normal (Minke, 1982), *trp* bump infrequency cannot be due to functional rhodopsin being exhausted. The crucial defect of *trp* is revealed when light adaptation is determined for *trp* retinas in varying levels of background light, and compared to wild-type. With increasing background light, the range of responses of *trp* retinas to additional light shrinks, while wild-type retinas adapt and remain able to generate widely variable currents. This can be expressed quantitatively by V/log[I] and V_{max}/log[σ]. Whereas wild-type V/log[I] lines shift rightward to higher log[I] values as background light increases, so that V_{max}/log[σ] has a negative linear slope, *trp* V/log[I] lines fail to respond to increased background light, so that log[σ] scarcely changes over greatly varying V_{max} values (Minke and Armon, 1980; Minke, 1982). More evidence that *trp* is not hyperadaptive comes from light-induced changes in photoreceptor latency: while wild-type photoreceptors become faster in their responses to test flashes with increased background light, *trp* photoreceptors are greatly *slowed*--despite the fact that they respond normally to the same test flashes when dark-adapted (Minke, 1982).

Isolated *trp* photoreceptors were characterized by Hardie and Minke (1992). *trp* photoreceptors are normal in dim light; but, in strong light pulses, they show a scaled-down equivalent of the *trp* ERG, with an initially normal spike of current followed by a rapid decline to zero. They also fail to accelerate their peak response if hyperpolarized, implying that excitatory Ca_0^{2+} influx is *trp*$^+$-dependent. More crucially, the reversal potential (E_{rev}) of *trp* peak current significantly differs from that of wild-type in varying cation solutions. By constant-field theory (Hille, 1992), such *trp* E_{rev}s imply a dramatic change in LSC cationic permeability. While wild-type LSCs have a Ca^{2+} : Mg^{2+} : Cs^+ : Na^+ permeability ratio of 40 : 8 : 1 : 1, *trp* LSCs have one of 3.5 : 1.9 : 1.0 : 0.7 (Hardie and

Minke, 1992). Unlike normal light-stimulted inward currents (predicted to contain 35-40% Ca^{2+}), *trp* currents should have only 10% Ca^{2+} (Peretz *et al.*, 1994a). In fact, voltage-clamped *trp* photoreceptors held at -50 mV and stimulated by a light flash display roughly normal inward currents, but only ~20% the normal rise in Ca_i^{2+} (Peretz *et al.*, 1994b); independent measurements of Ca_o^{2+} in *trp* retinas support this discrepancy (Peretz *et al.*, 1994a). Other data suggest that this is the only crucial defect of *trp* (Hardie and Minke, 1992). The altered LSC permeability ratios and peak response times of *trp* can be mimicked by treatment of wild-type photoreceptors with 10 μM La^{3+}, an inhibitor of calcium-binding proteins. Conversely, *trp* photoreceptors are unaltered by La^{3+} treatment. Finally, if photoreceptors are depleted of calcium by soaking for >60' in 50 nM Ca^{2+}, and then tested with a strong light pulse, they generate a *trp*-like current. These findings suggest that the *trp* phenotype can be summarized as two defects, one primary, one indirect: loss of a specific LSC polypeptide that mediates most Ca^{2+} permeability; and profound defects in regulation of the remaining LSCs, brought about by scarcity of Ca_i^{2+} during the photoresponse.

The *trp* gene encodes a putative membrane protein with 1275 residues expressed in all retinal and ocellar photoreceptors (Montell *et al.*, 1985; Montell and Rubin, 1989; Wong *et al.*, 1989), but not in Bolwig's organ (Pollock *et al.*, 1995); this correlates with the genetic requirement for *trp* in photoreceptors R1-R8 and ocelli (Hu *et al.*, 1978; Chen and Stark, 1983). Its N-terminal quarter contains four ankyrin repeats, thought to bind other (unknown) proteins (Bork, 1993). The next quarter of Trp is predicted to have six transmembrane sequences, with traces of similarity to those in the α_1 subunit of the brain dihydropyridine-sensitive voltage-dependent Ca^{2+} channel (Phillips *et al.*, 1992). However, the arginine residues of transmembrane helix S4 (which sense voltage in the latter channel) are not conserved in Trp, suggesting that Trp is not voltage-gated. The C-terminal half of Trp is predicted to have a single calmodulin-binding helix (Phillips *et al.*, 1992), and ends with nine repeats of the octapeptide DKDKKP[G/A]D. In retinal

photoreceptors, Trp protein resides in a narrow strip of plasma membrane at the roots of the rhabdomeres (Pollock *et al.*, 1995), coinciding with the initial site of light-stimulated calcium influx seen by Ranganathan *et al.* (1994). Although Ranganathan *et al.* (1994) also saw a general elevation of Ca_i^{2+} in the rhabdomeres themselves, Pollock *et al.* (1995) found that rhabdomere size completely fails to correlate with LSC function, while the area available for Trp at rhabdomere roots strongly correlates with it.

Heterologous Trp was assayed for Ca^{2+}-channel activity by expressing it in Sf9 cells with a baculovirus vector (Vaca *et al.*, 1994). Trp is inert in Sf9 cells until they are treated with thapsigargin, a specific inhibitor of the ER's Ca^{2+}-pump (Berridge, 1993) that causes the ER to leak Ca^{2+} into the cytosol. Upon thapsigargin treatment, the Sf9 cells become permeable to Na^+, Mg^{2+}, and Ca^{2+} currents, with Ca^{2+} permeability being greatest. Trp thus most likely encodes a channel that sustains phototransduction by maintaining Ca_o^{2+} influx during prolonged stimuli.

More LSC components?

With the large number of phototransduction mutations already in hand, and the straightforward methods for obtaining more, all LSC components might be genetically identifiable. But, at this writing, only *trp* is actually known to ablate *Drosophila* LSCs. Very recently, a new mutation (*P69*) has been reported that might disrupt a second channel component: while it has an ERG by itself, *P69* has no response to light if compounded with *trp* in a double mutant (Li *et al.*, 1995). The characterization of genes like *P69* will be essential to dispel the present fog that shrouds *Drosophila* LSC composition. At the same time, two possible LSC components (*trpl*, *DmCNGC*) have been cloned in advance of their being genetically tested for visual function. *trpl* is described here, *DmCNGC* somewhat later.

***trp-like* (*trpl*) and other *trp* homologs**

The *trpl* gene was isolated by expression cloning, as an adult head cDNA encoding a calmodulin-binding protein (Phillips *et al.*, 1992). Further study showed it to encode a novel protein of 1124 residues with no close relatives except Trp, to which it has 39% identity. Like Trp, Trpl has four N-terminal ankyrin repeats (Bork, 1993) and six transmembrane sequences weakly similar to the dihydropyridine receptor α_1 subunit (Phillips *et al.*, 1992). However, Trpl has two calmodulin-binding helices, and lacks the C-terminal DKDKKP[G/A]D repeat of Trp. The most conserved regions of Trpl are the N-terminal region containing ankyrin repeats (54% identity to Trp), and the region containing putative transmembrane helices 4-6 (74% identity); other regions are more variable (≤29% identity). Trpl, like Trp, lacks arginine residues in what would otherwise be a conserved, voltage-sensing S4 helix. In adult heads, a single 4.0 kb *trpl* transcript is specifically expressed in the photoreceptor level of the retina (Phillips *et al.*, 1992). Since no anti-Trpl sera exist, Trpl protein has yet to be histochemically detected; however, its relatively conserved N-terminus might lead it to colocalize with Trp. That Trp and Trpl are not arthropod-specific proteins has been demonstrated by the *C. elegans* genome project, which identified an open reading frame on chromosome III (ZC21.2) with 37% identity to Trp (Wilson *et al.*, 1992); like *trpl*, it has no extant mutations. More recently, there has appeared a preliminary report of at least three mammalian *trp* homologs (by Montell and coworkers; Clapham, 1995b).

No *trpl* mutations have been reported, making *trpl*'s function conjectural. However, studies of heterologous Trpl in Sf9 cells are consistent with Trpl being an LSC component. Hu *et al.* (1994b) found that *trpl* expression caused Sf9 cells to raise their basal Ca_i^{2+} level from ~90 nM to ~290 nM after 30-36 hours (Harteneck *et al.*, 1995; Hu *et al.*, 1994b). Such a change can arise from either inhibited Ca_i^{2+} efflux or increased Ca_o^{2+} influx. Ba^{2+}, a Ca^{2+} surrogate that permeates calcium channels but not calcium exporters, was used to test these two explanations; *trpl*-expressing Sf9 cells challenged

with Ba^{2+} display a pronounced increase of fura-2 fluorescence with respect to control cells, showing that *trpl* actually promotes cation influx (Hu *et al.*, 1994b). Whole-cell voltage clamps show that *trpl* generates a membrane conductance with an E_{rev} of 0 mV (Harteneck *et al.*, 1995; Hu *et al.*, 1994b). Replacing external cations with N-methyl-D-glucamine shifts this conductance's E_{rev} to -100 mV, while replacing all external ions with calcium gluconate has no effect (Harteneck *et al.*, 1995; Hu *et al.*, 1994b).

If *trpl* expression in Sf9 cells genuinely simulates a meaningful subset of *Drosophila* LSC function, it should be possible to induce Trpl to elevated activity by treatments of the Sf9 cells that generate internal IP_3 through PLC-β activation. Although neither IP_3 nor PLC-β has been directly studied in Sf9 cells, they do respond to octopamine treatment by activating endogeneous calcium channels, which are blocked by 10 μM La^{3+} (Hu *et al.*, 1994a). Octopamine belongs to a large class of molecules (including thromboxane, acetylcholine, and histamine) that, by binding specific heptahelical receptors, uniformly stimulate $G_{q\alpha}$, PLC-β, and IP_3 receptors (Berridge, 1993). Sf9 cells were therefore cotransformed with both *trpl* and a variety of heptahelical receptors (Harteneck *et al.*, 1995; Hu and Schilling, 1995). *trpl* coexpressed with M5 muscarinic receptor elevates basal Ca_i^{2+} to 200 nM, but carbachol addition induces an acute rise of Ca_i^{2+} to ~700 nM; this rise is poorly inhibited by 10 μM La^{3+}, demonstrating that Trpl is specifically activated and is more La^{3+}-resistant than Trp in vivo (Hu and Schilling, 1995). This elevation occurs with either Ca^{2+} or Ba^{2+} present outside the cell, and can also be induced by bradykinin treatment in cells coexpressing *trpl* with bradikinin receptor (Hu and Schilling, 1995). Similar Trpl activation by histamine, thrombin, and thromboxane A2 receptors has been observed by Harteneck *et al.* (1995). However, unlike Trp, Trpl channels are unaffected by thapsigargin treatment (Vaca *et al.*, 1994; Hu and Schilling, 1995). Also unlike Trp, Trpl channels have good permeability to Na^+, Ca^{2+}, and Ba^{2+}, but are impermeable to Mg^{2+} (Vaca *et al.*, 1994). This last point is significant because *trp*$^-$ LSCs are more permeable to Mg^{2+} than to Na^+ (Hardie and Minke, 1992). If Trpl is indeed, like

Trp, a LSC component, it seems that a third Mg^{2+}-permeable component must then exist; this might be a cGMP-gated channel (DmCNGC, detailed below), or a sodium-magnesium exchanger (Flatman, 1992) working in reverse as photoexcitation elevates intracellular Na^{+}.

Hu and Schilling (1995), noting the three-fold elevation of basal Ca_i^{2+} in Sf9 cells by *trpl* expression, speculated that Trpl may be artifactually deregulated by heterologous expression. While this possibility should be considered, not all of the basal permeability of Trpl need be artifactual. For heterologous Trpl generates a resting level of Ca_i^{2+} (~300 nM) which is comparable to the resting levels of Ca_i^{2+} actually observed in photoreceptors of blowfly (150 nM; Hochstrate and Juse, 1989) and *Apis* (90 nM; Walz *et al.*, 1994). The quantitative difference between these levels is modest, and might wholly be accounted for by failure to restrict Trpl to a limited portion of Sf9 cells. Moreover, mutant phenotypes of *inaC* and *InaD* (detailed below) suggest that moderately elevated resting Ca_i^{2+} is required for a basal level of adaptation in total darkness.

Despite the availability of heterologous Trp and Trpl, neither has been studied in patch-clamps to determine its precise conductance. However, Hardie and Minke (1994a) have ingeniously exploited an electrophysiological artifact to observe trp^{+}-dependent and trp^{+}-independent conductances indirectly. Dissociated *Drosophila* photoreceptors, after a delay of ≤20 min, suddenly display a spontaneous current without benefit of light-stimulation. This run-down current (RDC) desensitizes the photoreceptor to light by at least 100-fold. Its advantage for studying Trp and non-Trp conductances is that, while a normal photoreceptor's background noise is dominated by quantum bump kinetics, the RDC is entirely decoupled from photosensory mechanisms. Thus RDC noise directly reflects individual LSCs opening and closing. The RDC has a biphasic reversal potential, cation-specificity, and rectification like those of light-regulated current, indicating that both pass through the same LSCs. RDC is either absent or greatly diminished by either trp^{-} mutations or 10-20 μM La^{3+}; the same factors that cause trp^{+}-independent LSCs to close

rapidly in a normal light response may also prevent them from participating in the RDC. Still, noise analysis of both *trp*$^+$ and *trp*$^-$ RDCs is feasible, and shows that their average conductances greatly vary: *trp*$^+$ RDC has an average quantal conductance of ~1.5-4.5 pS, while *trp*$^-$ RDC's is 12-30 pS (Hardie and Minke, 1994a).

Because the power spectra of both genotypes are identical, Hardie and Minke (1994a) argue that the ~1.5-4.5 pS of *trp*$^+$ photoreceptors may actually represent a minority of 12-30 pS channels amid a great many *trp*$^+$-dependent RDCs with tiny (<1 pS) conductances. This has precedents elsewhere. The conductance of mammalian rod photoreceptor channels is kept at 0.1 pS by divalent cations, which allows rods to use a greater number of channels and therefore maximize signal resolution (Atwell, 1986; Kaupp and Koch, 1992). A closer analogy is the calcium release-activated calcium-selective current (I_{CRAC}) of mast cells, which (like Trp) is activated when ER is depleted of Ca^{2+} by thapsigargin, and which has undetectably low channel noise (Hoth and Penner, 1993). Trp and Trpl, despite their similarity, may be specialized to carry out quite different photosensory functions and to have different responses to Ca_o^{2+} influx, with Trpl providing rapid and robust depolarization and Trp providing sustained, slower, and more highly resolved waveforms. Their differences in ionic permeability are likely to be encoded by variations in transmembrane sequences (especially helices 1-3), while differences in regulation might arise from the Trp-specific C-terminal octapeptide repeat (Vaca *et al.*, 1994) and from their different number of calmodulin-binding sites (Phillips *et al.*, 1992).

Models for LSC activation

Characterizing Trp and Trpl addresses one important problem, the actual composition of *Drosophila* LSCs. It leaves another one, their activation, unsettled. As noted, it is not obvious how Dip activates channels in the plasma membrane. Three possible answers are discussed here.

cGMP-gating after Ca^{2+} elevation? Vertebrate photoreceptors use cGMP

levels to control whether their plasma membrane channels are open or shut. Since the channels are Ca^{2+}-permeable, and since the enzymes of cGMP metabolism are Ca^{2+}-regulated, Ca^{2+} and cGMP control one another's levels, with their actual quantities being determined by illumination levels (Kaupp and Koch, 1992). *Drosophila* phototransduction does not, like that of vertebrates, directly control cGMP metabolism through a G protein; however, there is some reason to think that it might do so indirectly by elevating cytoplasmic Ca^{2+} via Dip activation. The electrophysiological evidence for this comes from *Limulus*.

Like *Drosophila*, *Limulus* photoreceptors release Ca^{2+} from IP_3-gated stores in response to light (Brown *et al.*, 1984; Fein *et al.*, 1984; Bloomquist *et al.*, 1988; Payne *et al.*, 1988). However, unlike *Drosophila*, *Limulus* photoreceptors have been successfully loaded with calcium buffers, and *Limulus* light-stimulated channels have been isolated in patch clamps. Specifically, dissociated *Limulus* ventral photoreceptors were loaded by Shin *et al.* (1993) with large concentrations (100-200 mM) of 5,5'-dibromo-BAPTA (DBB), a calcium buffer that is both fast-binding and resistant to saturation by resting levels of cytoplasmic calcium. By varying the amounts of calcium coinjected with DBB, the entire cytoplasm of the injected photoreceptor could be temporarily compelled to assume a predetermined concentration of cytoplasmic Ca^{2+}, despite flooding of a tiny portion of the photoreceptor with Ca^{2+} from IP_3-gated internal stores. Shin *et al.* (1993) predicted that, if photoreceptor excitation uses Ca^{2+} as a necessary intermediate, it should never become resistant to incremental perturbation by repeated DBB injection. This prediction was verified with a DBB/Ca^{2+} solution designed to force cytoplasmic Ca^{2+} to resting levels (0.5 μM): repeated injection of this buffer eventually diminished light-induced depolarization 10^2-fold and slowed it 10^3-fold. A second set of injections with DBB/Ca^{2+} solutions set to 5.0 μM (the resting Ca^{2+} level in a light-illuminated photoreceptor) demonstrated that even this level weakened excitation, arguing against Ca^{2+} merely facilitating excitation. Finally, injections of DBB/Ca^{2+} set to either 5.0 or 45.0 μM evoked

small or large excitations in total darkness, indicating that Ca^{2+} is not only necessary but also sufficient to activate *Limulus* photoreceptors. The reversal potential of Ca^{2+}-induced current roughly equalled that of light-induced current, suggesting that they pass through identical channels.

Yet Ca^{2+}, while an obligatory intermediate, is not the direct agonist of light-activated membrane channels in *Limulus*. Bacigalupo *et al.* (1991) demonstrated this by patch-clamping *Limulus* ventral photoreceptors, demonstrating that a patch had captured a light-stimulated channel, and then excising the patch without damaging its channels. The cytoplasmic face of the patch could then be treated with Ca^{2+} or cGMP, and tested for channel opening. Ca^{2+} treatments of 0.01-1.00 mM had no effect on the patches; in contrast, 100 μM cGMP generally opened channels that had conductances, open times, and voltage-dependences indistinguishable from light-stimulated channels. Nonhydrolyzable cGMP derivatives worked more reliably than cGMP, suggesting that phosphodiesterases act near the channels to render cGMP signals fleeting. Independently, Feng *et al.* (1991) used nonhydrolyzable cGMP *and* cAMP derivatives to induce reliable excitation in dissociated *Limulus* photoreceptors; while supporting Bacigalupo *et al.* (1991), this also shows that the post-Ca^{2+} signal cannot yet be unambiguously specified.

Data of this sort are not yet available for *Drosophila*. In the case of DBB buffering, this may simply be because it has not yet been tried, since similar experiments have been successfully performed with caged calcium compounds (Hardie, 1995). In the case of patch clamping, tight junctions between the photoreceptors form a circular series of gaskets (Van Vactor *et al.*, 1988) that mechanically hinder access to the rhabdomere base, where patch clamps would ideally be placed. To overcome this, it might be possible to obtain dissociated single photoreceptors by macerating and glycolytically cleaning retinas (Ziemba *et al.*, 1995) that either contain excess photoreceptors (which might dissociate more readily; Renfranz and Benzer, 1989) or lack photoreceptors R1-R6 (leaving R7-R8 free to be patch-excised; Harris *et al.*, 1976).

But two *Drosophila* genes are known to exist which conceivably could mediate cGMP signalling in photoreceptors. The first, cloned by low-stringency hybridization and by differential cDNA screening, is *Dgcα1*, encoding an α-subunit of soluble guanylyl cyclase (Yoshikawa *et al.*, 1993; Liu *et al.*, 1995; Shah and Hyde, 1995). Dgcα1 protein is predicted to have 676 residues with 48% identity to mammalian GC α-subunits; like its mammalian homologs, it displays GC activity only if coexpressed with a (*Drosophila*) GC β-subunit, *Dgcβ1* (Shah and Hyde, 1995). In adults, *Dgcα1* is expressed in photoreceptors and neuropil (Liu *et al.*, 1995; Shah and Hyde, 1995); since *Dgcβ1* is not expressed in the retina, a different GC β-subunit must be expressed in photoreceptors if *Dgcα1* actually functions in them (Shah and Hyde, 1995).

The second gene, also cloned by low-stringency hybridization, is *DmCGNG*, encoding an cGMP-gated Ca^{2+} channel: DmCGNG has 665 residues with 62-64% identity to its bovine homologs (Baumann *et al.*, 1994). Like those homologs, DmCGNG is predicted to have a cytoplasmic N-terminal domain, six transmembrane sequences and a pore-forming loop in a central membrane-spanning domain, and a C-terminal cytoplasmic cGMP-binding domain. Nevertheless, heterologously expressed DmCGNG differs from mammalian channels: at -60 mV (the resting potential of *Drosophila* photoreceptors), DmCGNC is not blocked by extracellular divalent cations, so that its conductance is 36 pS rather than in the (mammalian) femtosiemen range. This conductance fits one seen in cGMP-activated *Limulus* photoreceptor patches (42 ± 4 pS; Bacigalupo *et al.*, 1991) quite closely, and roughly matches one inferred in *trp*$^-$ photoreceptors (12-30 pS; Hardie and Minke, 1994a). DmCGNC also has a range of permeabilities for $Ca^{2+} : Mg^{2+} : Cs^+ : Na^+$ (48 : 10 : 1 : 0.8) noticeably akin to that seen in *Drosophila* light-induced channels (40 : 8 : 1 : 1); and *DmCGNC* transcripts are detectable in dissected adult eyes by PCR of reverse-transcribed RNA (RT-PCR.)

Some caveats exist, though. RT-PCR cannot localize DmCGNC in photoreceptor plasma membranes; immunohistochemical work is needed. Worse, *trp* mutations alter the

permeability ratio of *Drosophila* light-induced channels from (40 : 8 : 1 : 1) to (3.5 : 1.9 : 1 : 0.7); since this is grossly different from the permeability ratios of DmCNGC, it must be at most a small fraction of all *Drosophila* light-induced channels. Furthermore, since low-stringency hybridization did not detect a second *DmCNGC* homolog in *Drosophila*, one cannot invoke a second cGMP-gated channel with different permeabilities (Baumann *et al.*, 1994). On the other hand, electrophysiological and pharmacological dissections of the *Limulus* photoreceptor light response by Nagy and coworkers (Deckert *et al.*, 1992; Nagy, 1993, 1994) have indicated that cGMP may be only one of two signals downstream of Ca^{2+} used to depolarize the *Limulus* photoreceptor, and that cGMP-gated channels may modulate the response rather than provide all of it. One is forced to conclude that, given present knowledge, cGMP is neither a convincing signal nor an impossible one.

Direct Ca^{2+}-activation? This model was initially suggested for *Limulus* photoreceptors, by experiments in which pressure injections of Ca^{2+} caused excitation resembling that caused by a light stimulus (Payne *et al.*, 1986). The model became reasonable for *Drosophila* as well, when it became clear that NorpA incites intracellular release of Ca^{2+} via Dip, and that sustained excitation requires a steady supply of Ca^{2+} to the photoreceptor cytoplasm through Trp. The data reviewed above demonstrate that injected Ca^{2+} must depolarize *Limulus* photoreceptors indirectly by elevating cGMP levels and activating cGMP-gated channels (Bacigalupo *et al.*, 1991; Shin *et al.*, 1993).

Two lines of evidence show that Ca_i^{2+} is necessary for LSC activation. The first comes from the effects of chelating Ca_i^{2+} in *Drosophila* photoreceptors with EGTA or BAPTA. Hardie and Minke (1992) bathed dissociated photoreceptors in ~2.5 mM Ca_o^{2+} for 30', while opening their LSC's with repeated adapting flashes (to leach out sequestered Ca^{2+}.) The photoreceptors were then perfused with EGTA/Ca^{2+} (set to a free Ca^{2+} concentration of either 50 nM or 700 nM), flash-stimulated, and recorded. 50 nM Ca_i^{2+} caused both wild-type and *trp* photoreceptors to desensitize ~300-fold to light, with some photoreceptors barely responding to the brightest available stimuli. With BAPTA in place

of EGTA, it is alleged that the light response is blocked entirely (unpublished observations cited by Peretz *et al.*, 1994b). Since normal sensitivity can be restored by raising Ca_i^{2+} to 700 nM, EGTA does not irreversibly impair the light-response (Hardie and Minke, 1992). Similar results were obtained by Ranganathan *et al.* (1994), who demonstrated that the response of dissociated Rh[1+4] photoreceptors to a light flash were greatly slowed by both internal BAPTA and internal Trans-5; since Trans-5's K_D is 6.0 μM, normal excitatory levels of Ca_i^{2+} must be in the range of micromolars rather than nanomolars.

Further support for the excitatory role of Ca_i^{2+} comes from developmental studies of the light response of photoreceptors in late *Drosophila* pupae (Hardie *et al.*, 1993a). Photoreceptors recorded <82 hours after pupariation are inert; but between 82-90 hours, photoreceptors display rapid microvillar growth (measurable through cell capacitance) and become able to respond to light *if* they are supplied with calcium in their recording pipet. With electrodes buffered to 25-150 nM they remain silent, but with 5 μM Ca^{2+} they become light-responsive. This conditional sensitivity is not due to a deficiency of Ca^{2+} in the surrounding hemolymph: it is observed in both *trp*$^+$ and *trp*$^-$ photoreceptors; and *trp*$^+$ photoreceptors display a *trp*$^-$ waveform when stimulated with sustained strong light at this developmental stage. This *trp*$^-$ phenocopy cannot be rescued by excess (10 mM) Ca_o^{2+}, and the E_{rev} of the "*trp*$^-$" pupal LSCs is wild-type, proving that Trp channels are present and functional (Hardie and Minke, 1992); it is thus improbable that the photoreceptors actually lack sufficient Ca_o^{2+} influx, once their LSCs have been induced to open at all. The simplest conclusion is that, during a limited pupal period, the photoreceptor is generally competent to detect light, but its SRC has not yet accumulated enough Ca^{2+} to initiate excitation through IP_3-gated Ca^{2+} release. All of the above findings make a strong case that Ca_i^{2+} elevation is required to activate *Drosophila* LSCs.

But showing calcium to be necessary does not prove it sufficient for excitation. Hardie (1995) addressed the latter question by loading *Drosophila* photoreceptors not with Ca^{2+} chelators, but with caged Ca^{2+}, which remains electrophysiologically inert until

photolytically freed. At the same time, fluorescent dyes were loaded into the photoreceptor to allow quantities of free Ca_i^{2+} to be dynamically quantitated. The photoreceptors were then subjected to flash photolysis either directly, or after their LSCs had already been activated by an ordinary flash stimulus (flash stimuli evoking full LSC activation are still so weak that they do not prematurely free caged Ca^{2+}). The results were mixed. Flash photolysis during a preestablished light response greatly facilitated and then immediately inactivated the LSCs. Facilitation could be observed in *trp*$^-$ or La^{3+}-blocked photoreceptors, showing that multiple LSC components were affected. However, flash photolysis alone had no effect on photoreceptors carrying null *ninaE* or *norpA* mutations, even though it might have been expected to bypass IP_3 production and induce depolarization. By using two different cage components, Hardie (1995) was able to induce either 26 ± 15 μM Ca_i^{2+} or 1-2 μM Ca_i^{2+} to appear within the photoreceptor: the former concentration was necessary to induce facilitation during a rising light response, while the latter was sufficient to inactivate the subsequent diminished plateau. Since caged calcium can facilitate LSC activation, it is implausible that it physically fails to reach the LSCs during flash photolysis.

One remaining caveat is that local concentrations of Ca_i^{2+} near an open Dip channel may actually be in the tens of micromolars (Shin *et al.*, 1993; Ranganathan *et al.*, 1994), and that the concentrations estimated for Ca_i^{2+} in the presence of caged compounds may be in error by a factor of 2-3 (Zucker, 1993). This suggests that LSCs might be activated by Ca_i^{2+} alone if much larger amounts of caged calcium were photolytically released. However, Shin *et al.* (1993) were able to activate *Limulus* photoreceptors weakly by buffering them to only 5 μM Ca_i^{2+}. It therefore seems likely that *Limulus* and *Drosophila* photoreceptors differ in this respect, and that Ca_i^{2+} elevation is necessary but not sufficient to activate *Drosophila* LSCs.

Allosteric activation by Dip? In mammals, the ryanodine receptor (a distant paralog of the IP_3 receptor) is positively known to be allosterically regulated in the muscle

sarcoplasmic reticulum by direct contact with a voltage-activated dihydropyridine receptor in the adjacent plasma membrane (Berridge, 1993). The conservation of IP_3 and ryanodine receptors between mammals and *Drosophila* hints that protein partners of these receptors will also be conserved (Takeshima *et al.*, 1994). For some time, IP_3 receptor activation has been known to trigger Ca_0^{2+} influx through I_{CRAC} channels (which have hitherto only been defined electrophysiologically--e.g., mast cell I_{CRAC}; Hoth and Penner, 1993). It is a reasonable speculation that I_{CRAC} channels might be allosterically triggered by IP_3 receptors in a manner analogous to ryanodine and dihydropyridine receptors (Berridge, 1993; Clapham, 1995a, 1995b). In some cases, mammalian I_{CRAC} activation appears to require calcium depletion in the ER lumen; the lumen is presumably invisible to I_{CRAC} save via the IP_3 receptor (Clapham, 1995a). Since Trp and Trpl have trace similarity to dihydropyridine receptors and depend on IP_3 generation, they could actually be *Drosophila* I_{CRAC} homologs triggered directly by Dip (Hardie and Minke, 1992; Phillips *et al.*, 1992). Trp, and perhaps other LSC components, are physically close enough to Dip (20 nm) to be sterically activated by it (Pollock *et al.*, 1995).

Unfortunately, data bearing on this issue are limited and mostly negative. Given the lumen-depletion model for allosteric I_{CRAC} activation, one might expect to be able to activate heterologously expressed Trp and Trpl with thapsigargin--an inhibitor of the ER's calcium pump that deprives the ER of luminal Ca^{2+}. Heterologous Trp is thapsigargin-activated (Vaca *et al.*, 1994), but Trpl is not (Hu and Schilling, 1995). Furthermore, dissociated *Drosophila* photoreceptors treated with thapsigargin do not spontaneously activate, though their Ca_i^{2+} indeed rises (Ranganathan *et al.*, 1994). Instead, their light-responses *weaken*, perhaps because their SRC becomes exhausted of Ca^{2+} (Hardie *et al.*, 1993b). These data do not address the issue of whether Dip allosterically activates LSCs only when it binds IP_3, or whether simultaneous dual triggers (allosteric Dip *and* sharply elevated Ca_i^{2+}) are necessary.

A final speculation. IP_4 might ultimately prove critical to solving the issue of

LSC agonists. In some systems where ER depletion is not sufficient to activate I_{CRAC}s, it has been suggested that they additionally require IP_4 stimulation (Berridge, 1993). All of the data reviewed so far are consistent with a model in which LSCs are triggered by simultaneously rising Ca_i^{2+} and IP_4. One virtue of this model is that it accounts for all of the data: the (probably) minor role of cGMP in *Drosophila* photoreceptors; the necessity of Ca_i^{2+} elevation, per se, to activation; the insufficiency of either Ca_i^{2+} or thapsigargin to excite *Drosophila* photoreceptors; the necessity of NorpA (generating the IP_4 precursor IP_3) to any photoresponse. In this view, Dip's role may be merely to provide an IP_3-induced local elevation of Ca_i^{2+}, with the last step of LSC activation not involving Dip at all. Another virtue of this model is that it should be testable by loading photoreceptors with a mixture of caged calcium and IP_4.

Calcium targets in excitation

Calcium influx is not an end in itself, but a means whereby phototransduction is achieved. For it to serve some purpose, it must activate or adapt the photoreceptor. The issue of activation can be more precisely defined as two problems: does Ca^{2+} influx activate LSCs? and does it promote photoreceptor neurotransmission in any other way besides activating LSCs? Direct LSC activation by Ca^{2+} has already been discussed at length. Three possible non-LSC targets are NorpA, Dip, and Dry. As described above, NorpA activity increases with Ca^{2+} up to 1 μM (Toyoshima *et al.*, 1990; Running Deer *et al.*, 1995), while that of Dip does so up to 0.28 μM (in *Apis*; Baumann and Walz, 1989b). Their parallel stimulation may account for the reduction of photoreceptor latency by prior light-induced Ca^{2+} influx (Hardie *et al.*, 1993b). Ryanodine receptors are activated by much higher Ca_i^{2+} levels than Dip (1-100 μM; Bezprozvanny *et al.*, 1991). Dry might therefore enable a second stage of Ca^{2+} release from the SRC, during a late phase of Ca_i^{2+} elevation that inactivates Dip. Whether other excitatory calcium targets exist besides NorpA, Dip, and Dry is unknown. However, some *rrp* and *non* genes may eventually be

found, upon molecular analysis, to encode Ca^{2+} targets that indirectly promote depolarization or that help start axonal transmission.

Calcium targets in adaptation

To adapt the photoreceptor, elevated Ca_i^{2+} must bind yet more targets. Several have been identified. Most of them appear to inhibit Ca_i^{2+} elevation. One (calmodulin) might both activate and inactivate Trpl. The last (rhodopsin phosphatase) restores rhodopsin to its original state.

Protein kinase C. NorpA is expected both to increase Ca_i^{2+} and to generate diacylglycerol. Jointly, these should activate any protein kinase C (PKC) present in the photoreceptor. Three PKCs are known to exist within *Drosophila* (Schaeffer *et al.*, 1989; Lindsley and Zimm, 1992), but only one (*inaC*) is eye-specific; it was first reported as a retinally transcribed PKC homolog (Schaeffer *et al.*, 1989), and later identified as *inaC* by transgenic rescue (Smith *et al.*, 1991). InaC has 700 residues with 51-53% identity to the bovine PKCs α-γ, and contains motifs typical of classical PKCs (a consensus ATP-binding site near its middle, cysteine-containing Zn^{2+}-fingers near its N-terminus, and an eight-residue psuedosubstrate domain.) Because *inaC* is only 20 kb 5'-ward of another PKC gene (*Pkc1*) and shares *Pkc1*'s transcriptional orientation, *inaC* and *Pkc1* may be divergent duplicates (Schaeffer *et al.*, 1989). InaC is specifically expressed in retinal and ocellal rhabdomeres (Smith *et al.*, 1991); two *inaC* alleles were shown to be either null or nearly so by immunoblotting and DNA sequencing.

inaC phenotypes vary depending on the environment of the photoreceptor and the type of illumination used to stimulate it. Given a brief light flash, an *inaC* photoreceptor in an intact retina depolarizes as swiftly as wild-type, and completes ~50% of repolarization normally. But it then slows its depolarization abruptly and profoundly, and completes it with a noisy, trailing waveform roughly seven-fold slower than wild-type (Ranganathan *et al.*, 1991a; Hardie *et al.*, 1993b). Given a sustained light pulse, *inaC* photoreceptors do

not rapidly (within ms) reach a peak current, partially curtail it, and then stably maintain a diminished current (as in wild-type); instead, they reach a normal peak of current, remain at it for many ms, and slowly fall from the peak to zero current with no intervening plateau (Hardie *et al.*, 1993b).

inaC$^-$ phenotypes are only discernable if extracellular calcium is actually present: in nominally zero-calcium buffer, dissociated *inaC*$^-$ -photoreceptors respond to light flashes or pulses like wild-type (with slow activation, slow inactivation, and complete blurring of the waveform; Ranganathan *et al.*, 1991a). Also, like wild-type, *inaC*$^-$ waveforms evoked by opposite voltages are asymmetrical if Ca_o^{2+} is present, but symmetrical if Ca_o^{2+} is absent (Ranganathan *et al.*, 1991a). These data show that InaC is likely to be a target of elevated Ca_i^{2+} in vivo. However, even the sluggish repolarization of dissociated *inaC*$^-$ photoreceptors is accelerated if their Ca_o^{2+} is raised from 1 mM to 10-20 mM (Ranganathan *et al.*, 1991a; Hardie *et al.*, 1993b). Both this and *inaC*'s partially normal repolarization in an intact retina (Hardie *et al.*, 1993b) are observed with the null allele *inaC*^{P209}: therefore, while *inaC* partially mediates Ca^{2+}-dependent adaptation, other mediators must also exist.

The primary defect of *inaC* was first proposed to be hyperadaptation, because an initial, adapting flash desensitizes *inaC* photoreceptors to light longer than wild-type (Smith *et al.*, 1991). However, as in *trp*, quantitative analysis shows *inaC* actually to be deficient in adaptation (Hardie *et al.*, 1993b). Where wild-type V/log[I] lines shift positively along the log[I] axis (as background light increases over 10^2-fold), *inaC* lines remain immobile. Given yet more background light, *inaC* lines do not adapt, but merely shrink in amplitude along the V axis; *inaC*'s σ remains virtually unchanged in all light intensities. *inaC* facilitation is also faulty: given two light flashes 4.5 s apart, normal photoreceptors respond more quickly to the second flash, while *inaC* photoreceptors are grossly weakened and slowed. Like *trp*, *inaC* permits normal (square-wave) responses to dim light pulses, but abruptly displays a mutant phenotype when challenged with stronger pulses (Minke, 1982;

Hardie *et al.*, 1993b). *inaC*, like *trp*, actually seems to cause response exhaustion.

But, at the level of quantum bumps, *inaC* has an entirely different phenotype from *trp*. *inaC* quantum bumps are not, as in *trp*, normally shaped (Minke *et al.*, 1975). Instead, they look like tiny versions of the waveform seen for an entire flash-stimulated *inaC* photoreceptor: a fast depolarization, 50% of a fast repolarization, but then a great slowing with a noisy tail of current (Hardie *et al.*, 1993b). These tails of current greatly increase the duration of quantum bumps, so that they no longer merely sum linearly to ragged square waves at low light intensities (Hardie, 1991); instead, they form abnormally large parabolic waves of current (Hardie *et al.*, 1993b). This is paradoxical: where the *trp* phenotype can be explained as exhaustion of the photoreceptor's Ca_i^{2+} by inadequate influx, it would seem that *inaC* is actually making the photoreceptor *more* open to Ca_o^{2+} than normal. This impression is correct: measurements of Ca_o^{2+} next to *inaC*$^-$ photoreceptors in vivo show that the light-induced drop in Ca_o^{2+} is two times that of wild-type (Peretz *et al.*, 1994a); and dissociated *inaC* photoreceptors loaded with calcium-dependent fluorescent dyes show three times the normal elevation of Ca_i^{2+} in response to either a flash or a pulse (Peretz *et al.*, 1994a; Ranganathan *et al.*, 1994). These differences vanish if photoreceptors are assayed in calcium-free medium (Peretz *et al.*, 1994a). It is thus clear that the primary defect of *inaC* is a failure to shut off LSCs during the latter half of their deactivation, and that this failure paradoxically floods the photoreceptor with calcium during the light response.

This immediately raises the question of which LSCs are regulated by InaC. The inactivations of both *trp* and *trp inaC* photoreceptors after a light flash are only slightly accelerated by raising Ca_o^{2+} from 1.5 mM to 10.0 mM (Hardie *et al.*, 1993b). The bulk of adaptive Ca_o^{2+} influx should thus be Trp-channeled, even if *trp*$^+$-independent LSCs are hyperactivated by *inaC* mutations. This is supported by Ca_o^{2+} measurements in *inaC* versus *trp inaC* retinas, which show that the excess Ca_o^{2+} influx of *inaC* photoreceptors is mostly blocked by an additional *trp* mutation (Peretz *et al.*, 1994a). Because the reversal

potential of LSCs is unchanged by *inaC* mutations, the excess current of *inaC* quantum bumps is probably carried by normal LSC components (Hardie *et al.*, 1993b). On the other hand, while *trp; inaC* photoreceptors inactivate far more quickly after a flash than *inaC*, they still take twice as long as *trp* photoreceptors (Hardie *et al.*, 1993b). Furthermore, there is a weak but discernable increase of Ca_o^{2+} influx for *trp inaC* versus *trp* photoreceptors (Peretz *et al.*, 1994a). It follows that InaC regulates both Trp and at least one *trp*$^+$-independent LSC component, but that all excess Ca_o^{2+} influx in *inaC* mutants is mediated by deregulated Trp.

A second cause of *inaC*'s excess Ca_i^{2+} becomes evident in Rh[1+4] photoreceptors loaded with calcium-sensitive dye, stimulated by a UV flash, and then probed at length with green light (Ranganathan *et al.*, 1994). Such photoreceptors can be monitored for post-flash currents and Ca_i^{2+} simultaneously: in wild-type, the current reaches baseline 900 times more quickly than Ca_i^{2+} (current τ, 33.7 ± 10.9 ms; Ca_i^{2+} τ, 30.2 ± 4.2 s.) Such prolonged Ca_i^{2+} reduction cannot simply reflect LSC closure, but must also depend on extrusion mechanisms such as ATP-driven pumps or sodium-calcium exchangers (Carafoli, 1991; Philipson and Nicoll, 1993). In *inaC* photoreceptors, Ca_i^{2+} decline is slowed 3.7-fold (Ranganathan *et al.*, 1994). Consequently, InaC must drive Ca_i^{2+} export as well as block its import.

How can *inaC* exhaust photoreceptors by flooding them with Ca_o^{2+}? One possible model is that Dip, like the LSCs, is abnormally active in *inaC* photoreceptors (Hardie *et al.*, 1993b). Such hyperactivity could be achieved either by failure to phosphorylate Dip, or simply by altering the quantity of Ca_i^{2+} (by which Dip must normally be regulated; Baumann and Walz, 1989b). This might then lead the SRC's stored Ca^{2+} to become exhausted, which in turn could silence the photoreceptor. Supporting data come from wild-type and *inaC* photoreceptors soaked in calcium-free solutions for 10'-40' before a light pulse. Wild-type photoreceptors increase their mean response to light from 10 pA (in normal Ca_o^{2+}) to 24 pA-- perhaps because calcium depletion forces Ca_i^{2+} downward from

inhibitory levels that it would normally reach during the photoresponse (Hardie *et al.*, 1993b; Hardie and Minke, 1994a). *inaC* mean responses, on the other hand, are reduced from 38 pA to 3 pA. This striking result is explicable if *inaC* photoreceptors, during their calcium-free bath, leak the SRC's Ca^{2+} through hyperactive Dip and LSCs. Another datum supporting Dip hyperactivity is that *inaC* photoreceptors are abnormally sensitive to very dim light (Hardie *et al.*, 1993b).

At least one *inaC* phenotype does *not* fit existing theory: *inaC* mutations suppress retinal degeneration caused by *rdgB* (Smith *et al.*, 1991). *rdgB* mutations ablate a phosphatidylinositol transfer protein located within the SRC membrane (Vihtelic *et al.*, 1993); their degenerative phenotypes can be induced by a single flash of light (Lindsley and Zimm, 1992). Two other genes can mutate to suppress *rdgB*: *ninaE* (Stark and Sapp, 1987) and *norpA* (Stark *et al.*, 1983). *ninaE* may suppress *rdgB* by merely blunting the photoreceptor, but *norpA*'s mechanism is more controversial. *norpA* has been proposed to suppress *rdgB* by slowing PIP_2 metabolism (Vihtelic *et al.*, 1993), but at least one allele ($norpA^{suII}$) suppresses *rdgB* despite having a very weak phenotype, and *norpA*'s suppression of *rdgB* is allele-specific (Stark *et al.*, 1983; Lindsley and Zimm, 1992). These data suggest that InaC may have an unsuspected role in excitation. They also suggest that screens for enhancers and suppressors of *rdgB* might allow InaC effectors to be genetically identified and ranked in importance (Smith *et al.*, 1991).

InaD. Four other *ina* loci besides *inaC* were identified by Pak (1979) and coworkers on the *Drosophila* autosomes. Given the similarity of their mutant phenotypes to *inaC*, the possibility that they have analogous functions is glaring. At this writing, all but *InaD* remain uncharacterized. $InaD^{P215}$ is the only known mutant allele of *InaD*, which in turn is the only *ina* gene with a semidominant mutant phenotype (Lindsley and Zimm, 1992). *InaD* was cloned by differential hybridization, and found to encode a novel polypeptide of 674 residues specifically expressed in retinal and ocellar rhabdomeres (Shieh and Niemeyer, 1995). InaD has no obvious transmembrane sequences or signal

sequence. 30% of InaD consists of acidic or basic residues (its predicted pI is 8.66), with one remarkable charge cluster of 14 residues solely containing glutamate and lysine; there is also a string of seven G(Q/M)s at around residue 150. Such clusters of biased composition are disproportionately found in regulatory proteins (Brendel *et al.*, 1992). The most striking part of InaD, spaced roughly evenly at its N-terminus and center, are two copies of a 40-residue motif found repeated in diverse proteins: *Drosophila* Discs large (Dlg1), a *Drosophila* hyperplasia suppressor; rat PSD95, found in post-synaptic densities; vertebrate ZO-1, a tight junction component; and human Ros, an epithelial tyrosine kinase suspected to regulate vertebrate development. These proteins have no common characteristics other than being signal transducers specifically localized to limited regions directly underneath the plasma membrane; presumably, in InaD, these motifs bind particular ligands in the highly specialized cytosol in or near rhabdomeres. Finally, InaD contains several possible substrates for cAMP- and cGMP-dependent kinases, tyrosine kinase, and protein kinases C. *InaD*^{P215} alters a methionine to lysine in one of the few hydrophobic stretches of the wild-type InaD sequence. This mutation does not qualitatively diminish the amount of InaD in adult heads, and has a stronger homozygous than heterozygous phenotype. It therefore is formally possible that null mutations might reveal nonvisual functions for this molecule. However, InaD's confinement to photoreceptors suggests it to be purely photosensory.

InaD photoreceptors in physiological Ca_o^{2+} levels (1 mM) respond to a light flash with a normal time to peak and with a roughly normal response amplitude. Like *inaC* photoreceptors, their inactivation is at first normal (during the first ~30% of the descending waveform) but then becomes abnormally slow; the time required for 75% deactivation is 5.9-fold longer in *InaD*^{P215} than wild-type. Like that of *inaC*, this phenotype depends on extracellular calcium: if Ca_o^{2+} is lowered to 0.1 mM, *InaD*^{P215}'s inactivation is only 3.4 times wild-type; in nominally Ca_o^{2+}-free buffer, the ratio drops to 0.9. Also like *inaC*, *InaD*^{P215} increases the sensitivity of photoreceptors to dim light: dark-adapted *InaD*^{P215}

photoreceptors generate a half-maximal depolarization in light intensities 10-fold lower than in wild-type. A more subtle phenotype indicating that *InaD*^{P215} causes abnormal dark-adaptation is that the latency of *InaD*^{P215} photoreceptors (65 ± 3 ms) is detectably longer than wild-type (53 ± 3 ms.) However, not all light adaptation is absent in *InaD*^{P215}. If presented with a light pulse, *InaD*^{P215} photoreceptors do partially repolarize as the pulse continues, albeit more sluggishly than normal.

No existing data rigorously determine the nature of InaD's calcium-dependence. An intriguing hypothesis, advanced by Shieh and Niemeyer (1995), is that InaD is activated by InaC phosphorylation, and in turn inhibits some earlier signalling step (e.g., NorpA activity). The multiple PKC substrates in InaD are consistent with this model, as is phenotypic similarity between *InaD* and *inaC*. However, 14% of InaD consists of acidic residues that might mediate Ca_i^{2+}-activation directly. One test of these competing models might be to express constitutively active InaC in a *InaD*^{P215} background and see if their phenotypes were additive or epistatic. Truncated, deregulated PKCs have been known for some time and could be used to design hypermorphic *inaC* transgenes (Schaeffer *et al.*, 1989).

Gβ subunit. Dissociated *Gβe*^{2} photoreceptors, upon flash stimulation, display normal latency and activation but delayed inactivation (1.9-fold slower than wild-type)--which, if Ca_o^{2+} is removed, worsens (to 9.2-fold slower than wild-type; Dolph *et al.*, 1994). This phenotype, and its intensification by Ca^{2+}-deprivation, are reminiscent of *inaC*; it suggests that the Gβe protein somehow links Ca_i^{2+} elevation to channel inactivation. Furthermore, the *Gβe*^{2} phenotype also appears in photoreceptors at the end of a PDA (at which metarhodopsin is instantly inactivated by orange light), demonstrating that the *Gβe*^{2} defect must lie downstream of rhodopsin (Dolph *et al.*, 1994). Protein kinase C is known to bind protein ligands in the cell membrane or cytoskeleton upon its activation in the cytoplasm ("receptors for activated protein kinase C," or RACKs: Mochly-Rosen *et al.*, 1991). One RACK has been cloned by Ron *et al.* (1992) and found to encode a divergent

Gβ subunit homolog, with ~25% identity to the orthodox mammalian Gβ subunits. This divergence is notable because Gβe is also quite divergent (55% identity) from Gβb, an orthodox Gβ subunit in *Drosophila* (Yarfitz *et al.*, 1991). Gβe may therefore structurally anchor InaC on cell membranes (in or near the rhabdomeres), and this anchoring may be essential for InaC's efficacy.

Dip and LSCs. The modulation of Dip's affinity for IP_3 by Ca^{2+} (Baumann and Walz, 1989), and the probability that Ca_i^{2+} in the vicinity of a Dip channel rises far above Dip's optimum of 0.24 μM Ca_i^{2+} (Ranganathan *et al.*, 1994), implies that light-activation necessarily causes negative feedback upon Dip itself. It is not known how Dip's affinity is actually altered, however; it might be a secondary event dependent on (for instance) InaC, or even more indirect.

On the other hand, the RDC allows LSCs to be studied in a constitutively active state, and this in turn allows their regulation by Ca_i^{2+} to be directly examined. The RDC is inhibited by Ca_o^{2+} influx even in an *inaC*$^-$ background (Hardie and Peretz, 1994b), demonstrating that at least one InaC-independent inhibitory pathway must exist in *Drosophila* photoreceptors. LSCs may be inhibited by direct binding of Ca_i^{2+}, or may encounter it indirectly as a complex with calmodulin.

Calmodulin and its ligands. Calcium can indirectly regulate a great many eukaryotic substrates, including ion channels, by forming a complex with calmodulin (Cohen and Klee, 1988; Saimi and Kung, 1994). Calmodulin can bind up to four Ca^{2+} ions via four EF-hand motifs that interact with distinct intracellular targets (Ohya and Botstein, 1994; Saimi and Kung, 1994). *Drosophila* calmodulin has 148 residues, of which 98% are shared with mammals (Yamanaka *et al.*, 1987). It is transcribed at elevated levels in the adult nervous system and retina (Hanson-Painton *et al.*, 1992); in retinal photoreceptors, calmodulin is heavily concentrated (~0.5 mM) within rhabdomeres (Porter *et al.*, 1993).

Calmodulin has four known or suspected targets in retinal photoreceptors. The first

two are Trp and Trpl; both proteins have 1-2 potential calmodulin-binding sites, which in Trpl's case have been proven real (Phillips *et al.*, 1992). These sites are obvious means whereby direct regulation of the LSCs by elevated Ca_i^{2+} (Hardie and Minke, 1994b) might be at least partially achieved. It is not known whether calmodulin actually causes Trp and Trpl to be activated, inactivated, or both: in Trpl's case, the presence of two binding sites raises the possibility of one being excitatory and one inhibitory.

The third target of calmodulin is NinaC, a photoreceptor-specific unorthodox myosin (Montell and Rubin, 1988). As its "*nina*" tag indicates, *ninaC*'s most obvious phenotype is failure of strong blue light to bleach mutant photoreceptors and induce a PDA (Pak, 1979). Adult *ninaC* photoreceptors are outwardly healthy, but their rhabdomeres are shrunken in size (Matsumoto *et al.*, 1987). In addition, the aqueous interiors of *ninaC* rhabdomeric villi completely lack the actin fibers found in wild-type (Matsumoto *et al.*, 1987), implying that *ninaC* reduces rhodopsin levels (and thus prevents a PDA) by preventing proper ultrastructural assembly of the rhabdomere. However, there are subtle complexities in the *ninaC* phenotype. If raised in darkness, *ninaC* flies have *normally* sized rhabdomeres (Porter *et al.*, 1992). Only if raised with normal illumination do *ninaC* flies have shrunken rhabdomeres, and this phenotype is age-dependent: the rhabdomeres are 80% normal size soon after eclosion, but then completely degenerate over a period of 21 days (Porter *et al.*, 1992). Furthermore, if dark-raised *ninaC* flies are stimulated with two successive light pulses, they show a distinctive ERG phenotype. The first *ninaC* photoreceptor response is *larger* than both wild-type and the second *ninaC* response; in wild-type, both responses are identically sized. *ninaC* shows exceedingly slow repolarization during the first pulse, towards a merely wild-type level. The first *ninaC* response therefore has a jagged-wave rather than a (normal) square-wave appearance. An off-transient (prominent in wild-type) is completely absent in the first *ninaC* response. Finally, repolarization after the first pulse ends is substantially slowed in *ninaC* versus wild-type. However, a *ninaC* response to the second pulse has normal magnitude, a

square-wave pattern, and a visible off transient. These phenotypes can be speculatively characterized as disruption of a process that is normally needed for adaptation on rapid (subsecond) time scales. After the first stimulus, this deficient process is presumably replaced by a slower, NinaC-independent process that makes later responses normal. Since *ninaC* does *not* show the response exhaustion seen in *trp* or *inaC*, it is unlikely to be grossly perturbing Ca_i^{2+}, but might instead disrupt a Ca_i^{2+}-dependent adaptive signal.

Molecular analyses of *ninaC* support this model. *ninaC* was cloned by subtractive hybridization and transgenic rescue; it encodes two NinaC isoforms, generated by alternate mRNA splicing, of 1501 residues (p174) and 1135 residues (p132; Montell and Rubin, 1988). Both isoforms begin identically and share 1081 residues, but have divergent 420-residue and 54-residue C-termini. Strikingly, the common NinaC sequence contains an N-terminal serine/threonine protein kinase domain fused to a C-terminal myosin head domain. The kinase domain has 266 residues with 24-26% identity to other kinases (e.g., Fps and Raf); out of 16 key residues found in many kinases, NinaC conserves 15. The myosin domain has 725 residues with 24-27% identity to the head domains of mammalian myosins I and II. It is less well conserved than in most members of the myosin superfamily, indicating that NinaC either represents a very divergent myosin family or is under weaker functional constraints than most myosins (Goodson, 1994).

p174 and p132 differ in their subcellular localization: while p174 is located within rhabdomeres, p132 is in the cytoplasm, with perhaps more p132 near the rhabdomeres than elsewhere (Hicks and Williams, 1992; Porter *et al.*, 1992). Since p172 and p132 only differ in their tail sequences, those must dictate localization. While p132's 54-residue tail has no similarities, that of p174 resembles the tail of myosin I: it is proline-rich, with a single run of seven consecutive prolines; and 30% of it has asparagine, glutamine, or arginine residues. Brush border myosin I requires its tail to bind acidic phospholipids with high affinity (K_D = 100-400 nM; Hayden *et al.*, 1990), so NinaC's tail may have this capacity as well. The N-terminal half of p172's tail binds calmodulin in vitro; this region

contains two IQ motifs, associated with calmodulin-binding in diverse myosins (Cheney and Mooseker, 1992). The p174 and p132 isoforms also differ in their activity within photoreceptors. Partial *ninaC* mutants, expressing only p132, are phenotypically indistinguishable from null *ninaC* mutants (Montell and Rubin, 1988; Porter *et al.*, 1992); conversely, transgenes encoding p172 completely rescue the *ninaC* phenotype (Porter *et al.*, 1992).

ninaC phenotypes are genetically and physically separable by targeted mutations in domains of p172, using p172 transgenes in a null *ninaC* genetic background (Porter and Montell, 1993; Porter *et al.*, 1993). Deletion of only the kinase domain causes an ERG phenotype that is neither wild-type, nor as severe as null *ninaC* (Porter and Montell, 1993); it shows a transient current dropping to a lessened plateau (which null *ninaC* does not), but the transient is greatly longer in duration than wild-type. Kinase-deficient p172 still prevents rhabdomeric degeneration, though. Deletion of the myosin domain causes a null *ninaC* phenotype, perhaps because myosin-deficient p172 fails to localize exclusively in rhabdomeres (Porter and Montell, 1993). However, two point mutations of the myosin domain have more specific phenotypes: they confer temperature-sensitive degeneration while having no ERG defect at all. These alleles also show mislocalized p172 at restrictive temperature. Finally, deletion of p172's calmodulin-binding site (Porter *et al.*, 1993) has several effects. It mislocalizes calmodulin away from rhabdomeres and into the extracellular space between them, perhaps through rhabdomere shedding. This is not due to calmodulin-dependence of p172's motility, because p172 remains in rhabdomeres. Calmodulin-deficient p172 also continues to prevent rhabdomeric degeneration. However, calmodulin-deficient p172 confers a null *ninaC* ERG phenotype. These data demonstrate that p172 has at least three independent functions: structural maintenance of the rhabdomere, which requires p172 to drive itself into the rhabdomere, and might involve bridging actin filaments and phospholipids; a specific inhibitory task in phototransduction, which requires p172's kinase activity within the rhabdomere; and a second inhibitory task,

which requires p172 to carry calmodulin with it into the rhabdomere. These two inhibitory tasks are likely to be parallel to the action of InaC; at least the latter is likely to depend on elevated Ca_i^{2+}.

Entirely independent work, on the classical biochemistry of *Drosophila*'s light response, has shown that calmodulin activates a protein kinase (CaMK) in photoreceptors (Matsumoto *et al.*, 1994). This Ca^{2+}/calmodulin-dependent protein kinase (CaMK) mediates the fastest known light-dependent phophorylation event in *Drosophila* photoreceptors (Matsumoto *et al.*, 1994). Specifically, CaMK phosphorylates Arr2 at a serine residue near its C-terminus (S_{366}), in 400 ± 50 ms after a light flash. Arr1 is phosphorylated later, presumably by the same kinase. Since Arr2 phosphorylation occurs in *inaC* null mutants, it cannot be due to InaC; and, given Arr1 and Arr2's location in the rhabdomeres (Dolph *et al.*, 1993), CaMK must also exist there. CaMK has not yet been purified, but might be identical to the kinase domain of p172. Were this true, it would imply that calmodulin-deficient p172 has a defective ERG both because of some (unknown) calmodulin target in the rhabdomere, and because the p172 kinase domain is allosterically dependent on p172-bound calmodulin for its activity. Alternatively, there may be multiple CaMK proteins in the rhabdomere: a faint 55 kD P^{32}-labelled band observed in active preparations of CaMK might represent autophosphorylation (Matsumoto *et al.*, 1994).

The primary role of Arr2 is to bind and silence metarhodopsin: because metarhodopsin persists far longer than the stimulus evoking it, Arr2 binding is essential for the temporal resolution of phototransduction (Byk *et al.*, 1993; Dolph *et al.*, 1994; Ranganathan and Stevens, 1995). S_{366} is in a C-terminal region of Arr2 that is dispensable for its basic function of quenching metarhodopsin (Dolph *et al.* 1993). However, an initial light stimulus of *Limulus* photoreceptors accelerates their rhodopsin inactivation during a subsequent stimulus (Richard and Lisman, 1992). Since Arr2 binding appears to be the rate-limiting event in *Drosophila* rhodopsin inactivation (Plangger *et al.*, 1994;

Ranganathan and Stevens, 1995), light-induced CaMK phosphorylation of S_{366} may mediate light-facilitated rhodopsin inactivation by increasing the rate of Arr2 binding.

Rhodopsin dephosphatase. Newly eclosed *rdgC* mutants display a normal ERG/PDA, but over 5-8 days of illumination their photoreceptors degenerate (Steele and O'Tousa, 1990). This phenotype is dependent on rhodopsin, since it is suppressed by either carotene deprivation or *ninaE* mutations; however, it is unsuppressed by *norpA* mutations that greatly reduce the ERG (Steele and O'Tousa, 1990; Lindsley and Zimm, 1992). The normal *rdgC* ERG demonstrates that *rdgC* does not impair Dgq or Gβe (Dolph *et al.*, 1994; Lee *et al.*, 1994); on purely genetic grounds, Steele and O'Tousa (1990) were thus able to deduce that *rdgC* impaired a second biochemical pathway that was downstream of rhodopsin but separate from Dgq/Gβe and NorpA.

rdgC was cloned by chromosome walking and transgenic rescue (Steele *et al.*, 1992). It encodes a 661-residue protein with two domains. The first, in residues 153-393, is 30-31% identical to type 1, 2A, and 2B serine/threonine phosphatases; it conserves all 17 residues known to be critical for enzymatic function. The second consists of 3-5 EF hands spanning residues 445-598; as in calmodulin/effector complexes, the EF hands are expected to regulate RdgC activity by Ca^{2+} binding. RdgC localizes to the retina, ocelli, and mushroom bodies of the central brain (Steele *et al.*, 1992). Since mushroom bodies are crucial for *Drosophila* memory, *rdgC* mutations may impair learning as well as photoreceptors (Davis, 1993). *Drosophila* rhodopsin kinase is activated merely by the presence of metarhodopsin (Doza *et al.*, 1992; Byk *et al.*, 1993). Rhodopsin dephosphorylation in *Drosophila* head membrane extracts requires Ca^{2+}, does *not* require calmodulin, is prevented by EGTA, and fails if the head genotype is *rdgC* (Byk *et al.*, 1993). RdgC is thus very probably a Ca^{2+}-activated rhodopsin dephosphatase. Its mutant phenotype is likely to arise from cumulative phosphorylation of rhodopsin, which might destabilize rhodopsin and gradually deplete it from the rhabdomeres (Selinger *et al.*, 1993). Since *norpA* alleles that completely silence phototransduction also cause a light-dependent

degeneration phenotype (Meyertholen *et al.*, 1987), it is plausible that the Ca_i^{2+} levels required for RdgC activity are only achieved by LSC activation during the photoresponse, and that *norpA* degeneration arises from inert RdgC. Ca_i^{2+} therefore participates in photosensory events acting over very long time scales.

Calcium extrusion

The delayed decrease of post-stimulus Ca_i^{2+} in *inaC* photoreceptors demonstrates that one target of InaC must be calcium exporters. These are logically the last step of calcium flux in *Drosophila* phototransduction. As such, they are poorly understood. Most of what might be true in *Drosophila* must presently be guessed at, by analogy with other systems where calcium extrusion is better studied.

In all eukaryotic cells, excess Ca_i^{2+} is removed through three pathways: calcium pumps in the plasma membrane; pumps in the ER; and sodium-calcium exchangers in the plasma membrane (Carafoli, 1987; Carafoli, 1991; Philipson and Nicoll, 1993; Clapham, 1995a). There are also sodium-calcium exchangers in the inner mitochondrial membrane (Philipson and Nicoll, 1993): while they can regulate oxidative activity by varying matrix calcium (Cox and Matlib, 1993), they are not otherwise thought to play a major role in calcium homeostasis (Carafoli, 1987).

Calcium pumps. These are integral membrane proteins of ~1000 residues, driven by ATP hydrolysis, that have a high affinity for Ca^{2+} ($K_m \approx 0.2$ μM; Carafoli, 1991) but a relatively low rate of ionic extrusion (0.5 nmol Ca^{2+} ions/[mg of pump protein·second]; Carafoli, 1987). Strictly speaking, they are not Ca^{2+} pumps, but ATP-driven $Ca^{2+}/2H^+$ antiporters (Carafoli, 1987). Calcium pumps comprise a protein superfamily, with two major subdivisions: those localized to the plasma membrane, and those in sarcoplasmic reticulum or the ER (Fagan and Saier, 1994). Calcium pumps are found in *Saccharomyces cerevisiae*, showing that they are eukaryotic in scope (Antebi and Fink, 1992; Cunningham and Fink, 1994).

One calcium pump gene of the ER class (*Ca-p*) has been isolated from *Drosophila*. *Ca-p* was isolated by degenerate PCR (Váradi *et al.*, 1989) and found to encode a 1003-residue protein with 67-71% identity to mammalian ER pumps (Magyar and Váradi, 1990). It has a single 4.5 kb transcript expressed most conspicuously in adults; Váradi *et al.* (1989) detected no transcripts before the adult stage, but this may only reflect low levels of expression. Given failure to detect multiple ER pump homologs by PCR, *Ca-p* is likely to encode the pump found in the *Drosophila* SRC. Since mammalian plasma pumps are only ~30% identical to ER pumps (instances for comparison: Lytton and MacLennan, 1988; Verma *et al.*, 1988), one would also expect a *Drosophila* plasma pump to exist; none has yet been reported.

Ranganathan *et al.* (1994) blocked the SRC pump of *Drosophila* photoreceptors with thapsigargin, and found that doing this both raised Ca_i^{2+} and diminished subsequent responses to test flashes. They interpreted this to be adaptation of the photoreceptor by increased Ca_i^{2+} in the region of the SRC/rhabdomere. This interpretation is debatable. Previous interpretations of the *inaC* phenotype as one of hyperadaptation, on exactly this basis (of diminished responses over time) have since been proven actually to represent exhaustion of the photoreceptor's SRC Ca^{2+}, with a complete *failure* of adaptation (Hardie *et al.*, 1993b). Furthermore, Ranganathan *et al.* (1994) did not observe adaptation in response to an alternative treatment (removing extracellular Na^+) that also increased Ca_i^{2+} in the photoreceptor. This is inconsistent with the hypothesis that microscopically quantifiable increases of Ca_i^{2+} can reliably modulate phototransduction. On the other hand, the data of Ranganathan *et al.* (1994) are entirely consistent with the SRC calcium pump maintaining SRC Ca^{2+}, and subsequent Ca^{2+} release from the SRC being necessary to activate LSCs. In this view, interrupting SRC pump function should immediately blunt phototransduction, and ultimately silence it entirely. Unfortunately, there seem to have been no experiments by any investigators using specific inhibitors of the plasma membrane calcium pump, so its role in phototransduction is entirely unknown.

Sodium-calcium exchangers. These have been recently reviewed by Philipson and Nicoll (1993). They have a lower affinity for Ca^{2+} ($K_m \approx 20$ μM; Philipson and Nicoll, 1993) but a much higher quantitative capacity for extrusion (~40 μmol Ca^{2+} ions/[mg of exchanger protein·second]; Hilgemann *et al.*, 1991) than calcium pumps. It is accordingly thought that, where the two exporters coexist, sodium-calcium exchangers act in the initial bulk phase of calcium extrusion, while calcium pumps act later to scavenge remaining Ca_i^{2+} and drive it down to nanomolar levels (Carafoli, 1987). However, the stoichiometry with which all known sodium-calcium exchangers act (either $3Na^+/1Ca^{2+}$ or, more rarely, $4Na^+/1Ca^{2+},1K^+$) is thermodynamically capable of itself forcing a cell down to low resting levels (Carafoli, 1987; Philipson and Nicoll, 1993). Indeed, in some tissues, sodium-calcium exchangers appear to actually be the only significant extrusion mechanism (e.g., mammalian heart muscle and rod photoreceptor cells; Philipson and Nicoll, 1993). Sodium-calcium exchangers are powered by excess extracellular Na^+ ions, which are in turn generated by the ATP-driven $3Na^+/2K^+$ pumps found in all eukaryotic cells.

Sodium-calcium exchange has been shown to exist in *Drosophila* photoreceptors by two experiments. First, Ranganathan *et al.* (1994) placed dissociated Rh[1+4] photoreceptors in Na^+-free extracellular buffer, subjected them to a series of flash stimuli, and then tested them for Ca_i^{2+} elevation and adaptation. With the exception of mitochondrial sodium-calcium exchangers (Li *et al.*, 1992), no known exchanger can trade Ca_i^{2+} for any monovalent cation other than Na^+; it was thus expected that Na^+ replacement would selectively block sodium-calcium exchange while leaving other processes (e.g., calcium pumping) intact. Ranganathan *et al.* (1994) found that, without extracellular Na^+, Ca_i^{2+} no longer returned to resting levels after strong flash stimuli, but instead increased with successive flash stimuli in a strikingly stepwise fashion. Yet this increase neither facilitated nor inhibited the response of photoreceptors to small flash stimuli. Therefore, *Drosophila* photoreceptors have a sodium-calcium exchanger; it is constantly needed to

keep overall levels of Ca_i^{2+} low; but inhibiting the exchanger does not immediately perturb phototransduction. This is consistent with a model for phototransduction in which only large changes in Ca_i^{2+} within narrowly limited microdomains (e.g., the SRC/rhabdomere gap) control signalling (Ranganathan *et al.*, 1994), while the bulk of the photoreceptor soma rapidly absorbs unextruded Ca_i^{2+} and muffles it. This last point is consistent with observations in both mammalian and invertebrate cells that suggest that most of the Ca^{2+} entering an electrically excited cell (e.g., a photoreceptor) is neither extruded nor allowed to remain free in the cytosol, but is instead buffered by intracellular protein ligands (Carafoli, 1987; O'Day and Gray-Keller, 1989; Peretz *et al.*, 1994a).

While the flash-release experiment of caged Ca^{2+} by Hardie (1995) was directly aimed at testing the excitatory role of Ca_i^{2+}, it had the indirect effect of revealing a novel inward current arising on flash photolysis. The current could not be blocked by depolarizing the photoreceptor to +80 mV, but halted at once if extracellullar Na^+ was replaced by Li^+. These characteristics are consistent with the properties of sodium-calcium exchangers, which are invariably electrogenic (with either $3Na^+/1Ca^{2+}$ or $4Na^+/1Ca^{2+},1K^+$ exchange), and which are expected to generate inward flows of Na^+-borne current if suddenly confronted with an instant elevation of Ca_i^{2+} to ~20 μM (Hardie, 1995). The quantity of this current (~18 pF/sec·cm^2) was very close to that observed for sodium-calcium exchange in *Limulus* (~16 pF/sec·cm^2; O'Day and Gray-Keller, 1989). Because the *Drosophila* photoreceptor's exchanger is unaffected by replacing the photoreceptor's internal K^+ with Cs^+ (Hardie, 1995), it is likely to fall into the $3Na^+/1Ca^{2+}$ class--in contrast to mammalian photoreceptors, where the $4Na^+/1Ca^{2+},1K^+$ class is used (Kaupp and Koch, 1992; Philipson and Nicoll, 1993).

The actual role of sodium-calcium exchange in *Drosophila* photoreceptors is still unclear. In dissociated photoreceptors, alterations in exchange do not have the prompt effect on phototransduction that altered SRC pumping has (Ranganathan *et al.*, 1994). On the other hand, the time scale examined in dissociated photoreceptors is quite short (never

more than 20 min; Hardie and Minke, 1994a), making prolonged examination of subtle modulations difficult (e.g., *inaC* adaptation; Hardie *et al.*, 1993b). In dissociated *Limulus* photoreceptors--which do not manifest run-down current, and can therefore be studied at length--inhibited sodium-calcium exchange has several photosensory effects, including desensitization of light-adapted photoreceptors, abnormally large desensitizations in response to light stimuli, and diminished readaptation of photoreceptors to darkness (O'Day *et al.*, 1991). It is thus possible that pumps and exchangers have a division of labor, in which the former govern rapid adaptive photoresponses, while the latter control chronic ones. Since an organism must both respond to brief stimuli and keep its photoreceptors in working order for longer than 20 min, both levels of adaptation are crucial.

Sodium-calcium exchangers have an ability, not shared by pumps, to reverse the direction of their calcium flow in response to transient changes in the prevailing sodium and voltage gradients. This ability is thought to be actively exploited in some mammalian cell types (e.g., neutrophils; Simchowitz *et al.*, 1990). Hardie and Minke (1992) observed that *Drosophila* photoreceptors, when deprived of external sodium and presented with even small amounts of extracellular calcium, irreversibly flooded with Ca_i^{2+}: plainly, photoreceptors have a substantial potential for reverse exchange. This reverse exchange has a probable role in mutant *Drosophila* and a possible one in wild-type. In *trp* photoreceptors, where LSC-mediated Ca^{2+} influx is deeply crippled, it has long been known that the photoresponse is somehow regained after 60 seconds of incubation in dark buffer, despite initial exhaustion of the photoreceptor (Cosens and Manning, 1969; Minke, 1982). One means whereby the slow rescuscitation of *trp* photoreceptors might occur is through reverse sodium-calcium exchange, followed by Ca_i^{2+} pumping into the SRC. While wild-type photoreceptors do not need an ersatz Trp channel, the hypersensitivity to dim light in *inaC* and *InaD* photoreceptors suggests that even dark-adapted $inaC^+$ $InaD^+$ photoreceptors maintain nonzero, basal light-adaptation (Hardie *et al.*, 1993b; Shieh and

Niemeyer, 1995). Given the centrality of Ca_i^{2+} to adaptation, basal dark adapation may entail keeping Ca_i^{2+} at a moderate concentration (~150 nM; Hochstrate and Juse, 1989) capable of slightly triggering InaC and calmodulin. Earlier, it was suggested that this might be achieved by spatially limited Ca^{2+} leakage through Trpl. It might also be achieved by the thermodynamic properties of sodium-calcium exchangers.

Regulation. How are either pumps or exchangers likely to be regulated by InaC? There is no good answer beyond the obvious, handwaving answer that they may be PKC targets in some way, as the LSCs seem to be. Calcium pumps are directly activated by calmodulin (Carafoli, 1991), but may be indirectly regulated by PKC as well (Carafoli, 1994). PKC regulation of exchangers has not been extensively studied (Philipson and Nicoll, 1993). InaC-independent means of regulating calcium extrusion are equally speculative. In the case of mammalian $3Na^+/1Ca^{2+}$ exchangers, it is positively known that the exchanger itself is regulated by cytoplasmic Ca^{2+} and Na^+ via an intracellular protein domain (Matsuoka *et al.*, 1993). It is also known that the exchanger may have a low-affinity calmodulin-binding site as well (Li *et al.*, 1991). Understanding the regulation of Ca^{2+} extrusion and its specific photosensory consequences will require a full characterization of Ca_i^{2+} exporters in the photoreceptor.

Future prospects

Many visual genes, found in mutant screens over the last two decades, remain uncloned (Lindsley and Zimm, 1992). Nor is there evidence that phototransduction is genetically saturated, since many loci have only one mutant allele (e.g., *InaD*). Saturation mutageneses and cloning are the obvious remedies; there are allusions to such efforts by Wu *et al.* (1995) and Pak (1991), so one may hope that full reports are forthcoming. Suppressor-enhancer screens are also underexploited. *rdgB* and *rdgC* (for instance) are suppressible by nonallelic mutations, yet systematic modifier hunts have only begun recently (Colley *et al.*, 1995; Kumar and O'Tousa, 1995). Full allelic spectra have not

been generated for most known visual genes. Screening for 10-100 alleles of a single gene identifies crucial residues in vivo, and is infeasible in more complex metazoa. Systematic mutageneses of *ninaE*/Rh1 (Colley *et al.*, 1995; Kumar and Pak, 1995) and NinaA (Ondek *et al.*, 1992) have shown the power of such screens, and should encourage others.

New techniques exist to assay protein domains for binding of suspected ligands, or to screen cDNA libraries with them for novel ligands (Phizicky and Fields, 1995). These methods could be fruitfully employed upon numerous proteins and motifs in *Drosophila* phototransduction (e.g., Gβe, Dip's cytoplasmic domain, the ankyrin repeats of Trp and Trpl, the Trp octapeptide repeat, InaC, and InaD). Heterologous expression has only begun to be exploited (with *trp*, *trpl*, and *DmCNGC*), but could be extensively used to verify the function of membrane proteins. Low-stringency hybridization, differential hybridization, and degenerate PCR have yielded many *Drosophila* genes that appear photosensory, but lack mutations demonstrating their actual function. Dominant mutant transgenes (Lee *et al.*, 1994) and immunoscreening (Dolph *et al.*, 1993; Dolph *et al.*, 1994) have provided such mutations in several cases; local transposition of P elements (Tower *et al.*, 1993; Zhang and Spradling, 1993) and saturation of the *Drosophila* genome with P insertions (Berkeley Drosophila Genome Project, pers. comm.) should facilitate more reverse genetics.

A central unsettled issue is the identity of LSC agonists. Solving it is likely to require developing patch-clamps for *Drosophila* LSCs and replicating experiments already performed in *Limulus* (Bacigalupo *et al.*, 1991; Shin *et al.*, 1993). Modifier screens and protein interaction assays should refine electrophysiological analyses, by winnowing out actual from merely hypothetical interactions between LSC components and ligands. The answers will be of profound interest, since they are likely to provide a general paradigm for the broader, and also unsettled issue of IP_3-induced Ca_o^{2+} influx in metazoan cells (Berridge, 1993; Clapham, 1995a, 1995b).

One equally unaddressed--and much less fashionable--question is the peculiarity of

Drosophila phototransduction. Is it a phylum-specific pathway? Is it, instead, more loosely confined to some group of "invertebrates" (e.g., phyla closely allied to arthropods)? Or, in contrast, is the vertebrate pathway an abbreviated derivative of a ubiquitous IP_3-regulated visual pathway? Evidence bearing on this is sparse but intriguing. Rhodopsin and arrestin mutations cause similar phenotypes in both *D. melanogaster* and *Homo sapiens* (Dolph *et al.*, 1993; Nathans, 1994; Colley *et al.*, 1995; Fuchs *et al.*, 1995; Kurada and O'Tousa, 1995). NinaA and NorpA homologs exist in the mammalian retina (Ferreira *et al.*, 1993; Ferreira and Pak, 1994; Ferreira *et al.*, 1995). Other *Drosophila* molecules (e.g., NinaC) currently have no close relatives (Goodson, 1994), but may in due course be found to have orthologs expressed in the mammalian retina. Genes promoting the determination and differentiation of *Drosophila* photoreceptors (e.g., *eyeless*, Halder *et al.*, 1995; *glass*, Sheshberadaran and Takahashi, 1994; and *sine oculis*, cited in Zuker, 1994) seem to have functional homologs in vertebrates, hinting that their target genes are likewise conserved. Outside of arthropods and vertebrates, little is known of phototranduction in most metazoan phyla (except, partially, in molluscs: Werner *et al.*, 1992; Gomez and Nasi, 1994). Such studies are needed to chart the phylogeny of phototransduction pathways.

More pragmatically, identifying photosensory molecules conserved between *Drosophila* and human beings defines candidates for new visual disease genes (Collins, 1995). Analysis of these genes can proceed more rapidly in *Drosophila* than in mammals, and can swiftly clarify the basis of a human ailment: this has already been done for retinitis pigmentosa and stationary night blindness (Nathans, 1994; Fuchs *et al.*, 1995), whose molecular defects have been recapitulated and characterized in *Drosophila* (Colley *et al.*, 1995; Kurada and O'Tousa, 1995; Ranganathan and Stevens, 1995). Finally, *Drosophila* photoreceptors afford a genetically malleable tissue in which defects of calcium homeostasis implicated in human disease can be characterized (Clapham, 1993; Brown, 1995; Hoffmann *et al.*, 1995).

Table 1. Known or suspected genes of *Drosophila* phototransduction. This briefly lists the names, products, and phenotypes of genes shown in Figure 1, described in this review, or (in some cases) merely alluded to in this review. Most genes are detailed and referenced in the main text; for some genes, a recent reference is included with its product description. For most genes listed here, more detailed descriptions are given by Lindsley and Zimm (1992).

Table 1:

Category	Gene	Product	Mutant phenotypes
Rhodopsins			
	ninaE/Rh1	Blue/UV-sensitive rhodopsin expressed in R1-R6 photoreceptors and Bolwig's organ	Blind R1-6 photoreceptors; "neither inactivation nor afterpotential" (*nina*) ERG; slow photoreceptor degeneration
	Rh2	Blue/UV-sensitive rhodopsin expressed in ocelli	---
	Rh3	UV-sensitive rhodopsin expressed in some R7 and R8 receptors	---
	Rh4	UV-sensitive rhodopsin expressed in some R7 and R8 receptors	---
Rhodopsin inhibitors			
	arr1	Arrestin 1: minor photoreceptor-specific metarhodopin-binding protein	Itself phenotypically normal, but enhances $arr2^-$ phenotype
	arr2	Arrestin 2: major photoreceptor-specific metarhodopin-binding protein	Delayed inactivation after light pulses; light-dependent photoreceptor degeneration
	RhK	Rhodopsin-specific kinase (Doza *et al.*, 1992)	---
Other genes perhaps regulating rhodopsin			
	ninaF-ninaJ	Unknown (Pak, 1991)	*nina* ERG

Table 1 (cont.):

Category	Gene	Product	Mutant phenotypes
Rhodopsin-specific ancillary proteins			
	ninaA	Proline isomerase required for the biosynthesis of Rh1 (Baker *et al.*, 1994)	Moderate *nina* ERG; reduced levels of mature rhodopsin per photoreceptor
	ninaB and *ninaD*	Unknown proteins required to generate the Rh1 chromophore 3-hydroxyretinal (Pak, 1979)	Resemble *ninaA*
Signal transduction			
	dgq	Photoreceptor-specific $G_{q\alpha}$ subunit	Artificial transgenic dominant mutations grossly desensitize photoreceptors and induce *rdgB*-dependent degeneration in dark
	Gβe	Photoreceptor-specific Gβ subunit	Defective photoreceptor excitation and adaptation
	norpA	Phosopholipase C-β4, expressed in photoreceptors and certain other tissues	Total blindness; photoreceptor degeneration
Lipid metabolism, known			
	rdgA	Photoreceptor-specific diacylglycerol kinase (DGK; Masai *et al.*, 1993)	Retinal degeneration, *independent* of light
	Dgk1	Broadly expressed DGK; might partially overlap *rdgA* function in photoreceptors (Masai *et al.*, 1992)	---

Table 1 (cont.):

Category	Gene	Product	Mutant phenotypes
	cds	Photoreceptor-specific CDP-diglyceride synthase (Wu *et al.*, 1995)	Reduced ERG and light-dependent retinal degeneration
	rdgB	Membrane-bound PI transport protein, activated by rhodopsin, Dgq, and InaC	Light-dependent retinal degeneration
Lipid metabolism, inferred from other organisms			
	[PIS]	Phosphatidylinositol synthase (Kent, 1995)	---
	[PIK]	Phosphatidylinositol 4-kinase (Kent, 1995)	---
	[PIPK]	Phosphatidylinositol-4-phosphate 5-kinase (Kent, 1995)	---
Ca^{2+} channels of the SRC			
	dip	IP_3 receptor	---
	dry	ryanodine receptor	---
Light-stimulated channel components (actual or potential)			
	trp	Novel cation (e.g. Ca^{2+}) channel with trace similarity to dihydryopyridine receptors; triggered by thapsigargin (and perhaps by $G_{q\alpha}$)	Normal responses to weak or transient light; failure to sustain responses to strong or sustained light

Table 1 (cont.):

Category	Gene	Product	Mutant phenotypes
	trpl	*trp* homolog; nonselective cation channel activated by $G_{q\alpha}$ but not thapsigargin	---
	DmCNGC	cGMP-gated channel with strong Ca^{2+} selectivity	---
Other genes that may encode or regulate ion channels			
	slrp	Unknown (Pak, 1975; Lindsley and Zimm, 1992)	Delayed currents in ERG; hypoactivity
	hrp	Unknown (Ranganathan *et al.*, 1991b)	Hyperpolarizing ERG (reversed polarity)
	*sudp**	Unknown (Ranganathan *et al.*, 1991b)	Superdepolarizing ERG (abnormally large amplitude)
cGMP signalling			
	Dgcα1	Guanylate cyclase α subunit, expressed in photoreceptors and other tissues	---
Excitatory Ca^{2+} targets?			
	rrpA-rrpD	Unknown (Ranganathan *et al.*, 1991b)	Reduced ERG

Table 1 (cont.):

Category	Gene	Product	Mutant phenotypes
	nonC, ~30 other *non* genes, and *ort*	Unknown (Ranganathan et al., 1991b; Pak, 1979, 1991; Lindsley and Zimm, 1992)	Failure of lamina to fire, manifested by a "no on transient" ERG; could represent either a failure of excitation or of neurotransmission
Inhibitory Ca^{2+} targets			
	inaC	Photoreceptor-specific protein kinase C	Loss of all inhibitory and adaptive responses to light
	InaD	Novel protein, with duplicated motifs thought to act in signal transduction	Resembles *inaC*
	inaA, *inaB* and *inaE*	Unknown (Pak 1979; Ranganathan *et al.*, 1991b)	Resemble *inaC*
	Calmodulin	Nearly invariant metazoan calmodulin	---
	ninaC	Complex unorthodox myosin with serine-threonine kinase, myosin motor, calmodulin-binding, and tail domains	Multiple and genetically seperable phenotypes: two distinct defects in adaptation, and retinal degeneration
	rdgC	Ca^{2+}-activated rhodopsin phosphatase	Light-dependent retinal degeneration
Ca^{2+} exporters, inferred to exist by comparison to other organisms			
	Ca-p	ATP-driven $Ca^{2+}/2H^{+}$ antiporter, ER variety	---

Table 1 (cont.):

Category	Gene	Product	Mutant phenotypes
	[Ca pump]	ATP-driven $Ca^{2+}/2H^{+}$ antiporter, plasma-membrane variety	---
	[Na-Ca exch.]	Sodium-calcium exchanger	---
Neurotransmission			
	ebony	β-alanyl-dopamine synthase? (Lindsley and Zimm, 1992)	Reduced or absent on- and off-transients in ERG; abnormally dark body pigment
	tan	β-alanyl-dopamine hydrolase? (Lindsley and Zimm, 1992)	Reduced or absent on- and off-transients in ERG; abnormally light (tan) body pigment
	nonA/diss	RNA-binding protein (Lindsley and Zimm, 1992; Stanewsky *et al.*, 1993)	Strong mutations are semilethal; some weak mutations (*nonA*) lack on- and off-transients in ERG; other weak mutations (*diss*) cause dissonant courtship song
	hdc	Histidine decarboxylase (Burg *et al.*, 1993)	Absent on- and off-transients in ERG; photoreceptors lack histamine neurotransmitter
	nonC, ~30 other *non* genes, and *ort*	[See above]	

*"*sdp*", the abbreviation used by Ranganathan *et al.* (1991), actually belongs to *sandpaper* (Lindsley and Zimm, 1992).

Figure 1. Diagram of *Drosophila* phototransduction. This summarizes the biochemical and regulatory events reviewed in the main text. Gene and protein symbols are explained in Table 1. Pointed arrows denote biochemical changes. Lines ending in "+" denote stimulation of a protein by another molecule (either another protein, or a metabolite). Lines ending in "-" denote inhibition. Suspected but uncertain interactions are shown with shaded rather than solid black lines. Intra- and extra-cellular membranes are marked as such, and shown as shaded rectangular barriers. Transmembrane channels are shown as clear boxes in the membranes. Some biochemical events (e.g., "Photoreceptor excitation") are summarized as a single node in the diagram out of both brevity and ignorance. The following symbols denote the following protein intermediates or small molecules: "R," resting active rhodopsin; "M*," activated metarhodopsin; "Arr," arrestin; "M+Arr," metarhodopsin inactivated by bound arrestin; "M-P_i," phosphorylated metarhodopsin (sometimes bound to arrestin); "R-P_i," phosphorylated rhodopsin; "PIP_2," phosphatidylinositol (4,5)bisphosphate; "IP_3," inositol (1,4,5)trisphosphate; "DAG," diacylglycerol; "PA," phosphatidic acid; "CDP-DG," CDP-diglyceride; "PI," phosphatidylinositol; "PIP," phosphatidylinositol 4-phosphate.

Figure 1:

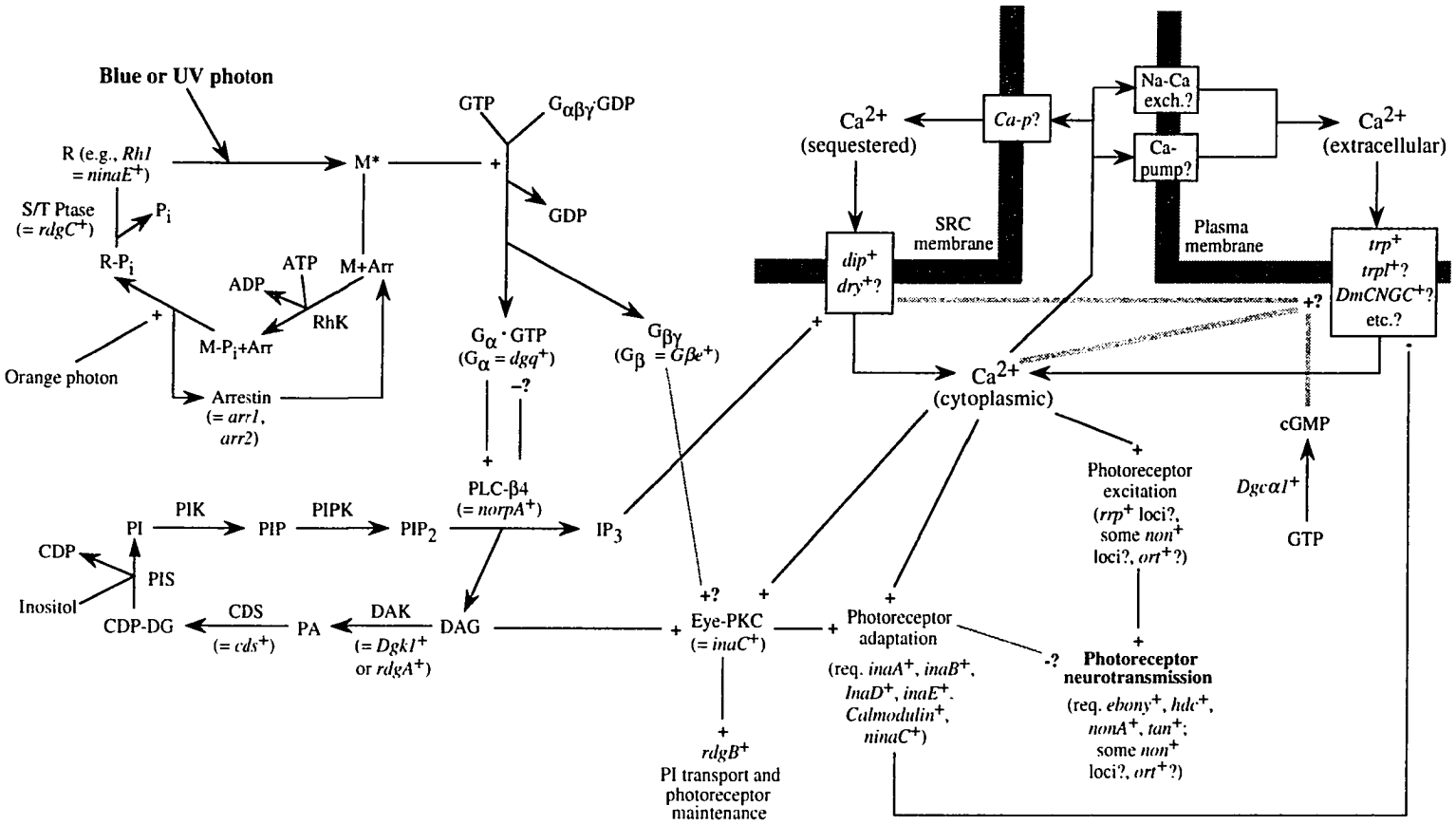
Blue or UV photon
R (e.g., Rh1 = ninaE+)
M*
GTP
Gαβγ·GDP
GDP
S/T Ptase (= rdgC+)
Pi
R-Pi
ATP
ADP
RhK
M+Arr
M-Pi+Arr
Orange photon
Arrestin (= arr1, arr2)
Gα · GTP (Gα = dgq+)
Gβγ (Gβ = Gβe+)
–?
PLC-β4 (= norpA+)
PI
PIK
PIP
PIPK
PIP2
IP3
CDP
Inositol
PIS
CDP-DG
CDS (= cds+)
PA
DAK (= Dgk1+ or rdgA+)
DAG
Eye-PKC (= inaC+)
rdgB+ PI transport and photoreceptor maintenance
Photoreceptor adaptation (req. inaA+, inaB+, InaD+, inaE+, Calmodulin+, ninaC+)
Photoreceptor neurotransmission (req. ebony+, hdc+, nonA+, tan+; some non+ loci?, ort+?)
Photoreceptor excitation (rrp+ loci?, some non+ loci?, ort+?)
Ca2+ (sequestered)
Ca-p?
Na-Ca exch.?
Ca-pump?
Ca2+ (extracellular)
SRC membrane
Plasma membrane
dip+ dry+?
trp+ trpl+? DmCNGC+? etc.?
Ca2+ (cytoplasmic)
cGMP
Dgcα1+
GTP

References

Ahmed, S., Maruyama, I.N., Kozma, R., Lee, J., Brenner, S., and Lim, L. (1992). The *Caenorhabditis elegans* UNC-13 gene-product is a phospholipid-dependent high-affinity phobol ester receptor. Biochem. J. *287*, 995-999.

Antebi, A. and Fink, G.R. (1992). The yeast Ca^{2+}-ATPase homologue, PMR1, is required for normal Golgi function and localizes in a novel Golgi-like distribution. Mol. Biol. Cell *3*, 633-654.

Applebury, M.L. (1994). Relationships of G-protein-coupled receptors: A survey with the photoreceptor opsin subfamily. In Molecular Evolution of Physiological Processes, D.M. Fambrough, ed. (Rockefeller University Press: New York), pp. 235-248.

Atwell, D. (1986). Ion channels and signal processing in the outer retina. Quart. J. Exp. Psych. *71*, 497-536.

Bacigalupo, J., Johnson, E.C., Vergara, C., and Lisman, J.E. (1991). Light-dependent channels from excised patches of *Limulus* ventral photoreceptors are opened by cGMP. Proc. Natl. Acad. Sci. U.S.A. *88*, 7938-7942.

Baker, E.K., Colley, N.J., and Zuker, C.S. (1994). The cyclophilin homolog NinaA functions as a chaperone, forming a stable complex *in vivo* with its protein target rhodopsin. EMBO J. *13*, 4886-4895.

Baumann, A., Frings, S., Godde, M., Seifert, R., and Kaupp, U.B. (1994). Primary structure and functional expression of a *Drosophila* cyclic nucleotide-gated channel present in eyes and antennae. EMBO J. *13*, 5040-5050.

Baumann, O. and Walz, B. (1989a). Topography of Ca^{2+}-sequestering endoplasmic reticulum in photoreceptors and pigmented glial cells in the compound eye of the honeybee drone. Cell Tissue Res. *255*, 511-522.

Baumann, O. and Walz, B. (1989b). Calcium and inositol polyphosphate-sensitivity of the calcium-sequestering endoplasmic reticulum in the photoreceptor cells of

the honeybee drone. J. Comp. Physiol. A *165*, 627-636.

Berridge, M.J. (1993). Inositol trisphosphate and calcium signalling. Nature *361*, 315-325.

Berstein, G., Blank, J.L., Jhon, D.-Y., Exton, J.H., Rhee, S.G., and Ross, E.M. (1992). Phospholipase C-β1 is a GTPase-activating protein for $G_{q/11}$, its physiologic regulator. Cell *70*, 411-418.

Bezprozvanny, I., Watras, J., and Erlich, B.E. (1991). Bell-shaped calcium response curves of Ins(1,4,5)P_3 and calcium-gated channels from endoplasmic reticulum of cerebellum. Nature *351*, 751-754.

Blaustein, M.P., DiPolo, R., and Reeves, J.P. (editors; 1991). Sodium-Calcium Exchange: Proceedings of the Second International Conference. Ann. N.Y. Acad. Sci., vol. 639.

Bloomquist, B.T., Shortridge, R.D., Schneuwly, S., Pedrew, M., Montell, C., Steller, H., Rubin, G., and Pak, W.L. (1988). Isolation of a putative phospholipase C gene of Drosophila, *norpA*, and its role in phototransduction. Cell *54*, 723-733.

Bolwig, N. (1946). Senses and sense organs of the anterior end of the housefly larva. Vidensk. Medd. fra Dansk. Naturh. Foren. *109*, 80-212.

Bork, P. (1993). Hundreds of ankyrin-like repeats in functionally diverse proteins: mobile modules that cross phyla horizontally? Proteins *17*, 363-374.

Brendel, V., Bucher, P., Nourbakhsh, I.R., Blaisdell, B.E., and Karlin, S. (1992). Methods and algorithms for statistical analysis of protein sequences. Proc. Natl. Acad. Sci. U.S.A. *89*, 2002-2006.

Britt, S.G., Feiler, R., Kirschfeld, K., and Zuker, C.S. (1993). Spectral tuning of rhodopsin and metarhodopsin in vivo. Neuron *11*, 29-39.

Britt, S. and Hall, K. (1995). Isolation and characterization of Rh5, a novel opsin gene. In 36th Annual Drosophila Research Conference, Program and Abstracts Volume (Genetics Society of America: Bethesda, Maryland), p. 8.

Brown, R.H., Jr. (1995). Amyotrophic lateral sclerosis: recent insights from genetics and transgenic mice. Cell *80*, 687-692.

Brown, J.E., Rubin, L.J., Ghalayini, A.J., Tarver, A.P., Irvine, R.F., Berridge, M.J., and Anderson, R.E. (1984). Myo-inositol polyphosphate may be a messenger for visual excitation in *Limulus* photoreceptors. Nature *311*, 160-163.

Brusca, R.C. and Brusca, G.J. (1990). Invertebrates (Sinauer Associates, Inc.: Sunderland, Massachusetts).

Burg, M.G., Sarthy, P.V., Koliantz, G., and Pak, W.L. (1993). Genetic and molecular identification of a *Drosophila* histidine decarboxylase gene required in photoreceptor transmitter synthesis. EMBO J. *12*, 911-919.

Byk, T., Bar-Yaacov, M., Doza, Y.N., Minke, B., and Selinger, Z. (1993). Regulatory arrestin cycle secures the fidelity and maintenance of the fly photoreceptor cell. Proc. Natl. Acad. Sci. U.S.A. *90*, 1907-1911.

Carafoli, E. (1987). Intracellular calcium homeostasis. Annu. Rev. Biochem. *56*, 395-433.

Carafoli, E. (1991). The calcium pumping ATPase of the plasma membrane. Annu. Rev. Physiol. *53*, 531-547.

Carafoli, E. (1994) Biogenesis: Plasma membrane calcium ATPase: 15 years of work on the purified enzyme. FASEB J. *8*, 993-1002.

Chen, D.-M. and Stark, W.S. (1983). Sensitivity and adaptation in the *Drosophila* phototransduction and photoreceptor degeneration mutants *trp* and *rdgB*. J. Insect Physiol. *29*, 133-140.

Cheney, R.E. and Mooseker, M.S. (1992). Unconventional myosins. Curr. Opin. Cell. Biol. *4*, 27-35.

Clapham, D.E. (1993). Mutations in G protein-linked receptors: novel insights on disease. Cell *75*, 1237-1239.

Clapham, D.E. (1995a). Calcium signalling. Cell *80*, 259-268.

Clapham, D.E. (1995b). Replenishing the stores. Nature *375*, 634-635.

Cohen, P. and Klee, C.B. (editors; 1988). Molecular Aspects of Cellular Regulation (Elsevier: New York).

Cohen, G.B., Ren, R., and Baltimore, D. (1995). Modular binding domains in signal transduction proteins. Cell *80*, 237-248.

Colley, N.J., Cassill, J.A., Baker, E.K., and Zuker, C.S. (1995). Defective intracellular transport is the molecular basis of rhodopsin-dependent dominant retinal degeneration. Proc. Natl. Acad. Sci. U.S.A. *92*, 3070-3074.

Collins, F.S. (1995). Positional cloning moves from perditional to traditional. Nature Genetics *9*, 347-350.

Conway Morris, S. (1993). The fossil record and the early evolution of the Metazoa. Nature *361*, 219-225.

Coombe, P.E. (1986). The large monopolar cells L1 and L2 are responsible for ERG transients in *Drosophila*. J. Comp. Physiol. A *159*, 655-665.

Cosens, D.J. and Briscoe, D. (1972). A switch phenomenon in the compound eye of the white-eyed mutant of *Drosophila melanogaster*. J. Insect Physiol. *18*, 627-632.

Cosens, D.J. and Manning, A. (1969). Abnormal electroretinogram from a *Drosophila* mutant. Nature *224*, 285-287.

Cowman, A.F., Zuker, C.S., and Rubin, G.M. (1986). An opsin gene expressed in only one photoreceptor cell type of the Drosophila eye. Cell *44*, 705-710.

Cox, D.A. and Matlib, M.A. (1993). A role for the mitochondrial Na^{+}-Ca^{2+} exchanger in the regulation of oxidative phosphorylation in isolated heart mitochondria. J. Biol. Chem. *268*, 938-947.

Cunningham, K.W. and Fink, G.R. (1994). Calcineurin-dependent growth control in *Saccharomyces cerevisiae* mutants lacking *PMC1*, a homolog of plasma membrane Ca^{2+} ATPases. J. Cell Biol. *124*, 351-363.

Davis, R.L. (1993). Mushroom bodies and *Drosophila* learning. Neuron *11*, 1-

14.

Deckert, A., Nagy, K., Helrich, C.S., and Stieve, H. (1992). Three components in the light-induced current of the *Limulus* ventral photoreceptor. J. Physiol. *453*, 69-96.

Deckert, A. and Stieve, H. (1991). Electrogenic Na^{+}-Ca^{2+} exchanger, the link between intra- and extracellular calcium in the *Limulus* ventral photoreceptor. J. Physiol. *433*, 467-482.

Dolph, P.J., Man-Son-Hing, H., Yarfitz, S., Colley, N.J., Running Deer, J., Spencer, M., Hurley, J.B., and Zuker, C.S. (1994). An eye-specific Gβ subunit essential for termination of the phototransduction cascade. Nature *370*, 59-61.

Dolph, P.J., Ranganathan, R., Colley, N.J., Hardy, R.W., Socolich, M., and Zuker, C.S. (1993). Arrestin function in inactivation of G-protein-coupled receptor rhodopsin *in vivo*. Science *260*, 1910-1916.

Doza, Y.N., Minke, B., Chorev, M., and Selinger, Z. (1992). Characterization of fly rhodopsin kinase. Eur. J. Biochem. *209*, 1035-1040.

Fagan, M.J. and Saier, M.H., Jr. (1994). P-type ATPases of eukaryotes and bacteria: sequence analyses and construction of phylogenetic trees. J. Mol. Evol. *38*, 57-99.

Fein, A., Payne, R., Corson, D.W., Berridge, M.J., and Irvine, R.F. (1984). Photoreceptor excitation and adaptation by inositol 1,4,5-trisphosphate. Nature *311*, 157-160.

Feng, J.J., Frank, T.M., and Fein, A. (1991). Excitation of *Limulus* photoreceptors by hydrolysis-resistant analogs of cGMP and cAMP. Brain Research *552*, 291-294.

Ferreira, P.A. and Pak, W.L. (1994). Bovine phospholipase C highly homologous to the NorpA protein of *Drosophila* is expressed specifically in cones. J. Biol. Chem. *269*, 3129-3131.

Ferreira, P.A., Shortridge, R.D., and Pak, W.L. (1993). Distinctive subtypes of

bovine phospholipase C that have preferential expression in the retina and high homology to the *norpA* gene product of *Drosophila*. Proc. Natl. Acad. Sci. U.S.A. *90*, 6042-6046.

Ferreira, P.A., Travis, G.H., and Pak, W.L. (1995). Characterization of the vertebrate homologs of 2 *Drosophila* photoreceptor proteins. Invest. Opthamol. Vis. Sci. *36*, S403.

Finch, E.A., Turner, T.J., and Goldin, S.M. (1991). Calcium as a co-agonist of inositol 1,4,5-trisphosphate-induced calcium release. Science *252*, 443-446.

Fitch, C.L., de Sousa, S.M., O'Day, P.M., Neubert, T.A., Plantilla, C.M., Spencer, M., Yarfitz, S., Apte, D., and Hurley, J.B. (1993). Pertussis toxin expression in *Drosophila* alters the visual response and blocks eating behaviour. Cellular Signalling *5*, 187-207.

Flatman, P.W. (1992). Mechanisms of magnesium transport. Annu. Rev. Physiol. *53*, 259-271.

Franceschini, N. (1975). Sampling of the visual environment by the compound eye of the fly: fundamentals and applications. In Photoreceptor Optics, A.W. Snyder and R. Menzel, eds. (Springer Verlag: New York), pp. 97-125.

Fryxell, K.J. and Meyerowitz, E.M. (1987). An opsin gene that is expressed only in the R7 photoreceptor cell of *Drosophila*. EMBO J. *6*, 443-451.

Fryxell, K.J. and Meyerowitz, E.M. (1991). The evolution of rhodopsins and neurotransmitter receptors. J. Mol. Evol. *33*, 367-378.

Fuchs, S., Nakazawa, M., Maw, M., Tamai, M., Oguchi, Y., and Gal, A. (1995). A homozygous 1-base pair deletion in the arrestin gene is a frequent cause of Oguchi disease in Japanese. Nature Genetics *10*, 360-362.

Gomez, M.D. and Nasi, E. (1994). The light-sensitive conductance of hyperpolarizing invertebrate photoreceptors: a patch-clamp study. J. Gen. Physiol. *103*, 939-956.

Goodson, H.V. (1994). Molecular evolution of the myosin superfamily:

application of phylogenetic techniques to cell biological questions. In Molecular Evolution of Physiological Processes, D.M. Fambrough, ed. (Rockefeller University Press), pp. 141-157.

Gordesky-Gold, B., Warrick, J.M., Bixler, A., Beasley, J.E., and Tompkins, L. (1995). Hypomorphic mutations in the *larval photokinesis A* (*lphA*) gene have stage-specific effects on visual system function in *Drosophila melanogaster*. Genetics *139*, 1623-1629.

Halder, G., Callaerts, P., and Gehring, W.J. (1995). Induction of ectopic eyes by targeted expression of the *eyeless* gene in *Drosophila*. Science *267*, 1788-1792.

Hall, J.C. (1995) Tripping along the trail to the molecular mechanisms of biological clocks. Trends Neurosci. *18*, 230-240.

Hanson-Painton, O., Randolph, V., Saugstad, J.A., Oh, S.-K., and Tobin, S.L. (1992). Developmental expression of the *Drosophila melanogaster* calmodulin gene. Int. J. Dev. Biol. *36*, 343-351.

Hardie, R.C. (1991). Whole-cell recordings of the light induced current in dissociated *Drosophila* photoreceptors: evidence for feedback by calcium permeating the light-sensitive channels. Proc. R. Soc. Lond. (B) *245*, 203-210.

Hardie, R.C. (1995). Photolysis of caged Ca^{2+} facilitates and inactivates but does not directly excite light-sensitive channels in *Drosophila* photoreceptors. J. Neurosci. *15*, 889-902.

Hardie, R.C. and Minke, B. (1992). The *trp* gene is essential for a light-activated Ca^{2+} channel in Drosophila photoreceptors. Neuron *8*, 643-651.

Hardie, R.C. and Minke, B. (1993). Novel Ca^{2+} channels underlying transduction in *Drosophila* photoreceptors: implications for phosphoinositide-mediated Ca^{2+} mobilization. Trends Neurosci. *16*, 371-376.

Hardie, R.C. and Minke, B. (1994a). Spontaneous activation of light-sensitive channels in *Drosophila* photoreceptors. J. Gen. Physiol. *103*, 389-407.

Hardie, R.C. and Minke, B. (1994b). Calcium-dependent inactivation of light-sensitive channels in *Drosophila* photoreceptors. J. Gen. Physiol. *103*, 409-427.

Hardie, R.C., Peretz, A., Pollock, J.A., and Minke, B. (1993a). Ca^{2+} limits the development of the light response in *Drosophila* photoreceptors. Proc. R. Soc. Lond. (B) *252*, 223-229.

Hardie, R.C., Peretz, A., Suss-Toby, E., Rom-Glas, A., Bishop, S.A., Selinger, Z., and Minke, B. (1993b). Protein kinase C is required for light adaptation in *Drosophila* photoreceptors. Nature *363*, 634-637.

Harlan, J.E., Hajduk, P.J., Yoon, H.S., and Fesik, S.W. (1994). Pleckstrin homology domains bind to phosphatidylinositol-4,5-bisphosphate. Nature *371*, 168-170.

Harris, W.A., Stark, W.S., and Walker, J.A. (1976). Genetic dissection of the photoreceptor system in the compound eye of *Drosophila melanogaster.* J. Physiol. *256*, 415-439.

Harteneck, C., Obukhov, A.G., Zobel, A., Kalkbrenner, F., and Schultz, G. (1995). The *Drosophila* cation channel *trpl* expressed in insect *Sf9* cells is stimulated by agonists of G-protein-coupled receptors. FEBS Lett. *358*, 297-300.

Hasan, G. and Rosbash, M. (1992). *Drosophila* homologs of two mammalian intracellular Ca^{2+}-release channels: identification and expression patterns of the inositol 1,4,5-triphosphate and the ryanodine receptor genes. Development *116*, 967-975.

Hayden, S.M., Wolenski, J.S., and Mooseker, M.S. (1990). Binding of brush border myosin-I to phospholipid vesicles. J. Cell Biol. *111*, 443-451.

Heisenberg, M. and Buchner, E. (1977). The role of retinula cell types in visual behavior of *Drosophila melanogaster.* J. Comp. Physiol. A *117*, 127-162.

Heisenberg, M. and Götz, K.G. (1975). The use of mutations for the partial degradation of vision in *Drosophila melanogaster.* J. Comp. Physiol. A *98*, 217-241.

Heisenberg, M. and Wolf, R. (1984). Vision in Drosophila: Genetics of Microbehavior. Springer-Verlag: New York. Pp. 10-24.

Hevers, W. and Hardie, R.C. (1995). Serotonin modulates the voltage dependence of delayed rectifier and *Shaker* potassium channels in Drosophila photoreceptors. Neuron *14*, 845-856.

Hicks, J.L. and Williams, D.S. (1992). Distribution of the myosin I-like *ninaC* proteins in the *Drosophila* retina and ultrastructural analysis of mutant phenotypes. J. Cell Sci. *101*, 247-254.

Hilgemann, D.W., Nicoll, D.A., and Philipson, K.D. (1991). Charge movement during Na^+ translocation by native and cloned cardiac Na^+/Ca^{2+} exchanger. Nature *352*, 715-718.

Hille, B. (1992). Ionic Channels of Excitable Membranes, 2cd. ed. (Sinauer Associates Inc.: Sunderland, Massachusetts).

Hochstrate, P. and Juse, A. (1991). Intercellular free calcium concentration in the blowfly retina studied by Fura-2. Cell Calcium *12*, 695-712.

Hoffman, E.P., Lehmann-Horn, F., and Rüdel, R. (1995). Overexcited or inactive: ion channels in muscle disease. Cell *80*, 681-686.

Horridge, G.A. (1977). The compound eye of insects. Sci. Am. *237*, 108-120.

Hoth, M. and Penner, R. (1993). Calcium release-activated calcium current in rat mast cells. J. Physiol. *465*, 359-386.

Hotta, Y. and Benzer, S. (1970). Genetic dissection of the *Drosophila* nervous system by means of mosaics. Proc. Natl. Acad. Sci. U.S.A. *67*, 1156-1163.

Hotta, Y. and Keng, Z.C. (1984). Genetic dissection of larval photoreceptors in *Drosophila*. In Animal Behavior: Neurophysiological and Ethological Approaches, K. Aoki, S. Ishii, and H. Morita, eds. (Springer-Verlag: Berlin), pp. 49-60.

Hu, K.G., Reichert, H., and Stark, W.S. (1978). Electrophysiological characterization of *Drosophila* ocelli. J. Comp. Physiol. A *126*, 15-24.

Hu, Y., Rajan, L., and Schilling, W.P. (1994a). Ca^{2+} signalling in Sf9 insect cells and the functional expression of a rat brain M_5 muscarinic receptor. Am. J. Physiol.

266, C1736-C1743.

Hu, Y. and Schilling, W.P. (1995). Receptor-mediated activation of recombinant Trpl expressed in Sf9 insect cells. Biochem. J. *305*, 605-611.

Hu, Y., Vaca, L., Zhu, X., Birnbaumer, L., Kunze, D.L., and Schilling, W.P. (1994b). Appearance of a novel Ca^{2+} influx pathway in Sf9 insect cells following expression of the transient receptor potential-like (*trpl*) protein of *Drosophila*. Biochem. Biophys. Res. Comm. *201*, 1050-1056.

Hyde, D.R., Mecklenburg, K.L., Pollock, J.A., Vihtelic, T.S., and Benzer, S. (1990). Twenty *Drosophila* visual system cDNA clones: one is a homolog of human arrestin. Proc. Natl. Acad. Sci. U.S.A. *87*, 1008-1012.

Johnson, E.C. and Pak, W.L. (1986). Electrophysiological study of *Drosophila* rhodopsin mutants. J. Gen. Physiol. *88*, 651-673.

Kaupp, U.B. and Koch, K.-W. (1992). Role of cGMP and Ca^{2+} in vertebrate photoreceptor excitation and adaptation. Annu. Rev. Physiol. *54*, 153-175.

Kent, C. (1995). Eukaryotic phospholipid biosynthesis. Annu. Rev. Biochem. *64*, 315-343.

Kingsolver, J.G. and Koehl, M.A.R. (1994). Selective factors in the evolution of insect wings. Annu. Rev. Entomol. *39*, 425-451.

Kurada, P. and O'Tousa, J.E. (1995). Retinal degeneration caused by dominant rhodopsin mutations in Drosophila. Neuron *14*, 571-579.

Lee, C.-W., Lee, K.-H., Lee, S.-B., Park, D., and Rhee, S.G. (1994a). Regulation of phospholipase C-β4 by ribonucleotides and the α-subunit of G_q. J. Biol. Chem. *269*, 25335-25338.

Lee, C.-W., Park, D.J., Lee, K.-H., Kim, C.G., and Rhee, S.G. (1993). Purification, molecular cloning, and sequencing of phopholipase C-β4. J. Biol. Chem. *268*, 21318-21327.

Lee, Y.-J., Shah, S., Suzuki, E., Zars, T., O'Day, P.M., and Hyde, D.R.

(1994b). The Drosophila *dgq* gene encodes a G_α protein that mediates phototransduction. Neuron *13*, 1143-1157.

Li, C., Randell, L., Koliantz, G., and Pak, W.L. (1995). Novel component of *Drosophila* phototransduction pathway. Invest. Opthamol. Vis. Sci. *36*, S381.

Lindsley, D.L. and Zimm, G.G. (1992). The Genome of *Drosophila melanogaster*. (Academic Press, Inc.: San Diego.)

Liu, W., Yoon, J., Burg, M., Chen, L., and Pak, W.L. (1995). Molecular characterization of two *Drosophila* guanylate cyclases expressed in the nervous system. J. Biol. Chem. *270*, 12418-12427.

Lytton, J. and MacLennan, D.H. (1988). Molecular cloning of cDNAs from human kidney coding for 2 alternatively spliced products of the cardiac Ca^{2+}-ATPase gene. J. Biol. Chem. *263*, 15024-15031.

Magyar, A. and Váradi, A. (1990). Molecular cloning and chromosomal localization of a sarco/endoplasmic reticulum-type Ca^{2+}-ATPase of *Drosophila melanogaster*. Biochem. Biophys. Res. Comm. *173*, 872-877.

Majerus, P.W. (1992). Inositol phosphate biochemistry. Annu. Rev. Biochem. *61*, 225-250.

Masai, I., Hosoya, T., Kojima, S., and Hotta, Y. (1992). Molecular cloning of a *Drosophila* diacylglycerol kinase gene that is expressed in the nervous system and muscle. Proc. Natl. Acad. Sci. U.S.A. *89*, 6030-6034.

Masai, I., Okazaki, A., Hosoya, T., and Hotta, Y. (1993). *Drosophila* retinal degeneration A gene encodes an eye-specific diacylglycerol kinase with cysteine-rich zinc-finger motifs and ankyrin repeats. Proc. Natl. Acad. Sci. U.S.A. *90*, 11157-11161.

Matsumoto, H., Isono, K., Pye, Q., and Pak, W.L. (1987). Gene encoding cytoskeletal proteins in *Drosophila* rhabdomeres. Proc. Natl. Acad. Sci. U.S.A. *84*, 985-989.

Matsumoto, H., Kurien, B.T., Takagi, Y., Kahn, E.S., Kinumi, T., Komori, N.,

Yamada, T., Hayashi, F., Isono, K., Pak, W.L., Jackson, K.W., and Tobin, S.L. (1994). Phosrestin I undergoes the earliest light-induced phosphorylation by a calcium/calmodulin-dependent protein kinase in Drosophila photoreceptors. Neuron *12*, 997-1010.

Matsumoto-Suzuki, E., Hirosawa, K., and Hotta, Y. (1989). Structure of the subrhabdomeric cisternae in the photoreceptor cells of *Drosophila melanogaster*. J. Neurocytol. *18*, 87-93.

McKay, R.R., Chen, D.-M., Miller, K., Kim, S., Stark, W.S., and Shortridge, R.D. (1995). Phospholipase C rescues visual defect in *norpA* mutant of *Drosophila melanogaster*. J. Biol. Chem. *270*, 13271-13276.

McKay, R.R., Zhu, L., and Shortridge, R.D. (1994). Membrane association of phospholipase C encoded by the *norpA* gene of *Drosophila melanogaster*. Neuroscience *61*, 141-148.

Meyertholen, E.P., Stein, P.J., Williams, M.A., and Ostroy, S.E. (1987). Studies of the *Drosophila norpA* phototransduction mutant. J. Comp. Physiol. A *161*, 793-798.

Miller, G.V., Hansen, K.N., and Stark, W.S. (1981). Phototaxis in *Drosophila*: R1-6 input and interaction among ocellar and compound eye receptors. J. Insect Physiol. *27*, 813-819.

Minke, B. (1982). Light-induced reduction in excitation efficiency in the *trp* mutant of *Drosophila*. J. Gen. Physiol. *79*, 361-385.

Minke, B. (1983). The *trp* is a *Drosophila* mutant sensitive to developmental temperature. J. Comp. Physiol. *151*, 483-486.

Minke, B. and Armon, E. (1980). Intermediate processes in phototransduction: a study in *Drosophila* mutants. Photochem. Photobiol. *32*, 553-562.

Minke, B., Wu, C.-F., and Pak, W.L. (1975). Induction of photoreceptor voltage noise in the dark in *Drosophila* mutant. Nature *258*, 84-87.

Mismer, D., Michael, W.M., Laverty, T.R., and Rubin, G.M. (1988). Analysis

of the promoter of the Rh2 opsin gene in *Drosophila melanogaster*. Genetics *120*, 173-180.

Montell, C., Jones, K., Hafen, E., and Rubin, G. (1985). Rescue of the *Drosophila* phototransduction mutation *trp* by germline transformation. Science *230*, 1040-1043.

Montell, C., Jones, K., Zuker, C., and Rubin, G. (1987). A second opsin gene expressed in the ultraviolet-sensitive R7 photoreceptor cells in *Drosophila melanogaster*. J. Neurosci. *7*, 1558-1566.

Montell, C. and Rubin, G.M. (1988). The Drosophila *ninaC* locus encodes two photoreceptor cell specific proteins with domains homologous to protein kinases and the myosin heavy chain head. Cell *52*, 757-772.

Montell, C. and Rubin, G.M. (1989). Molecular characterization of the Drosophila *trp* locus: a putative integral membrane protein required for phototransduction. Neuron *2*, 1313-1323.

Nagy, K. (1993). Cyclic nucleotides and inositol trisphosphate activate different components of the receptor current in *Limulus* ventral nerve photoreceptors. Neurosci. Lett. *152*, 1-4.

Nagy, K. (1994). Inhibition of the first component of the receptor current in *Limulus* photoreceptor. NeuroReport *5*, 847-849.

Nathans, J. (1994). In the eye of the beholder: visual pigments and inherited variation in human vision. Cell *78*, 357-360.

O'Day, P.M. and Gray-Keller, M.P. (1989). Evidence for electrogenic Na^+/Ca^{2+} exchange in *Limulus* ventral photoreceptors. J. Gen. Physiol. *93*, 473-492.

O'Day, P.M., Gray-Keller, M.P., and Lonergan, M. (1991). Physiological roles of Na^+/Ca^{2+} exchange in *Limulus* ventral photoreceptors. J. Gen. Physiol. *97*, 369-391.

Ohya, Y. and Botstein, D. (1994). Diverse essential functions revealed by complementing yeast calmodulin mutants. Science *263*, 963-966.

Ondek, B., Hardy, R., Baker, E., Stamnes, M., Shieh, B., and Zuker, C. (1992). Genetic dissection of cyclophilin function: saturation mutagenesis of the *Drosophila* cyclophilin homolog *ninaA*. J. Biol. Chem. *267*, 16460-16466.

O'Tousa, J.E., Baehr, W., Martin, R.L., Hirsh, J., Pak, W.L., and Applebury, M.L. (1985). The Drosophila *ninaE* gene encodes an opsin. Cell *40*, 839-850.

O'Tousa, J.E., Leonard, D.S., and Pak, W.L. (1989). Morphological defects in ora^{JK84} photoreceptors caused by mutation in R1-6 opsin gene of *Drosophila*. J. Neurogenet. *6*, 41-52.

Pak, W.L. (1975). Mutations affecting the vision of *Drosophila melanogaster*. In Handbook of Genetics, Volume 3: Invertebrates of Genetic Interest, R.C. King, ed. (Plenum Press: New York), pp. 703-733.

Pak, W.L. (1979). Study of photoreceptor function using *Drosophila* mutants. In Neurogenetics: Genetic Approaches to the Nervous System, X.O. Breakefield, ed. (Elsevier: New York), pp. 67-99.

Pak, W.L. (1991). Molecular genetic studies of photoreceptor function using *Drosophila* mutants. Prog. Clin. Biol. Res. *362*, 1-32.

Pak, W.L., Grossfield, J., and Arnold, K.S. (1970). Mutants of the visual pathway of *Drosophila melanogaster*. Nature *227*, 518-520.

Palazzollo, M.J., Hyde, D.R., VijayRaghavan, K., Mecklenburg, K., Benzer, S., and Meyerowitz, E. (1989). Use of a new strategy to isolate and characterize 436 Drosophila cDNA clones corresponding to RNAs detected in adult heads but not in early embryos. Neuron *3*, 527-539.

Parker, P.J., Hemmings, B.A., and Gierschik, P. (1994). PH domains and phospholipases--a meaningful relationship? Trends Biochem. *19*, 54-55.

Payne, R., Corson, D.W., and Fein, A. (1986). Pressure injection of calcium both excites and adapts *Limulus* ventral photoreceptors. J. Gen. Physiol. *88*, 107-126.

Payne, R., Flores, T.M., and Fein, A. (1990). Feedback inhibition by calcium

limits the release of calcium by inositol trisphosphate in *Limulus* ventral photoreceptors. Neuron *4*, 547-555.

Payne, R., Walz, B., Levy, S., and Fein, A. (1988). The localization of calcium release by inositol trisphosphate in *Limulus* photoreceptors and its control by negative feedback. Phil. Trans. R. Soc. Lond. B *320*, 359-379.

Peretz, A., Sandler, C., Kirschfeld, K., Hardie, R.C., and Minke, B. (1994a). Genetic dissection of light-induced Ca^{2+} influx into *Drosophila* photoreceptors. J. Gen. Physiol. *104*, 1057-1077.

Peretz, A., Suss-Toby, E., Rom-Glas, A., Arnon, A., Payne, R., and Minke, B. (1994b). The light response of Drosophila photoreceptors is accompanied by an increase in cellular calcium: effects of specific mutations. Neuron *12*, 1257-1267.

Philipson, K.D. and Nicoll, D.A. (1993). Molecular and kinetic aspects of sodium-calcium exchange. Int. Rev. Cytol. *137C*, 199-227.

Phillips, A.M., Bull, A., and Kelly, L.E. (1992). Identification of a Drosophila gene encoding a calmodulin-binding protein with homology to the *trp* phototransduction gene. Neuron *8*, 631-642.

Phizicky, E.M. and Fields, S. (1995). Protein-protein interactions: methods for detection and analysis. Microbiol. Rev. *59*, 94-123.

Plangger, A., Malicki, D., Whitney, M., and Paulsen, R. (1994). Mechanism of arrestin 2 function in rhabdomeric photoreceptors. J. Biol. Chem. *269*, 26969-26975.

Pollock, J.A., Assaf, A., Peretz, A., Nichols, C.D., Mojet, M.H., Hardie, R.C., and Minke, B. (1995). TRP, a protein essential for inositide-mediated Ca^{2+} influx is localized adjacent to the calcium stores in *Drosophila* photoreceptors. J. Neurosci. *15*, 3747-3760.

Pollock, J.A. and Benzer, S. (1988). Transcript localization of four opsin genes in the three visual organs of *Drosophila*; RH2 is ocellus specific. Nature *333*, 779-782.

Porter, J.A., Hicks, J.L., Williams, D.S., and Montell, C. (1992). Differential

localizations of and requirements for the two Drosophila *ninaC* kinase/myosins in photoreceptor cells. J. Cell Biol. *116*, 683-693.

Porter, J.A. and Montell, C. (1993). Distinct roles of the *Drosophila ninaC* kinase and myosin domains revealed by systematic mutagenesis. J. Cell Biol. *122*, 601-612.

Porter, J.A., Yu, M., Doberstein, S.K., Pollard, T.D., and Montell, C. (1993). Dependence of calmodulin localization in the retina on the NINAC unconventional myosin. Science *262*, 1038-1042.

Provost, N.M., Somers, D.E., and Hurley, J.B. (1988). A *Drosophila melanogaster* G protein α subunit gene is expressed primarily in embryos and pupae. J. Biol. Chem. *263*, 12070-12076.

Raff, R.A., Marshall, C.R., and Turbeville, J.M. (1994). Using DNA sequences to unravel the cambrian radiation of the animal phyla. Annu. Rev. Ecol. Syst. *25*, 351-375.

Ranganathan, R., Bacskai, B.J., Tsien, R.Y., and Zuker, C.S. (1994). Cytosolic calcium transients: spatial localization and role in Drosophila photoreceptor cell function. Neuron *13*, 837-848.

Ranganathan, R., Harris, G.L., Stevens, C.F., and Zuker, C.S. (1991a). A *Drosophila* mutant defective in extracellular calcium-dependent photoreceptor deactivation and rapid desensitization. Nature *354*, 230-232.

Ranganathan, R., Harris, W.A., and Zuker, C.S. (1991b). The molecular genetics of invertebrate phototransduction. Trends Neur. Sci. *14*, 486-493.

Ranganathan, R. and Stevens, C.F. (1995). Arresting binding determines the rate of inactivation of the G protein-coupled receptor rhodopsin in vivo. Cell *81*, 841-848.

Renfranz, P.J. and Benzer, S. (1989). Monoclonal antibody probes discriminate early and late mutant defects in development of the *Drosophila* retina. Dev. Biol. *136*, 411-429.

Richard, E.A. and Lisman, J.E. (1992). Rhodopsin inactivation is a modulated

process in *Limulus* photoreceptors. Nature *356*, 336-338.

Riek, E.F. (1970). Fossil history. In The Insects of Australia, sponsored by CSIRO (Melbourne University Press: Carlton, Victoria), pp. 168-188.

Rom-Glas, A., Sandler, C., Kirschfeld, K., and Minke, B. (1992). The *nss* mutation or lanthanum inhibits light-induced Ca^{2+} influx into fly photoreceptors. J. Gen. Physiol. *100*, 767-781.

Ron, D., Chen, C.-H., Caldwell, J., Jamieson, L., Orr, E., and Mochly-Rosen, D. (1994). Cloning of an intracellular receptor for protein kinase C: a homolog of the β subunit of G proteins. Proc. Natl. Acad. Sci. U.S.A. *91*, 839-843.

Rosenthal, A., Rhee, L., Yadegari, R., Paro, R., Ullrich, A., and Goeddel, D.V. (1987). Structure and nucleotide sequence of a *Drosophila melanogaster* protein kinase C gene. EMBO J. *6*, 433-441.

Running Deer, J.L., Hurley, J.B., and Yarfitz, S.L. (1995). G protein control of *Drosophila* photoreceptor phospholipase C. J. Biol. Chem. *270*, 12623-12628.

Sahly, I., Schröder, W.H., Zierold, K., and Minke, B. (1994). Accumulation of calcium in degenerating photoreceptors of several *Drosophila* mutants. Visual Neurosci. *11*, 763-772.

Saimi, Y. and Kung, C. (1994). Ion channel regulation by calmodulin binding. FEBS Lett. *350*, 155-158.

Schaeffer, E., Smith, D., Mardon, G., Quinn, W., and Zuker, C. (1989). Isolation and characterization of two new Drosophila protein kinase C genes, including one specifically expressed in photoreceptor cells. Cell *57*, 403-412.

Schneuwly, S., Burg, M.G., Lending, C., Perdew, M.H., and Pak, W.L. (1991). Properties of photoreceptor-specific phospholipase C encoded by the *norpA* gene of *Drosophila melanogaster*. J. Biol. Chem. *266*, 24314-24319.

Selinger, Z., Doza, Y.N., and Minke, B. (1993). Mechanisms and genetics of photoreceptors desensitization in *Drosophila* flies. Biochem. Biophys. Acta *1179*, 283-

299.

Shah, S. and Hyde, D.R. (1995). Two *Drosophila* genes that encode the α and β subunits of the brain soluble guanylyl cyclase. J. Biol. Chem. *270*, 15368-15376.

Sheshberadaran, H. and Takahashi, J.S. (1994). Characterization of the chicken rhodopsin promoter: identification of retina-specific and *glass*-like protein binding domains. Mol. Cell. Neurosci. *5*, 309-318.

Shieh, B.-H. and Niemeyer, B. (1995). A novel protein encoded by the *InaD* gene regulates recovery of visual transduction in Drosophila. Neuron *14*, 201-210.

Shin, J., Richard, E.A., Lisman, J.E. (1993). Ca^{2+} is an obligatory intermediate in the excitation cascade of Limulus photoreceptors. Neuron *11*, 845-855.

Simchowitz, L., Foy, M.A., and Cragoe, E.J., Jr. (1990). A role for Na^{+}/Ca^{2+} exchange in the generation of superoxide radicals by human neutrophils. J. Biol. Chem. *265*, 13449-13456.

Smith, D.P., Ranganathan, R., Hardy, R.W., Marx, J., Tsuchida, T., and Zuker, C.S. (1991). Photoreceptor deactivation and retinal degeneration mediated by a photoreceptor-specific protein kinase C. Science *254*, 1478-1484.

Snyder, A.W. (1975). Optical properties of invertebrate photoreceptors. In The Compound Eye and Vision of Insects, G.A. Horridge, ed. (Clarendon Press: Oxford), pp. 179-235.

Stanewsky, R., Rendahl, K.G., Dill, M., and Saumweber, H. (1993). Genetic and molecular analysis of the *X* chromosomal region 14B17-14C4 in *Drosophila melanogaster*: loss of function in NONA, a nuclear protein common to many cell types, results in specific physiological and behavioral defects. Genetics *135*, 419-442.

Stark, W.S. (1975). Spectral selectivity of visual response alterations mediated by interconversions of native and intermediate photopigments in *Drosophila*. J. Comp. Physiol. A *96*, 343-356.

Stark, W.S., Chen, D.-M., Johnson, M.A., and Frayer, K.L. (1983). The *rdgB*

gene in *Drosophila*: retinal degeneration in different mutant alleles and inhibition of degeneration by *norpA*. J. Insect Physiol. *29*, 123-131.

Stark, W.S. and Sapp, R. (1987). Ultrastructure of the retina of *Drosophila melanogaster*: the mutant *ora* (outer rhabdomeres absent) and its inhibition of degeneration in *rdgB* (retinal degeneration-B). J. Neurogenet. *4*, 227-240.

Stark, W.S., Sapp, R., and Carlson, S.D. (1989). Ultrastructure of the ocellar visual system in normal and mutant *Drosophila melanogaster*. J. Neurosci. *5*, 127-153.

Steele, F. and O'Tousa, J.E. (1990). Rhodopsin activation causes retinal degeneration in Drosophila *rdgC* mutant. Neuron *4*, 883-890.

Steele, F.R., Washburn, T., Rieger, R., and O'Tousa, J.E. (1992). Drosophila *retinal degeneration C* (*rdgC*) encodes a novel serine/threonine protein phosphatase. Cell *69*, 669-676.

Steller, H., Fischbach, K.-F., and Rubin, G.M. (1987). *disconnected*: a locus required for neuronal pathway formation in the visual system of Drosophila. Cell *50*, 1139-1153.

Suzuki, E. and Hirosawa, K. (1991). Immunoelectron microscopic study of the opsin distribution in the photoreceptor cells of *Drosophila melanogaster*. J. Electron Microsc. *40*, 187-192.

Suzuki, E., Katayama, E., and Hirosawa, K. (1993). Structure of photoreceptive membranes of Drosophila compound eyes as studied by quick-freezing electron microscopy. J. Electron Microsc. *42*, 178-184.

Takeshima, H., Nishi, M., Iwabe, N., Miyata, T., Hosoya, T., Masai, I., and Hotta, Y. (1994). Isolation and characterization of a gene for a ryanodine receptor/calcium release channel in *Drosophila melanogaster*. FEBS Lett. *337*, 81-87.

Touhara, K., Inglese, J., Pitcher, J.A., Shaw, G., and Lefkowitz, R.J. (1994). Binding of G protein βγ-subunits to pleckstrin homology domains. J. Biol. Chem. *269*, 10217-10220.

Tower, J., Karpen, G.H., Craig, N., and Spradling, A.C. (1993). Preferential transposition of Drosophila *P* elements to nearby chromosomal sites. Genetics *133*, 347-359.

Toyoshima, N., Matsumoto, P., Wang, P., Inoue, H., Yoshioka, T., Hotta, Y., and Osawa, T. (1990). Purification and partial amino acid sequences of phosphoinositide-specific phospholipase C of *Drosophila* eye. J. Biol. Chem. *265*, 14842-14848.

Vaca, L., Sinkins, W.G., Hu, Y., Kunze, D.L., and Schilling, W.P. (1994). Activation of recombinant *trp* by thapsigargin in Sf9 insect cells. Am. J. Physiol. *267*, C1501-C1505.

Van Vactor, D., Jr., Krantz, D.E., Reinke, R., and Zipursky, S.L. (1988). Analysis of mutants in chaoptin, a cell-specific glycoprotein in Drosophila, reveals its role in cellular morphogenesis. Cell *52*, 281-290.

Váradi, A., Gilmore-Heber, M., and Benz, E.J., Jr. (1989). Amplification of the phosphorylation site--ATP-binding site cDNA fragment of the Na^+,K^+-ATPase and the Ca^{2+}-ATPase of *Drosophila melanogaster* by polymerase chain reaction. FEBS Lett. *258*, 203-207.

Verma, A.K., Filoteo, A.G., Stanford, D.R., Wieben, E.D., Penniston, J.T., Strehler, E.E., Fischer, R., Heim, R., Vogel, G., Mathews, S., Strehler-Page, M.-A., James, P., Vorherr, T., Krebs, J., and Carafoli, E. (1988). Complete primary structure of a human plasma membrane Ca^{2+} pump. J. Biol. Chem. *263*, 14152-14159.

Vihtelic, T.S., Goebl, M., Milligan, S., O'Tousa, J.E., and Hyde, D.R. (1993). Localization of *Drosophila retinal degeneration B*, a membrane-associated phosphatidylinositol transfer portein. J. Cell Biol. *122*, 1013-1022.

Walz, B., Baumann, O., Zimmermann, B., and Ciriacy-Wantrup, E.V. (1995). Caffeine- and ryanodine-sensitive Ca^{2+}-induced Ca^{2+} release from the endoplasmic reticulum in honeybee photoreceptors. J. Gen. Physiol. *105*, 537-567.

Walz, B., Zimmermann, B., and Seidl, S. (1994). Intracellular Ca^{2+} concentration

and latency of light-induced Ca^{2+} changes in photoreceptors of the honeybee drone. J. Comp. Physiol. A *174*, 421-431.

Werner, U., Suss-Toby, E., Rom, A., and Minke, B. (1992). Calcium is necessary for light excitation in barnacle photoreceptors. J. Comp. Physiol. A *170*, 427-434.

Wilson, R., Ainscough, R., Anderson, K., Baynes, C., Berks, M., Bonfield, J., Burton, J., Connell, M., Copsey, T., Cooper, J., Coulson, A., Craxton, M., Dear, S., Du, Z., Durbin, R., Favello, A., Fraser, A., Fulton, L., Gardner, A., Green, P., Hawkins, T., Hillier, L., Jier, M., Johnston, L., Jones, M., Kershaw, J., Kirsten, J., Laisster, N., Latreille, P., Lightning, J., Lloyd, C., Mortimore, B., O'Callaghan, M., Parsons, J., Percy, C., Rifken, L., Roopra, A., Saunders, D., Shownkeen, R., Sims, M., Smaldon, N., Smith, A., Smith, M., Sonnhammer, E., Staden, R., Sulston, J., Thierry-Mieg, J., Thomas, K., Vaudin, M., Vaughan, K., Waterston, R., Watson, A., Weinstock, L., Wilkinson-Sproat, J., and Wohldman, P. (1994). 2.2 Mb of contiguous nucleotide sequence from chromosome III of *C. elegans*. Nature *368*, 32-38.

Wolff, T. and Ready, D.F. (1993). Pattern formation in the *Drosophila* retina. In The Development of *Drosophila melanogaster*, M. Bate and A. Martinez Arias, eds. (CSHL Press: Cold Spring Harbor Laboratory), pp. 1277-1325.

Wong, F., Schaefer, E.L., Roop, B.C., LaMendola, J.N., Johnson-Seaton, D., and Shao, D. (1989). Proper function of the Drosophila *trp* gene product during pupal development is important for normal visual transduction in the adult. Neuron *3*, 81-94.

Wu, L., Niemeyer, B., Colley, N., Socolich, M., and Zuker, C.S. (1995). Regulation of PLC-mediated signalling in vivo by CDP-diacylglycerol synthase. Nature *373*, 216-222.

Wu, C.-F. and Pak, W.L. (1975). Quantal basis of photoreceptor spectral sensitivity of *Drosophila melanogaster*. J. Gen. Physiol. *66*, 149-168.

Wu, C.-F. and Pak, W.L. (1978). Light-induced voltage noise in the

photoreceptor of *Drosophila melanogaster*. J. Gen. Physiol. *71*, 249-268.

Yamanaka, M.K., Saugstad, J.A., Hanson-Painton, O., McCarthy, B.J., and Tobin, S.L. (1987). Structure and expression of the *Drosophila* calmodulin gene. Nucl. Acids Res. *15*, 3335-3348.

Yarfitz, S., Niemi, G., McConnell, J., Fitch, C., and Hurley, J. (1991). A G_β protein in the Drosophila compound eye is different from that in the brain. Neuron *7*, 429-438.

Yarfitz, S.L., Running Deer, J.L., Froelick, G., Colley, N.J., and Hurley, J.B. (1994). *In situ* assay of light-stimulated G protein activity in *Drosophila* photoreceptor G protein β mutants. J. Biol. Chem. *269*, 30340-30344.

Yoon, J., Shortridge, R.D., Bloomquist, B.T., Schneuwly, S., Pendew, M.H., and Pak, W.L. (1989). Molecular characterization of *Drosophila* gene encoding G_o α subunit homolog. J. Biol. Chem. *264*, 18536-18543.

Yoshikawa, S., Miyamoto, I., Aruga, J., Furuichi, T., Okano, H., and Mikoshiba, K. (1993). Isolation of a *Drosophila* gene encoding a head-specific guanylyl cyclase. J. Neurochem. *60*, 1570-1573.

Yoshikawa, S., Tanimura, T., Miyawaki, A., Nakamura, M., Yazaki, M., Furuichi, T., and Mikoshiba, K. (1992). Molecular cloning and characterization of the inositol 1,4,5-trisphosphate receptor in *Drosophila melanogaster*. J. Biol. Chem. *267*, 16613-16619.

Zhang, P. and Spradling, A.C. (1993). Efficient and dispersed local *P* element transposition from Drosophila females. Genetics *132*, 361-373.

Zhu, L., McKay, R.R., and Shortridge, R.D. (1993). Tissue-specific expression of phospholipase C encoded by the *norpA* gene of *Drosophila melanogaster*. J. Biol. Chem. *268*, 15994-16001.

Ziemba, S.E., Saks, S., Janviriya, Y., and Stephenson, R.S. (1995). Dissociation of photoreceptors from whole heads of the fruit fly, *Drosophila melanogaster*. Cell Tissue

Res. *280*, 473-477.

Zipursky, S.L. and Rubin, G.M. (1994). Determination of neuronal cell fate: lessons from the R7 neuron of *Drosophila*. Annu. Rev. Neurosci. *17*, 373-397.

Zucker, R.S. (1993). The calcium concentration clamp: spikes and reversible pulses using the photolabile chelator DM-nitrophen. Cell Calcium *14*, 87-100.

Zuker, C.S. (1994). On the evolution of eyes: would you like it simple or compound? Science *265*, 742-743.

Zuker, C.S., Cowman, A.F., and Rubin, G.M. (1985). Isolation and structure of a rhodopsin gene from D. melanogaster. Cell *40*, 851-858.

Zuker, C.S., Montell, C., Jones, K., Laverty, T., and Rubin, G.M. (1987). A rhodopsin gene expressed in photoreceptor cell R7 of the *Drosophila* eye: homologies with other signal-transducing molecules. J. Neurosci. *7*, 1550-1557.

Expression and evolution of *Calx*, a sodium-calcium exchanger of *Drosophila melanogaster*

Erich M. Schwarz and Seymour Benzer
Division of Biology, 156-29, California Institute of Technology, Pasadena, CA, 91125

Summary

We have cloned *Calx*, which encodes a sodium-calcium exchanger of *Drosophila melanogaster*. *Calx* is ubiquitously expressed in embryos and adult heads; it has multiple transcripts in adults, including one expressed in the retina. In *Xenopus* oocytes, microinjected *Calx* cRNA induces calcium uptake like that of its homolog, the $3Na^+/1Ca^{2+}$ exchanger of mammalian heart. *Calx* encodes two repeated motifs, *Calx*-α and *Calx*-β, that overlap domains required for exchanger activity and regulation. Analysis of these motifs suggests that *Calx* arose from several gene duplications in the Precambrian.

Introduction

Both animals and protists use Ca^{2+} as an excitatory intracellular signal in response to external stimuli, suggesting that cells co-opted this ion very early in life's history (Hille, 1992). However, excitation cannot recur unless Ca^{2+} influxes are followed by effluxes; moreover, prolonged cytoplasmic residence of excess Ca^{2+} is lethal (Carafoli, 1987; Choi, 1992; Nicotera *et al.*, 1992; Cunningham and Fink, 1994). To maintain homeostasis, cells expel calcium with calcium pumps and sodium-calcium exchangers (Carafoli, 1991; Philipson and Nicoll, 1993). These two systems complement one another: exchangers have a low affinity, but a high capacity, for intracellular calcium; pumps have low capacity, but high affinity (Carafoli, 1987).

Sodium-calcium exchange has been observed in diverse vertebrate tissues: central and motor neurons (Dahan *et al.*, 1991; Luther *et al.*, 1992; Marlier *et al.*, 1993); rod and cone photoreceptors (Nakatani and Yau, 1989; Haase *et al.*, 1990); cardiac and smooth muscle (Frank *et al.*, 1992; Moore *et al.*, 1993); kidney (Kofuji *et al.*, 1993; Reilly *et al.*,

1993); red blood cells (Milanick, 1992); B cells (Herschuelz and Lebrun, 1993); neutrophils (Simchowitz *et al.*, 1990); platelets (Kimura *et al.*, 1993); and osteoclasts (Krieger, 1991). Furthermore, distinct sodium-calcium exchangers are found in cellular versus mitochondrial membranes (Frank *et al.*, 1992; Li *et al.*, 1992; Reilly *et al.*, 1993). Finally, sodium-calcium exchange has been observed in arthropods and molluscs, and thus may exist in all metazoans (Allen, 1991; O'Day *et al.*, 1991). In *Drosophila*, photoreceptors admit calcium to their cytoplasms in response to light; this serves the dual purpose of both activating photoreceptors and adapting them to continued illumination (Hardie and Minke, 1993). The photoreceptors of at least four arthropods (honeybees, horseshoe crabs, houseflies, and *Drosophila*) display sodium-dependent calcium export (Minke and Armon, 1984; Minke and Tsacopoulos, 1986; O'Day *et al.*, 1991; Ranganathan *et al.*, 1994; Hardie, 1995). This suggests that sodium-calcium exchange may act in *Drosophila* photoreceptors to restore activated *Drosophila* photoreceptors to their resting state.

Despite their ubiquity, genes known to encode sodium-calcium exchangers have only been isolated from mammals (Nicoll *et al.*, 1990; Reiländer *et al.*, 1992). Cloned sodium-calcium exchangers fall into two classes, based on amino acid identity and stoichiometry of action. The cardiac exchanger (NCX1) trades three extracellular Na^+ ions for one cytoplasmic Ca^{2+} ion (Philipson and Nicoll, 1993). Its gene produces, by alternative splicing, renal and brain isoforms with 95% identity to that found in heart (Reilly and Shugrue, 1992; Furman *et al.*, 1993). A paralogous exchanger (NCX2), expressed in brain and skeletal muscle, has 68% identity to NCX1 (Li *et al.*, 1994). Both renal NCX1 and NCX2 behave similarly to cardiac NCX1 in patch clamps, and thus probably also perform $3Na^+/1Ca^{2+}$ exchange (Matsuoka et al., 1993; Li *et al.*, 1994). In contrast, the retinal exchanger (henceforth "RetX") is expressed on the surface of the outer segments of rod photoreceptors, has only 21-25% identity to NCX1-2, and has $4Na^+/1Ca^{2+},1K^+$ stoichiometry (Reiländer *et al.*, 1992; Philipson and Nicoll, 1993).

While NCX2 and RetX have so far only been cloned from rat and cow (Reiländer *et al.*, 1992; Li *et al.*, 1994), NCX1 has been cloned from diverse mammalian species (e.g., cow [Aceto *et al.*, 1992], dog [Nicoll *et al.*, 1990], rabbit [Reilly and Shugrue, 1992], and rat [Furman *et al.* 1993]); mammalian NCX1s are 95% identical to one another. It is thus likely that NCX1, NCX2, and RetX are largely invariant within all mammalian species. Finally, large-scale genomic sequencing has revealed a conceptual protein from the nematode *Caenorhabditis elegans* (C07A9.4) with 23% identity to RetX (Wilson *et al.*, 1994). C07A9.4 could be either a very divergent $4Na^+/1Ca^{2+},1K^+$ exchanger, or a new molecule of unknown function.

We and others have worked to identify possible components of *Drosophila* phototransduction, by isolating cDNAs of genes expressed in the visual system (Hyde *et al.*, 1990; Lee *et al.*, 1990; Smith *et al.*, 1990). One such cDNA proved to arise from a *Drosophila* homolog of NCX1 and NCX2, designated *Calx*. We show here that *Calx* is a fully functional sodium-calcium exchanger, expressed in many tissues including the retina. We also show that *Calx* encodes novel protein motifs.

Results

***Calx* cDNAs.** The original *Calx* cDNA, 9C5-o, is from a subtractive cDNA library (Palazzollo *et al.*, 1989) and is 377 bp long; Hyde *et al.* (1990) used it to detect a novel retinal transcript. We therefore isolated five more cDNAs from a λgt11 library (Itoh *et al.*, 1985) and partially sequenced three of them. Initial sequence data were then compared to known sequences with the program BLASTX (Altschul *et al.*, 1994). We found that the cDNAs had partial open reading frames (ORFs) resembling the cardiac $3Na^+/1Ca^{2+}$ exchanger, NCX1 (Nicoll *et al.*, 1990). These ORFs were on the *same* strand as had been primed by oligo-dT synthesis in 9C5-o, suggesting that 9C5-o might be a second-strand synthesis product. We used the longest cDNA (9C5-E) to confirm this hypothesis.

The annotated sequence of 9C5-E (5408 bp) is shown in Figure 1. Exchanger similarity plainly maps to the major ORF of 9C5-E, which has a complex pattern of similarities to other known or suspected exchangers (Figure 2). We henceforth term the 9C5 gene "*Calx*," and the protein product of its major ORF "Calx." Calx is predicted to have a leader sequence of 20 residues (2.3 kD), followed by a mature protein of 930 residues (104 kD, before glycosylation). Proteolytic cleavage of the Calx cytoplasmic domain, which is seen in vivo for its ortholog NCX1 (Nicoll *et al.*, 1990), could liberate a ~70 kD polypeptide as well. The 5' untranslated region (5'-UTR) of 9C5-E has seven minor non-overlapping ORFs. This was unexpected, but minor ORFs in 5'-UTRs occur in cDNAs from several *Drosophila* genes (OH *et al.*, 1992) and from bovine NCX1 (Aceto *et al.*, 1992). The translational start site of *Calx* (5'-GTAACCAGCCATGCA-3') strikingly differs from the *Drosophila* consensus (5'-CACAACCAAAATGGC-3') defined by Cavener and Ray (1991). While the 9C5-E cDNA has no large and unambiguous poly(A)$^+$ tail, it does have three polyadenylation signals (Angelichio *et al.*, 1991; Sachs and Wahle, 1993) near its oligo(A)$^+$ 3' terminus. We have observed, by partial sequencing of other cDNAs, five Calx residues encoded by alternately spliced cDNA (Figure 3). They fall in a region poorly conserved between Calx, NCX1, and NCX2 (Figures 2-3); indeed, alternate splicing occurs in the same region of NCX1 as in Calx (Figure 3; Nicoll *et al.*, 1990; Reilly and Shugrue, 1992; Lee *et al.*, 1994).

Sequence analysis of the *Calx* ORF. All mammalian sodium-calcium exchangers share common structural features (Philipson and Nicoll, 1993). They have two regions of six potential transmembrane sequences, split by a cytoplasmic domain. The first membrane sequence is transient, being proximal to a signal sequence cleavage site. The mature N-terminus is followed by one or more possible extracellular glycosylation sites. The cytoplasmic domain bears many acidic residues: an especially prominent acid cluster sits immediately before the seventh membrane sequence, where the cytoplasmic domain ends. Calx is predicted to possess all of these traits (Figures 1-2, 5). In addition, we

report several features shared by Calx and its mammalian homologs that have not been previously described.

Multiple alignment. We used BLASTP (Altschul *et al.*, 1994) to screen the non-redundant protein database of the NCBI for Calx homologs. In addition to NCX1, NCX2, RetX, and C07A9.4, we found significant similarity to two unannotated coding sequences from the *C. elegans* and *Escherichia coli* genome projects (C07A9.11 and ORF_o325). No homologs were encoded by *Haemophilus influenzae* Rd (Fleischmann *et al.*, 1995). We then used the Multiple Alignment Construction and Analysis Workbench (MACAW; Schuler *et al.*, 1991) to align these seven proteins globally (Figure 2). MACAW yielded many ungapped blocks of multiple similarity, with low probabilities (from $1.4 \cdot 10^{-4}$ to 0) of being spurious. Calx is globally similar to NCX1 and NCX2, having 52-54% identity out of 736 aligned amino acids. There are five N- and two C-terminal blocks in which Calx is discernably similar to all six metazoan proteins in Figure 2. Two of the N-terminal blocks and both of the C-terminal blocks show similarity to the *E. coli* protein ORF_o325 as well. Within these most-conserved 126 residues, Calx has: 75% identity to NCX1 and NCX2; 36% to RetX; and 25% to C07A9.4, C07A9.11, and ORF_o325. All of these alignments have z-scores of 19-77; a z-score of 6 is probably significant, and one of 9 highly significant (Methods; Pearson and Lipman, 1988). An acid cluster, previously observed in all mammalian sodium-calcium exchangers near their second transmembrane region (Figure 2), is plainly shared by Calx; however, it is not found in the *C. elegans* or *E. coli* proteins.

α-helical transmembrane sequences for the proteins in Figure 2 were predicted essentially as in Eisenberg *et al.* (1984; Figure 2). We found that this yields the expected 2x6 conformation of transmembrane sequences for Calx, NCX1, and NCX2, with two caveats. There exist two membrane sequences predicted only to occur once among these three proteins; since gaining or losing a transmembrane sequence is expected to alter a protein's structure grossly, we assume that these predictions are mistaken. More notably,

there is a consistent prediction--not made in the original analysis of NCX1 (Nicoll *et al.*, 1990)--that a 13th transmembrane sequence exists in Calx, NCX1, and NCX2 outside of their two transmembrane regions. Since this sequence overlaps a water-soluble calcium-binding domain of NCX1 (Matsuoka *et al.*, 1995), it may be the hydrophobic core of that domain.

The cytoplasmic domain of NCX1 has been shown to possess at least three functionally distinct regions (Figures 2, 5). One has possible amphipathic helicity and calmodulin-binding, and from it an autoinhibitory peptide has been derived (Li *et al.*, 1991). The second is required both for inhibition by elevated intracellular sodium (Na_i^+) and for high-affinity Ca^{2+} binding (Matsuoka *et al.*, 1993, 1995). The third is solely required for activation by elevated intracellular calcium (Ca_i^{2+}; Matsuoka *et al.*, 1993). The high-affinity Ca^{2+}-binding site is thought to regulate NCX1 by allosteric contacts with the Ca_i^{2+}-stimulatory domain, which does not itself bind Ca^{2+} in vitro (Matsuoka *et al.*, 1995). The first two regions are well conserved between Calx and NCX1 (61% and 49% identity); the last is less well conserved (33% identity). This correlates with the behavior of Calx in patch clamps: Calx displays inhibition by autoinhibitory peptide and elevated Na_i^+, but is partially *inhibited* by elevated Ca_i^{2+} (Hryshko *et al.*, 1995).

Protein kinase C (PKC) stimulates calcium extrusion in *Drosophila* photoreceptors, and a significant amount of such extrusion depends on sodium-calcium exchange (Ranganathan *et al.*, 1994). To identify plausible targets for stimulatory PKC, we scanned Calx, NCX1, and NCX2 for sites that were both potential PKC substrates and conserved between all three proteins. One such site actually exists: it is 12-13 residues N-terminal from the acid cluster (Figure 2), in a region of NCX1 not yet characterized by deletion analysis (Matsuoka *et al.*, 1993).

Intragenic repeats. To check for recurring motifs within Calx, we performed dot matrix analyses (States and Boguski, 1991), and discovered two new motifs (hereafter called *Calx*-α and *Calx*-β). While initially found in Calx, they are in fact reiterated within

all homologs of Calx (Figure 4). The statistical significance of these motifs is demonstrable by calculating the z-scores for matches between paired motifs (Methods). Any *Calx*-α motif has a z-score of 7.2-17.8, when nonidentically paired with either *Calx*-α motif from RetX or ORF_o325. Other pairings of *Calx*-α motifs generally (31/44 pairs) have z-scores over 9. All pairs of *Calx*-β motifs whatsoever have z-scores of 15.2-90.6.

The *Calx*-α motif is duplicated in all exchanger sequences, in equivalent locations within each transmembrane region (Figures 1, 4-5). It is tripartite: it begins with an extremely conserved N-terminal half (24/46+ residues); proceeds into a nonconserved linker (6-9 residues); and ends with a C-terminal third (16/46+ residues) that is moderately conserved, but nevertheless statistically convincing. In each of the four proven sodium-calcium exchangers, the *Calx*-α motifs are predicted to bridge the membrane, comprising most of the sequences and N-terminal vicinities of transmembrane sequences 2-3 and 9-10 (Figures 4-5). The *Calx*-β motif has four conserved blocks (Figure 4). Unlike the *Calx*-α motif, *Calx*-β is only found in Calx, NCX1, and NCX2. Yet an isolated *Calx*-β motif exists in human and murine integrin-β4 (Hynes, 1992; Spinardi *et al.*, 1993; Vidal *et al.*, 1995). In both exchangers and integrins, *Calx*-β motifs are predicted to be cytoplasmic. In Calx, NCX1, and NCX2 they exist as tandem repeats in the core of the cytoplasmic domain, separated by a highly variable region of 4-21 residues (Figures 1-2, 4-5); in mammalian integrin-β4 they exist as solo elements, N-terminal to four fibronectin-III repeats (Suzuki and Naitoh, 1990).

Predicted secondary structures. The PHD neural network (Rost and Sander, 1994) was used to predict the secondary structure of Calx, with special attention being paid to the *Calx*-α and *Calx*-β motifs (Methods; Figures 2, 4). Where a sequence was predicted to be membrane-spanning, we disregarded PHD, since it was specifically trained to determine globular secondary structures. *Calx*-α motifs are predicted to have a loop between their two transmembrane sequences. *Calx*-β motifs are predicted to have a series of β-strands and turns; this is consistent with the *Calx*-β motif being a self-contained β-sheet

of seven strands. The N-terminal intracellular region of Calx, NCX1, and NCX2 is predicted to be primarily α-helical; this includes the possible calmodulin-binding region of NCX1 (Figure 2; Li *et al.*, 1991).

***Calx* tissue expression.** We tested the transcriptional polarity and tissue specificity of *Calx* by probing RNA blots with strand-specific 9C5-E probes (Figures 6-7). Probes antisense to the major 9C5-E ORF revealed at least three transcripts in adult *Drosophila*; probes comprising the same strand as the major ORF yielded no signals, even against 10 μg of poly(A)$^+$ RNA from adult heads (Figure 6). The RNAs observed with antisense probes and high-resolution blots (Figure 7) include a transcript in both heads and bodies (4.9 kb); a body-specific transcript (4.0 kb); and three head-specific transcripts that appear unaffected by the presence or absence of the visual system (8.2, 9.0, and ≥~15 kb). A fifth head-specific transcript is enriched in eyeless heads, and thus appears to be primarily expressed outside the visual system (7.0 kb). A sixth transcript (5.6 kb, close in size to 9C5-E) is expressed both within the visual system and elsewhere in the head.

To determine the spatial distribution of *Calx* transcripts, tissue in situ hybridization was performed with digoxigenin-riboprobes on both adult head sections and embryos (Figure 8). In heads, antisense probes reveal *Calx* expression in the retina, optic ganglia, and central brain. Retinal expression is uniform, with no hint of expression only in specific cell types; we conclude that *Calx* is expressed in both photoreceptors and auxiliary cells. In the peripheral head, there is a sponge-like pattern of dark staining thoroughly peppered with white spots; we interpret these to be neuronal cell bodies whose nuclei do not stain. Further into the head, there is a halo of stain outlining the neuropil. In embryos, *Calx* transcripts are ubiquitously present at all stages from syncytial blastoderm to organogenesis. Since *Drosophila* embryos begin to transcribe zygotic genes at the syncytial blastoderm stage (Wilkins, 1986), their *Calx* transcripts are probably maternally loaded. Sense *Calx* riboprobes elicit no signals in embryos and weak signals in heads.

To localize Calx protein, polyclonal antisera were raised against a *Calx* peptide (C1-

15: KYMDKNYRVNKRGTC) conjugated to keyhole limpet hemocyanin (KLH). KLH-C1-15 elicted a polyclonal ascites that stains retinal and ocellar photoreceptors, as well neuropil of the optic ganglia and brain (Figure 9); no such pattern was seen with preimmune serum. Staining of photoreceptors and visual neuropil by the ascites can be specifically prevented with competing ovalbumin-conjugated C1-15, but not with ovalbumin conjugated to a different peptide (Figure 9; Methods). Given that the ascites' staining parallels the expression seen with riboprobes, we conclude that this staining actually represents Calx protein expression. However, the anti-KLH-C1-15 antiserum detects multiple bands in immunoblotted head protein, only one of which fits the predicted mass of Calx's cytoplasmic loop (~70 kD; data not shown); this may account for the diffuse background seen with competing C1-15 (Figure 9). We thus intend to generate a monospecific subset of anti-KLH-C1-15 serum through affinity purification by beads conjugated with C1-15 (Harlow and Lane, 1988).

***Calx* genomic region**. The genomic DNA from which *Calx* transcripts arise is at least 32 kb long (Figure 10); it is located in the 93B1,2 doublet of chromosome 3 (N. Bonini, pers. comm.). The 5' UTR of 9C5-E is plainly generated by splicing from a genomic region far larger than itself. The minimum 5' extent of *Calx* can be roughly defined by genomic DNA fragments that cross-hybridize to 9C5-o. This end is immediately downstream (Figure 10) of the 3' end of the $3Na^+/2K^+$ ATP-driven pump α-subunit gene (*Na-p*; Lebovitz et al., 1989), also mapped by Schubiger *et al.* (1994) to 93B1-2. *Calx* is also 14-21 kb from genomic DNA that cross-hybridizes with the plasmid-rescued insertion site of P997 (Figure 10), a lethal P element insertion isolated and mapped to 93B by Wilson *et al.* (1989). The P997 insertion clone hybridizes to a single-copy sequence in *Drosophila* genomic DNA (data not shown). P997 thus should disrupt *Na-p*.

The 3' ends of cosmids W8, W5, and S6 (Figure 10) have several EcoRI fragments with sizes identical to EcoRI fragments in the proximal genomic region of *rudimentary-like* (*r-l*), a UMP synthase gene in 93B6-7 (Eisenberg *et al.*, 1990). We accordingly probed

proximal *r-l* genomic phage DNA with a 5.0 kb EcoRI fragment from cosmid W5 (just off the 3' end of the *Calx* region in Figure 10). The W5 fragment recognized an identically sized fragment at the very proximal end of the *r-l* genomic walk, which had been chromosomally oriented by Eisenberg *et al.* (1990). This physically links *Na-p* and *r-l* via *Calx*, and yields the chromosomal orientation of both *Calx* and *Na-p* (Figure 10).

There exist three more lethal P insertions in the 93B1,2 doublet: P633 was isolated by Cooley *et al.* (1988); P1523 and P1533 were generated as gene tags in the *Drosophila* genome project (Karpen and Spradling, 1992). Furthermore, Rawls and coworkers have identified two non-allelic, chemically-induced lethal mutations in the vicinity of 93B1,2 (*l(3)rlr1* and *l(3)rlr2*; Eisenberg *et al.*, 1990). We have tested these mutations for allelism by noncomplementation (Roberts, 1987); all of the P insertions comprise a single complementation group that is distinct from both of the EMS lethals (Table 1). The Berkeley Drosophila Genome Project (pers. comm.) has very recently generated another lethal P insertion in 93B2-3, *l(3)j2B1*. At this writing it has just emerged from the Benzer laboratory's stock quarantine (Roberts, 1987); it will, like P997, be physically mapped by plasmid rescue.

Direct assays of sodium-calcium exchanger activity. The 49% identity of Calx to NCX1 does not make functional identity a foregone conclusion. Paralogous membrane proteins, despite amino acid identities of 42-55%, can still transport different molecules (e.g., GAT1/5HTT and LacY/RafB; Aslanidis *et al.*, 1989; Blakely *et al.*, 1991; Guastella *et al.*, 1990; Hoffman *et al.*, 1991; Kaback, 1992). To ascertain if Calx is a genuine sodium-calcium exchanger, we chose to express Calx in *Xenopus* oocytes (Nicoll *et al.*, 1990). Capped *Calx* cRNAs were synthesized from pXexCalx, a HindIII/SspI subclone of 9C5-E containing the major ORF (Figure 1). Plasmids encoding NCX1 and the *Drosophila* potassium channel *Shaker* (*Sh*; Hille, 1992) were used as templates for capped NCX1 and *Sh* cRNAs; these plasmids encode 5' and 3' UTRs designed to optimize cRNA translation (C. Labarca, pers. comm.; Matsuoka *et al.*, 1993). Finally, we

synthesized a template for translationally optimized *Calx* cRNAs ("PCR-Calx") by PCR. All four templates were used to make standardized aliquots of cRNA.

These cRNAs, in parallel with blank buffer, were microinjected into *Xenopus* oocytes (5 ng/oocyte). After 4.5-8 days of expression, these oocytes were loaded with internal sodium via nystatin (Holz, 1979; Longoni *et al.*, 1988), challenged with $^{45}Ca^{2+}$, washed, and assayed for $^{45}Ca^{2+}$ uptake. Calcium uptake was induced by *Calx* cRNAs (Table 2; Figure 11). This uptake occurred with external potassium or choline; however, it was absent from oocytes that were either challenged by external sodium or not loaded with internal sodium. While pXexCalx-induced uptake (2-7 times background) was significantly weaker than that induced by NCX1 (9-35 times background), an uptake overlapping NCX1's was induced by both PCR-Calx (7-21 times background) and 50 ng of pXexCalx cRNA (15 times background). The lack of a requirement for K^+ to be cotransported with Ca^{2+} is consistent with the observation of Hardie (1995) that sodium-calcium exchange in *Drosophila* photoreceptors is K^+-independent.

We observed that the sodium-unloaded controls, while they reduced calcium uptake, nevertheless permitted above-background uptake in oocytes vigorously expressing sodium-calcium exchangers (Table 2; Figure 11). We thought that this might be due to residual sodium within the unloaded oocyte: given a resting concentration of 1-6 mM for Na_i^+ (Dascal, 1987), and a K_m of 20-30 mM Na_i^+ for the cytoplasmic face of the exchanger (Philipson and Nicoll, 1993), trace $^{45}Ca^{2+}$ uptake might be possible. To test this explanation, we loaded *Calx*-expressing oocytes with lithium or potassium cations, and found that this abolished calcium uptake (Table 2; Figure 11). Aceto *et al.* (1992) had similar results with bovine NCX1.

A background uptake of 0.3-1.8 pmol of calcium per oocyte was observed after injecting 50 nl of buffer or 5 ng of *Sh* cRNA (Table 2; Figure 11). This background was small but reproducibly higher in choline$^+$/$^{45}Ca^{2+}$ or K^+/$^{45}Ca^{2+}$ versus Na^+/$^{45}Ca^{2+}$ solutions; this may be due to a *Xenopus* sodium-calcium exchanger. Longoni *et al.* (1988)

did not observe such an activity: one difference between our experiments and theirs is that we treated oocytes with horse serum prior to assay. Serum, which can improve oocyte viability and cRNA expression, can also evoke endogenous ion transporters (Quick *et al.*, 1992).

Phylogenetic analysis of *Calx* motifs. Repeated protein motifs are thought to arise through intragenic duplications, and to survive if they functionally augment their protein (Li and Graur, 1991). The analyses above imply that *Calx*-α and *Calx*-β motifs are related, but do not show the manner in which they arose. Evolutionary trees were therefore calculated for the seven proteins in Figure 2, and for their *Calx*-α/-β motifs (Figure 12-14; Methods; Hillis *et al.*, 1993). These phylogenies are based on the assumption that modern proteins and motifs evolved from a single common ancestor by undergoing the minimum number of nonsynonymous codon changes necessary, and the specific evolutionary tree consistent with this minimum is thus most consistent with the data. The *general* assumptions of this approach have been defended by Hillis *et al.* (1994). The *specific* assumption that the proteins and motifs in Figures 12-14 share a common ancestor is justified by their high z-scores when aligned as pairs (Pearson and Lipman, 1988). The evolutionary starting point (root) of each tree cannot be placed infallibly, because codon changes are reversible and because we have no previously established outgroup for any tree. However, it is possible to make plausible guesses at where the roots lie, which we have marked in Figures 12-14.

The protein tree (Figure 12) shows a trichotomy of Calx/NCX1/NCX2, RetX, and C07A9.4/C07A9.11, with no hint of any affinities bringing one group closer to another. Of 1000 bootstrap trees constructed from 1000 random subsets of each sequence set, 100% supported this branching order. This implies that the difference in stoichiometry between NCX1 and RetX reflects an evolutionary split between them that substantially antedates the fly-mammalian split (visible in Figure 12 as the splitting of Calx from the lineage leading to NCX1). The further deep branching of C07A9.4/C07A9.11 from both RetX and Calx

means that either all exchangers other than Calx/NCX1/NCX2 are evolving much more quickly than Calx, or there are *three* classes of exchangers with distinct stoichiometries of action. Two data are consistent with the latter interpretation. First, Philipson and coworkers (pers. comm.) have found that C07A9.4, when expressed in *Xenopus* oocytes, does not behave like either NCX1 or RetX; its true substrates are unknown. Second, a human cDNA has been identified with strong similarity to C07A9.4 and C07A9.11 (gnl R53500; WashU-Merck EST Project, unpub.). Despite the evolutionary distance of eubacteria from metazoa, ORF_o325 is plainly closer to RetX, C07A9.4, and C07A9.11 than to Calx. ORF_o325 is difficult to cluster with greater precision: it weakly groups with RetX instead of with C07A9.4/C07A9.11, but only with 19% confidence in 1000 bootstrap trees.

In both the *Calx*-α and *Calx*-β motif trees (Figures 13-14), N- and C-terminal motifs group together. This indicates that, for both *Calx*-α and *Calx*-β, intragenic duplication to produce two motifs in one exchanger occurred before diversification of the exchangers carrying them. In the *Calx*-β tree (Figure 14), both N- and C-terminal groups show the same branching pattern (Calx splits from an ancestral NCX, which in turn splits into NCX1 and NCX2). This pattern implies that *Calx*-β motifs appeared in sodium-calcium exchangers, and underwent a tandem duplication, before the divergence of Metazoa (≥~540 My ago; Conway Morris, 1993). The integrin *Calx*-β motifs form a third group that branches very deeply from the exchanger motifs, and upon which the mammalian radiation (indicated by the human/murine split) appears relatively recent. Therefore, the *Calx*-β motif is very unlikely to be present in integrin-β4 through a recent, functionally neutral exon shuffle; it must instead be long-standing and necessary. The *Calx*-β data set supports all but a single subbranch of this tree in Figure 14 with 97-100% reliability; since bootstrap values are conservative, the actual reliability of the NCX1-β2/NCX2-β2 group may be higher than 76% (Felsenstein and Kishino, 1993).

In contrast, the *Calx*-α motif tree (Figure 13) does not have enough evolutionary

signal to allow any one pattern of branching to be unequivocally supported. However, two groups of *Calx*-α motifs tend to segregate into distinct groups: N-terminal versus C-terminal motifs; and motifs from Calx, NCX1, and NCX2 versus those from RetX, C07A9.4, and C07A9.11. Strikingly, the N- and C-terminal ORF_o325 motifs comprise a branch of their own, which splits off from the branch leading to the RetX C-terminal motif. This finding is consistent with the ORF_o325 motifs having arisen from an intragenic duplication after the eubacterial-eukaryotic split, and with the grouping of RetX with ORF_o325 in the protein tree (Figure 12).

Discussion

Possible roles of *Calx* in vivo. Excess cytoplasmic Ca^{2+} is thought to kill cells by several possible means: titrating intracellular oligophosphates such as ATP (Carafoli, 1987); deranging calcium-dependent proteases, lipases, and DNAses (Nicotera *et al.*, 1992); generating excess free radicals (Choi, 1992); or hyperactivating protein phosphatases such as calcineurin (Cunningham and Fink, 1994). *Calx* may thus be an essential gene; indeed, one of the lethal mutations *l(3)rlr1*, *l(3)rlr2*, or *l(3)j2B1* might inactivate *Calx*. There are other purposes that sodium-calcium exchangers are thought to serve beyond mere viability. One is to quench an electrically excited cell by expelling intracellular calcium: the most studied examples to date are photoreceptors and muscle cells in both vertebrates and invertebrates (Philipson and Nicoll, 1993). A more subtle role of sodium-calcium exchangers might be to modulate synaptic transmission, by varying the rate at which calcium is expelled from axonal terminals (Blaustein *et al.*, 1991). Alternatively, sodium-calcium exchangers may act to *import* calcium into kidney tubules, neutrophils, osteoclasts, platelets, and red blood cells (Simchowitz *et al.*, 1990; Krieger, 1991; Windhager *et al.*, 1991; Milanick, 1992; Kimura *et al.*, 1993). Our data (Figure 11) show that reverse exchange is possible for both *Calx* and NCX1 in *Xenopus* oocytes, even with biologically low levels of intracellular sodium, *if* extracellular sodium is absent; but it

remains to be seen whether this capacity is actually exploited by *Drosophila* in any way. Yet another role for sodium-calcium exchange is to regulate the activity of mitochondria, by varying the levels of matrix calcium (Cox and Matlib, 1993). However, our data show that *Calx* does not have the capacity to exchange calcium for lithium, while Li *et al.* (1992) have shown that the mitochondrial exchanger does.

The role of sodium-calcium exchange in photoreception has been most thoroughly studied in mammals (Kaupp and Koch, 1992) and the horseshoe crab *Limulus* (O'Day *et al.*, 1991). In the outer segments of mammalian photoreceptors, Ca^{2+} is incessantly admitted to the cytoplasm by cGMP-gated channels that are constitutively open to both Ca^{2+} and Na^{+} in the dark. To expel Ca^{2+} under these unfavorable conditions, a $4Na^{+}/1Ca^{2+},1K^{+}$ exchanger is thermodynamically preferable to a $3Na^{+}/1Ca^{2+}$ exchanger (Cervetto *et al.*, 1989; Schnetkamp *et al.*, 1989). In contrast, Drosophila photoreceptors only depolarize when stimulated by light (Hardie and Minke, 1993), and their sodium-calcium exchangers do not require K^{+} to expel Ca^{2+} (Hardie, 1995). In isolated *Drosophila* photoreceptors, 5 light flashes over 4 minutes, with extracellular Na^{+} removed to block sodium-calcium exchange, can cause a stepwise increase in cytoplasmic Ca^{2+} without altering photoreceptor function (Ranganathan *et al.*, 1994). Since the light-induced Ca^{2+} influxes occur in a limited (subrhabdomeric) region of the *Drosophila* photoreceptor, the buffering effect of the whole cell's volume may be enough to make sodium-calcium exchange unnecessary for such limited stimuli. On the other hand, *Limulus* photoreceptors are desensitized after sodium-calcium exchange is blocked during $\geq$15 flashes spanning $\geq$1 minute (O'Day *et al.*, 1991); and *Drosophila* phototransduction requires calcium influxes for both excitation and adaptation by light (Hardie and Minke, 1993; Ranganathan *et al.*, 1994). These facts, and the expression of *Calx* in the *Drosophila* retina, suggest that Calx may adjust *Drosophila* photoreceptors to exposures of light which would otherwise irreversibly bleach them.

5' UTRs. Kozak (1991) has argued that, in mRNAs, extended 5' UTRs

containing miniature ORFs are likely to be either crossed by tenacious ribosomes or spliced away; in either case, long 5' UTRs should confer "throttled" translation upon the major ORF following them, or no translation at all. On the other hand, synthetic bicistronic mRNAs have been shown to be translatable from their second ORF (OH *et al.*, 1992). Furthermore, there exist 5' UTRs containing mini-ORFs in the mRNAs of other ion transporters and channels (Kozak, 1991), including bovine cardiac NCX1 (Aceto *et al.*, 1992). These considerations, with our data, suggest that internal ribosome priming is performed upon *Calx* mRNAs in vivo. Since the mRNAs for the $3Na^+/1Ca^{2+}$ and $4Na^+/1Ca^{2+},1K^+$ exchangers are ~3.5 kb longer than protein-coding alone would seem to require (Nicoll *et al.*, 1990; Reilländer *et al.*, 1992), extensive 5' UTRs may be necessary for some aspect of sodium-calcium exchanger gene expression.

***Calx*-α and *Calx*-β motifs: possible evolution and function.** The evolutionary trees computed for exchanger proteins and *Calx* motifs (Figures 12-14) are consistent with the following model for *Calx* evolution. Certainly prior to the last common ancestor of metazoa (Conway Morris, 1993), and conceivably much earlier (Doolittle and Brown, 1994), there existed a single sodium-calcium exchanger with six transmembrane sequences. In vivo it would have formed a dimer, as many six-spanner proteins belonging to the ABC transporter family do even today (Higgins, 1992). This would have caused the *Calx*-α motifs to oppose one another symmetrically across an internal pore spanning the membrane (Klingenberg, 1981; Kyte, 1981). The gene encoding the primitive exchanger then underwent an internal duplication, causing the exchanger to have two separate lobes folding onto one another to form a pseudodimer. There followed a series of extragenic duplications that brought the first distinct ancestors of Calx/NCX1/NCX2, RetX, and C07A9.4/C07A9.11 into being. These ancestors could then have diverged (by point mutations in their *Calx*-α sequences?) to acquire distinct stoichiometries of action.

The clustering of ORF_o325's *Calx*-α motifs is inconsistent with the general split between N- and C-terminal *Calx*-α motifs (Figure 13). There is a trace of intragenic

duplication in ORF_o325 C-terminal to its *Calx*-α motifs (not shown), which suggests that its original condition was that of a single *Calx*-α motif. It is presently impossible to date *Calx*-α evolution with respect to organismal evolution, but ORF_o325 appears to have arisen *after* the divergence of Calx from RetX, and it is not conserved between *E. coli* and *H. influenzae* (Fleischmann *et al.*, 1995). Yet the conservation and duplication of *Calx*-α motifs in ORF_o325 implies that they are functional in *E. coli*. One possible explanation is that ORF_o325 was scavenged from eukaryotes by horizontal gene transfer (Syvanen, 1994). Alternatively, *Calx*-α motifs may antedate the divergence of eubacteria and eukaryotes (Doolittle and Brown, 1994), but only have been retained in complex eubacteria.

In our model, the *Calx*-β motif arose independently of *Calx*-α, and was distributed by exon shuffling to $3Na^+/1Ca^{2+}$ exchangers and integrin-β4 subunits. The *Calx*-β motif tandemly duplicated within exchangers before metazoa diverged. Consistent with this model, NCX1 and NCX2 map to chromosomal regions descended from a single, multiply duplicated region of the early vertebrate genome (Shieh *et al.*, 1992; Lundin, 1993; Li *et al.*, 1994).

This model has nontrivial implications for the mechanism of sodium-calcium exchange. Electrophysiology has shown that both $3Na^+/1Ca^{2+}$ and $4Na^+/1Ca^{2+},1K^+$ exchangers (i.e., NCX1 and RetX) have, respectively, two or three negative charges which are totally neutralized by $Ca^{2+} \pm K^+$ passing through the exchanger (Hilgemann *et al.*, 1991; Perry and McNaughton, 1993). In both NCX1 and RetX, the passage of $(3\pm1)Na^+$ leaves a single unneutralized cation, and renders the Na^+-transport step of sodium-calcium exchange electrogenic. Furthermore, RetX may superimpose an extra monovalent cation binding step onto an exchange mechanism otherwise like that of NCX1 (Perry and McNaughton, 1993). In other words, both NCX1 and RetX appear in patch clamps to have two anions that completely neutralize either Ca^{2+} or $2Na^+$ during the sodium-calcium exchange cycle. Evolutionary parsimony suggests that such anions would be present in the

common ancestor of NCX1 and RetX; however, no location for such an anion pair has so far been proposed for either NCX1 or RetX. Our analysis shows that only one anionic (D or E) residue is completely conserved in all *Calx*-α motifs (Figure 4). According to the model above, this residue would be one member of a symmetrical pair of two invariant anions flanking the exchanger channel. The plausibility of this is increased when one observes that this D/E residue is invariably adjacent to a helix-breaking residue (generally proline, occasionally glycine; Figure 4). Such a P/G site would be well-suited to form a constricting bend in a transmembrane α-helix; this is observed in the M2 helix of acetylcholine receptors, which forms the wall of the receptor channel (Unwin, 1993). We therefore predict that these D/E residues are in fact the two anions used for Ca^{2+} and $2Na^{+}$ binding in both $3Na^{+}/1Ca^{2+}$ and $4Na^{+}/1Ca^{2+},1K^{+}$ exchange. NCX1 would, in this model, require no further anions to account for its electrogenicity, whereas RetX would require an anion not found in the NCX1 *Calx*-α motifs. In our view, the best candidate for such a third RetX anion is D_{1113} (Figure 4): it is predicted to have roughly the same altitude in the membrane as the invariant D/E residues; furthermore, it resides at a well-conserved site, yet differs from the residue seen in most other *Calx*-α motifs (asparagine).

In contrast, it is difficult to assign a function even speculatively to the *Calx*-β motif because existing data are consistent with its having any of several roles. NCX1's two *Calx*-β motifs precisely overlap a proven high-affinity Ca_i^{2+}-binding site (Figure 2; Matsuoka *et al.*, 1995). However, the protein region required for Ca_i^{2+}-binding only comprises slightly over half of the full tandem pair of *Calx*-β motifs, which has been conserved in sodium-calcium exchangers for over half a billion years (Figure 14). Thus the full *Calx*-β pair may have other roles besides Ca_i^{2+}-binding. The *Calx*-β pair overlaps with a region of NCX1 that negatively regulates NCX1 in response to elevated intracellular sodium (Matsuoka *et al.*, 1993), and that may also bind NCX1 to ankyrin (Li *et al.*, 1993). Any of the above functions would be consistent with the presence of *Calx*-β in integrin, since integrin-β4 is known to connect hemidesmosomes with the cytoskeleton (Spinardi *et*

al., 1993), yet is also suspected to mediate signal transduction (Hynes, 1992). In either case, the perinatal lethality caused by cytoplasmic truncations of human integrin-β4 (Vidal *et al.*, 1995) indicates that integrin-β4's *Calx*-β motif may be strongly selected for continued function.

Methods

General methods. Most methods roughly resembled those of Sambrook *et al.* (1989). However, modifications to "standard methods" often proved necessary. These include both minor details of procedure, and variations on the "standard methods", which collectively represent a significant deviation from Sambrook *et al.* (1989) or manufacturer's protocols.

Nomenclature and origin of *Calx*. *Calx* was previously called 9C5, one of 20 genes active in the *Drosophila* visual system (Hyde *et al.*, 1990). Because *Calx* denotes a gene product rather than a mutant phenotype, we capitalize it (Lindsley and Zimm, 1992). We selected the name *Calx* on mnemonic grounds ("*Cal*cium exchanger") and etymological grounds: *calx* (Classical Latin, "limestone") yielded the New Latin *calcium*. (Morris, 1975). We renamed the original *Calx* cDNA "9C5-o" (formerly "9C5"; Hyde *et al.*, 1990); longer *Calx* cDNAs were termed "9C5-A" through "-E." The three EcoRI fragments of 9C5-E, in 5' to 3' order, were named "9C5-E1," "-E3," and "-E2." The plasmid pXex9C5-E, used for making native *Calx* cRNAs by in vitro transcription, was renamed pXexCalx in this manuscript. The PCR-generated template 5'3'Xex9C5-E, used making for translationally optimized *Calx* cRNAs, was renamed PCR-Calx in this manuscript.

Reagents. Restriction enzymes, non-*Taq* DNA polymerases, ligases and their incubation buffers were from Boehringer Mannheim or Stratagene. *Taq* DNA polymerase was from Boehringer Mannheim or Perkin-Elmer. α-^{32}P- or α-^{35}S-labelled nucleotides were from Amersham; $^{45}CaCl_2$ was from ICN. 10x reaction salt for either PCR or serial primer elongation consisted of 200 mM Tris·HCl (pH 8.3 at room temperature) + 15 mM $MgCl_2$ + 250 mM KCl + 0.5% v/v Tween-20 + 1 mg/ml gelatin. After mixing, 10xPCR/SPE salt was autoclaved, aliquoted into disposable polyethylene tubes, and stored at -20° C. between uses. 10 mM dNTPs for PCR or SPE were obtained from the Perkin-Elmer PCR Kit. Most other reagents were obtained from Boehringer Mannheim, Fisher, Mallinckrodt, and Sigma.

All water was double-distilled on a Corning ACS Mega-PureTM system, fed by nominally distilled water from the Caltech physical plant. For purifying oligonucleotides, ersatz "HPLC-grade" water was made by filtering 500 ml of double-distilled water through a Nalgene 0.2-μm filter unit. For PCR, serial probe elongation (SPE), or solutions of cloned DNA, water was autoclaved. Frozen molecular-biology-grade phenol was purchased from Fischer Biotech in 500 g batches, melted at ≤65° C., mixed with 0.5 g 8-hydroxyquinone, and successively equilibrated with 500 ml of: double-distilled H_2O; 1 M Tris + 0.1 M EDTA, pH 8.0; and 100 mM Tris + 10 mM EDTA + 0.2% β-mercaptoethanol, pH 8.0. After checking its aqueous phase for a pH >7.6, the phenol was stored in the dark at 4° C. under equilbration buffer until use. Salmon sperm DNA was obtained as 2.5-3.0 g clumps from Sigma. Each such clump was dissolved overnight in 250-300 ml of 111 mM NaCl at room temperature; the solution was extracted and centrifuged with one volume of phenol and chloroform, sheared with a Polytron sonicator (Brinkman Instruments) at 400 W for 10 min, precipitated with 530-750 ml of 95% EtOH, washed by vortexing with 250-300 ml of 70-80% EtOH, centrifuged, air-dried for ≥10', resuspended overnight in 250-300 ml H_2O, aliquoted into 50-ml polyethylene tubes, vortexed to homogeneity, and stored at 4° C. 100% ethanol was purchased from Quantum Chemical Corporation.

Strains. The *Drosophila* strains Canton-S (wild-type; Lindsley and Zimm, 1992) and *eya*^{1} (Bonini *et al.*, 1993) were obtained from E.B. Lewis and N.M. Bonini (Cal. Inst. of Tech.); balanced single-P-insertion lethals in the 93B region were obtained from the Bloomington *Drosophila* stock center (P633, P997, P1523, P1533) or from Allan Spradling (*l(3)j2B1*); EMS-induced lethals in the 93B region (*l(3)rlr1*, *l(3)rlr2*; Eisenberg *et al.*, 1990) were obtained from J. Rawls (Univ. of Kentucky, Lexington). Fly strains were cultured at 25° C. by standard methods (Roberts, 1987) on the food medium of Lewis (1960). The *E. coli* strains C600, Y1090, and VCS257 were from Stratagene; the strain DH10B™ (Grant *et al.*, 1990) was from Gibco BRL. We found DH10B to be preferable

for electrotransformation and γδ-mediated sequencing, on account of both its lack of enzymes hostile to cloned DNA and its streptomycin resistance.

Isolation of DNA restriction fragments. For radiolabelling or subcloning, DNA restriction fragments were purified by electrophoresis through low-melt agarose (BRL or FMC; Sambrook *et al.*, 1989). To remove agarose efficiently, freshly melted gel slices (at ~55° C.) were extracted with phenol before standard phenol-chloroform and chloroform extractions. To abolish trace contamination by aberrantly comigrating DNA, desired DNA fragments were run through two successive gels with different concentrations (typically a succession of 1.0% and 0.7% gels, grafting razor-excised DNA fragments into the 0.7% gel with ~10 ml of molten 1.0% low-melt agarose).

Blots, radioactive probes, autoradiography, and radiolabelling. DNA blots were done essentially as in Sambrook *et al.* (1989), onto reinforced nitrocellulose or Hybond-N paper; RNA blots are described below. Both DNA and RNA blots were stored in plastic wrap at -20° C. between uses. Radioactive probes were made at a final concentration of $0.5\text{-}2.0 \cdot 10^6$ cpm/ml, $1.0 \cdot 10^6$ cpm/ml being preferred. 6xSSPE + 5x Denhardt's solution + 0.1 (mg/ml) boiled/sonicated salmon sperm DNA + 0.1-0.5% SDS was generally used as the hybridization buffer for both DNA and RNA blots; the original isolation of *Calx* cDNAs used 4xSET (0.6 M NaCl + 0.12 M Tris + 8 mM EDTA, pH 7.0) instead of 6xSSPE. Autoradiography was at -70° C. with X-omat AR film (Kodak) and optional intensifying screens (Du Pont); cardboard exposure holders (Kodak) were preferred to steel because they thawed more readily. Double-stranded ^{32}P-DNA probes were produced with the Random Priming Kit of Boehringer Mannheim (Sambrook *et al.*, 1989). Generally, ^{32}P-α-dCTP was the radioactive nucleotide; the original isolation of *Calx* cDNAs was done with ^{32}P-α-dATP.

Single-stranded radioactive probes. Single-stranded, ^{32}P-DNA probes were generated by repeatedly extending ^{32}P-α-dCTP-labelled DNA from an oligonucleotide annealed to a denatured double-stranded DNA template ("serial probe elongation," or SPE).

Equal volumes of H_2O, 10 mM dATP, 10 mM dGTP, and 10 mM dTTP were mixed to make "SPE-dNTPs" and stored between uses at -20° C. Immediately before each SPE, solutions A and B were mixed. Solution A: 4.2 µl 10x PCR/SPE rxn. salt; 1.0 µl (100 ng/µl) DNA template; *either* 2.3 µl 20 µM oligonucleotide plus 0.5 µl H_2O, *or* 2.8 µl H_2O; and 0.6 µl SPE dNTPs. Solution B: 4.0 µl 10x PCR/SPE rxn. salt; *either* 35.5 µl H_2O; *or* 10.4 µl 20 µM oligonucleotide plus 25.1 µl H_2O; and 0.5 µl 5 U/µl *Taq* DNA polymerase. The following were then mixed by pipetting in an autoclaved 500 µl Eppendorf tube: 0.5 µl solution A; 0.5 µl solution B; and 1.6 µl ^{32}P-α-dCTP (Amersham). 40 µl of mineral oil was then added, and the total mixture was microfuged down briefly to form an airtight droplet under oil. In a Perkin Elmer thermal cycler, the reaction tube was first heated to 94° C. for 5', and then cycled 35 times through 94° C. (for 1.0-1.5'), T_{ann}° (for 1.0-1.5'), and 72° C. for t_{clong}'. T_{ann}° generally is set at 5° C. below the estimated half-dissociation temperature (T_{diss}°) for the oligonucleotide as defined by either of two formulae in Sambrook *et al.* (1989). t_{clong} equals the length of the template in kb, rounded up to the nearest minute. T_{ann}° and t_{clong}' can range from 55°-72° C. and 1.0'-4.0' in a normal SPE.

Screening phage and cosmid libraries. We obtained a subclone of the 9C5-o cDNA in pBluescript ("p9C5-o") from K. Mecklenburg (U. Indiana, South Bend). p9C5-o consists of both a directional cDNA (with EcoRI and XbaI ends) and a ~13-bp EcoRI-XbaI fragment, subcloned into an EcoRI site. To screen phage libraries, 9C5-o DNA was amplified from p9C5-o by PCR, using the commercially available M13 -20 and M13 REV oligonucleotides (USB) and the PCR conditions of Ballinger and Benzer (1989); 9C5-o DNA was then isolated from the purified PCR products, and radiolabelled. *Calx* cDNA phage clones were obtained from $2.2 \cdot 10^6$ plaques of a *Drosophila* adult head cDNA library in the phage λgt11 (Itoh *et al.*, 1985), by cross-hybridization to 9C5-o. cDNA phage were first propagated in VCS257 (a derivative of DP50 *supF*; Stratagene); later Y1090r was used (Sambrook *et al.*, 1989). Each recombinant phage was rescreened until

all plaques were distinguishable and positive; this prevented trace contamination of positive plaques by diffusing non-positive phage. *Calx* genomic clones were obtained by screening ~33,000 colonies from the cosmid library of Tamkun *et al.* (1992) with radiolabelled 9C5-E DNA. Hybond-N or reinforced nitrocellulose was used for plating and rescreening both phage and cosmid clones.

Mapping *Calx* genomic DNA. Partially overlapping cosmid clones that collectively spanned the *Calx* locus were digested with EcoRI or HpaI, gel-electrophoresed through agarose + 1xTBE + EtBr (Sambrook *et al.*, 1989), and photographed. To resolve ≥10-kb fragments differing by ~1 kb, digests were electrophoresed through 0.5% w/v agarose; otherwise 0.7-1.0% agarose was used. Gels of all fragments at all resolutions were blotted and probed with 9C5-o, -E1, -E2, or -E3. EcoRI and HpaI fragment maps were deduced from DNA fragments, based on their being shared between cosmids and on their cross-hybridization to cDNA segments. Doublets were deduced from disparities between the EcoRI and HpaI maps, and confirmed by visually comparing their fluorescent intensity to neighboring DNA bands; in one case a doublet was rechecked by laser-scanning its photograph. The EcoRI and HpaI maps were then fused into a single map by double-digestion of gel-isolated DNA fragments.

The insertion site of P997 (Wilson *et al.*, 1989) was cloned by plasmid rescue: high-molecular-weight P997 genomic DNA was isolated from adult heterozygotes (Ashburner, 1989b), digested with SalI, autoligated (Collins and Weissman, 1984), and electrotransformed into DH10B, yielding a subclone of the P997 locus. This was gel-isolated and mapped to the 5' end of the cloned *Calx* genomic region by cross-hybridization to DNA blots.

Isolating phage DNA. Our protocol was derived from that of E. Hafen (Rubin Lab Manual). 10 µl of phage plate lysate were mixed with 300 µl of bacteria (grown overnight in LB + 0.2% w/v maltose), incubated 10-15', mixed with 9 ml molten NCZYM top agarose, pipetted onto a 150 mm NCZYM agarose plate, allowed to gel, and grown at

37° C. for ≥6 hours (Sambrook *et al.*, 1989). The plates were layered with 10 ml 1xTM10 (5 mM Tris + 5 mM $MgSO_4$, pH 7.5) and 0.1-1.0 ml chloroform, and incubated (preferably with gentle shaking) at 4-6° C. for ≥2 hours. 2 ml of 1xTM10 were added to the eluate, which was then pipetted off; a second 2 ml of 1xTM10 were used to rinse the plate and pooled with the eluate in a Falcon 2059 tube. Bacterial debris was removed by centrifugation for ~10' at 8000 rpm in a Sorvall centrifuge. DNAse I (final concentration, 1 μg/ml) and RNAse A (f.c. 2 μg/ml) were mixed with the supernatant in a fresh 2059 tube by gentle inversion, incubated at 37° C. for ≥30', and split into a second 2059 tube. An equal volume of 20% w/v polyethylene glycol + 1xTM10 + 2 M NaCl was mixed during the incubation, and then added to the nucleased phage suspensions; these in turn were mixed by inversion and cooled to 0-6° C. for ≥2 hours. The phage generally formed a slurry if precipitated overnight; slurried phage were centrifuged at 8000 rpm in a Sorvall for ~≤5', while unslurried phage required 20'. The split PEG-phage pellets were rejoined in 500 μl 1xTM10, mixed with one volume of chloroform by vortexing, and microfuged at 4-6° C. for 3-5'. The upper phase was removed, mixed with 2.5 μl 20% SDS and 5.0 μl 0.5 M EDTA, incubated at 65-70° C. for ≥10', and extracted with one volume each of phenol, phenol-chloroform, and chloroform. We found that phenol is essential and that, contrary to Hafen, extractions must be done with *vigorous* vortexing. Purified phage DNA was precipitated by inversion with one volume isopropanol, washed by vortexing with 70% EtOH, air dried for 10', and resuspended overnight at 4° C. in 50-100 μl of TE plus 0.1 μg/μl DNAse-free RNAse A (Sambrook *et al.*, 1989). The resuspended DNA was incubated at 37° C. for ≥30', *re*extracted with one volume of phenol-chloroform and chloroform, precipitated with 10 μl 3 M sodium acetate plus 110 μl isopropanol by inversion, washed and air dried as before, and resuspended in 50 μl TE overnight at 4° C. With this procedure, we find that ~80-bp fragments of 50 kb cDNA phages can be gel-isolated from a double miniprep, essentially no minipreps are indigestable by restriction enzymes, and many DNAs can be prepared in parallel.

Preparations of plasmid and cosmid DNA. Minipreps of plasmid DNA were done roughly by the alkali method of Sambrook *et al.* (1989); lysozyme was used to predigest cells (Maniatis *et al.*, 1982). Large scale preparations of both plasmids and cosmids were done largely by the alkali method of Sambrook *et al.* (1989), but with these variations: EtBr + CsCl + crude DNA solutions were separated from their crude protein precipitates by centrifugation in an HB-4 (typically 8000 rpm for 15 minutes); solutions were brought up to at least 11.0 ml by added EtBr + CsCl buffer; balanced aliquots of ~5.5 ml of each EtBr + CsCl + DNA solution were used to load pairs of VTi65 tubes completely (Beckman), which were then heat-sealed; centrifugations were carried out at 53,000 rpm for ≥18 hours in a Beckman LB-M ultracentrifuge; and only one CsCl centrifugation was carried out.

Restriction digests, transformations, and ligations. These generally followed Sambrook *et al.* (1989).

We found that multiple restriction digests were most easily done with the modified KGB buffer of Stratagene (1x concentrations: 0.1 M potassium acetate + 25 mM Tris-Acetate, pH 7.6 + 10 mM magnesium acetate + 0.5 mM β-mercaptoethanol + 10 μg/ml DNAse-free bovine serum albumin). KGB concentrations for a given set of enzymes were selected by consulting Sambrook *et al.* (1989).

Chemical transformations of *E. coli* roughly followed Protocol II of Sambrook *et al.* (1989). Electrotransformations of *E. coli* were performed with a Bio-Rad Gene Pulser™ and Pulse Controller; cells were prepared for electrotransformation by the Bio-Rad protocol. We preferred to use ultra-pure redistilled glycerol (Gibco BRL) for this, in the suspicion that trace contaminants from less fastidious glycerols may impair transformation. We found DH10B™ (Gibco BRL) greatly superior to DH5α (Sambrook *et al.*, 1989) as a recipient *E. coli* strain.

Some *Calx* cDNA fragments proved difficult to ligate into the sequencing vector pMOB (Strathmann *et al.*, 1989). This may be because pMOB, having been reduced to

indispensable sequences, lacks plasmid sequences that stabilize large plasmid inserts (C. Martin, pers. comm.). Difficult ligations were sometimes achieved by coprecipitating the vector and insert to be ligated, resuspending them in a 1.5-µl volume of 1xT4 ligase buffer and 0.1 Weiss U/µl of T4 DNA ligase (both from Boehringer Mannheim), sealing them from evaporation with 40 µl of light mineral oil, and incubating the "microligation" for ≥16 hr. at 16° C. This concentrated ligands fivefold without requiring more DNA.

Oligonucleotide synthesis, purification, and quantification. Oligonucleotides were synthesized in 0.2-µM quantities on a Cyclone Plus DNA Synthesizer (Millipore). Oligonucleotides to be used for PCR were synthesized with their trityl groups on, and purified by NENsorb chromatography (Johnson *et al.*, 1990). Oligonucleotides to be used exclusively for DNA sequencing were sometimes synthesized with trityl groups off and used without purification. All oligonucleotides were resuspended after their final lyophilization in T_{10} (10 mM Tris, pH 8.0) and stored at -20° C. when not in use. NENsorb-purified oligonucleotides were UV-quantitated by the ε coefficient of Sambrook et al. (1989), as defined on page 11.30; unpurified oligonucleotides were roughly quantitated in the same way, by a "crude" ε coefficient defined as half that of pure oligonucleotides (based on a guess that 50% of unpurified UV-chromophores were unwanted by-products).

PCRs. Amplification of the 9C5-o insert for phage screening from p9C5-o was performed as in Ballinger and Benzer (1989). All other PCRs were performed on the Perkin-Elmer Cetus thermal cycler, with the following concentrations of reagents: 1xPCR/SPE reaction salt, 0.2 mM for each dNTP, 1 µM for each oligonucleotide, and ≥25 mU/µl for Taq DNA polymerase. Reaction cocktails were first mixed from aliquots of concentrated stock solutions and then mixed with individual templates; negative control PCRs, consisting of aliquoted reaction cocktail without a template, guarded against spurious amplification. All reaction components were pipetted during PCR assembly with Aero-Gard filter-blocked micropipet tips (VWR), after these became available.

Isolation of variable cDNA regions. The cDNA library of Zinsmaier *et al.* (1990) was screened with 9C5-E3 DNA; ~40 positive plaques were picked and stored at 4° C. PCRs were performed directly on 1 µl aliquots from each plaque's eluate, with the oligonucleotides 5'VarI and 3'VarI. These oligonucleotides were designed to detect alternative splicing of *Calx* ORFs, on the basis of variation between canine cardiac NCX1 and rabbit renal NCX1 (Figure 3). 5'VarI (5'-CCIG-GAT-CCIG-GCG-AAC-TTG-TCT-TCG-AA-3') was directed against the antisense strand encoding GELVFE, with a CC clamp and BamHI site; 3'VarI (5'-CCIT-CTA-GAIC-TTG-TCG-ACT-GTA-GCC-TT-3') was directed against the sense strand encoding KATVDK, with a CC clamp and XbaI site. 19 plaques gave products when used as templates for high-fidelity PCR (Barnes, 1993). These were gel-purified and sequenced directly with 5'VarI and 3'VarI; 14 products have been sequenced at this writing. The near-identity of all 14 PCR products to 9C5-E confirms that they represent *Calx* cDNAs.

DNA sequencing. Both strands of 9C5-E were sequenced. The bulk of sequencing was done upon EcoRI fragments of 9C5-E in pMOB; to determine their order in 9C5-E, and ensure that small internal EcoRI fragments were not being overlooked, we sequenced across internal EcoRI sites in a KpnI-SacI subclone containing the entire 9C5-E cDNA, plus ~1 kb of flanking λgt11 DNA on each side, as a single fragment in pBluescript. The sequences were read into a VAX and assembled manually, using the Wisconsin Package (Genetics Computer Group, 1991). DNA sequencing reactions were performed on double-stranded templates with Sequenase 2.0 (USB) and S^{35}-α-thio-dATP, essentially as advised by USB. Sequencing reactions were electrophoresed at ≥2000 V, through 60-cm x 20-cm x 0.2 mm gels composed of either 5-6% acrylamide or Long Ranger matrix (AT Biochem). Gels were either dried immediately after electrophoresis, or dried after fixation with 15% acetic acid and 30% *ethanol* to avoid methanol toxicity. Autoradiography was at room temperature in steel exposure frames with XAR film (Kodak).

Initial sequencing was performed on the ends of inserts subcloned in pBluescript with the -20 and REV oligonucleotides. Most sequencing of 9C5-E's EcoRI fragments was performed by subcloning DNA fragments into pMOB and creating sequencing sites throughout the insert with γδ-transposons (Strathmann *et al.*, 1991). Residual gaps in the γδ-derived 9C5-E sequence, the full 9C5-o sequence, and the sequences of variable cDNA PCR products were determined at the Caltech Sequencing Facility with gene-specific oligonucleotides.

We modified the original transposon-facilitated sequencing technique of Strathmann *et al.* (1991). First, our recipient strain was DH10B instead of JGM, and was selected with streptomycin at 50 μg/ml instead of with kanamycin. Next, possible derivative clones were picked directly from the mating plate with sterile toothpicks and resusupended in 100 μl of sterile LB, for short-term storage at ~6° C. and for PCR-screening. 120 possible derivative clones were picked. The first 24 clones picked were then screened by PCR as in Strathmann *et al.* (1989), with 1 μl from each resuspended derivative as a PCR substrate; typically, this would yield a set of derivatives adequate to sequence ~70%-100% of an insert. The remaining ~≤30% was then provided with derivatives, if need be, by PCR-screening the next 96 derivatives: 12 8-μl mixtures of 1-μl aliquots from 12 sets of 8 resuspended derivatives were made, and 1 μl of each mixture was then subjecting to mapping PCRs as if it represented a single colony. While in some cases the PCR products were unintelligible, in other cases multiple, discrete products arose that could be screened to identify rare γδ-insertions into coldspots within the derivatized insert. Where a set of 8 derivatives displayed a possible coldspot insertion, its members were then reexamined by PCR individually. In this manner, we saturated most of the *Calx* cDNA 9C5-E with γδ-insertions. Regions that resisted any γδ-insertions were sequenced by gene-specific oligonucleotides, as were the junctions of internal EcoRI sites in the subclone pBloc9C5-E.

Once selected for sequencing, derivatives were isolated from their resuspensions by streaking to clonality on LB Amp agar plates with sterile toothpicks, and permanently

stored at -80° C. in 15% w/v glycerol (Sambrook *et al.*, 1989). Derivative DNA was prepared for sequencing by culturing the derivatives in Super Broth (25 g/l Bacto-Tryptone + 15 g/l Bacto-Yeast + 5 g/l NaCl) + 100 μg/ml ampicillin before minipreps, and by thorough purification of miniprepped DNA (an extra phenol extraction of the alkaline lysate, and an extra phenol-chloroform purification of the DNA after resuspension in TE + 20 μg/ml RNAse A). Orthodox alkaline minipreps of γδ-derivatives yielded blurry sequencing reactions; orthodox boiling minipreps gave no visible sequencing products at all. In sequencing, ambiguities and compressions were resolved by resequencing with dITP or aza-dGTP. We found that aza-dGTP was essential for readable sequencing ladders from γδ-derivatives, perhaps because the γδ primer sites are C/G-rich and readily form secondary structures when sequenced with dGTP; we thus used aza-dGTP for most DNA sequencing.

Sequence analysis. The GCG Package was used to analyse the major ORF of 9C5-E (Genetics Computer Group, 1991). All analytical programs were operated with standard defaults. BLASTX and BLASTP were performed at the National Center for Biotechnology Information using the BLAST network service (cruncher.nlm.nih.gov). Possible membrane-spanning sequences were initially predicted as in Eisenberg *et al.* (1984). Where such sequences appeared in only one of several homologous positions, they were disregarded; and where naive predictions placed two spanners adjacent to one another (sterically implausible), slightly suboptimal sites were chosen that had a more physically plausible spacing. Signal sequences were predicted by SigCleave (von Heijne, 1986). Potential protein kinase C phosphorylation sites were predicted by Prosite (Bairoch and Bucher, 1994) and checked for conservation manually. For general purposes of description, the amino acid identities of entire proteins were calculated by GAP; contrariwise, for describing multiple alignments, identities were instead calculated solely from sequence regions actually aligned within ungapped blocks (Figures 2, 4).

Intragenic repeats in the Calx protein (*Calx*-α and *Calx*-β) were first detected by

dot-matrix analyses. They were further defined by reiterated Needleman-Wunsch alignments. A later influx of sequence data (Kennel *et al.*, 1993; Li *et al.*, 1994; Plunkett, unpublished, Genbank ECOUW67; Wilson *et al.*, 1994) rendered these methods plainly inadequate. We thus globally aligned all suspected Calx homologs by the MACAW program (Schuler *et al.*, 1991; version Mac68K was obtained by anonymous ftp from ncbi.nlm.nih.gov). Global protein alignments were achieved solely by segment pairing; redefining the intragenically repeated *Calx*-α and *Calx*-β elements also required Gibbs sampling (Lawrence *et al.*, 1993). The significance of all pairwise alignments, whether of entire protein sequences or of sequence motifs, was verified by RSS (Fasta v1.6c2; available from W.R. Pearson at wrp@virginia.edu). RSS is an improved version of the RDF2 program (Pearson and Lipman, 1988) which uses a rigorous Smith-Waterman calculation to score similarities (Huang *et al.*, 1990). In each RSS run, 200 local shuffles were performed with a window size of 10 residues, and with the BLOSUM62 matrix rather than a PAM matrix (via the "-s" option) to maximize sensitivity (Henikoff and Henikoff, 1992).

Generating phylogenetic trees of *Calx* motifs. Proteins and motifs were multiply aligned (Figures 2, 4). Before analysis with RSS or PAUP, a *concatenated derivative* of each sequence was generated by excising those portions of a protein or motif unshared by all known homologs, and then fusing the remainder to form a single conserved subsequence. This removed regions that might be randomized with respect to evolution, while preserving sequence alignments. Concatenated derivatives were then used as the basis for trees measured in *minimal replacements*: the minimal number of nonsynonymous changes in codons necessitated by an evolutionary tree was computed from the tree's topology (Swofford, 1990; Maddison and Maddison, 1992).

We justify this approach by two suppositions. First, concatenated derivatives probably represent protein regions in which most changes are functionally important, and thus only tolerated by evolution when they are (rarely) beneficial. Second, while excess

mutations may have *actually* occurred in the divergence of two taxa, the most *probable* path of divergence between taxa is the most direct one: i.e., that path requiring a minimum of codon changes. In other words, we assume that the DNA sequences encoding the proteins and motifs analyzed in Figures 12-14 have had no significant constraints on their evolution other than (1) an improbability of nonsynonymous codon changes and (2) a very great improbability of redundant nonsynonymous codon changes, so that their phylogenies can be sensibly constructed on the basis of parsimony (Hillis *et al.*, 1994; Swofford, 1990). Other approaches exist that are statistically more sophisticated than ours (Felsenstein, 1988); but we are unconvinced that they are necessary in this instance, since empirical and computational evidence shows that parsimony is both reliable and sensitive (Hillis *et al.*, 1994).

Phylogenic analyses of the sevenfold conserved regions of Calx *et al.*, or of the *Calx*-α and -β repeats, were performed by Paup 3.0o (Swofford, 1990) using the modified PROTPARS matrix of Swofford (1990) in which non-contiguous serine codons are distinguished. Each sequence set was first checked for the presence of evolutionary signal by computing the skew (g_1) of the distribution of its possible tree lengths, since evolutionarily informative sequence sets (which preserve evolutionary information) display more negative skews than those from uninformative sets (which, over time, have become randomized with respect to evolutionary history; Hillis and Huelsenbeck, 1992). Each data set yielded a skew indicating a >99% probability that its most parsimonious tree would resemble its true phylogeny (Figures 12-14). For trees containing 7-8 taxa, skews were obtained by exhaustive searching with PAUP (Figures 12, 14). For a tree containing 14 taxa (Figure 13), skew was calculated by using PAUP 3.1 (Mark Siddall, University of Virginia) for an exhaustive search with the following required groupings: [(Calx-α1, (NCX1-α1, NCX2-α1)), RetX-α1, (C07A9.4-α1, C07A9.11-α1), ORF_o325-α1, (Calx-α2, (NCX1-α2, NCX2-α2)), RetX-α2, (C07A9.4-α2, C07A9.11-α2), ORF_o325-α2]. This constraint on groupings was imposed in order to demonstrate that, even after

subtracting the contribution of obvious groupings, phylogenetic signal remains in the *Calx*-α motif data. We also calculated the lengths of 10,000 unconstrained equiprobable random trees for Figure 13 by MacClade (Maddison and Maddison, 1992), after which their skew was calculated by StatView II SE+Graphics (Abacus Concepts Inc.) The g_1 value obtained (-0.97) was even stronger than that obtained for constrained trees (-0.44).

We thus proceeded to calculate the most parsimonious set of trees for each sequence set (Figures 12-14), by selecting for minimal tree-length through either exhaustive or branch-and-bound searching. Confidence levels for trees were obtained by bootstrapping (Felsenstein and Kishino, 1993): 100-1000 bootstrap trees per data set were generated and compiled by PAUP into a consensus tree, with each branch assigned a percentage of individual trees that supported it. Bootstrap trees were generated by branch-and-bound for the tree in Figure 12, and by heuristic search (using tree-bisection-reconnection branch-swapping and 3-10 random addition sequences per bootstrap tree) for the trees in Figures 13-14. It is important to note that we chose, for Figures 12-14, the shortest tree (out of several which were at or near the minimum length) that was *topologically identical* to the consensus tree derived by bootstrapping. For the *Calx*-β motifs, this was in fact the absolutely shortest tree possible. For the proteins and *Calx*-α motifs, this was a tree only *one* step longer than the absolutely shortest possible tree. In these latter two cases, the alternative trees in question were hundreds of steps long, and the tree we actually chose was in a small subset of trees that clustered near the tree-length minimum. Given these conditions, we considered a tree of slightly over minimal tree-length, topologically matching the bootstrap consensus tree, to be rationally preferable to a barely shorter tree that did not match.

Predictions of secondary structure were performed by the PHD neural network system (Rost and Sander, 1994; predict-help@embl-heidelberg.de). The PHD server was fed an alignment identical to that in Figure 2, except that all protein segments not aligned with Calx in a block were first deleted from the alignment. Similar alignments of the N-

and C- terminal *Calx*-α and -β motifs from Calx, shown in Figure 4, were also sent to the server. The resulting structural predictions are shown in Figures 2 and 4, with the following caveats. First, since predictions about the *Calx*-α and -β motifs are based upon greater evolutionary depth, they were taken to supercede predictions based on the Figure 2 alignment where a conflict arose. Second, since the PHD server is intended solely to predict globular structures, any prediction from it was overridden by a predicted transmembrane sequence (Eisenberg *et al.*, 1984).

RNA. All aqueous solutions to be used with RNA were rendered RNAse-free by filtering them through two 0.2-μm nitrocellulose Nalgene filter units in series. RNA was electrophoresed through formaldehyde-MOPS gels according to Sambrook *et al.* (1989); the modifications of Tsang *et al.* (1993) were used in Figure 7 to enhance gel resolution. Equal loading of RNAs was primarily ensured by UV-quantitation, but rechecked with *RpA1* probes. The *ninaE* and *RpA1* genes (Lindsley and Zimm, 1992) were obtained as subcloned cDNA and genomic DNA (p5D; Qian *et al.*, 1987) clones from K. Zinsmaier (Caltech) and M. Jacobs-Lorena (Case Western Reserve); each was subcloned into pBluescript for further use (Sambrook *et al.*, 1989). Double-stranded *ninaE* and *RpA1* ^{32}P probes were made, mixed, and hybridized to RNA blots (Figures 6-7). This was done to check both against contamination of non-*eya*$^{+}$ head RNA with retinal transcripts and against unequal loading of RNAs. We observe what we guess to be a five-fold elevation of steady-state *RpA1* in adult bodies with respect to adult heads (Figure 7); this is probably due to elevated synthesis of ribosomal proteins in *Drosophila* ovaries with respect to most other (nonmitotic) adult fly tissues (Al-Atia *et al.*, 1985).

To harvest adult fly tissues for RNA extraction, wild-type or *eya*^{1} adult *Drosophila* were collected, and stored at -70° C. in 50-ml Corning polyethylene tubes. The tubes were struck forcibly several times against a benchtop (snapping adult heads, legs, etc. from adult bodies) and rechilled in liquid nitrogen. The detritus was passed through a stack of N_2(l)-prechilled 800 μm and 300 μm nylon meshes over dry ice, separating bodies (retained in

the 720 μm mesh), heads (405 μm mesh), and legs, etc. (into the dry ice). Wild-type bodies were stored in a second tube, rechilled with N_2(l), and stored at -70° C. for later extraction; *eya*^{1} bodies were discarded; heads of either genotype were extracted immediately after harvesting.

Bulk RNA was extracted from ~2 g of frozen fly tissues as follows. Tissues were ground to powder by hand, with a Coors mortar (and pestle) resting in (or precooled by) liquid nitrogen. The powder was poured on top of a slowly stirring 60 ml aliquot of CHAOS buffer (4.2 M guanidinium thiocyanate + 0.5% w/v N-laurylsarcosine) with 420 μl of freshly added β-mercaptoethanol. The stirring was then sped up to force the powder into solution immediately. Dissolved fly powder was further liquefied by two or more passes of an "A" pestle in a Wheaton homogenizer. The liquid was then split into five 50-ml Nalgene polyethylene tubes, each containing 20 ml phenol-chloroform and 12 ml PEB (0.1 M Tris + 10 mM EDTA + 1% w/v SDS, pH 8.0); the tubes were mixed by gentle inversion and centrifuged for ≥10' at full speed in a Damon tabletop centrifuge. Two more extractions were performed with phenol-chloroform and chloroform; the RNA was then precipitated with 5x24 ml isopropanol overnight at -20° C. The bulk of solution was decanted; 5x~8 ml of loosely precipitated nucleic acids and their mother liquor were then transferred to Falcon 2059 tubes, centrifuged at 8000 rpm in a Sorvall centrifuge for ≥5', washed by vortexing with 80% EtOH, recentrifuged, air-dried for ~3', and resuspended in a final volume of 9 ml TE.

Poly(A)$^+$ RNA was selected from bulk RNA with oligo-dT cellulose tablets (Invitrogen). Bulk RNA-TE was heated to 65° C. for ≥5', cooled to room temperature in a water bath, and mixed with 1 ml of 5 M NaCl. An oligo-dT tablet was then dissolved in the RNA-NaCl-TE, rocked for 15-30', and centrifuged at 4000 rpm in an HB-4 rotor (Du Pont) for 5'; ~9.5 ml of supernatant was transferred to a fresh tube, reheated to 65° C. and recooled, and reselected with the oligo-dT cellulose. The supernatant was then discarded; the oligo-dT cellulose was washed twice with 10 ml TEN_{500} (10 mM Tris + 1 mM EDTA

+ 0.5 M NaCl, pH 8.0). The bulk of the supernatant was removed; ~0.5 ml oligo-dT cellulose in TEN_{500} were transferred to an Eppendorf tube, microfuged, dried, and washed with 500 µl TEN_{100} (10 mM Tris + 1 mM EDTA + 0.1 M EDTA, pH 8.0). To elute poly(A)$^+$ RNA, four aliquots of 500 µl TE were preheated to 65° C. in Eppendorf tubes, and successively mixed with the oligo-dT cellulose. The first three were microfuged clear of most cellulose, and transferred to fresh tubes. The fourth was kept in the original tube. All four aliquots, in their order of elution, were then spun through an Invitrogen microcentrifuge spin column to rid them of remaining cellulose. All cleansed aliquots were removed to fresh Eppendorf tubes, and precipitated with 30 µl 3.2 M sodium acetate (pH 5.0-5.2) and 550 µl isopropanol at -20° C. for ≥1 hour. After microfuging ≥30' and vortexing/microfuging in 80% EtOH, the RNA was air-dried ≥10', resuspended in 4x 5 µl TE, and pooled. A 1-µl aliquot of the final solution was quantitated by UV spectrophotometry at a 1:100 dilution in H_20; the remaining RNA was stored at -70° C.

0.24-9.5 kb molecular weight markers (Gibco BRL) were mixed with 1.0 µl 1 µg/µl ethidium bromide (EtBr) just before heating to 65° C. and loading into the gel. We found no difference in mobility between markers prestained with EtBr and those stained/destained in an fully run gel, whether the formaldehyde distribution of Sambrook *et al.* (1989) or of Tsang *et al.* (1993) is used (data not shown.) For tests of cRNA integrity, cRNA aliquots were prestained with EtBr and then photographed in the completed gel. For RNA blots, the unstained poly(A)$^+$ RNA was blotted onto Hybond-N paper overnight with 20xSSPE, cooked in vacuo for ≥2 hours at 80° C., and cross-linked by 60 seconds of irradiation atop a UV transilluminator (Ultra Violet Products, Inc.). The blot was then photographed with UV light. RNA molecular weight markers, having retained their EtBr, fluoresced on the blot: this provided both proof of efficient blotting and a permanent record of the markers' final position. Blots were stored at -20° C.

cRNA templates and syntheses. A plasmid template for *Calx* cRNAs ("pXexCalx") was made as follows. A ~3 kb HindIII-SspI fragment was gel-isolated from

digested pBloc9C5-E; HindIII/EcoRV-digested pBluescript SK+ was gel-isolated from its severed polylinker; these two molecules were then ligated to one another via successive intermolecular cohesive-end and intramolecular blunt-end protocols (Sambrook *et al.*, 1989; Collins and Weissman, 1984), and transformed into DH5α. A successful transformant was isolated carrying the HindIII-SspI 9C5-E fragment antisense to the *lacP* promoter of pBluescript SK+. pXexCalx can be propagated in the *lacI*- host DH5α; in contrast, *Calx* subclones in pBluescript KS+ proved inviable in DH5α, perhaps because of trace *Calx* expression from *lacP*. A plasmid template for translationally optimized NCX1 cRNAs ("exchanger clone M"; Matsuoka *et al.*, 1992) was obtained from K. Philipson (UCLA); one for *Shaker* cRNAs ("H4 NcoI") was obtained from C. Labarca (Caltech); these templates were transformed into XL-1. pXexCalx, ex. clone M, and H4 NcoI were miniprepped and linearized with SacI (pXexCalx) or HindIII (ex. clone M and H4 NcoI). Digested pXexCalx was polished with T4 DNA polymerase to prevent artifactual transcripts from protruding 3' ends (Sambrook *et al.*, 1989). Linearized templates were then extracted with phenol-chloroform and chloroform, precipitated with 3 M sodium acetate and isopropanol, washed with 70% EtOH, and resuspended in TE; all reagents after the chloroform extraction were RNAse-free.

A template for translationally optimized *Calx* cRNAs ("PCR-Calx") was constructed by a method similar to that of Mager *et al.* (1993), as follows. The oligonucleotides 5'Xex (5'-GCG-CGT|-AAT-ACG-ACT-CAC-TAT-AGG-GAG-A|TA-ATT-TTC-TTT-CAA-ATA-CT|G-CCA-CCA-TG|C-AGT-TGC-TCC-TTA-AAT-C-3') and 3'Xex (5'-$[TTT]_6$-TT|A-GCT-TCT-AAG-TAT-CGG-TTA-CGT-CTG-TT-3') were synthesized, NENsorb-purified, quantitated, diluted to 20 μM in T_{10}, and stored at -20° C. between uses. 5'Xex consists of the following elements, separated by staves above: a GC-clamp and landing space for T7 RNA polymerase; a T7 promoter (Dunn and Studier, 1981); nt 26-7 from the 3' end of the alfalfa mosaic virus 5'UTR (Jobling and Gehrke, 1987); an optimal vertebrate initiation site for translation (Kozak, 1991); and nt 4-20 of the

Calx major ORF (Figure 1). 3'Xex consists of the template for an A_{20} cRNA tail, and antisense nt 120-94 of the *Calx* 3' UTR (Figure 1). 5'Xex and 3'Xex were then used in a 800-µl PCR mix at a final concentration of 1 µM, other reagents being standard (see above); as template, we added 43 ng of the ~3.0 kb HindIII-SspI 9C5-E DNA fragment that had been used to construct pXexCalx. The reaction mixture was split into eight 500-µl Eppendorf tubes and sealed with 100 µl mineral oil per tube. Amplification was then begun with at 94° C. for 5'; there followed 20 cycles of 94° C. (1'), 62° C. (1'), and 72° C. (3'); ragged ends were polished with a final incubation at 72° C. (7'), the reaction then being soaked at 4° C. until retrieval. Under these conditions, amplification is inefficient and its output varies roughly linearly with the amount of input DNA template (data not shown). Amplification products were pooled, extracted with phenol-chloroform/chloroform, precipitated, and resuspended in 11 µl T_{10}. Since *Taq* DNA polymerase tends to place protruding adenine residues on the 3' ends of double-stranded DNA (Clark, 1988), and since such ends might promote unwanted T7 transcription, we then polished the 5'Xex/3'Xex products with T4 DNA polymerase (Sambrook *et al.*, 1989). Any residual Taq DNA polymerase (Barnes, 1992) was not expected to counteract the polishing efficiently at 12° C. Polished 5'Xex/3'Xex products were reextracted, precipitated, and resuspended in 11 µl RNAse-free TE.

Both the finished PCR cRNA template ("PCR-Calx") and finished plasmid cRNA templates were UV-quantitated, and checked for proper amplification and linearization by gel electrophoresis.

Capped cRNAs were synthesized with Stratagene's kit, supplemented by RNAsin from BMB, following manufacturer's instructions: all templates were transcribed with T7 RNA polymerase, except for exchanger clone M which used T3 RNA polymerase. cRNAs were resuspended in small volumes (5-10 µl) of injection buffer (RNAse-free 10 mM Hepes, pH 7.4). They were quantitated by UV spectophotometry (Sambrook *et al.*, 1989). The remaining cRNA was then diluted to a final concentration of 0.1 µg/µl or 1.0 µg/µl

with injection buffer, split into 4.0-µl aliquots, chilled to -70° C., and stored frozen until immediately before use. Before use of a cRNA mass-preparation, one aliquot from it was thawed, EtBr-stained, and checked for integrity by formaldehyde-MOPS gel electrophoresis (Sambrook *et al.*, 1989; Tsang *et al.*, 1993).

Assaying sodium-calcium exchange in *Xenopus* oocytes. Sodium-calcium exchange was assayed by an amalgamation of the methods of Kimura *et al.* (1993), Longoni *et al.* (1988), Mager *et al.* (1993), and Quick *et al.* (1992). The following stock solutions were used to generate assay buffers: 10xND96 (0.96 M NaCl + 20 mM KCl + 10 mM $MgCl_2$ + 18 mM $CaCl_2$ + 50 mM Hepes, pH 7.4); 10xND96-Ca^{2+} (10xND96 without $CaCl_2$); 10xNa-EB (0.96 M NaCl + 0.2 M Hepes, pH 7.4); 10xK-EB (0.96 M KCl + 0.2 M Hepes, pH 7.4); 10xCh-EB (0.96 mM choline chloride + 0.2 M Hepes, pH 7.4); 10xStup (10xK-EB + 10 mM EGTA); and 5% w/v BSA in 10 mM Hepes (pH ~7.4). The following media were used for oocyte culture: ND96+HS (1xND96 + 50 mg/ml gentamycin + 2.5 mM sodium pyruvate + 1-5% v/v horse serum); and ND96+PG (ND96+HS without horse serum). Horse serum was obtained from Irvine Scientific (cat. no. #4023). For the non-BSA rinsed oocytes (Results and below), 1-5% horse serum was used to stimulate cRNA expression in culture media; for the BSA-rinsed oocytes 5% serum was used (Quick *et al.*, 1992).

Oocytes were harvested, defolliculated, aged in ND96+HS for 1-3 days, and microinjected by the methods of Quick and Lester (1994). 50 nl of either blank buffer or cRNA were dispensed in all injections. We slightly dissent from Quick and Lester (1994), in that we found the most useful microinjection needles to be 27 µm instead of 20 µm wide. After injection, oocytes were returned to ND96+HS; ailing oocytes were culled after 1-2 days and their healthy mates transferred to fresh ND96+HS. After 3.5-5.0 days in ND96+HS, oocytes were transferred to ND96+PG for 1-3 days, and then assayed. Before beginning the assay, $^{45}Ca^{2+}$ was thawed, serially diluted from ~70-110 mM to 10-20 mM (in H_20) and then to 10-20 µM (in 1xK-EB, 1xCh-EB, or 1xNa-EB); solutions of

1xK/Ch/Na-EB + 10-20 μM $^{45}Ca^{2+}$ were kept at room temperature until being used to start $^{45}Ca^{2+}$ uptake.

All rinses and soaks save the uptake itself were carried out in disposable 60 mm Petri dishes (Falcon). Oocytes to be loaded with internal sodium were first rinsed by passage through two 6 ml baths of 1xND96-Ca^{2+}, then soaked at 4-6° C. with rotary shaking in 6 ml of 1xND96-Ca^{2+} + 30 μM nystatin for ≥30'; nystatin was stored as a 10 mM stock solution in DMSO at -20° C. and only mixed with aqueous solutions immediately before use. After sodium-loading, the nystatin was washed off the oocytes by extensive rinsing (~≥15'/rinse) in four soaks of either 6 ml 1xNa-EB or of 6 ml 1xNa-EB + 0.1% w/v BSA; the BSA was diluted from a 5% stock stored at 4° C. The first two rinses were at 4-6° C. with rotary shaking, the latter two at room temperature without shaking. Sodium-loaded oocytes were passed through two rinses of 6 ml of 1xK-EB, 1xCh-EB, or 1-Na-EB. Meanwhile, oocytes not loaded with sodium were kept in their 1xOM-hs culture until the final rinses of the sodium-loaded oocytes, at which point unloaded oocytes were passed through three 6 ml rinses of 1xK-EB, 1xCh-EB, or 1xNa-EB. Finally, oocytes were transferred to 1 ml of 1xK/Ch/Na-EB in a 35 mm disposable Petri dish, to which was added 1 ml (1xK/Ch/Na-EB + $^{45}Ca^{2+}$), producing a final concentration of 5-10 μM $^{45}Ca^{2+}$ and igniting calcium uptake. After 10' the uptake was quenched by pipetting 2 ml of 1xStup into each dish. The oocytes in each dish were washed three times by pipetting almost all of the fluid from their dish and replacing it with 4 ml 1xStup; washed individual oocytes were dropped via Pasteur pipet into 7-ml scintillation tubes (cat. no. 125508, Research Products International) containing 500 μl 20% SDS. To obtain a crude measure of background noise, 1-3 drops of the final rinse solution from each assay dish were also dropped into individual scintillation tubes. The oocytes were liquefied by rotary shaking of their sealed tubes in a 42-50° C. water bath for ≥45', cooled to room temperature, mixed with 3.0 ml of scintillation fluid, sealed, vortexed to homogeneity, and scintillation-counted. Uptake data were initially recorded and

calculated in terms of cpm/sample; for their presentation in Table 2, they were converted to mol/sample by the formula $M = O \cdot [S \cdot (40\ g/mol) \cdot 0.5^{(t/164)}]^{-1}$, where M = (moles of Ca in a sample), S = (specific activity on its reference date, provided by ICN, for the $^{45}Ca^{2+}$ batch used in the assay), t = (time elapsed in days from the reference date to the time of the assay). Note that the preponderance of calcium in "$^{45}Ca^{2+}$" is in fact nonradioactive $^{40}Ca^{2+}$ (Francis *et al.*, 1959).

We observe that including BSA (USB, cat. no. 10868) in the nystatin rinse solutions prevents oocytes from sticking to the dish wall during subsequent rinses; this substantially increases the ease of assaying large numbers and reduces the lysis of oocytes during assay from annoying levels to essentially zero. We thus prefer and recommend rinsing with BSA (Kimura *et al.*, 1993) as opposed to pure buffer (Longoni *et al.*, 1988). However, for controls in which non-Na alkali cations are loaded, BSA seems to have the effect of artifactually stimulating $^{45}Ca^{2+}$ uptake, perhaps by introducing trace sodium into the oocytes before they have resealed (data not shown). We successfully circumvented this by performing the first two of four rinses *without* BSA, but in petri dishes that do *not* stick to nystatin-treated oocytes. Such dishes are available from Lux (Quick and Lester, 1994) or Corning (P. Deshpande, pers. comm.).

In situ localization of *Calx* gene products. Sense and antisense digoxigenin-labelled RNA probes were transcribed in vitro, from pXexCalx that had been linearized with either HindIII or XbaI (Boehringer). Detailed methods were as provided by Stratagene, Boehringer Mannheim, and Sambrook *et al.* (1989). Dig-RNA products were precipitated and resuspended into RNAse-free T_{10}, quantitated by UV, and diluted into hybridization buffer (50% deionized formamide + 5xSSC + 2% blocking reagent [Boehringer] + 0.1% N-laurylsarcosine + 0.05% SDS + 10% dextran sulfate). 0.1 mg/ml yeast type III RNA (Sigma) was generally included in the hybridization buffer as a further blocking agent. For hybridization, probes were diluted to ≥10 μg/ml.

For whole-mount hybridization to embryos, embryos were harvested, and prepared

for hybridization, and stored at -20° C. essentially as in Ashburner (1989b); details are given below. For sectioning, OCT-embedded adult tissues were cryostat-sectioned, mounted onto gelatin-treated slides and stored at -20° C. Processing, hybridization and wash procedures for both whole-mounted and sectioned tissues resembled those of Tautz and Pfeifle (1989), with the addition of a 30' post-hybridization wash step at 37° C. with 2-5 µg/ml of DNAse-free RNAse (Boehringer) in TE + 500 mM NaCl. Further details of processing, hybridization and wash procedures are given below. To diminish background staining, anti-digoxigenin AP-conjugated Fab-fragments were preabsorbed against fixed fly embryos for 60' prior to use. Staining was performed with BM purple AP-substrate (Boehringer) instead of with NBT/BCIP, essentially by manufacturer's instructions.

The detailed protocols below were first devised by Dali Ding and Kellie Whittaker in the laboratory of Howard Lipshitz, and by Doris Kretschmar in our laboratory. They appear to be ultimately based on protocols of Ashburner (1989b) and Tautz and Pfeifle (1989). However, to the best of our knowledge, they have not in fact been explicitly and plainly described in any prior publication.

In situ localization: collection and initial fixation of embryos. An embryo sieve was made from a nylon filter mounted on a 50-ml disposable screwtop tube, with both the bottom of the tube and the top of the cap cut off. Embryos were collected from population cages for ~16 hours on trays of standard medium (Lewis, 1960). They were then washed onto the sieve with a paintbrush and a squirt bottle of distilled water. To dechorionate the embryos, the sieve was rinsed with, and then soaked in, a 1:1 mixture of commercial bleach and distilled water for 2 minutes at room temperature. The embryos in the sieve were thoroughly rinsed for 60 seconds with a squirt bottle of 1% v/v Triton X-100 in distilled water, and then for 60 seconds with distilled water from a tap. The nylon filter carrying the dechorionated embryos was then dismounted from its tube, and the embryos were washed off the filter into a monolayer of heptane in a glass scintillation vial. The embryos were swirled into a monolayer; if they were unable to form a monolayer, they

were distributed among several scintillation vials. Fixative (10% paraformaldehyde in 1xPBS, pH 7.0-7.2, made on the day of use) was then added, which caused the embryos to float at the interface. The vials were then sealed tightly, shaken vigorously by hand for one minute, and then rotated at 200 RPM on a shaker for 19 minutes. The lower (fixative) phase was then removed by Pasteur pipette and three volumes (with respect to heptane) of methanol were added. The vials were resealed and shaken gently but thoroughly by hand for 2 minutes. Devitellinized embryos were then collected from the bottoms of the vials, washed several times with ethanol, and then stored at -20° C. until use (embryos remain usable for many months).

In situ localization: collection and initial fixation of adult flies. White-eyed adult flies (double *cinnabar brown* mutants; Lindsley and Zimm, 1992) were etherized, mounted in OCT compound (Tissue-Tek), locked into it by freezing, and sectioned on a cryostat. Cryostat sections were stored dry at -20° C. until use. Immediately before use they were heated to 42° C. on a hot plate for 1' and then incubated at room temperature for 10', to ensure that they were dry prior to fixation.

In situ localization: hybridization of digoxigenin-RNA probes to tissues. The protocol will be given in full for embryos; modifications required for heads sections instead of embryos will then be briefly listed. All solutions used in or prior to hybridization were made RNAse-free by double-filtration through 0.2 μm-nitrocellulose Nalgene filter units.

Fixative was made on the same day as the experiment (4% paraformaldehyde + 1xPBS [pH 7.1] + 0.1% Tween-20). We initially titrated the fixative to 7.0-7.2 with concentrated HCl prior to filtraton; later we found that this was superfluous, since the paraformaldehyde/1xPBS mixture spontaneously attains pH ~7.5. Small aliquots (~≤50 μl/tube) of embryos were removed with a 5-ml disposable pipet from storage at -20° C. into individual tubes. Pre-siliconized, RNAse-free, graduated microcentrifuge tubes (National Scientific Supply Co, Inc.; VWR# 20172-945) were used at all steps. One aliquot of

embryos, in a single tube, was set up for each probe solution; an additional aliquot was set up for eventual use in preabsorbing AP-conjugated anti-digoxigenin Fab fragments. Since, throughout the procedure, solutions were changed while embryos remained in their tube, relatively few embryos were lost. All steps were done with 1 ml volumes unless otherwise indicated. All steps, including hybridization, were performed on a Nutator (Adams) to keep embryos well-suspended in solution.

The embryos were rinsed twice with methanol, and once with a 1:1 mixture of methanol:fixative. They were then fixed for 20+'; rinsed 2' in PTw (1xPBS + 0.1% Tween-20), 3 times; etched 20' in 0.2 M HCl + 0.1% Tween-20; washed 5' in 2xSSCTw (2xSSC + 0.1% Tween-20), 3 times; incubated 30' without rocking in a 68° C. water bath in 2xSSCTw; rinsed 5' in PTw, 3 times; digested 3' in 25 mg/ml Proteinase K (diluted from a concentrated stock solution; Boehringer) + PTw; quenched 2' in 2 mg/ml glycine (diluted from an RNAse-free 100 mg/ml stock solution of glycine) + PTw, 2 times; rinsed ~1' in PTw, 3 times; refixed 20+' in fixative; washed ~1' in PTw, 3 times; acetylated 10' with 0.128% v/v acetic anhydride (diluted from 100% acetic anhydride; Fisher) + 0.1 M triethanolamine; washed 5' with PTw, 3 times.

At this point, one aliquot of embryos was stored at 4° C. for later use in preabsorbing antibodies. The remaining aliquots were then: incubated 15' with a 1:1 mixture of PTw and hybridization buffer without dextran sulfate ("hybb.-DS"); incubate 15' with hybb.-DS; incubated at 48-55° C. with hybb.-DS, for 1-24 hours.

The composition of hybb.-DS is: 50% deionized formamide + 5xSSC + 2% blocking reagent (Boehringer) + 0.1% N-laurylsarcosine + 0.05% SDS. The composition of "hybb.+DS" is the same as hybb.-DS, with 10% dextran sulfate added. As a further blocking agent, 0.1 mg/ml yeast type III RNA (Sigma) was generally also included in the hybridization buffer.

Probe synthesis is described above. Probes were mixed to a final concentration of ≥10 μg/ml in 300-500 ml of hybb.+DS, boiled for 3', cooled to room temperature in a

water bath for 2', mixed with embryos immediately after removal of their last prehybridization solution, and incubated with the embryos for 12-36 hours at 48-55° C.

It was typically not possible to separate embryos from probe solution due to the latter's viscosity. After hybridization, the probe was therefore diluted with 0.5-1.0 ml of 2xSSCTw to allow both the embryos to settle to the bottom of the tube and the probe to be discarded. The embryos were then rinsed for at least 3 hours with three changes of 2xSSCTw at 48-55° C. They were then rinsed 5' in TEN_{500} (10 mM Tris [pH 8.0] + 1 mM EDTA + 500 mM NaCl), 3 times; incubated 30' at 37° C. in TEN_{500} + 5 µg/ml RNAse (diluted from 0.5 mg/ml stock solution; Boehringer); rinsed 2' with 2xSSCTw, 3 times; incubated 30' at 48-55° C. in 2xSSCTw; washed 5' in 0.1xSSCTw (0.1xSSC + 0.1% Tween-20); incubated 15' at 48-55° C. in 0.1xSSCTw.

After the non-hybridizing probe had been removed, probe detection began. The embryos were washed 5' in PTw, 3 times; incubated 30' in 0.5% blocking reagent (Boehringer) + PTw; washed 5' in PTw, 3 times; incubated 60' with 1:2000 preabsorbed AP-conjugated anti-digoxigenin Fab fragments (Boehringer); washed for at least 100' with at least 10 changes of PTw; and stored at 4° C. until staining.

Preabsorbed anti-dig. Fab solutions and 0.5% blocking reagent took time to make and thus were best made while embryos were being cleansed of excess probe. To preabsorb anti-digoxigenin Fab, 1.5-5.0 µl of concentrated AP-conjugated anti-digoxigenin Fab were mixed with 300-1000 µl of PTw to yield a 1:200 solution; this was mixed with an aliquot of fixed embryos (stored overnight at 4° C.) with rocking for at least 60'. The supernatant was then transferred by pipetting to a fresh Eppendorf tube, microfuged briefly to pellet any straggling embryos, retransferred to yet another Eppendorf, diluted tenfold with more PTw, and stored until use. 0.5% w/v blocking reagent in PTw was easy to mix at 48-55° C. on a Nutator, but very difficult to mix any other way; this was most conveniently done at the time embryos were being RNAse-treated.

A subset of embryos from each set were stained by pipetting them into a fresh siliconized microfuge tube; washing them 5' with 1 mM levimasole (diluted from a 250 mM stock solution, kept frozen between uses) in distilled water, 2-4 times; then soaking them in BM Purple AP stain (Boehringer) for 30', under foil to keep out light. The stain was stopped by several rinses with PTw. Stained embryos were then mounted in gelatin-glycerol mountant (Ashburner, 1989b) for light microscopy.

The differences between this protocol and that used for head sections are as follows. Head sections were thawed at 42° C. for 1', then at room temperature for 10', and then immediately fixed; no rehydration with methanol was needed. Tween-20 (used in all steps of the embryo protocol to prevent sticking) was *omitted* from all solutions in the head section protocol; e.g., 1xPBS instead of PTw was used for several of the rinse steps. The sections were kept in a humidified plastic box, on top of rubber stoppers to prevent wicking of solutions, in all stages of the hybridization; solutions were pipetted onto and drained off of the slides individually, and typically 1-4 ml of a given solution per slide would be atop the slides at any given stage of the experiment. This was done both to prevent RNAse contamination in the early stages of the hybridization and to prevent contaminating common laboratory glassware with RNAses in the late stages. For the actual hybridization, we placed 100 µl of probe atop the head sections (which occupied roughly a 20x20 mm^2 area) and then placed a 22x22 mm^2 coverslip over the head sections; instead of sealing them with rubber cement, we instead placed enough 50% formamide + 5xSSC in the box to keep the slides humidified for 12-36 hours. The probe solutions and coverslips were removed by soaking the entire slide in 50 ml of 2xSSC in a disposable tube; given proper humidification, the coverslips and probes would spontaneously slough off, leaving sections unharmed. The staining with AP purple worked best if done for 3 hours, rather than 30' as with the embryos; somewhat shorter times (75-105') gave better discrimination between sense and antisense probes, but also gave considerably less pleasing signal intensities with the antisense probe.

Polyclonal ascites generation. Peptides C1-15 (KYMDKNYRVNKRGTC) and C2-17 (PDDELAAKIKEVEKKPC) were selected from the cytoplasmic loop of Calx for antibody generation, on the basis of predicted antigenicity (Jameson and Wolf, 1988); a C-terminal cysteine residue was included in each peptide for linkage. They were synthesized and linked to KLH by the Caltech Biomolecular Synthesis and Analysis Center. The linking agent was succinimidyl 4-(N-maleimido methyl) cyclohexane--equivalent in principle to m-maleimidobenzoyl-N-hydroxysuccinimide ester (Harlow and Lane, 1988). KLH-C1-15 and KLH-C2-17 were then used by Dr. Susan Ou (Caltech Monoclonal Antibody Facility) to immunize two sets of three Swiss Webster mice five times, with tail bleeds being taken for testing after the first three boosts (Ou *et al.*, 1993). Two criteria were used to identify a potentially valid anti-KLH-C1-15 antiserum (Hockfield *et al.*, 1993): visible histochemical signals in cryostat sections of adult heads; and positive signals with dot-blotted BSA- and ovalbumin-conjugated C1-15, but not with BSA- or ovalbumin-conjugated C2-17. Neither histochemical signals nor specific detection of conjugated C1-15 were observed with either preimmune serum; nor was C1-15 specifically detected with sera elicited by KLH-C2-17. A histochemically and antigenically positive anti-KLH-C1-15 serum was obtained from one of three mice after the fifth boost. It was converted into a polyclonal ascites by a final KLH-C1-15 immunization, followed by ascites generation and collection (Ou *et al.*, 1993). It was then retested by immunohistochemistry, competition with ovalbumin-conjugated C1-15 versus C2-17, and immunoblotting (Hockfield *et al.*, 1993).

Immunohistochemistry. This was performed upon frozen sections of adult heads essentially as in Hockfield *et al.* (1993), but with the following notable points. After fixation, 10 mg/ml glycine was used to block excess linking groups. 0.1% Tween-20 was used at all antibody incubation and wash stages. Primary sera were used at 1:2000 to 1:20,000, and were blocked with 1% w/v BSA (USB, cat. no. 10868), 0.1 mg/ml ovalbumin (Sigma, cat no. A-5378), and 0.1 mg/ml KLH (Sigma, cat. no. H-2133). Anti-

KLH-C1-15 serum was tested for specificity by two methods: preabsorption to nitrocellulose strips carrying ovalbumin-C1-15 or ov.-C2-17; or blocking in solution, with added 0.4 mg/ml Ov.-C1-15 or Ov.-C2-17. The secondary antibody was Cy3™-conjugated Goat Anti-Mouse IgG+M (Jackson ImmunoResearch Laboratories, Inc., cat. no. 115-165-044), used at 1:250 dilution, with 1% w/v BSA to block irrelevant binding.

Acknowledgements

We thank the following: Eveline Eichenberger, Lynette Dowling, Heather Davis, Amparo Gomez, and Jeremy Gollub for excellent technical assistance; David Hyde and Kirk Mecklenburg for cooperation in the early stages of this project; John Rawls, the Indiana *Drosophila* Stock Center, and the Berkeley Drosophila Genome Project for providing *Drosophila* stocks; Uptal Banerjee, Konrad Zinsmaier, and John Tamkun for providing cDNA and genomic libraries; Nancy Bonini for determining the chromosomal location of *Calx*; William Leiserson, Brian Mozer, and Faiz Kayyem for RNA blot protocols; Henry Lester for his generous support of our *Xenopus* expression work; Mike Quick for excellent instruction in *Xenopus* techniques; Janis Corey and Purnima Deshpande for short-order *Xenopus* information; Debora Nicoll for providing NCX1 clones and reagents; Ron Davis for discussing *Calx*-β; Doris Kretschmar and Kellie Whittaker for RNA in situ hybridization protocols; Susan Ou for generating polyclonal antisera; David Mathog for computational support; Mark Siddall for phylogenetic discussions and outputs from PAUP 3.1; Nancy Bonini, Konrad Zinsmaier, and members of the Benzer laboratory for criticism of both this work and its manuscripts; Dan Schulze for collegial exchange of unpublished information; and Ken Philipson for support, advice, and encouragement in several of the areas listed above. This work was supported by the NIH, the NSF, and the Beckman Institute.

Table 1. Complementation data for lethal mutations in the *Calx* genomic region. *Drosophila* strains were intercrossed by standard methods (Roberts, 1987). "P" denotes a lethal single P insertion in the 93B1,2 region collected by the Berkeley Drosophila Genome Project (pers. comm.), while "*l(3)rlr*" denotes a chemically induced lethal mutation near 93B1,2 (Eisenberg *et al.*, 1990). In the strains crossed, both sets of mutations were maintained over a third chromosomal balancer carrying the dominant visible, recessive lethal marker *Stubble*^{1} (*Sb*^{1}: Roberts, 1987; Lindsley and Zimm, 1992). The adult progeny of each cross were therefore expected to possibly include *Sb*$^{+}$/*Sb*$^{+}$ flies and certainly include *Sb*^{1}/*Sb*$^{+}$ flies. Absence of the former class demonstrates noncomplementation, most likely due to allelism of the lethal mutations; presence of *Sb*$^{+}$/*Sb*$^{+}$ progeny demonstrates the reverse. A numerical ratio (X/Y) shows the numbers of Sb progeny (X) and *Sb*^{1}/*Sb*$^{+}$ F1 progeny (Y) from a given cross; "---" denotes a cross that was not performed. The results define three nonallelic vital genes in the *Calx* region, one of which is ablated by all P insertions so far tested.

	Female F0:				
	P997	P633	P1523	P1533	*l(3)rlr2*
Male F0:					
P997	0/86	0/113	0/50	0/121	---
P633	0/76	0/89	0/80	0/132	---
P1523	0/105	0/109	0/51	0/70	---
P1533	0/111	0/129	0/69	0/116	---
l(3)rlr1	40/48	62/46	---	27/44	15/46
l(3)rlr2	21/28	72/47	---	18/59	---

Table 2. Expression of Calx in *Xenopus* oocytes. Oocytes were microinjected, incubated for several days, loaded with intracellular sodium, challenged with $^{45}Ca^{2+}$ along with a variable monovalent cation, and allowed to take up $^{45}Ca^{2+}$ via reverse sodium-calcium exchange for 10'. They were then rinsed and individually assayed by scintillation counting. "Injected" refers to the substance injected; "Ion_o^+," the primary monovalent cation placed outside the oocytes being assayed for $^{45}Ca^{2+}$ uptake; "Ion_i^+," the primary monovalent cation loaded into the oocytes; "No. inj.," the number of oocytes injected with a particular solution; "Uptake," the mean quantity and standard deviation of $^{45}Ca^{2+}$ taken up per oocyte; "Range," the range of uptakes observed; "Background," the amount of radiation seen in a drop of rinse buffer lacking an oocyte. These data are displayed graphically in Figure 11.

Injected:	Ion_o^+:	Ion_i^+:	No. inj.:	Uptake (pmol Ca/oocyte, mean ± σn-1):	Range (pmol Ca/oocyte):	Background: (pmol Ca/drop):
Set 1	**(Aged 2.5 d.; +HS 4.5 d.; -HS 3 d. BSA-washed; 6.2 μM Ca_o; 680 cpm/1.0 pmol Ca):**					
Hepes	Ch	Na	13	0.46 ± 0.14	0.31-0.74	0.07-0.09
	Ch	(no load)	16	0.26 ± 0.08	0.14-0.33	0.06-0.10
	Na	Na	14	0.26 ± 0.05	0.18-0.33	0.09-0.12
NCX1	Ch	Na	18	16.0 ± 6.4	4.7-33.0	1.7-2.0
	Ch	(no load)	18	8.9 ± 4.0	2.1-13.0	0.63-0.73
	Na	Na	17	2.8 ± 1.0	1.6-5.2	0.17-0.27
pXexCalx	Ch	Na	14	3.18 ± 0.45	2.6-4.4	0.09-0.10
	Ch	(no load)	13	0.24 ± 0.10	0.16-0.40	0.05-0.08
	Na	Na	11	0.24 ± 0.04	0.15-0.31	0.12-0.16
pXexCalx, 50 ng	Ch	Na	17	6.8 ± 2.2	2.8-11.0	0.26-0.29
	Ch	(no load)	18	0.48 ± 0.23	0.28-1.15	0.08-0.12
	Na	Na	17	0.37 ± 0.05	0.28-0.45	0.16-0.17
PCR-Calx	Ch	Na	18	8.9 ± 2.5	3.5-13.0	0.40-0.57
	Ch	(no load)	17	3.5 ± 1.1	1.7-6.1	0.19-0.23
	Na	Na	16	0.56 ± 0.15	0.28-0.70	0.08-0.11
Set 2A	**(Aged 3 d.; +HS 4.0 d.; -HS 1.5 d. Buffer-washed; 6.7 μM Ca_o; 1100 cpm/1.0 pmol Ca):**					
Hepes	K	Na	13	1.63 ± 0.27	1.2-2.2	0.13
	K	(no load)	16	1.80 ± 0.46	1.2-2.5	0.39
Shaker	K	Na	14	1.20 ± 0.33	1.0-2.1	0.22
	K	(no load)	13	0.78 ± 0.23	0.48-1.3	0.14
NCX1	K	Na	11	16.0 ± 4.7	9.6-22.0	1.9
	K	(no load)	9	9.0 ± 3.0	4.9-13.0	1.6
pXexCalx	K	Na	15	5.2 ± 1.4	1.8-7.5	0.70
	K	(no load)	17	1.2 ± 0.25	0.89-1.48	0.58
PCR-Calx	K	Na	11	14.9 ± 4.7	5.9-21.0	1.1
	K	(no load)	11	4.3 ± 1.6	2.1-7.2	1.0

Set 2B (Aged 1 d.; +HS 4.5 d.; -HS 1.5 d. Buffer-washed; 5.7 μM Ca_o; 930 cpm/1.0 pmol Ca):

Hepes	Ch	Na	9	1.65 ± 0.60	0.60-2.25	0.05-0.09
	Na	Na	12	0.56 ± 0.42	0.09-1.24	0.08-0.12
Shaker	Ch	Na	6	1.84 ± 0.55	1.2-2.6	0.13-0.15
	Na	Na	11	0.69 ± 0.35	0.2-1.1	0.04-0.08
NCX1	Ch	Na	7	17.0 ± 7.0	9.1-28.2	0.49-0.88
	Na	Na	15	1.8 ± 0.78	0.57-3.4	0.11-0.18
pXexCalx	Ch	Na	6	3.2 ± 0.55	2.9-4.2	0.09-0.12
	Na	Na	11	0.23 ± 0.20	0.09-0.78	0.04-0.10
PCR-Calx	Ch	Na	9	14.0 ± 3.6	9.7-18.0	0.41-0.58
	Na	Na	12	0.75 ± 0.43	0.39-1.5	0.16-0.36

Set 3A (Aged 3 d.; +HS 4.5 d.; -HS 1.5 d. BSA-washed; 6.9 μM Ca_o; 800 cpm/1.0 pmol Ca):

Hepes	Ch	Na	17	0.63 ± 0.18	0.30-0.98	0.09-0.10
	Ch	(no load)	22	0.61 ± 0.24	0.16-1.16	0.09-0.19
	Na	Na	20	0.34 ± 0.07	0.20-0.46	0.14-0.15
Shaker	Ch	Na	17	0.68 ± 0.16	0.45-1.05	0.07-0.14
	Ch	(no load)	20	0.90 ± 0.32	0.45-1.50	0.27-0.46
	Na	Na	20	0.49 ± 0.09	0.30-0.69	0.24-0.45
NCX1	Ch	Na	29	19.0 ± 6.5	3.0-37.0	2.2-2.5
	Ch	(no load)	33	9.7 ± 4.5	3.3-23.0	1.6-2.3
	Na	Na	32	2.3 ± 0.8	0.79-4.1	0.38-0.46

Set 3B (Aged 3 d.; +HS 5.0 d.; -HS 1.0 d. BSA-washed; 5.9 μM Ca_o; 710 cpm/1.0 pmol Ca):

pXexCalx	Ch	Na	11	4.3 ± 1.1	2.2-6.1	0.07-0.13
	Ch	(no load)	13	0.75 ± 0.27	0.52-1.54	0.08-0.17
	Na	Na	14	0.35 ± 0.12	0.17-0.59	0.07-0.10
pXexCalx, 50 ng	Ch	Na	14	14.0 ± 3.4	7.0-21.0	0.18-0.31
	Ch	(no load)	17	2.0 ± 0.78	1.1-4.3	0.11-0.21
	Na	Na	16	0.57 ± 0.14	0.25-0.76	0.06-0.11
PCR-Calx	Ch	Na	16	7.3 ± 2.6	3.3-13.0	0.06-0.17
	Ch	(no load)	17	2.0 ± 0.80	0.80-3.5	0.07-0.18
	Na	Na	15	0.51 ± 0.12	0.30-0.68	0.06-0.13

Set 4 (Aged 2 d.; +HS 3.0 d.; -HS 1.0 d. Buffer-washed; 6.5 μM Ca_o; 360 cpm/1.0 pmol Ca):

Hepes	Ch	Na	41	2.53 ± 0.52	1.4-3.7	0.70-0.90
PCR-*Calx*	Ch	Na	12	17.2 ± 8.6	3.6-29.0	1.4-1.9
	Ch	Li	12	3.0 ± 0.9	0.87-4.1	0.34-0.45
	Ch	K	12	4.4 ± 1.3	2.3-7.1	0.48-0.73
	K	Na	12	11.7 ± 10.7	3.1-33.5	1.4-2.2
	K	Li	12	1.9 ± 0.5	1.4-2.7	0.25-0.42
	K	K	12	1.64 ± 0.58	0.87-2.6	0.25-0.34
	Na	Na	10	4.7 ± 2.4	1.6-9.4	0.14-0.20
	Na	Li	10	4.0 ± 1.7	2.4-5.9	0.20-0.31
	Na	K	11	3.5 ± 1.9	1.8-7.9	0.23-0.39

Figure 1. Features of a *Calx* cDNA. Internal restriction sites relevant to cRNA template construction and ssDNA probe generation (HindIII, EcoRI and SspI) are shown. The sequence overlap of 9C5-E with 9C5-o (Hyde *et al.*, 1990), in the 5' end of 9C5-E, is underlined; two small gaps within 9C5-o lack 2- and 4-bp parts of 9C5-E. Non-overlapping miniORFs in the 5'UTR are shown, as is the major *Calx* ORF. The predicted mature N-terminus of signal-cleaved Calx protein is marked with "§." Two possible N-glycosylation sites in the mature N-terminal region of Calx are marked with superimposed "gly" signs. Predicted membrane-spanning sequences in the major Calx ORF are underlined. The residues used in peptide C1-15 are italicized. Finally, three potential polyadenylation signals near the 3' end of the cDNA are underlined. The 5' end of 9C5-E has been compared to genomic DNA and to the 5' ends of two other *Calx* cDNAs (9C5--A and D; data not shown). All three cDNAs end within 12 bp of one another, at sites 80-92 bp upstream of 9C5-o's 5'-end, with no intervening genomic sequences.

Figure 1:

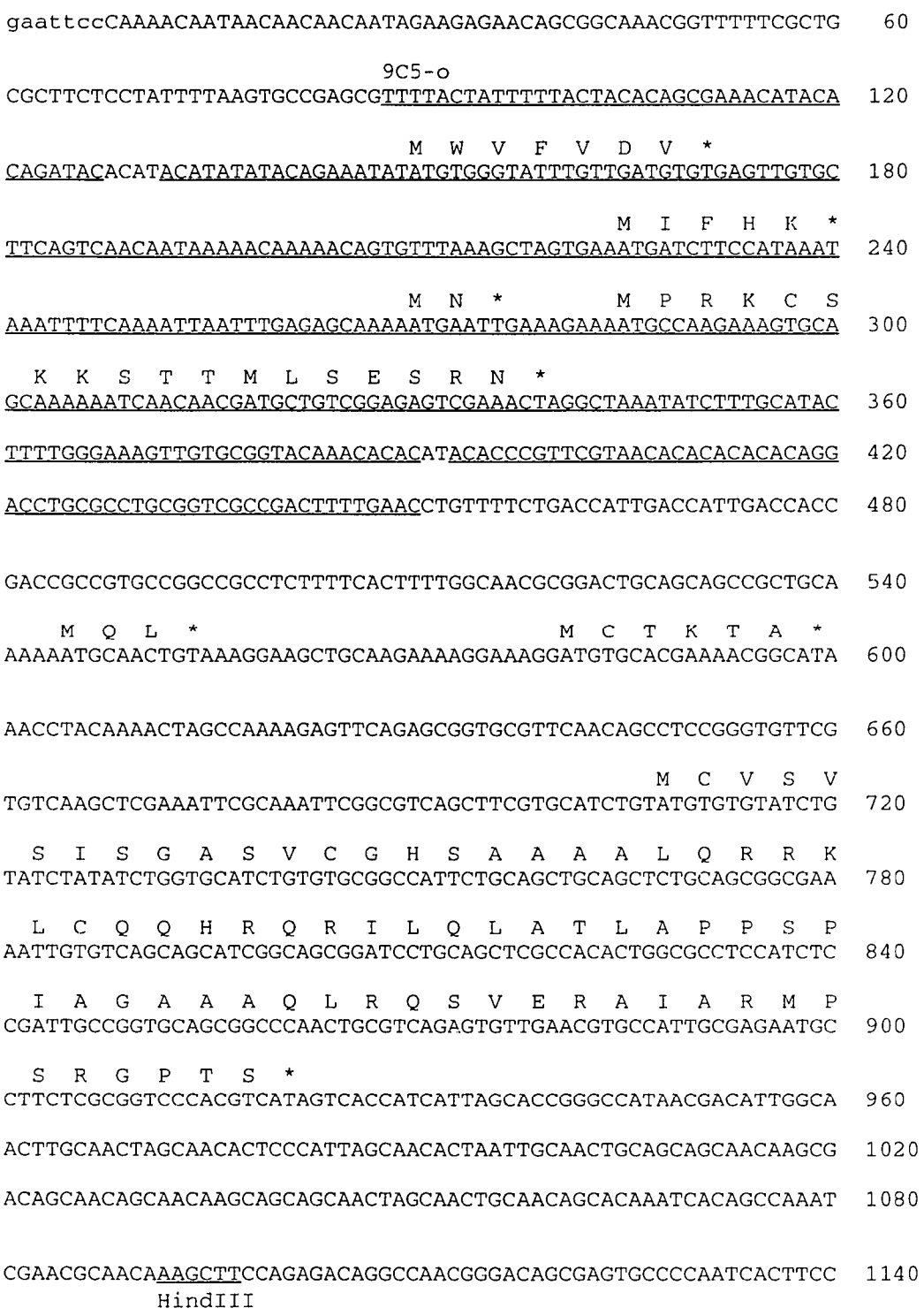
1 gaattccCAAAACAATAACAACAACAATAGAAGAGAACAGCGGCAAACGGTTTTTCGCTG 60
9C5-o
61 CGCTTCTCCTATTTTAAGTGCCGAGCGTTTTACTATTTTTACTACACAGCGAAACATACA 120
M W V F V D V *
121 CAGATACACATACATATATACAGAAATATATGTGGGTATTTGTTGATGTGTGAGTTGTGC 180
M I F H K *
181 TTCAGTCAACAATAAAAACAAAAACAGTGTTTAAAGCTAGTGAAATGATCTTCCATAAAT 240
M N * M P R K C S
241 AAATTTTCAAAATTAATTTGAGAGCAAAAATGAATTGAAAGAAAATGCCAAGAAAGTGCA 300
K K S T T M L S E S R N *
301 GCAAAAAATCAACAACGATGCTGTCGGAGAGTCGAAACTAGGCTAAATATCTTTGCATAC 360
361 TTTTGGGAAAGTTGTGCGGTACAAACACACATACACCCGTTCGTAACACACACACACAGG 420
421 ACCTGCGCCTGCGGTCGCCGACTTTTGAACCTGTTTTCTGACCATTGACCATTGACCACC 480
481 GACCGCCGTGCCGGCCGCCTCTTTTCACTTTTGGCAACGCGGACTGCAGCAGCCGCTGCA 540
M Q L * M C T K T A *
541 AAAAATGCAACTGTAAAGGAAGCTGCAAGAAAAGGAAAGGATGTGCACGAAAACGGCATA 600
601 AACCTACAAAACTAGCCAAAAGAGTTCAGAGCGGTGCGTTCAACAGCCTCCGGGTGTTCG 660
M C V S V
661 TGTCAAGCTCGAAATTCGCAAATTCGGCGTCAGCTTCGTGCATCTGTATGTGTGTATCTG 720
S I S G A S V C G H S A A A A L Q R R K
721 TATCTATATCTGGTGCATCTGTGTGCGGCCATTCTGCAGCTGCAGCTCTGCAGCGGCGAA 780
L C Q Q H R Q R I L Q L A T L A P P S P
781 AATTGTGTCAGCAGCATCGGCAGCGGATCCTGCAGCTCGCCACACTGGCGCCTCCATCTC 840
I A G A A A Q L R Q S V E R A I A R M P
841 CGATTGCCGGTGCAGCGGCCCAACTGCGTCAGAGTGTTGAACGTGCCATTGCGAGAATGC 900
S R G P T S *
901 CTTCTCGCGGTCCCACGTCATAGTCACCATCATTAGCACCGGGCCATAACGACATTGGCA 960
961 ACTTGCAACTAGCAACACTCCCATTAGCAACACTAATTGCAACTGCAGCAGCAACAAGCG 1020
1021 ACAGCAACAGCAACAAGCAGCAGCAACTAGCAACTGCAACAGCACAAATCACAGCCAAAT 1080
1081 CGAACGCAACAAAGCTTCCAGAGACAGGCCAACGGGACAGCGAGTGCCCCAATCACTTCC 1140
HindIII

```
                                                  M  Q  L  L  L  K  S  I .
1141 AGGATAAGGAGAAGCCATCCCAGTTAGTAACCAGCCATGCAGTTGCTCCTTAAATCGATA 1200

                                                  §
     F  T  C  A  L  F  V  I  F  V  Y  A  T  A  Q  S  L  L  K  V
1201 TTCACCTGCGCACTATTCGTGATCTTTGTGTATGCCACCGCCCAGTCGCTGCTCAAAGTC 1260

                                        gly                    gly
     Q  E  T  E  A  R  Q  A  Y  L  N  V  T  S  S  S  S  S  N  L
1261 CAGGAGACAGAAGCGCGGCAGGCGTACCTTAATGTTACCTCCTCCAGCAGTAGTAATCTC 1320

     S  Q  D  D  G  H  F  L  S  R  R  L  R  Q  V  S  H  G  E  E
1321 AGCCAGGACGATGGCCACTTCCTCAGCCGGCGACTAAGGCAGGTCAGCCATGGCGAGGAG 1380

     G  D  E  G  A  P  S  Q  M  D  D  E  L  E  Q  M  T  K  V  H
1381 GGCGACGAGGGCGCGCCGTCCCAAATGGACGACGAGTTGGAACAGATGACCAAGGTGCAT 1440

     G  E  A  P  D  A  E  D  V  R  E  C  S  E  G  L  V  L  P  L
1441 GGAGAAGCACCGGACGCGGAGGACGTGCGCGAATGCAGCGAGGGTCTTGTCCTGCCACTC 1500

     W  M  P  Q  R  N  I  S  V  G  D  R  L  V  R  G  F  V  Y  F .
1501 TGGATGCCGCAACGCAACATTTCGGTGGGTGACCGCCTCGTCCGCGGCTTTGTTTACTTC 1560

     V  L  L  I  Y  L  F  V  G  V  S  I  I  A  D  R  F  M  A  A
1561 GTCCTACTGATCTACCTGTTTGTGGGTGTGTCCATCATTGCGGATCGCTTCATGGCCGCC 1620

     I  E  A  I  T  S  I  E  R  A  V  V  V  K  G  P  N  N  T  K
1621 ATCGAGGCAATCACATCGATTGAACGGGCGGTGGTGGTCAAGGGACCCAACAACACCAAG 1680

     Q  V  M  H  V  R  I  W  N  E  T  V  A  N  L  T  L  M  A  L .
1681 CAGGTGATGCACGTGCGCATCTGGAACGAAACGGTGGCGAATCTAACGCTAATGGCCCTG 1740

     G  S  S  A  P  E  I  L  L  S  V  I  E  I  Y  A  K  D  F  E
1741 GGATCGAGTGCCCCCGAGATCCTGCTCTCGGTTATTGAGATTTATGCGAAGGACTTCGAG 1800

     S  G  D  L  G  P  G  T  I  V  G  S  A  A  Y  N  L  F  M  I .
1801 AGCGGTGACTTGGGACCTGGCACCATCGTGGGATCAGCTGCCTACAACCTGTTTATGATT 1860

     I  A  V  C  M  I  W  I  P  A  G  E  V  R  R  I  R  H  L  R
1861 ATCGCCGTATGCATGATCTGGATACCGGCGGGCGAGGTACGAAGGATCCGGCATCTGCGA 1920

     V  F  F  V  T  A  L  F  S  V  F  A  Y  V  W  L  W  L  I  L .
1921 GTCTTCTTCGTTACCGCCCTCTTCTCGGTCTTCGCCTATGTGTGGCTGTGGCTCATCCTA 1980

     S  V  F  T  P  G  V  I  L  V  W  E  A  I  V  T  L  L  F  F .
1981 TCCGTGTTCACGCCCGGCGTGATCCTGGTCTGGGAGGCGATCGTGACCTTGCTATTCTTC 2040

     P  L  T  V  L  W  A  Y  I  A  E  R  R  L  L  V  Y  K  Y  M
2041 CCGCTGACCGTGCTGTGGGCCTACATCGCCGAGCGGCGTCTTCTGGTCTACAAATACATG 2100

     D  K  N  Y  R  V  N  K  R  G  T  V  V  A  G  E  H  D  Q  V
2101 GACAAGAACTACCGGGTCAATAAGCGCGGCACCGTGGTGGCCGGCGAGCACGACCAGGTG 2160

     E  M  D  A  E  K  G  P  K  Q  P  M  V  T  S  A  R  G  N  D
2161 GAGATGGATGCGGAGAAGGGCCCCAAACAACCAATGGTCACATCCGCTCGCGGAAACGAC 2220
```

```
      A  E  A  F  D  E  A  R  R  E  Y  I  T  L  L  T  E  L  R  Q
2221  GCCGAGGCCTTCGACGAGGCCCGTCGCGAGTACATCACTTTGCTGACGGAGCTACGCCAG  2280

      K  Y  P  D  A  D  L  E  Q  L  E  M  M  A  Q  E  Q  V  L  A
2281  AAGTACCCCGACGCCGATCTCGAACAGCTGGAGATGATGGCCCAGGAGCAGGTGCTGGCG  2340

      R  S  G  R  S  R  A  F  Y  R  I  Q  A  T  R  K  M  V  G  S
2341  CGGAGCGGCAGGTCGCGCGCCTTTTATCGCATCCAGGCCACCCGCAAGATGGTCGGCAGC  2400

      G  N  L  M  R  K  I  Q  E  R  A  H  S  D  L  T  G  V  K  A
2401  GGCAACCTGATGCGCAAGATCCAGGAACGCGCTCACAGCGATCTCACCGGGGTTAAAGCC  2460

      Q  L  H  A  G  D  D  E  E  A  D  D  P  I  R  M  Y  F  E  P
2461  CAGCTGCATGCGGGCGATGACGAGGAGGCGGACGATCCCATCCGAATGTACTTCGAGCCG  2520

      G  H  Y  T  V  M  E  N  C  G  E  F  E  V  R  V  V  R  R  G
2521  GGTCACTACACCGTCATGGAGAACTGCGGCGAGTTTGAGGTGCGCGTGGTGCGCCGTGGC  2580

      D  I  S  T  Y  A  S  V  E  Y  E  T  Q  D  G  T  A  S  A  G
2581  GACATCTCCACCTACGCCAGCGTGGAGTACGAAACGCAGGACGGCACCGCCTCCGCCGGC  2640

      T  D  F  V  G  R  K  G  L  L  S  F  P  P  G  V  D  E  Q  R
2641  ACCGATTTCGTCGGACGGAAGGGACTGCTTAGCTTCCCGCCGGGGGTCGACGAGCAGCGC  2700

      F  R  I  E  V  I  D  D  D  V  F  E  E  D  E  C  F  Y  I  R
2701  TTCCGCATCGAGGTGATCGACGATGACGTATTTGAGGAGGACGAGTGCTTCTACATTCGA  2760

      L  F  N  P  S  E  G  V  K  L  A  V  P  M  I  A  T  V  M  I
2761  CTCTTCAATCCCTCCGAGGGCGTGAAGCTAGCCGTGCCAATGATCGCCACCGTCATGATC  2820

      L  D  D  D  H  A  G  I  F  A  F  T  D  S  V  F  E  I  T  E
2821  CTGGACGACGACCACGCGGGCATCTTTGCCTTCACAGACTCGGTATTCGAGATCACGGAG  2880

      S  V  G  R  F  E  L  K  V  M  R  Y  S  G  A  R  G  T  V  I
2881  TCCGTCGGCCGGTTCGAGCTGAAGGTAATGCGCTACTCCGGCGCCCGCGGCACCGTCATA  2940

      V  P  Y  W  T  E  N  D  T  A  T  E  S  K  D  Y  E  G  A  R
2941  GTGCCCTACTGGACAGAGAACGACACGGCCACCGAATCCAAGGACTACGAGGGGGCCCGC  3000

      G  E  L  V  F  E  N  N  E  S  E  K  F  I  D  L  F  I  L  E
3001  GGCGAACTTGTCTTCGAAAACAATGAATCCGAGAAATTCATCGATCTGTTCATCCTGGAG  3060

      E  S  S  Y  E  K  D  V  S  F  K  V  H  I  G  E  P  R  L  A
3061  GAGAGCAGCTACGAGAAGGACGTCAGCTTCAAGGTGCACATCGGAGAACCTCGATTGGCG  3120

      P  D  D  E  L  A  A  K  I  K  E  V  E  K  K  P  V  Q  D  L
3121  CCAGACGATGAATTGGCAGCCAAAATCAAGGAGGTCGAGAAAAAACCCGTTCAAGATCTG  3180

      T  E  L  D  R  I  L  L  L  S  K  P  R  N  G  E  L  T  T  A
3181  ACCGAACTGGATCGCATCCTGCTGCTGAGTAAGCCGAGAAACGGAGAACTGACCACCGCA  3240

      Y  V  R  I  R  E  S  Q  E  F  K  A  T  V  D  K  L  V  A  K
3241  TATGTGCGCATTCGAGAGAGCCAGGAATTCAAGGCTACAGTCGACAAGCTGGTGGCAAAA  3300
                              EcoRI

      A  N  V  S  A  V  L  G  T  S  S  W  K  E  Q  F  K  D  A  L
3301  GCGAACGTTTCTGCCGTCCTTGGCACTTCATCGTGGAAGGAACAGTTCAAAGATGCCCTC  3360
```

```
      T  V  I  P  A  D  E  S  E  F  D  N  D  D  E  E  E  E  V  P
3361  ACCGTTATCCCAGCCGATGAAAGTGAGTTTGATAACGATGATGAGGAGGAGGAGGTGCCC  3420

      S  C  F  S  Y  V  S  H  F  V  C  L  F  W  K  V  L  F  A  F  .
3421  AGTTGCTTCAGCTACGTGAGCCACTTCGTCTGCCTCTTCTGGAAGGTTCTCTTTGCATTT  3480

      V  P  P  T  D  I  C  G  G  Y  V  T  F  V  V  S  I  F  V  I  .
3481  GTGCCGCCCACTGACATTTGCGGCGGCTACGTTACCTTTGTGGTATCCATATTCGTGATT  3540

      G  V  I  T  A  I  I  G  D  A  A  S  Y  F  G  C  A  L  N  I
3541  GGCGTCATCACTGCCATCATCGGAGATGCCGCCTCCTATTTCGGCTGCGCCCTCAACATC  3600

      K  D  S  V  T  A  I  L  F  V  A  L  G  T  S  I  P  D  T  F  .
3601  AAGGACTCGGTAACGGCCATTCTGTTTGTCGCCCTGGGCACAAGCATACCAGATACATTC  3660

      A  S  M  I  A  A  K  H  D  E  G  A  D  N  C  I  G  N  V  T
3661  GCCAGCATGATTGCCGCCAAGCATGACGAGGGTGCCGATAATTGCATCGGCAATGTCACG  3720

      G  S  N  A  V  N  V  F  L  G  I  G  L  A  W  T  I  A  A  V  .
3721  GGCAGCAATGCGGTCAACGTGTTCCTGGGCATCGGCCTGGCCTGGACCATCGCCGCCGTC  3780

      Y  H  S  S  H  G  M  T  F  N  V  E  P  G  T  I  G  F  A  V  .
3781  TACCACAGCTCCCATGGCATGACCTTCAACGTGGAGCCGGGAACCATTGGATTCGCCGTG  3840

      A  L  F  C  G  E  A  L  I  A  I  M  L  I  M  F  R  R  W  H
3841  GCGCTCTTCTGCGGCGAGGCCCTGATTGCCATAATGCTCATCATGTTCCGGCGCTGGCAC  3900

      K  G  I  G  A  E  L  G  G  P  K  V  S  K  Y  I  S  A  A  I  .
3901  AAGGGCATTGGCGCCGAGCTGGGCGGTCCGAAAGTATCGAAGTACATCAGCGCAGCGATC  3960

      L  V  F  L  W  V  F  Y  V  V  I  C  I  L  E  A  Y  D  V  I
3961  CTGGTATTCCTTTGGGTGTTCTACGTGGTTATATGCATACTGGAAGCCTACGACGTCATC  4020

      R  V  *
4021  CGGGTTTAAGGAATTCGCAGCCGCGTTGGTTTGGCTTTGGCTTGATTATTCGCAATGGCG  4080
                 EcoRI

4081  TTGGACTTTTCCGTCAAATTGAAGAGGATCGTTACGGCGGAAAACAGAGCTAACCGATAC  4140

4141  TTAGAAGCTATCGAAAGATGCTGTAGATGCAGTTTTTATATGTAAACTTATGAAATTGAT  4200

4201  TTATACATATATGTGCTCGGCGCGATATATAAATATTTCTTGTGTAAAATTTATGTTAAT  4260
            SspI

4261  ACTAAAAGTAAAATTTAAAAGTTTAACTAGGTTTAAGCCAGGCTTACATACAAACCATTT  4320

4321  TTACGATTATTGTCTCTATTCATATATGAATTGTAAATACAGAAAGGCTGCCACGGCTCA  4380

4381  GCAATCTTGTAATCGTAACGAGATCATTTACTGTTATGCCATATATACTTAATTTACTTT  4440

4441  CTAAAGAATACTATTATATTTATTATATCATTCTGTGTATAACTTAAGTCATTGTTGTTG  4500

4501  TTTGTTAAAGCTGTACTTAATCGACCCCATAAAATCAAAACGGGAAAATCGGAATCGATT  4560

4561  TAGAGTTTAAATCGTGTTCCGTACTCCAAACTCGATATTGTCTCTCCATTTGCCGAAAAC  4620
```

4621 CATTGTTAATTTAATACATGTGTAAGTTTTAGGAAAGATCTAAAGGTTTTAGCCAAGAAG 4680

4681 AAACGCAGTCCCTCTAGCCATCTACTACAAATACTACAATTATAACTACTACTACTGAAT 4740

4741 AGGGGCCTCCTTGACAACTAGTTCTAGTCACCTCACACTATCGACACAAGTCCAACTAGC 4800

4801 AACACTTTCATTAACTCTGACCAAAGCAAAAGGCGGCACTACTTACTAGCGATTAGCTGT 4860

4861 TAGCGATTAGCCAGAAAGACCATCAGTGTGTCTACACTGCACTATGAAGAACTACACGTA 4920

4921 CTACCAGTGAGCACTAATCAATTTACTTAAAAAAAGACTTTCTATTCGCTTACGTCGCTG 4980

4981 GTATCGAAGTAGACAAAACTGGATATTAAGGCAAACACCAAAACAATAGCGAAATAAAAA 5040

5041 GGAGAATTACTAGAATTGATTGTAAACCAAATGTAACGAGCAGGTACATATTTTTTGTAT 5100

5101 AATGTTGTACTATTTTTCATATAACAAAATTCTAGCAAATTAATGGTGAGAAGAGAAGCC 5160

5161 TAATGATATTTATAGCCACATGCATAAATTTGTATTATATATTTGGGGTCACACAACTGT 5220

5221 ACGGGGAACTCGTTGAGAAAACTGCGCCAAATTTAGACGTAATTGATTATTAATTACTGC 5280

5281 ATATACGAACTATTAAACAATTTAATAAATATACAAACATGAATAAATAATAATGTACTA 5340

5341 AGTTATACTGTCAACGTTTATTGCTAGATATTATAATTAAATTTCTTTTTAAATTTAAAA 5400

5401 Aggaattc 5408

Figure 2. Alignment of Calx with its homologs. The sequences of non-Calx proteins were from the following studies: canine NCX1, Nicoll *et al.* (1990); rat NCX2, Li *et al.* (1994); bovine RetX, Reiländer *et al.* (1992); *C. elegans* C07A9.4 and C07A9.11, Wilson *et al.* (1994); and *E. coli* ORF_o325, Plunkett (unpublished; GenBank ECOUW67). For Calx, NCX1, and NCX2, the number of the rightmost residue in each line is shown. For consistency, all protein sequences are numbered from "1," although this has not always been done in previous studies of NCX1. Where RetX, C07A9.4, C07A9.11, and ORF_o325 can be aligned significantly to Calx by MACAW, they are also shown. Sequences aligned into an ungapped block are shown in capital letters; unblocked sequences are in lowercase; residues identical to Calx are shown in boldface. Dashes mark alignment gaps due to length variation in unconserved regions. Above each block is shown the probability, given a random sequence model of proteins, of that block arising by chance (Schuler *et al.*, 1991); "Xe-Y" denotes $X \cdot 10^{-Y}$. Predicted cleavage sites for signal sequences are shown with "/"; predicted transmembrane sequences are underlined. "2° prediction" denotes secondary structure predictions made for Calx by the algorithms of Rost and Sander (1994) and Eisenberg *et al.* (1984). "H" denotes a residue predicted to be in either an α- or a 3_{10}-helix; "E," in an extended strand (e.g., a β-strand); "L," in a loop; and "T," in an α-helical transmembrane sequence. "." denotes a residue for which no strong prediction was made. All "H," "E," and "L" residues shown were from a subset predicted with 82% accuracy; adjacent "." residues were generally predicted to have similar structures, but with only 72% accuracy (not shown). While these predictions were made specifically for Calx, NCX1 and NCX2 are expected to be very similar. Structural features of the NCX1 cytoplasmic domain defined in vitro (Li *et al.*, 1991; Matsuoka *et al.*, 1993; Matsuoka *et al.*, 1995) are shown underneath the alignment in italics. Likewise shown in italics are the acid cluster shared by all proven sodium-calcium exchangers, and the single potential protein kinase C phosphorylation site conserved between Calx, NCX1, and NCX2.

Figure 2:


2° str.
Calx
NCX1
NCX2
RetX
C07A9.4
C07A9.11
ORF_o325
P = 5.6e-8
P ≈ 0
P = 1.8e-5
P = 9.5e-9
P ≈ 0
P ≈ 0
P ≈ 5.4e-20
P ≈ 0
| NCX1 calm. targ.? |
| Regulatory region of NCX1 ->

Figure 2 (cont.):

Figure 2 (cont.):

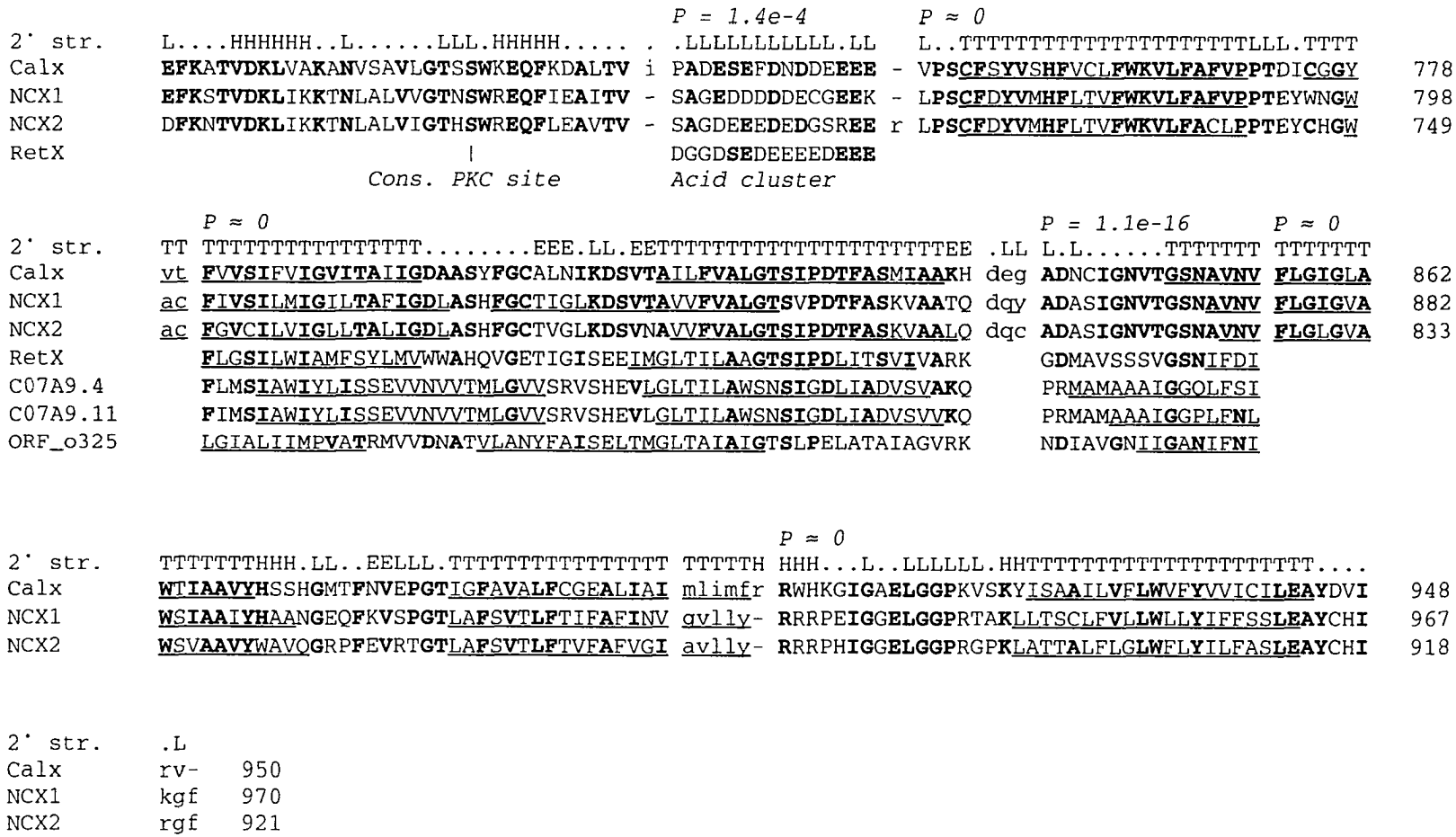

Figure 3. Variable region of *Calx* ORFs. Figure 2's format is used, with the addition of dots to separate variable coding sequences from invariant sequences: two blocks of conserved sequences flank a variable region of Calx and NCX1. 14 *Calx* ORFs were determined in this coding region, by directly sequencing PCR products generated from independent cDNA clones. All Calx cDNAs examined are nearly identical save for a variation of five codons, highlighted with carats. This variation falls in a region where NCX1 also shows variation; NCX1's is much more extensive than that so far observed in Calx. The NCX1 isoforms shown are merely two out of many alternatively spliced NCX1 ORFs, but show maximum divergence among the known variants (Lee *et al.*, 1994). Note that in the N-terminal aligned block, cardiac and renal NCX1 still have alternately spliced sequences, but that these sequences appear to be subject to evolutionary conservation. The rabbit renal NCX1 isoform sequence is from Reilly and Shugrue (1992). Other sequences are as in Figure 2. The difference between 3 *Calx* cDNAs and the others arises from a precise replacement of 5'-CGATGAATTGGCAG-3' (in 9C5-E) with 5'-TTCCACTCACTACC-3'. In addition, there are two silent nucleotide differences between 9C5-E and the other cDNAs: C_{3081} -> T (13 cDNAs) and A_{3174} -> G (14 cDNAs.) No other nucleotide differences between 9C5-E and the other 14 *Calx* sequences were observed in this coding region.

Figure 3:

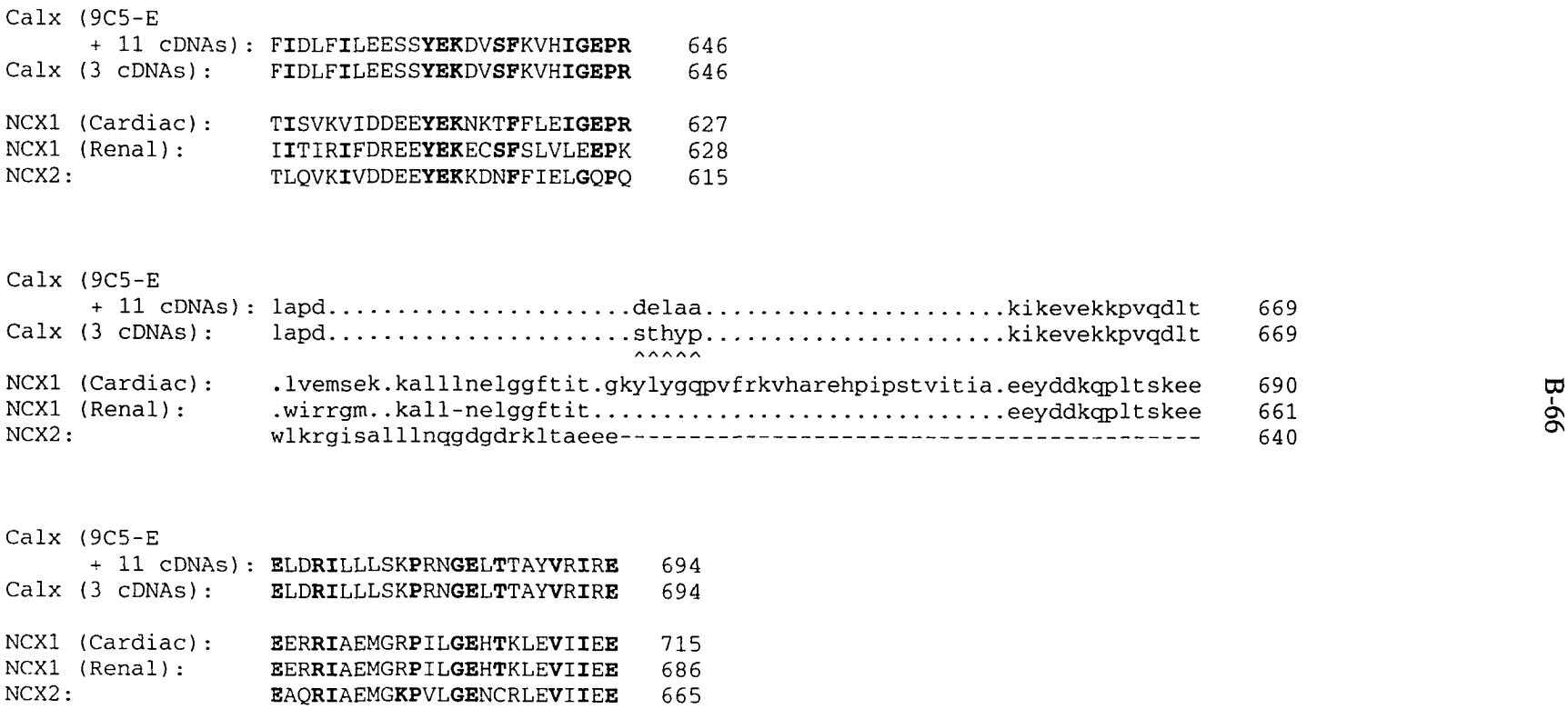
Calx (9C5-E
+ 11 cDNAs): FIDLFILEESSYEKDVSFKVHIGEPR 646
Calx (3 cDNAs): FIDLFILEESSYEKDVSFKVHIGEPR 646
NCX1 (Cardiac): TISVKVIDDEEYEKNKTFFLEIGEPR 627
NCX1 (Renal): IITIRIFDREEYEKECSFSLVLEEPK 628
NCX2: TLQVKIVDDEEYEKKDNFFIELGQPQ 615
Calx (9C5-E
+ 11 cDNAs): lapd.....delaa.....kikevekkpvqdlt 669
Calx (3 cDNAs): lapd.....sthyp.....kikevekkpvqdlt 669
^^^^^
NCX1 (Cardiac): .lvemsek.kalllnelggftit.gkylygqpvfrkvharehpipstvitia.eeyddkqpltskee 690
NCX1 (Renal): .wirrgm..kall-nelggftit.....eeyddkqpltskee 661
NCX2: wlkrgisalllnqgdgdrkltaeee----------640
Calx (9C5-E
+ 11 cDNAs): ELDRILLLSKPRNGELTTAYVRIRE 694
Calx (3 cDNAs): ELDRILLLSKPRNGELTTAYVRIRE 694
NCX1 (Cardiac): EERRIAEMGRPILGEHTKLEVIIEE 715
NCX1 (Renal): EERRIAEMGRPILGEHTKLEVIIEE 686
NCX2: EAQRIAEMGKPVLGENCRLEVIIEE 665

Figure 4. The *Calx*-α and *Calx*-β motifs. The sequences of human and murine integrin-β4 were from Suzuki and Naitoh (1990) and Kennel *et al.* (1993). (References for other non-Calx sequences are given in Figure 2.) The format here resembles that of Figure 2, but with some important differences. First, individual motif names are more complicated than protein names. For instance, in "NCX1-α2," the first part ("NCX1") denotes the *specific protein* in which the motif was detected; the second "α" denotes the *type* of motif; the third "2" denotes that this is the *second* of one or more *Calx*-α motifs in the protein. When repeated within a protein, the motifs are numbered in the order of their appearance in that protein from its N- to its C-terminus. While all motifs are collectively called *Calx*-α or *Calx*-β motifs, a specific motif called (for instance) "Calx-β1" comes specifically from the Calx protein (instead of NCX1-2 or integrin-β4). Second, boldface residues are *not* those identical to Calx, but those which are conserved between two or more paralogous motifs. The consensus sequence underneath the aligned motifs is identical to those residues boldfaced in the alignment; note that sometimes more than one residue is conserved at a position. Third, secondary structure predictions are the consensus of predictions for N- and C-terminal motifs in Calx. Two extremely conserved sites in the *Calx*-α motif may be functionally important, and are thus set aside by spaces from the rest of the *Calx*-α alignment. "P(D/E)" might identify a proline-acid kink in opposed transmembrane sequences that binds pairs of positive charges as they transverse the membrane. "N" may identify an asparagine site, alongside the P(D/E) in the membrane, whose variation in RetX-α2 might be involved in the difference between RetX's and NCX1's stoichiometries of action.

Figure 4:

Calx–α motifs:

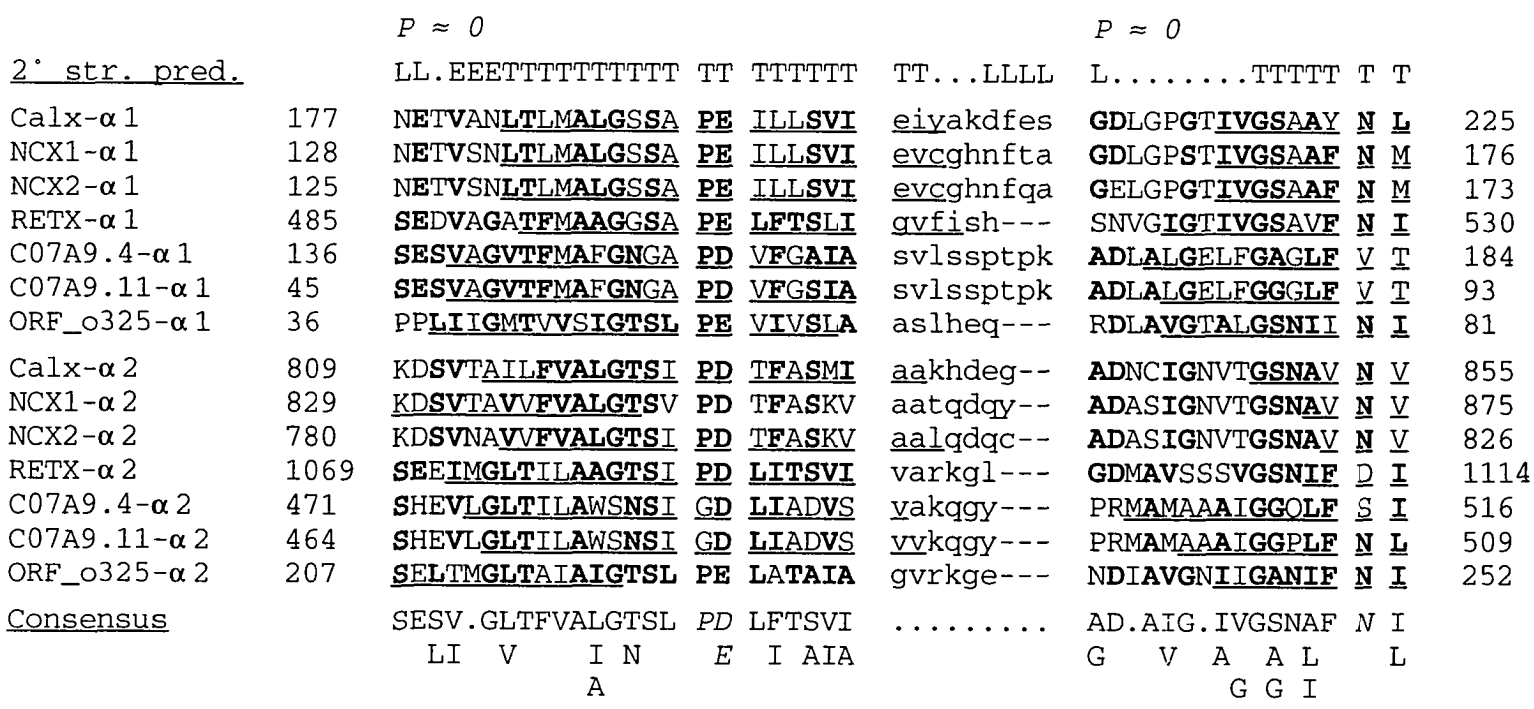

		P ≈ 0				*P ≈ 0*			
2° str. pred.		LL.EEETTTTTTTTT	TT	TTTTTT	TT...LLLL	L.....TTTTT	T	T	
Calx-α1	177	NETVANLTLMALGSSA	PE	ILLSVI	eiyakdfes	GDLGPGTIVGSAAY	N	L	225
NCX1-α1	128	NETVSNLTLMALGSSA	PE	ILLSVI	evcghnfta	GDLGPSTIVGSAAF	N	M	176
NCX2-α1	125	NETVSNLTLMALGSSA	PE	ILLSVI	evcghnfqa	GELGPGTIVGSAAF	N	M	173
RETX-α1	485	SEDVAGATFMAAGGSA	PE	LFTSLI	gvfish---	SNVGIGTIVGSAVF	N	I	530
C07A9.4-α1	136	SESVAGVTFMAFGNGA	PD	VFGAIA	svlssptpk	ADLALGELFGAGLF	V	T	184
C07A9.11-α1	45	SESVAGVTFMAFGNGA	PD	VFGSIA	svlssptpk	ADLALGELFGGGLF	V	T	93
ORF_o325-α1	36	PPLIIGMTVVSIGTSL	PE	VIVSLA	aslheq---	RDLAVGTALGSNII	N	I	81
Calx-α2	809	KDSVTAILFVALGTSI	PD	TFASMI	aakhdeg--	ADNCIGNVTGSNAV	N	V	855
NCX1-α2	829	KDSVTAVVFVALGTSV	PD	TFASKV	aatqdqy--	ADASIGNVTGSNAV	N	V	875
NCX2-α2	780	KDSVNAVVFVALGTSI	PD	TFASKV	aalqdqc--	ADASIGNVTGSNAV	N	V	826
RETX-α2	1069	SEEIMGLTILAAGTSI	PD	LITSVI	varkgl---	GDMAVSSSVGSNIF	D	I	1114
C07A9.4-α2	471	SHEVLGLTILAWSNSI	GD	LIADVS	vakqgy---	PRMAMAAAIGGQLF	S	I	516
C07A9.11-α2	464	SHEVLGLTILAWSNSI	GD	LIADVS	vvkqgy---	PRMAMAAAIGGPLF	N	L	509
ORF_o325-α2	207	SELTMGLTAIAIGTSL	PE	LATAIA	gvrkge---	NDIAVGNIIGANIF	N	I	252
Consensus		SESV.GLTFVALGTSL LI V I N A	*PD* *E*	LFTSVI I AIA	.....	AD.AIG.IVGSNAF G V A A L G G I	*N*	I L	

Figure 4 (cont.):

Calx–β motifs:

```
                    P ≈ 0                                                P ≈ 2.2e-19
2° str. pred.       LLLL..EEEE..L.EEE..LL.EEEEEEEEE..LLL .EEE EEE...LL.. LL

Calx-β 1    437     EADDPIRMYFEPGHYTVMENCGEFEVRVVRRGDIST yas- VEYETQDGTA s-   486
NCX1-β 1    399     ENDPVSKIFFEQGTYQCLENCGTVALTIIRRGGDLT ntvf VDFRTEDGTA n-   449
NCX2-β 1    389     EDDGASRIFFEPSLYHCLENCGSVLLSVACQGGEGN stfy VDYRTEDGSA k-   439

Calx-β 2    550     DDDHAGIFAFTDSVFEITESVGRFELKVMRYSGARG tvi- VPYWTENDTA t-   599
NCX1-β 2    530     DDDHAGIFTFEEPVTHVSESIGIMEVKVLRTSGARG nvi- VPYKTIEGTA rg   580
NCX2-β 2    518     DDDHAGIFSFQDRLLHVSECMGTVDVRVVRSSGARG tvr- LPYRTVDGTA rg   568

HumInt-bt4-β 985    KEQARDVVSFEQPEFSVSRGDQVARIPVIRRVLDGG ksq- VSYRTQDGTA q-   1034
MurInt-bt4-β 985    KEQASGVVSFEQPEYSVSRGDQVARIPVIRHILDNG ksq- VSYSTQDNTA h-   1034

Consensus           .DD.AG..SFEQPLYHVSE..GTVEVRVIRR.GDGG .... V.YRTEDGTA ..
                              S F       F L  V                  Q

                    P ≈ 0                                                P ≈ 4.3e-8
2° str. pred.       LL.......EEEE.LLL....EEEEEE...L...                  ....EEEEE.LLL

Calx-β 1    487     AGTDFVGRKGLLSFPPGVDEQRFRIEVIDDDVFE ------ EDECFYIRLFNPS  533
NCX1-β 1    450     AGSDYEFTEGTVVFKPGETQKEIRVGIIDDDIFE ------ EDENFLVHLSNVK  496
NCX2-β 1    440     AGSDYEYSEGTLVFKPGETQKELRIGIIDDDIFE ------ EDEHFFVRLLNLR  486

Calx-β 2    600     ESKDYEGARGELVFENNESEKFIDLFILEESSYE ------ KDVSFKVHIGEPR  646
NCX1-β 2    581     GGEDFEDTCGELEFQNDEIVKTISVKVIDDEEYE ------ KNKTFFLEIGEPR  627
NCX2-β 2    569     GGVHYEDACGELEFGDDETMKTLQVKIVDDEEYE ------ KKDNFFIELGQPQ  615

HumInt-bt4-β 1035   GNRDYIPVEGELLFQPGEAWKELQVKLLELQEVD sllrgr QVRRFHVQLSNPK  1087
MurInt-bt4-β 1035   GHRDYVPVEGELLFHPGETWKELQVKLLELQEVD sllrgr QVRRFQVQLSNPK  1087

Consensus           GG.DYEGTEGELVFQPGETEKELQVKIIDD.E.E ------ .D.NFFVHLSNPK
                        FV                 I    LE                I     R
```

Figure 5. Schematic diagram of the Calx protein. The overall predicted structure of Calx is shown. The ion flows predicted for Calx during a single outward calcium exchange are shown to the left. In this diagram, it is easy to see that the *Calx*-α and *Calx*-β motifs map onto regions already known (in NCX1) to be necessary and sufficient for ion transport, high-affinity binding of intracellular calcium, and inactivation by elevated intracellular sodium (Matsuoka *et al.*, 1993). It is also evident that the motifs are precisely repeated: the *Calx*-α motifs occupy identical positions within their respective blocks of membrane sequences, while the *Calx*-β motifs are tandem.

Figure 5:

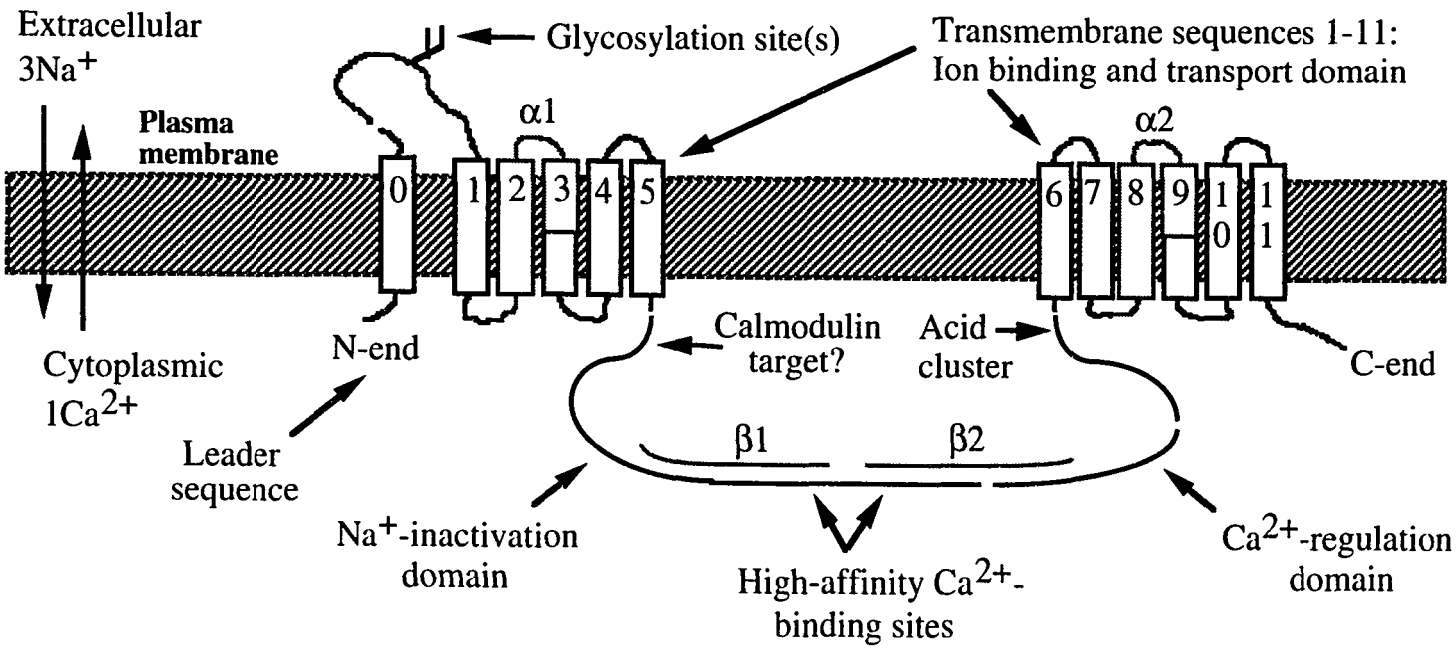
Extracellular
3Na+
Plasma membrane
Cytoplasmic
1Ca2+
Glycosylation site(s)
α1
α2
Transmembrane sequences 1-11:
Ion binding and transport domain
0
1
2
3
4
5
6
7
8
9
10
11
N-end
Leader sequence
Calmodulin target?
Acid cluster
C-end
β1
β2
Na+-inactivation domain
High-affinity Ca2+-binding sites
Ca2+-regulation domain

Figure 6. Strand-specificity of *Calx* transcripts. 6A-6F: RNA and DNA blots were hybridized to strand-specific *Calx* and control *RpA1* (ribosomal protein A1) probes. The blots in 6A/6C and 6D/6F, as well as in 6B and 6E, were made in parallel from the same RNA or DNA gel with equal aliquots of nucleic acid. The positions of molecular weight markers are shown alongside the blots; sizes are in kilobases. **6A**: Head RNA probed with antisense *Calx* ^{32}P-DNA. Three *Calx* transcripts of 8.7, 7.0, and 6.4 kb are seen. 10 μg of poly(A)$^+$ adult head RNA was blotted; the probe strength was $1.2 \cdot 10^6$ cpm/ml. The autoradiograph was exposed for 19 days without an intensifying screen. **6B**: The same probe as in 6A, hybridized to 1 μg of genomic DNA; a single EcoRI fragment of 4.2 kb is seen after the same exposure conditions as in 6A. **6C**: The same head RNA blot as in 6A, now hybridized to *RpA1* double-stranded ^{32}P-DNA; a single 0.68 kb transcript is seen, after an exposure of 19 hours with an intensifying screen. The probe strength was $0.74 \cdot 10^6$ cpm/ml. **6D**: Poly(A)$^+$ adult head RNA probed with sense *Calx* ^{32}P-DNA. 10 μg of poly(A)$^+$ adult head RNA was blotted; the probe strength was $1.7 \cdot 10^6$ cpm/ml; the exposure conditions were identical to those of 6A and 6B. No discrete transcripts were seen. **6E**: The same probe as in 6D, hybridized to 1 μg of genomic DNA, with the same exposure as 6A-6B and 6D; again, a single EcoRI fragment of 4.2 kb is seen. Note that the signal here is, if anything, stronger than in 6B. **6F**: The same head RNA blot as in 6D, now hybridized to the same *RpA1* probe used in 6C, with an identical 0.68 kb transcript detected after 19 hours with an intensifying screen.

Figure 6:

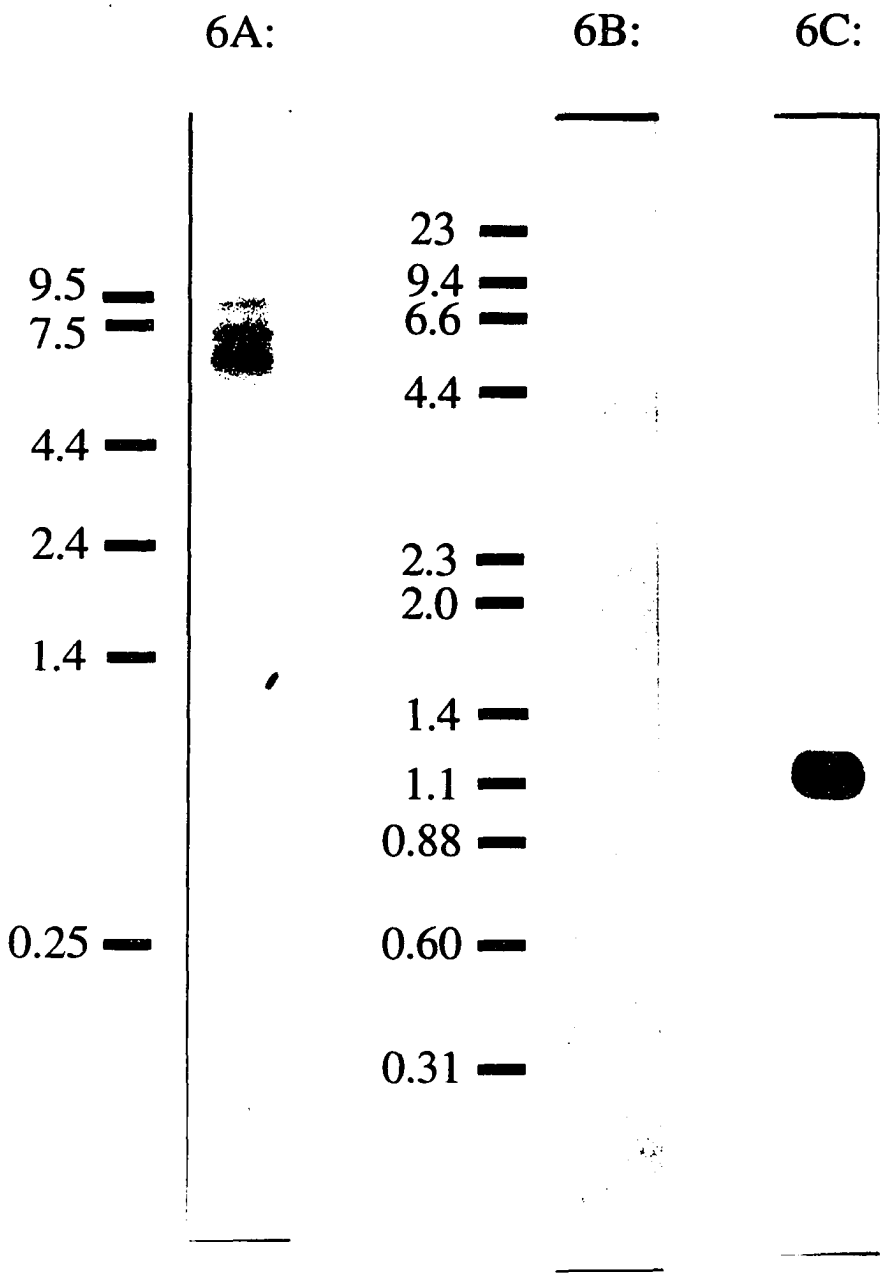

Figure 6:

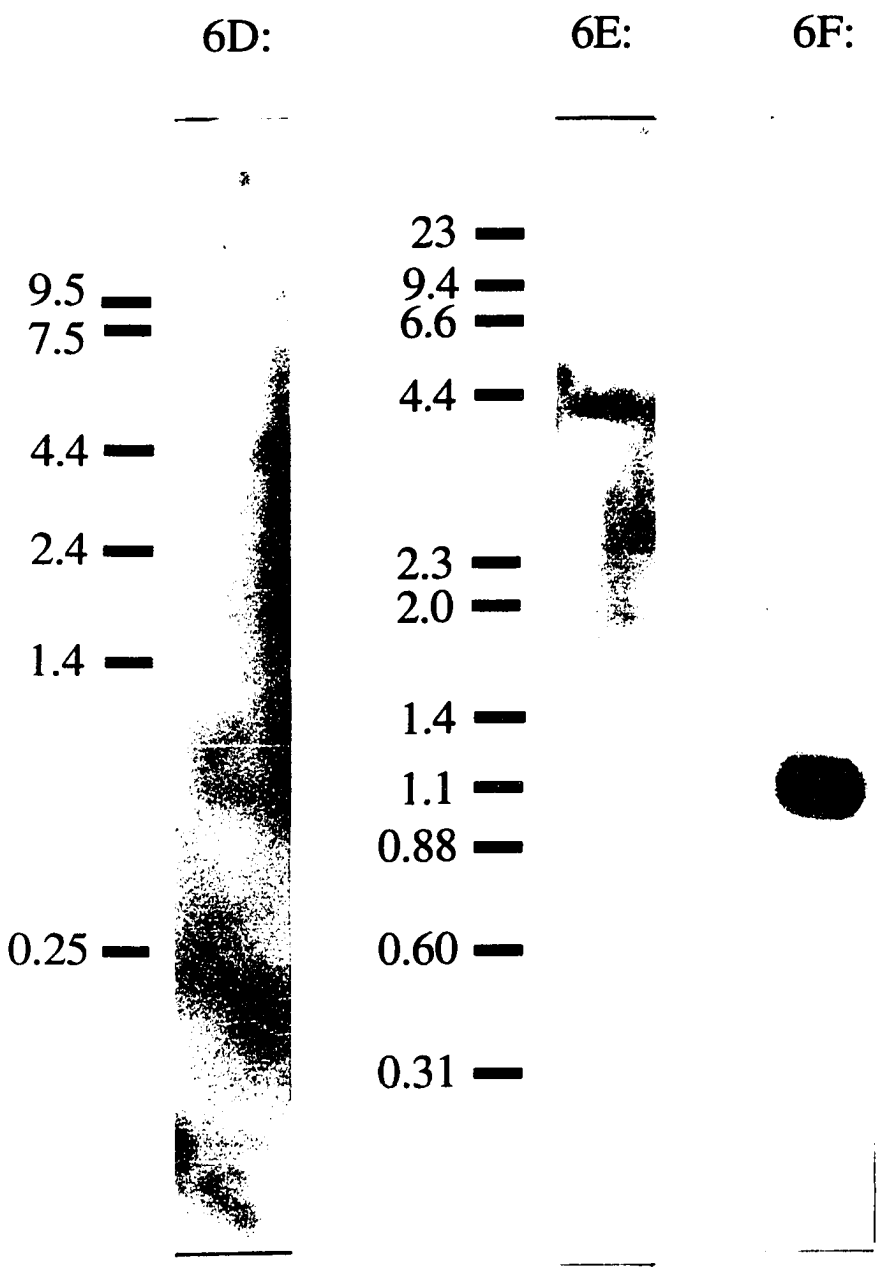

Figure 7. Multiple *Calx* transcripts in adult tissues. **7A**: Antisense *Calx* probe hybridized to poly(A)$^+$ RNAs. From left to right, the poly(A)$^+$ RNAs consist of 5 μg from wild-type heads (h), 5 μg from eyeless (*eyes absent*) heads (e), and 10 μg from wild-type bodies (b). In adult heads, transcripts with the following sizes are observed: ≥~15, 9.0, 8.2, 7.0, 5.6, and 4.9 kb. The first three transcripts are scarce but visibly unchanged between normal and eyeless heads: this serves as a useful control for integrity and equal loading of high molecular weight RNAs. The 7.0 kb transcript is enriched in eyeless heads; the 5.6 kb transcript is enriched in normal heads. In wild-type bodies, there is a trace of what might be the 5.6 kb transcript, plainly visible 4.9 kb transcript, and a body-specific 4.0 kb transcript. The probe strength was $1.0 \cdot 10^6$ cpm/ml; the exposure time was 25 days without an intensifying screen. Because the high-resolution RNA gel technique of Tsang *et al.* (1993) was used, the molecular weights seen for *Calx* transcripts here are more reliable than those in Figure 6A. **7B**: The same blot as in 7A, rehybridized with mixed *ninaE* (rhodopsin) and *RpA1* probes. The retina-specific *ninaE* transcript (1.7 kb) and the ubiquitous *RpA1* transcript (0.68 kb) are both seen. There is no trace of *ninaE* signal in either eyeless head or body RNAs, confirming their purity. The probe strength was $0.37 \cdot 10^6$ cpm/ml for *ninaE* and $0.38 \cdot 10^6$ cpm/ml for *RpA1*; the exposure was 14 hours without an intensifying screen.

Figure 7:

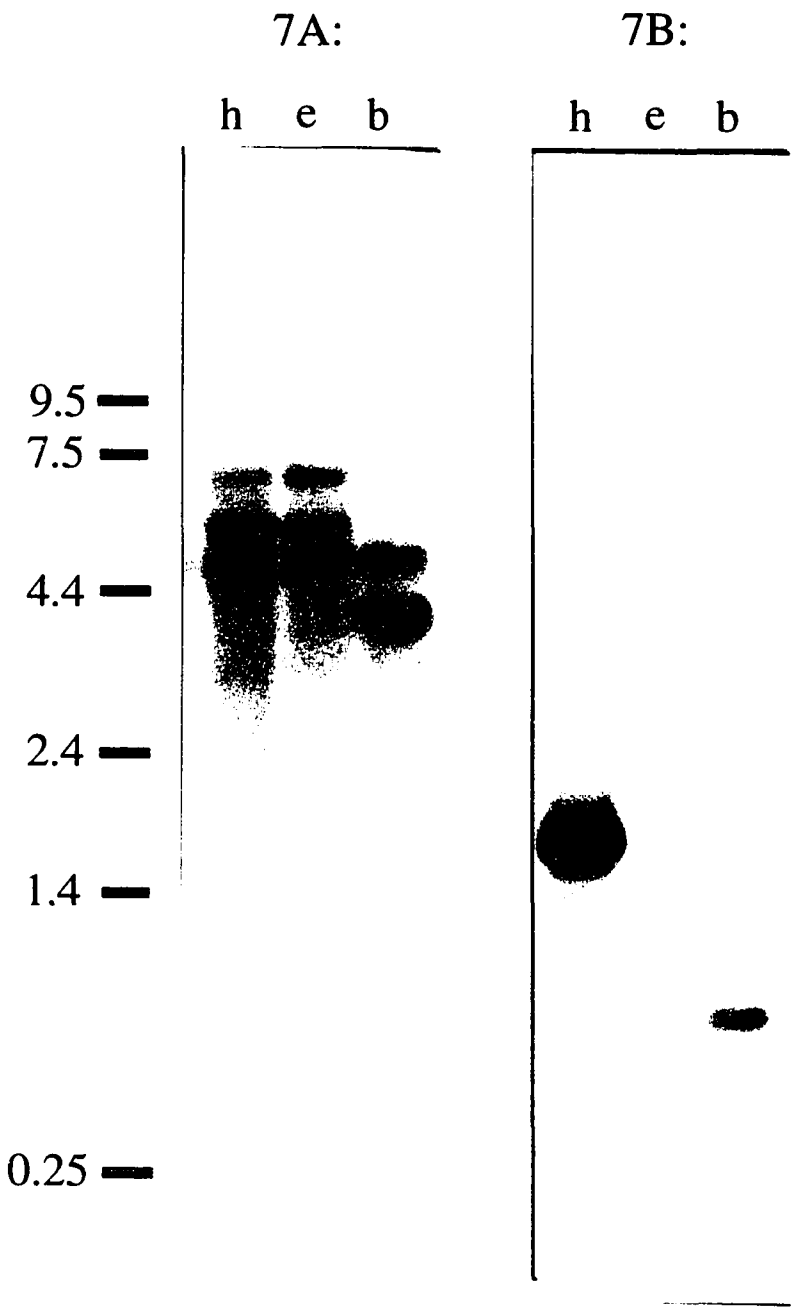

Figure 8. Spatial distribution of *Calx* transcripts in embryos and adult heads. Unless otherwise noted, all visible light images had Nomarski optics. All scale bars denote 100 μm.

8A-8H: *Calx* transcripts are ubiquitously expressed in embryos. The background signal elicited in embryos by sense *Calx* probes is very low. Embryonic stages are detailed in Ashburner (1989a). All images are magnified 180x. **8A-8B**: Precellular blastoderm hybridized with *Calx* antisense probe (**8A**) or sense probe (**8B**). **8C-8D**: Cellular blastoderm with antisense (**8C**) or sense probe (**8D**). **8E-8F**: Gastrula (in germ band elongation) with antisense (**8E**) or sense (**8F**) probe. **8G-8H**: Late embryo (undergoing head involution and organogenesis) with antisense (**8G**) or sense (**8H**) probe. Observe that, in 8H, the sense probe has been caught and protected from washing by the embryo's tracheae. This shows that the absence of sense signal in 8B, 8D, 8F, and 8H is due to effective probe washing, and not to failed probe synthesis.

8I-8L: *Calx* transcripts in embryos, while ubiquitous, are still localized to some extent. **8I**: They delineate the boundaries of cells, in a cellular blastoderm probed with antisense *Calx*. (Here, Nomarski optics is omitted, so that only variations of color staining are seen.) Magnfication is 580x. **8J**: Under the surface epithelium of a cellular blastoderm, *Calx* transcripts are enriched within a subcortical region (seen without Nomarski). Magnification is 580x. **8K-8L**: They also line cell boundaries in a later stage, germ band elongation. Here a gastrulating embryo probed with antisense *Calx* is shown with (**8K**) and without (**8L**) Nomarski optics. The correspondence of cell membranes and transcripts can be seen despite the curvature of embryonic epithelium. Magnification is 290x.

8M-8P: *Calx* transcripts in the adult head: magnfication is 150x. **8M**: In adult heads probed with antisense *Calx* probes, *Calx* transcripts are found in retina, optic ganglia, and cortical cells. They show a halo of staining surrounding the neuropil. **8N**: But, sense *Calx* probes in adult heads--unlike in embryos--give visible background signals.

Like antisense signals, the sense signals are ubiquitous in the adult head, but are consistently weaker than antisense signals. Both the antisense and sense probes used here are identical to those used on embryos, as are the hybridization and wash protocols. The RNA data of Figure 7, and the embryo data in 8A-8H, suggest that the signal seen with sense probe may arise from nonspecific adhesion to head tissue. We know, from mock hybridizations, that it is not due to an endogenous alkaline phosphatase (data not shown). **8O-8P**: Another view of adult tissues hybridized to antisense (**8O**) and sense (**8P**) *Calx* probes. Note the signal in thoracic muscle, seen only with antisense probe.

8Q-8R: Two views of *Calx* transcription in the retina detected by antisense probes. There is no obvious subset of cells failing to express *Calx*. Magnification is 580x.

8S: View of a proximal retina (upper left corner), optic ganglion (to upper left of center, a narrow ellipse of staining surrounding weakly-stained neuropil), and lateral brain (in the center of view, an inverted V of cortical staining, surrounding a halo of stain bordering the neuropil). Increased magnification shows a honeycomb of small unstained voids in the cortex of both the optic lobe and the brain, perhaps due to unstained cortical nuclei. This cortical staining surrounds a region of uniform staining that is dark at its outer edge but grades rapidly off to invisibility further into the optic lobe and brain neuropil. Magnification is 580x.

Figure 8:

8A:

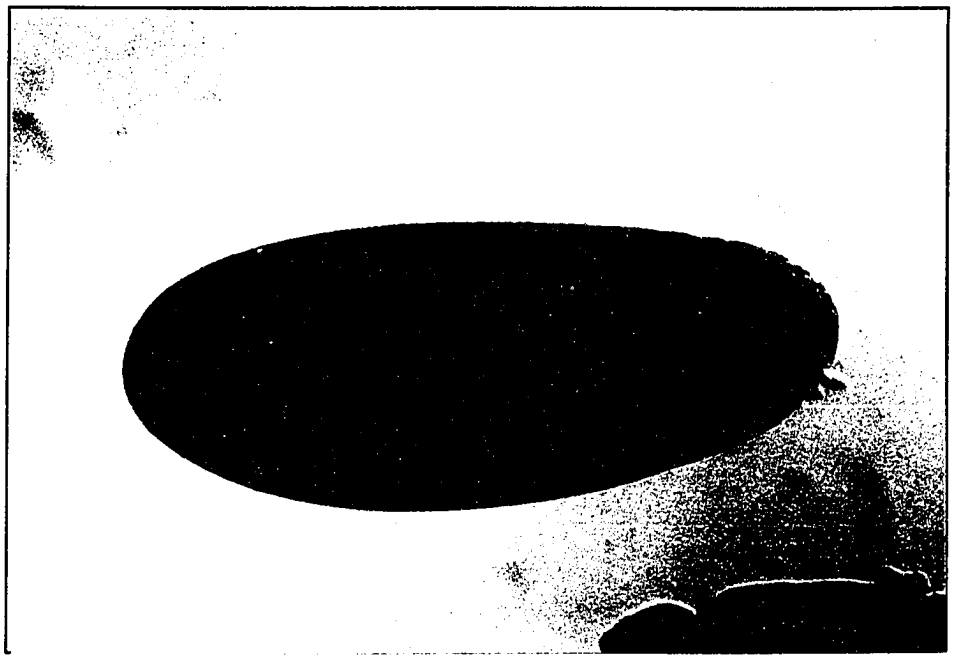

8B:

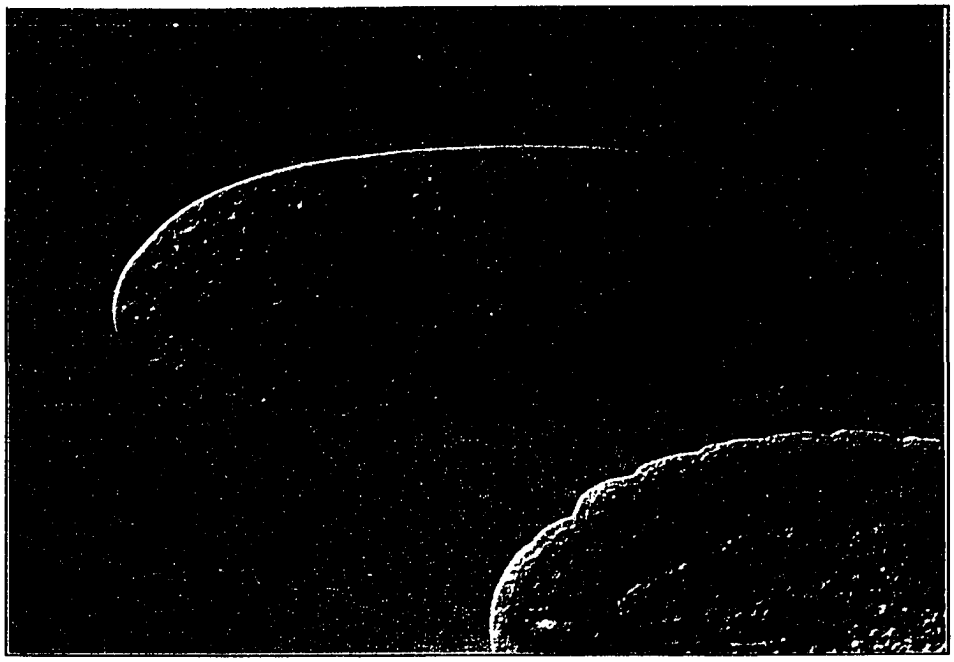

Figure 8:

8C:

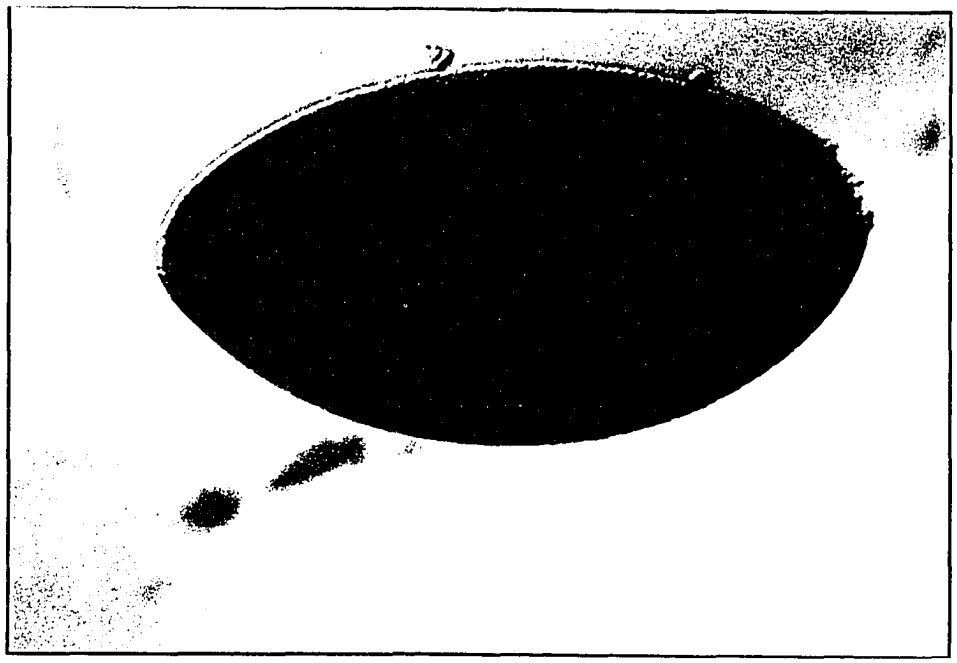

8D:

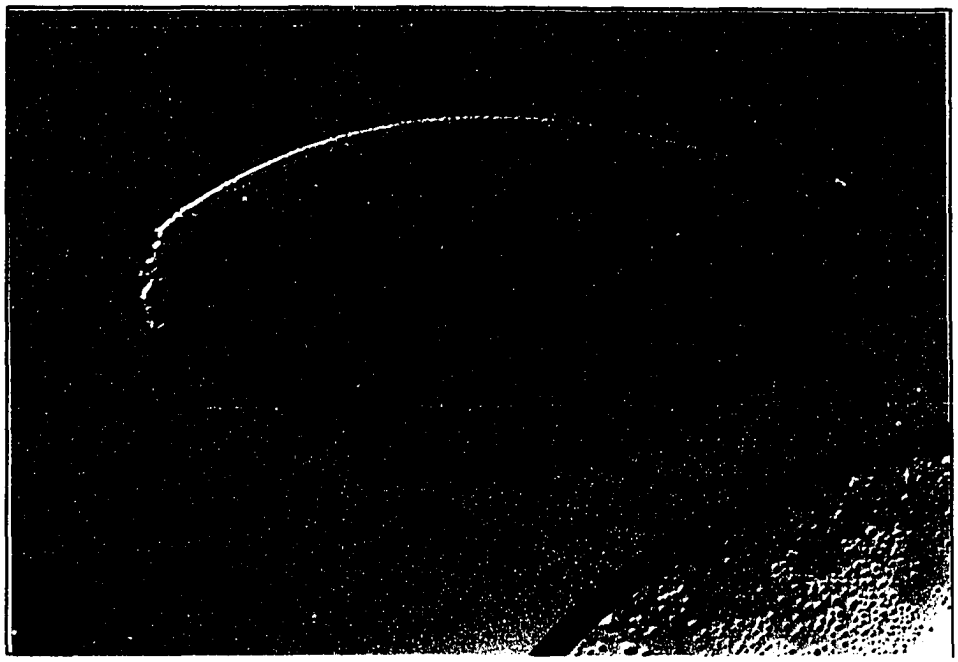

Figure 8:

8E:

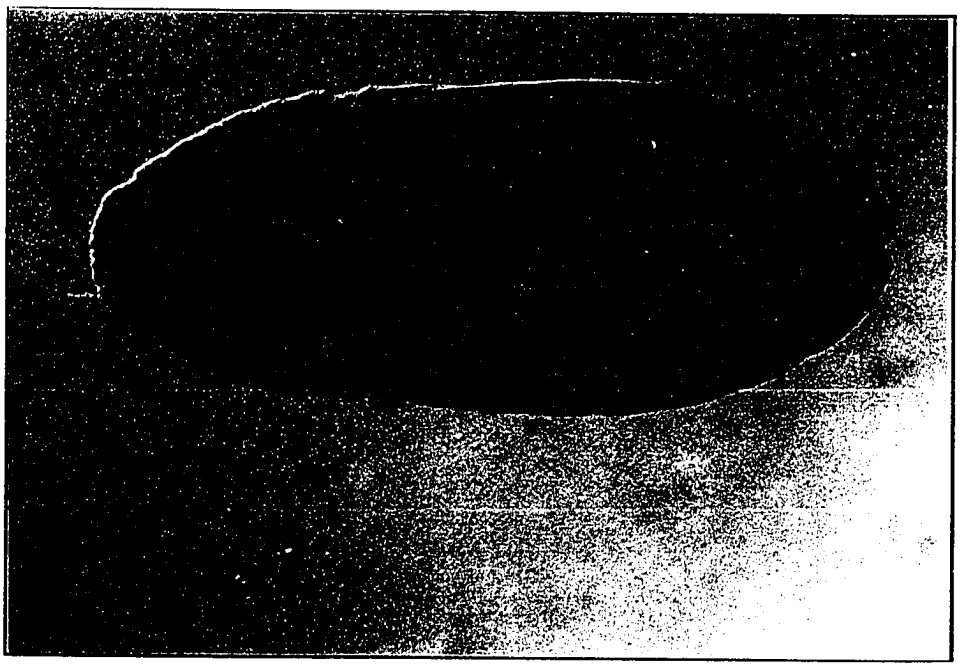

8F:

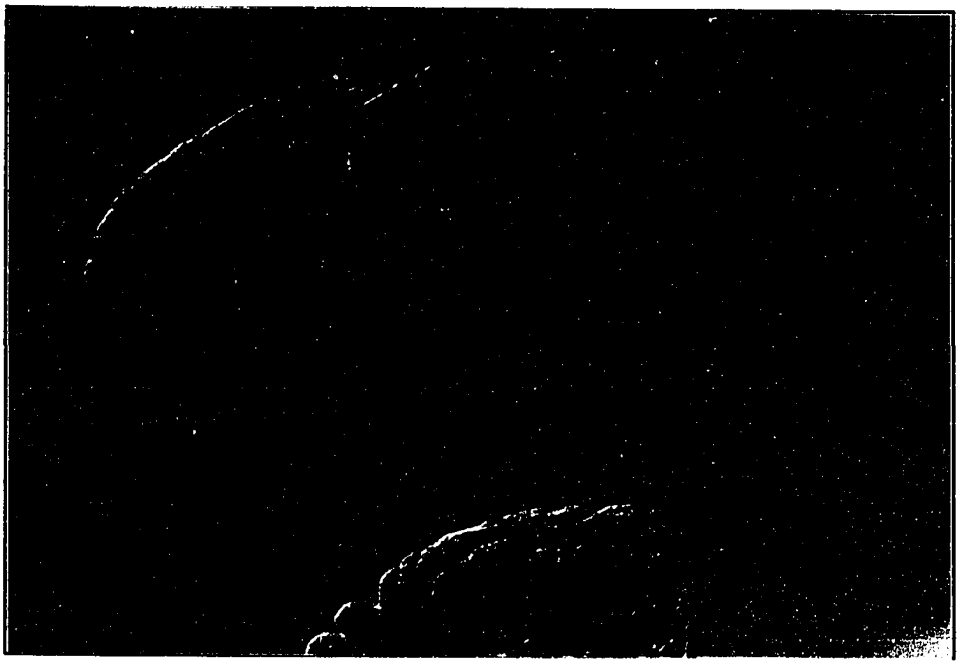

Figure 8:

8G:

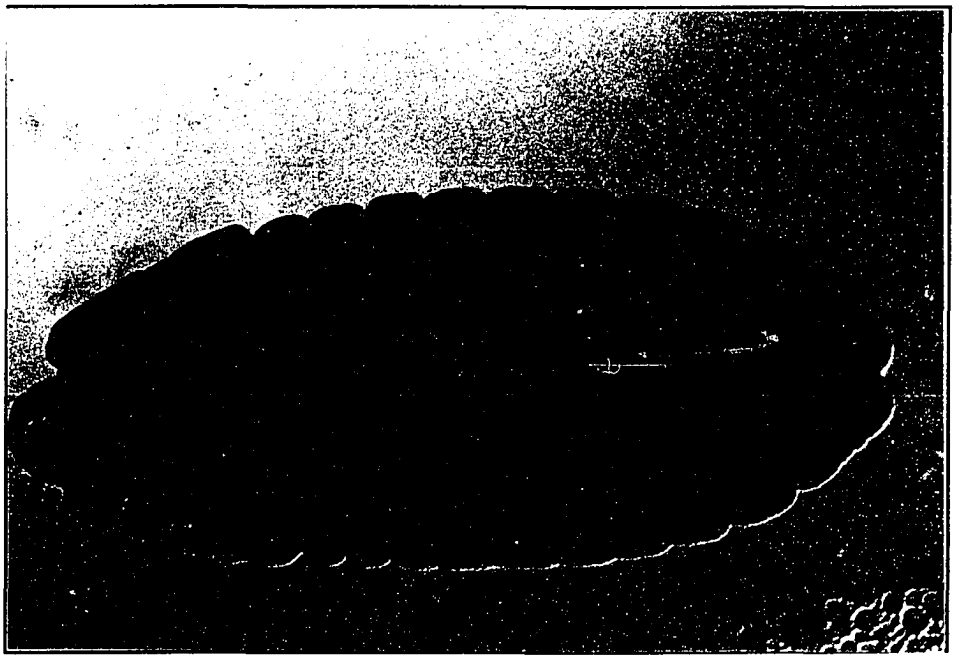

8H:

Figure 8:

8I:

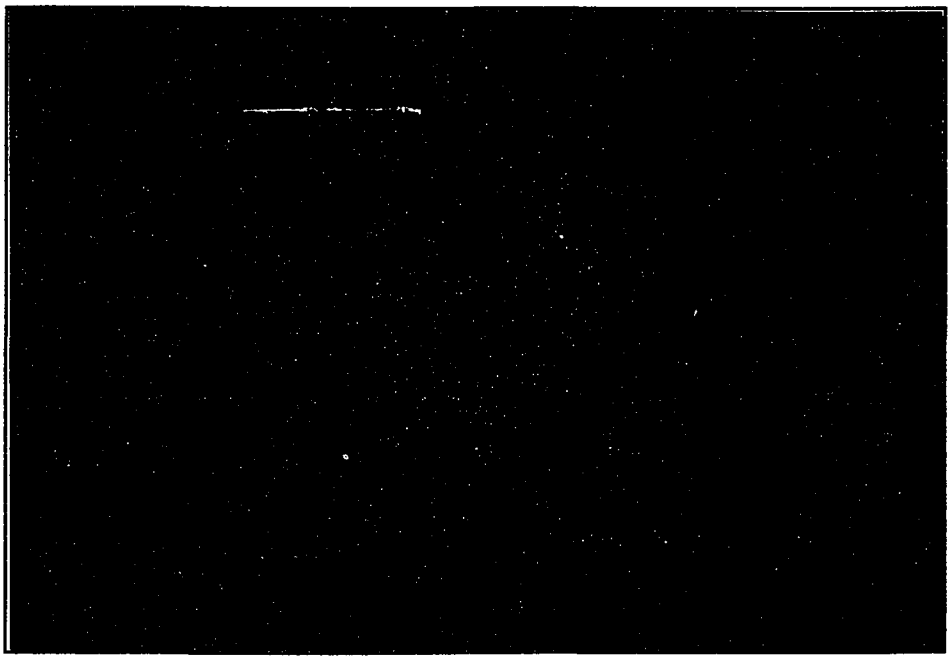

8J:

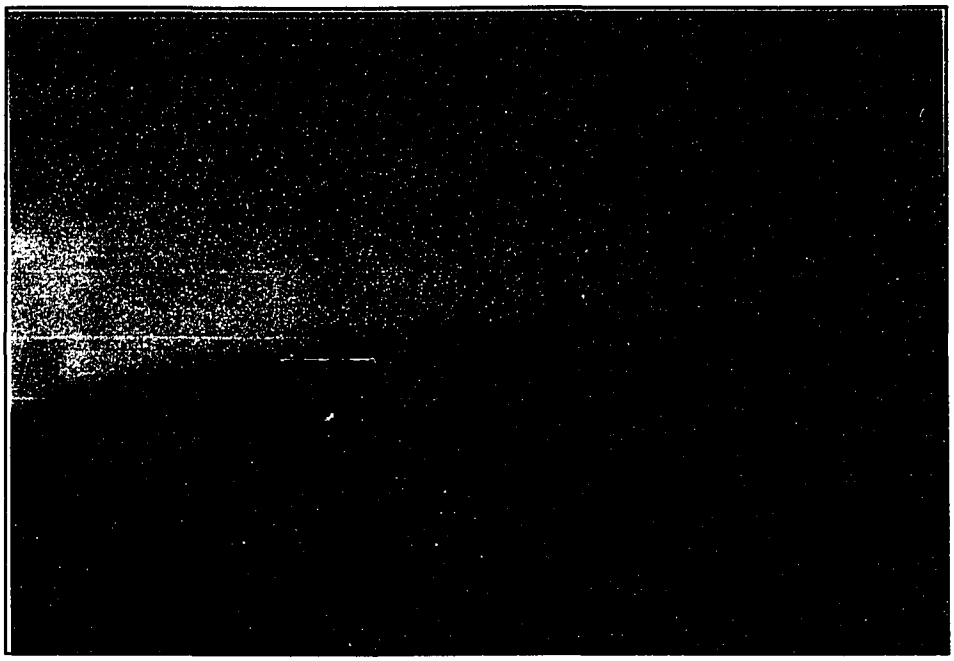

Figure 8:

8K:

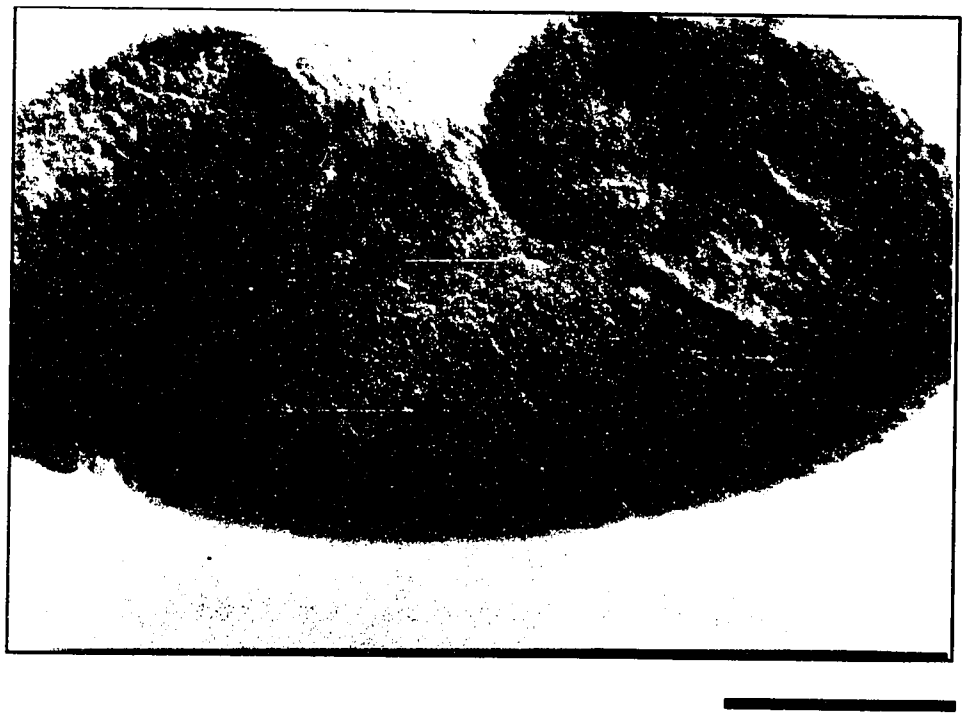

8L:

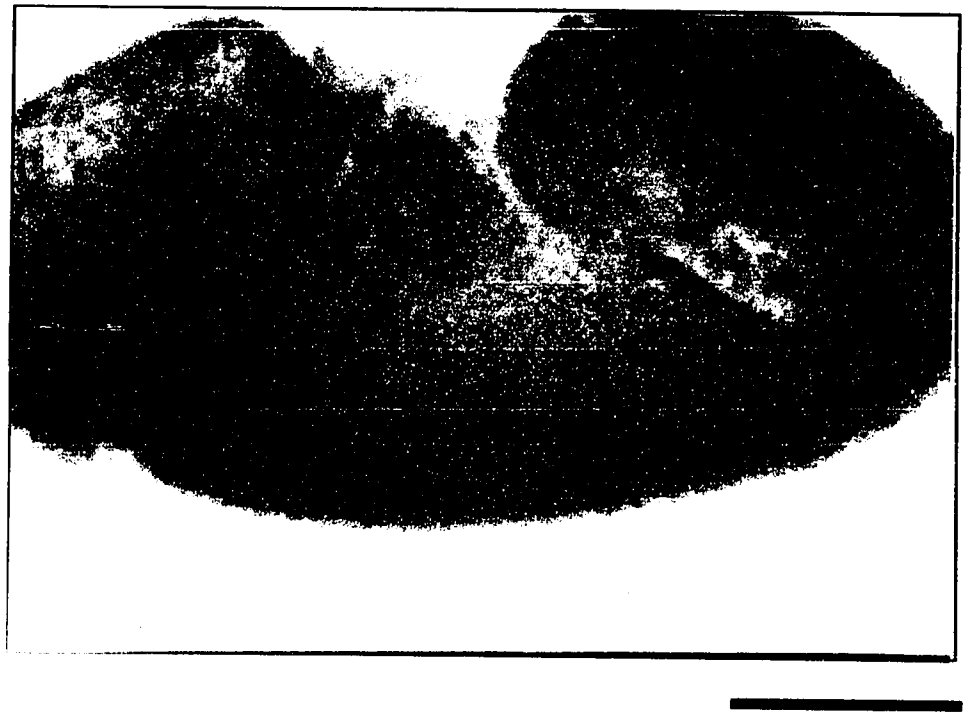

Figure 8:

8M:

8N:

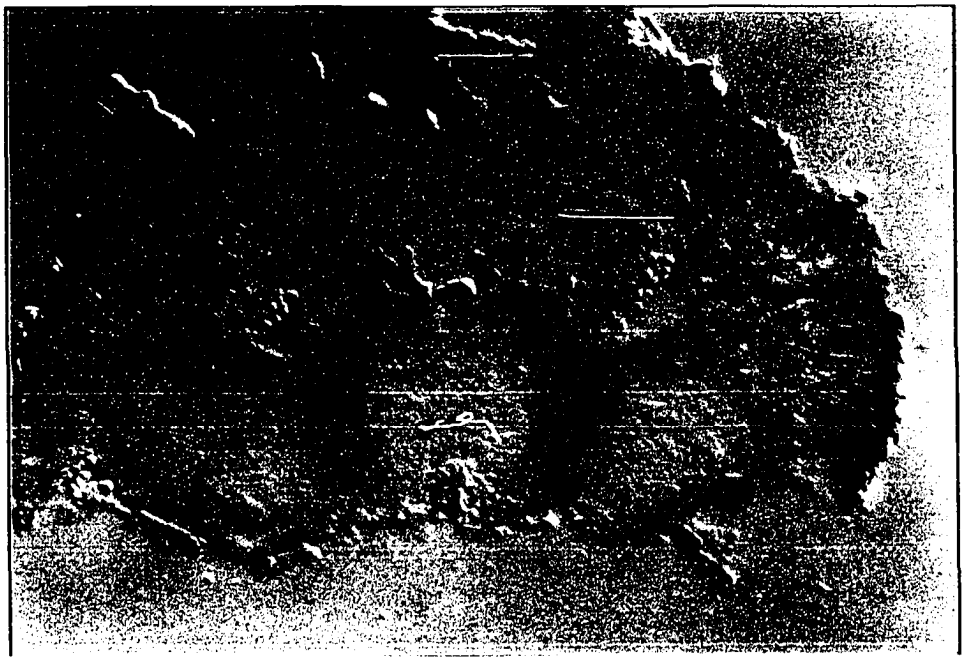

Figure 8:

8O:

8P:

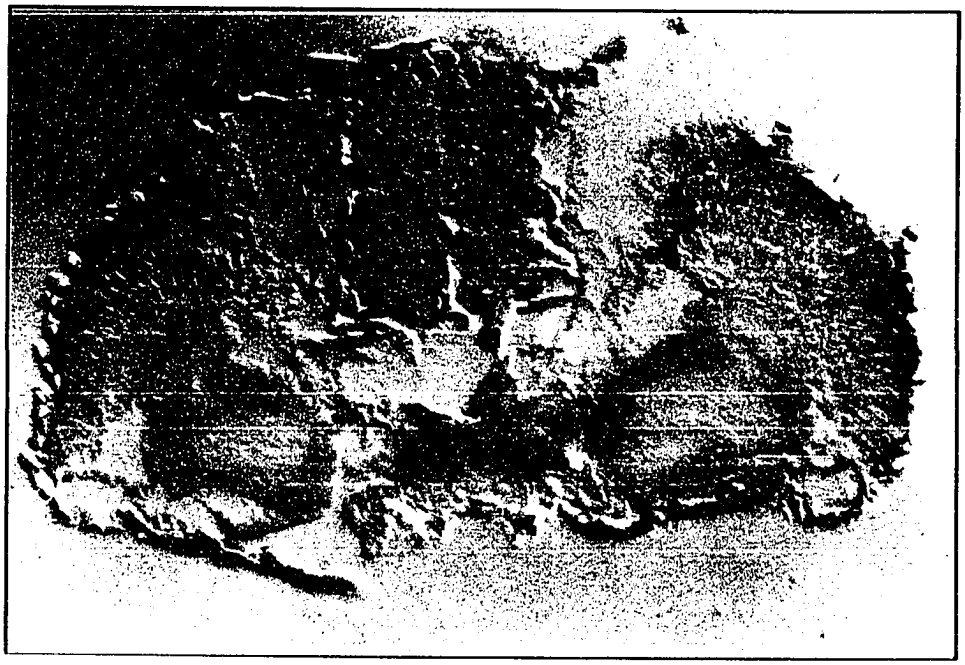

Figure 8:

8Q:

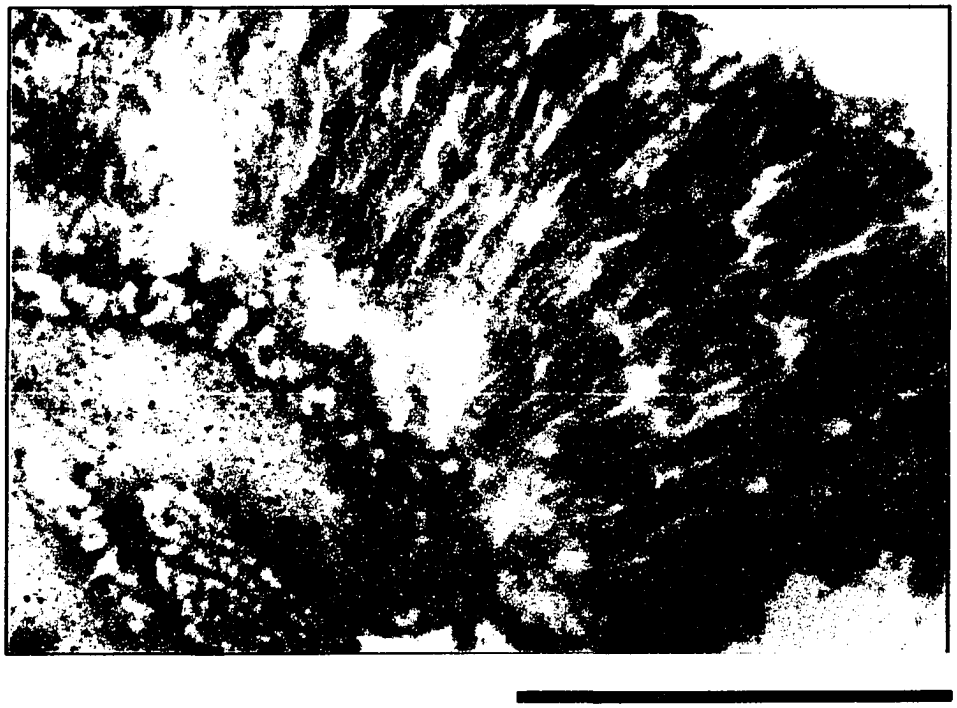

8R:

Figure 8:

8S:

Figure 9. Spatial distribution of Calx in adult heads. Antiserum raised against the KLH-conjugated Calx peptide C1-15 was used to visualize Calx distribution in adult *Drosophila* head sections by indirect immunofluorescence. All visible light images have Nomarski optics. All scale bars denote 100 μm. None of the specific patterns here were seen with preimmune serum or early stages of antiserum generation (data not shown.)

9A-9D: Adult tissues probed with anti-KLH-C1-15 polyclonal serum at 1:2000 dilution. The signals complement those seen for *Calx* transcripts: retinal and thoracic muscular expression is prominent. Where transcripts were expressed in cortical nuclei and the borders of the neuropil, proteins are found predominantly in the neuropil rather than in cortices. **9A**: From right to left, staining is seen in: adult retina; neuropil of the lamina (first optic ganglion); and neuropil of the underlying optic lobe. Magnification is 360x. **9B**: A sagittal view of the adult head. The sides show prominent retinal staining. Concentrated whorls of neuropil staining are seen in the center. The small points of bright staining on the top of the head are ocellar photoreceptors. Magnfication is 180x. **9C**: A detailed view of ocellar photoreceptor staining, from the same head as in 9B; magnification is 360x. **9D**: Strong staining in the thoracic muscle; magnification is 180x.

9E-9H: Retinal and neuropil staining is specifically abolished by competition with peptide C1-15. All magnifications are 360x. Photographic exposure times in 9F and 9H were both 30 seconds. **9E**: A double exposure (Nomarski visible and DAPI-filtered UV light) to show cells and nuclei in an adult head section. The photoreceptors are on the right, with nuclei near the retina surface. Trapezoids of nuclei further inside the head mark cells of the optic ganglia. **9F**: The same head section as in 9E, now viewed with UV light and a rhodamine red filter to visualize *Calx* antigens. The serum used here is at 1:20,000 dilution and was competed with ovalbumin-conjugated C2-17 (a distinct peptide from C1-15.) Other than being weaker (and thus less detailed), the staining here is qualitatively like that in Figure 9A. Specifically, retinal staining remains prominent, and the neuropil of optic ganglia is unquestionably delineated. **9G**: A similar view as in 9E above. Note that

photoreceptors are in the same focus as in 9E. **9H**: Exactly as in 9F, except the serum used here was competed with ovalbumin-conjugated C1-15 instead of C2-17. Staining is abolished in both the retina and the optic neuropil. Attempts to carry out competition with serum at 1:2000 dilution have not been successful, perhaps because our polyclonal ascites has a high titer.

Figure 9:

9A:

9B:

Figure 9:

9C:

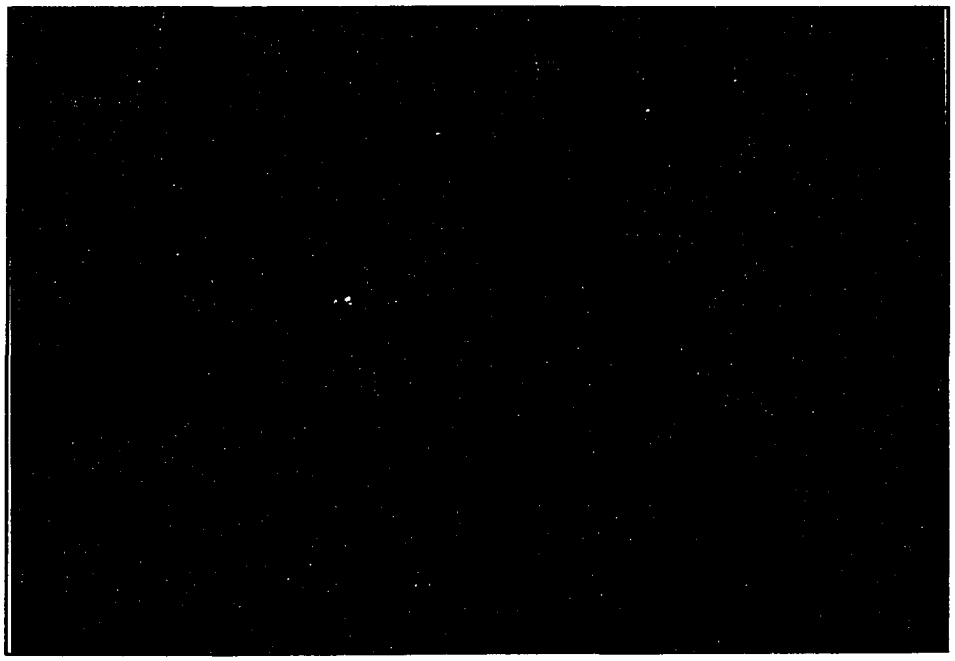

9D:

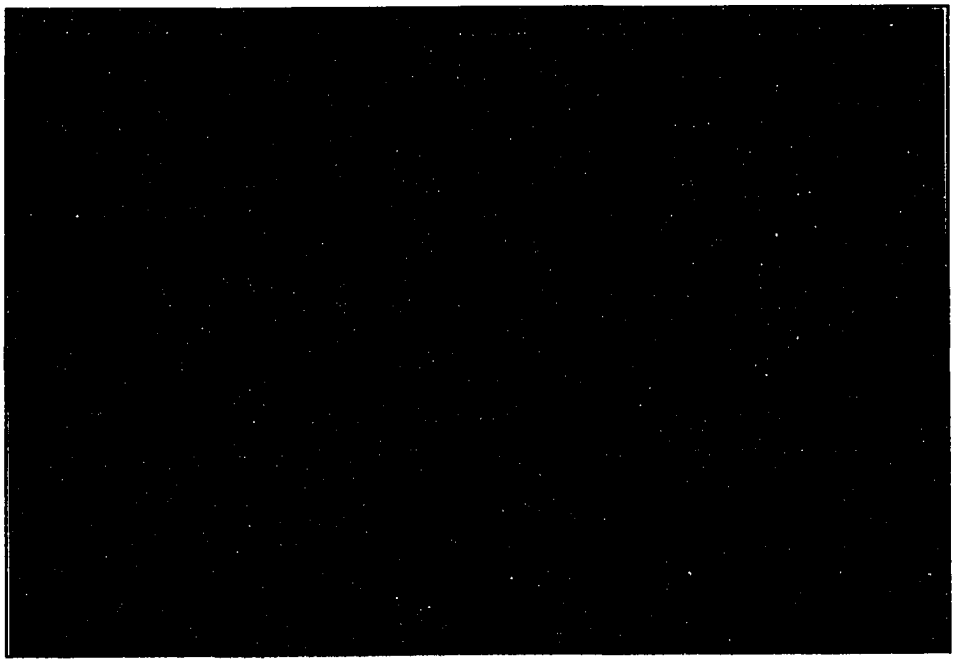

Figure 9:

9E:

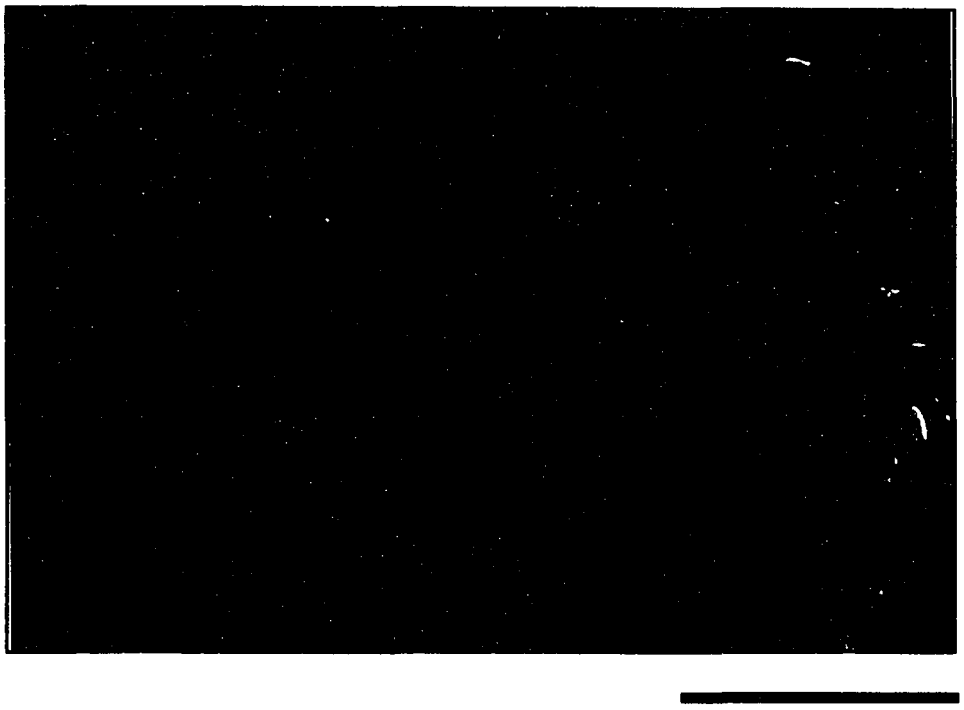

9F:

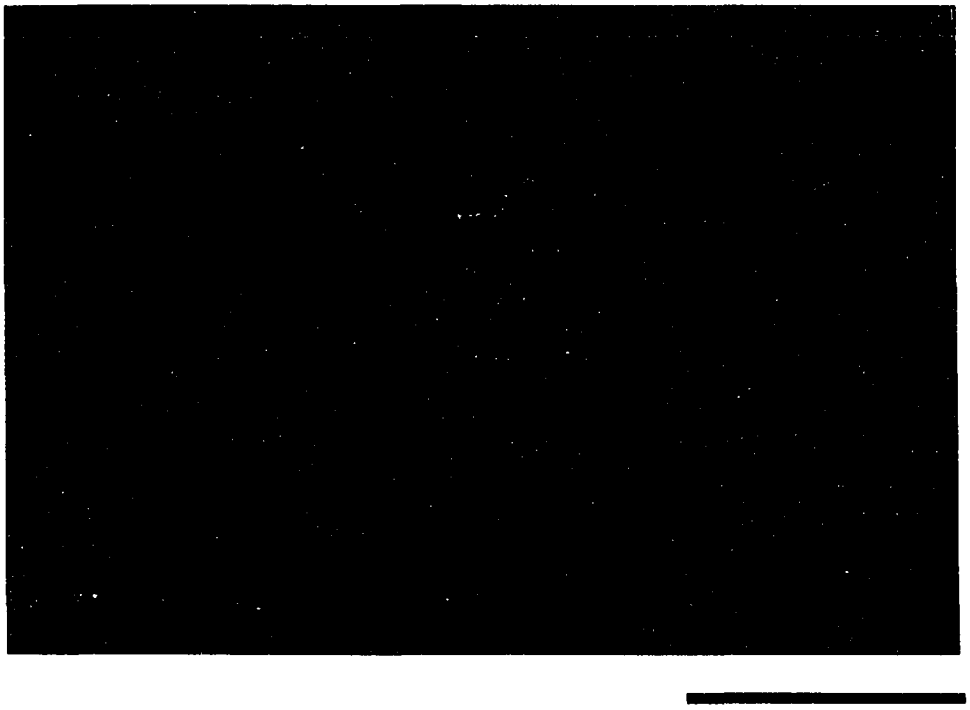

Figure 9:

9G:

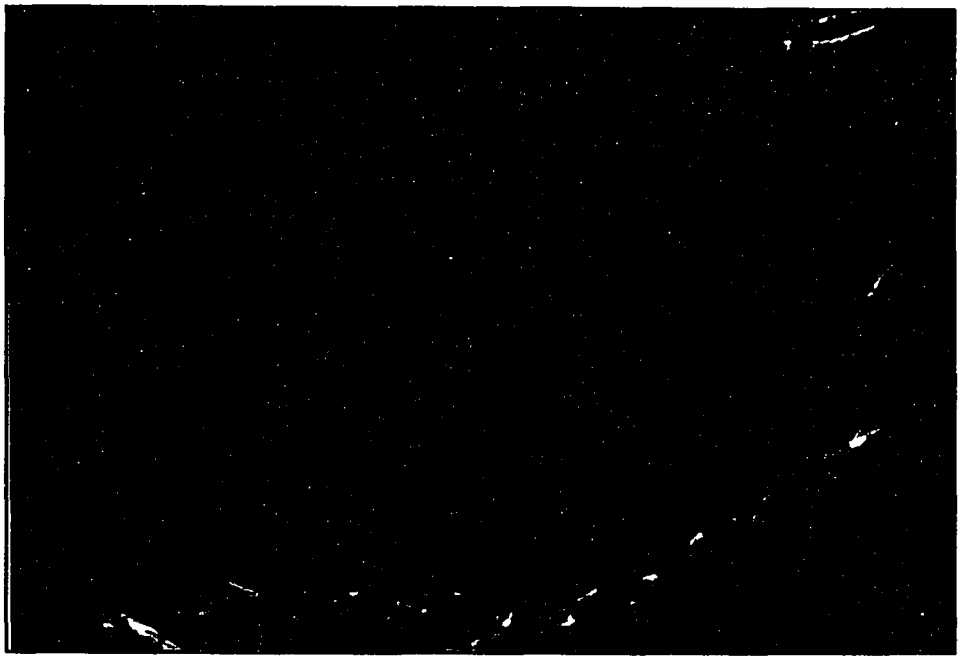

9H:

Figure 10. The *Calx* genomic region. 65 kb of genomic DNA encompassing the *Calx* transcription unit are shown. The topmost continuous line shows a restriction map, with upper ticks denoting EcoRI sites and lower ticks denoting HpaI sites. One HpaI site (at about -5.0 kb) separates two HpaI-HpaI fragments (1.18 and 1.05 kb in size) whose order was not determined. Immediately above the restriction map, DNA fragments are denoted that crosshybridize to plasmid-rescued DNA from the P997 lethal mutation, to the Na^+/K^+ pump α-subunit (*Na-p*) gene (Lebovitz *et al.*, 1989), and to the *Calx* cDNAs 9C5-o and 9C5-E. The proximal end of the *r-l* genomic walk (Eisenberg *et al.*, 1990) begins with a 5.0 kb EcoRI fragment immediately to the right of the genomic DNA shown here. The chromosomal orientation of *Calx* and *Na-p* are shown with arrows at top. DNA fragments cross-hybridizing to *Calx* cDNA are shown as solid parts of the *Calx* transcript arrow; other fragments are shown as stippled parts of the line, to indicate that the precise disposition of *Calx* exons awaits future genomic sequencing. The direction of *Calx* transcription was deduced from ordered cDNA probes and strand-specific RNA blots (Figure 6). Immediately underneath the restriction map, a scale bar shows distances in kb; the +0.00 kb coordinate is set at the first restriction site 5'-ward of the *Calx* locus. Beneath the scale bar, the inserts of six cosmids covering the region are shown.

Figure 10:

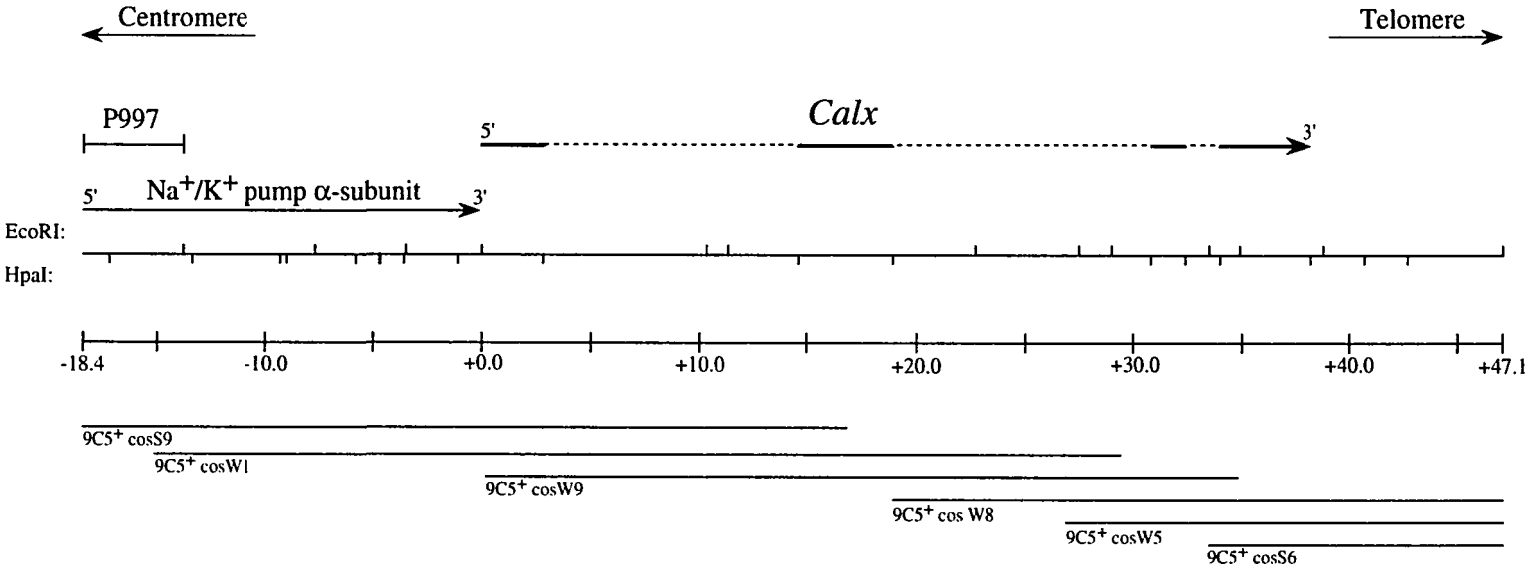
Centromere
Telomere
P997
Calx
5'
3'
5'
Na+/K+ pump α-subunit
3'
EcoRI:
HpaI:
-18.4
-10.0
+0.0
+10.0
+20.0
+30.0
+40.0
+47.1
9C5+ cosS9
9C5+ cosW1
9C5+ cosW9
9C5+ cos W8
9C5+ cosW5
9C5+ cosS6

Figure 11. Expression of Calx in *Xenopus* oocytes. This shows the data in Table 2 graphically. All symbols here have the same significance as in Table 2.

Figure 11:

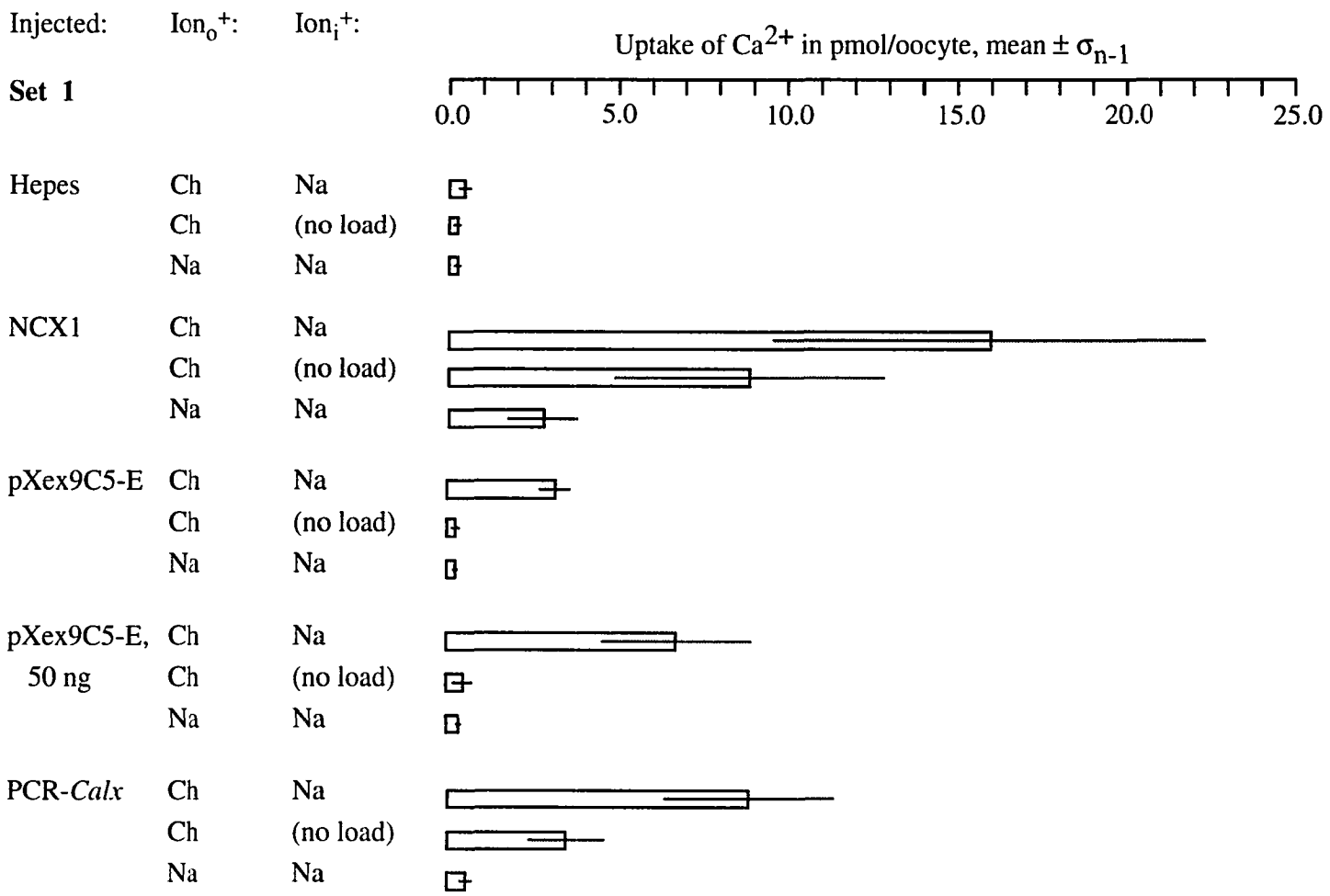
Injected:
Ion$_o^+$:
Ion$_i^+$:
Uptake of Ca^{2+} in pmol/oocyte, mean ± σ_{n-1}
Set 1
0.0
5.0
10.0
15.0
20.0
25.0
Hepes
Ch
Na
Ch
(no load)
Na
Na
NCX1
Ch
Na
Ch
(no load)
Na
Na
pXex9C5-E
Ch
Na
Ch
(no load)
Na
Na
pXex9C5-E,
50 ng
Ch
Na
Ch
(no load)
Na
Na
PCR-*Calx*
Ch
Na
Ch
(no load)
Na
Na

Figure 11 (cont.):

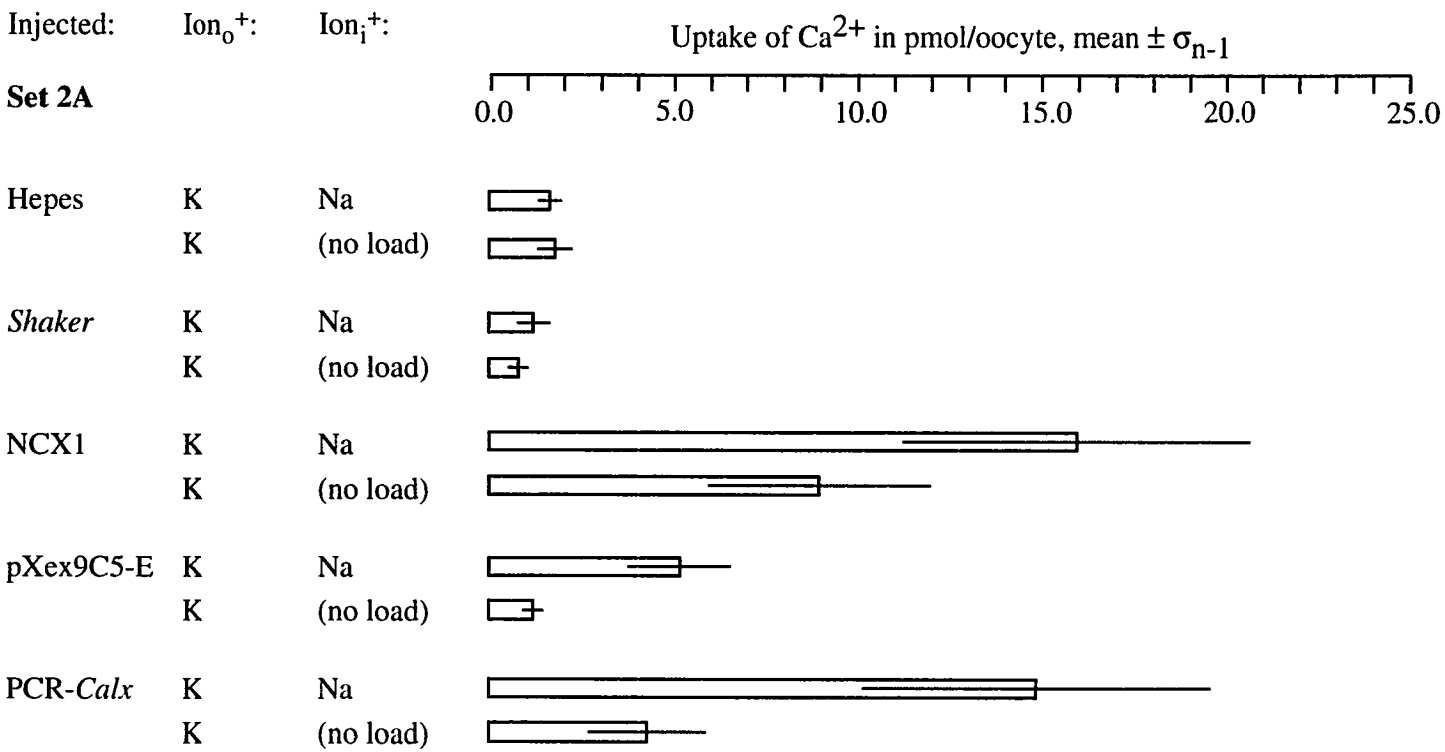

Figure 11 (cont.):

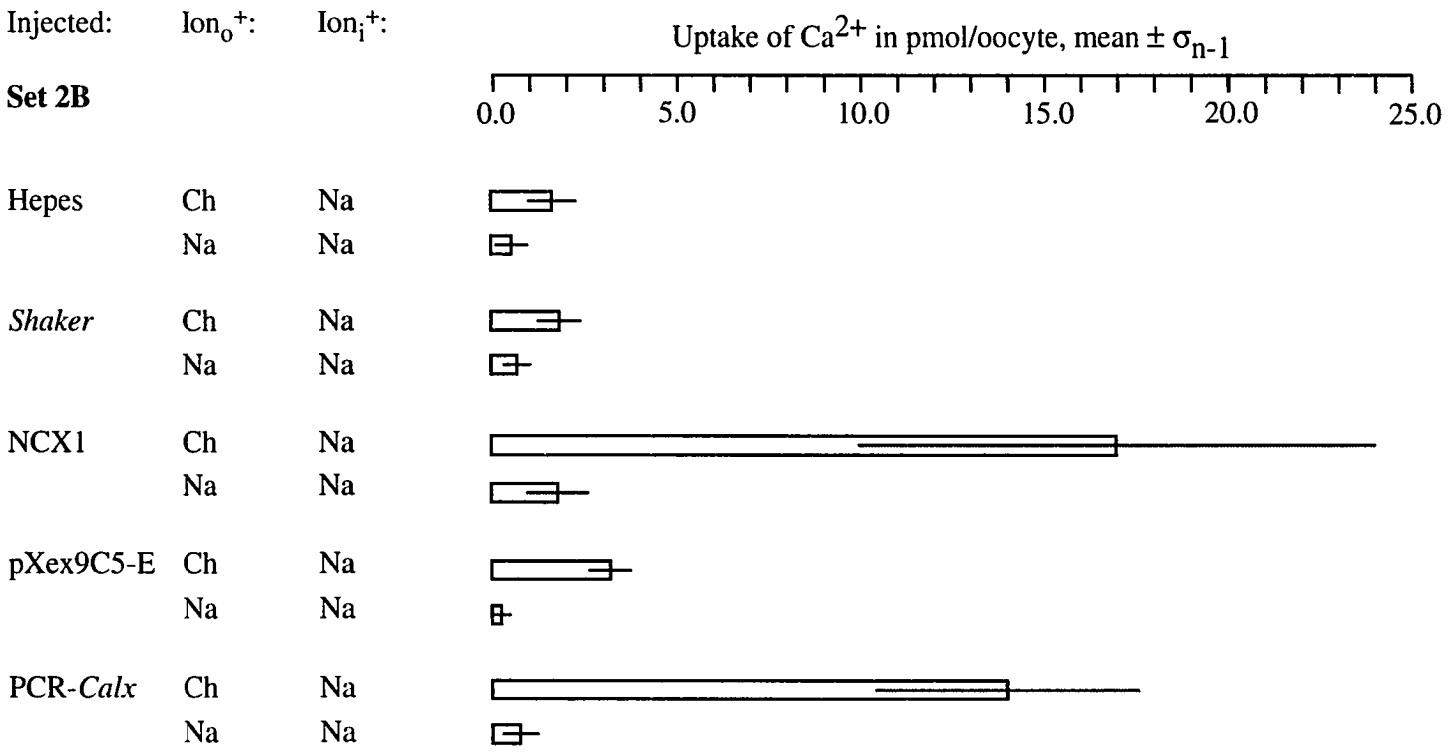

Figure 11 (cont.):

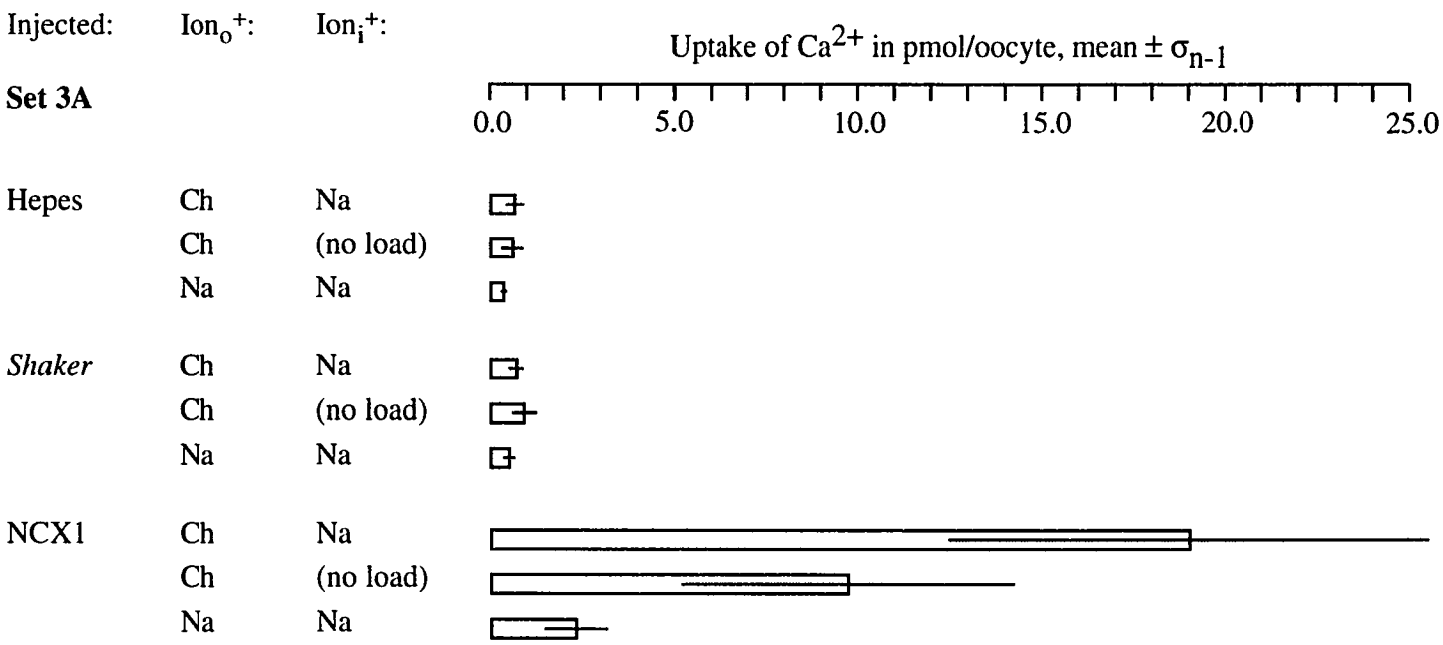

Figure 11 (cont.):

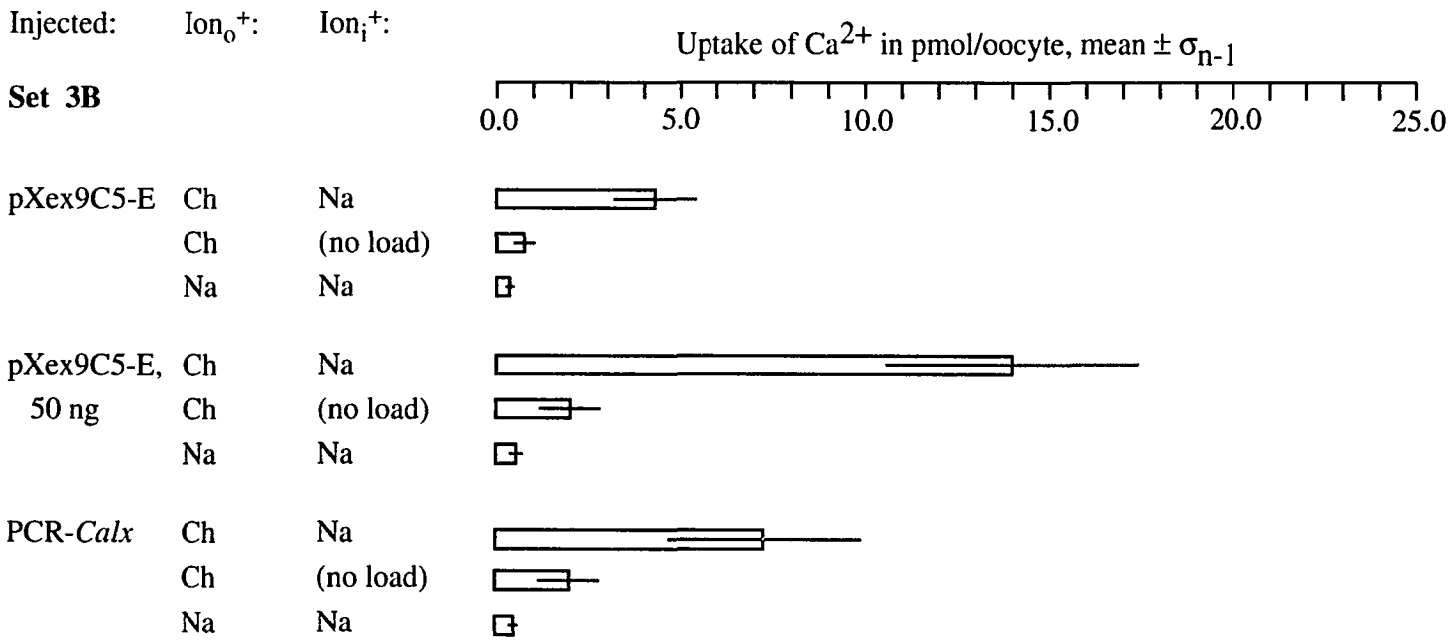

Figure 11 (cont.):

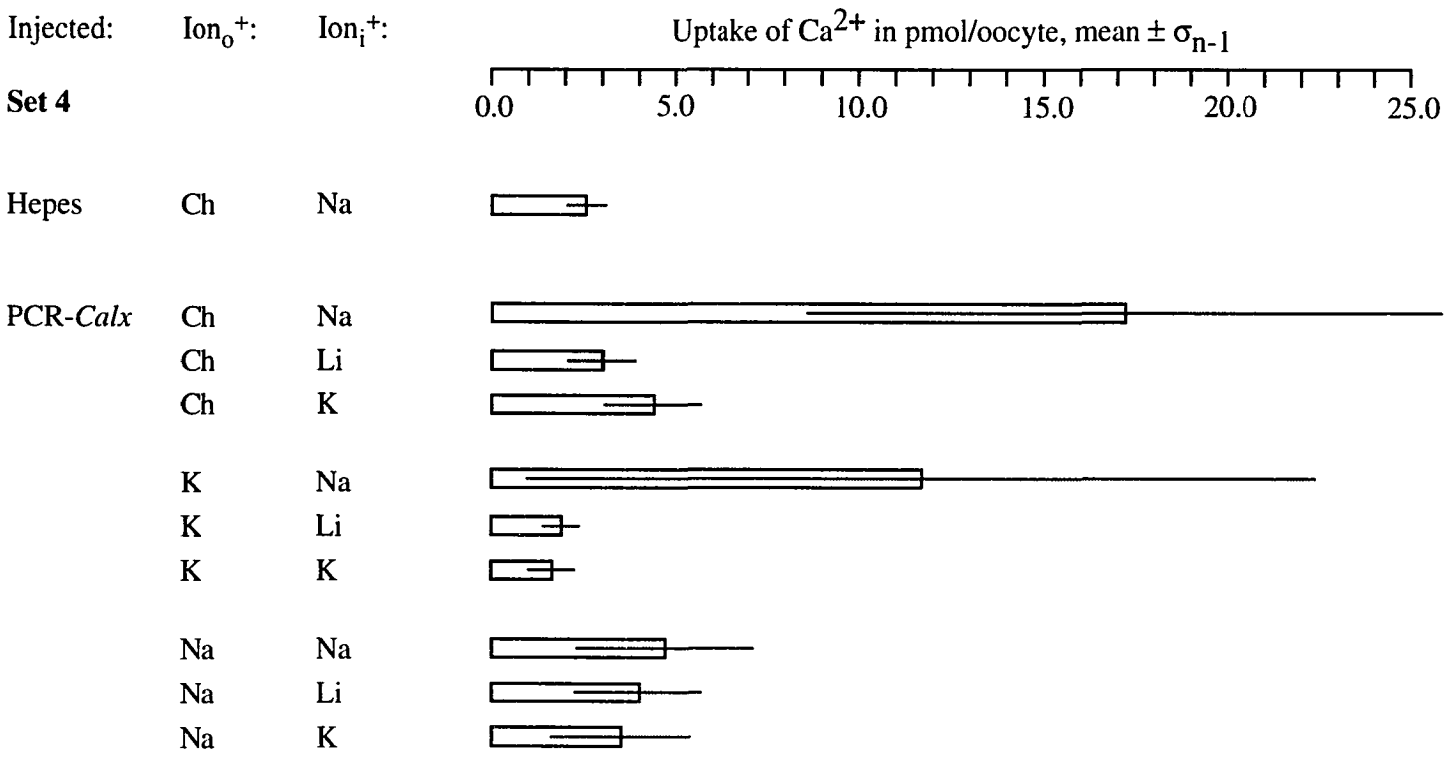

Figure 12. Evolutionary tree of Calx homologs. This tree shows a branched pathway for evolution of the modern Calx homologs (Figure 2) from a common ancestor (hypothetically placed at "Root?"). The horizontal parts of the tree show evolutionary change (nonsynonymous codon changes); a scale bar for this is given. Note that this change only applies to universally conserved regions of the proteins (Figure 2); no attempt was made to calculate evolutionary change for rapidly evolving, unconserved regions. The vertical distances serve solely to keep tips of the tree apart, and have solely graphic significance. We judge this tree, of all possible trees, to be the one most strongly supported by the modern protein-sequence data, through reasoning detailed elsewhere (Methods; Hillis and Huelsenbeck, 1992; Hillis *et al.*, 1993, 1994). The sequence data that yielded this tree also yield a highly skewed length distribution of other, less probable trees. The precise value of this distribution's skew (g_1) is shown; it indicates (Hillis and Huelsenbeck, 1992) that the sequence data are >99% likely to be evolutionarily informative (as opposed to being so randomized, with the passage of time, as to be useless for evolutionary inference). The numbers alongside horizontal branches show the frequency with which each branch recurs in a set of 100-1000 trees generated from random *subsets* of the protein data used to generate the tree shown here. These "bootstrap" frequencies give a conservative indication (Felsenstein and Kishino, 1993) of the soundness with which a given branch can be inferred from a given set of sequence data. Given the strong skew value, we interpret bootstrap values of <95% to mean that a given branch is reasonable, but must be considered tentative until more sequence data become available. Since there is no automatically valid outgroup for any of the proteins, and since codon changes are nondirectional, the trees are necessarily unrooted as computed (Swofford, 1990); the root indicated in the figure is speculative.

Figure 12:

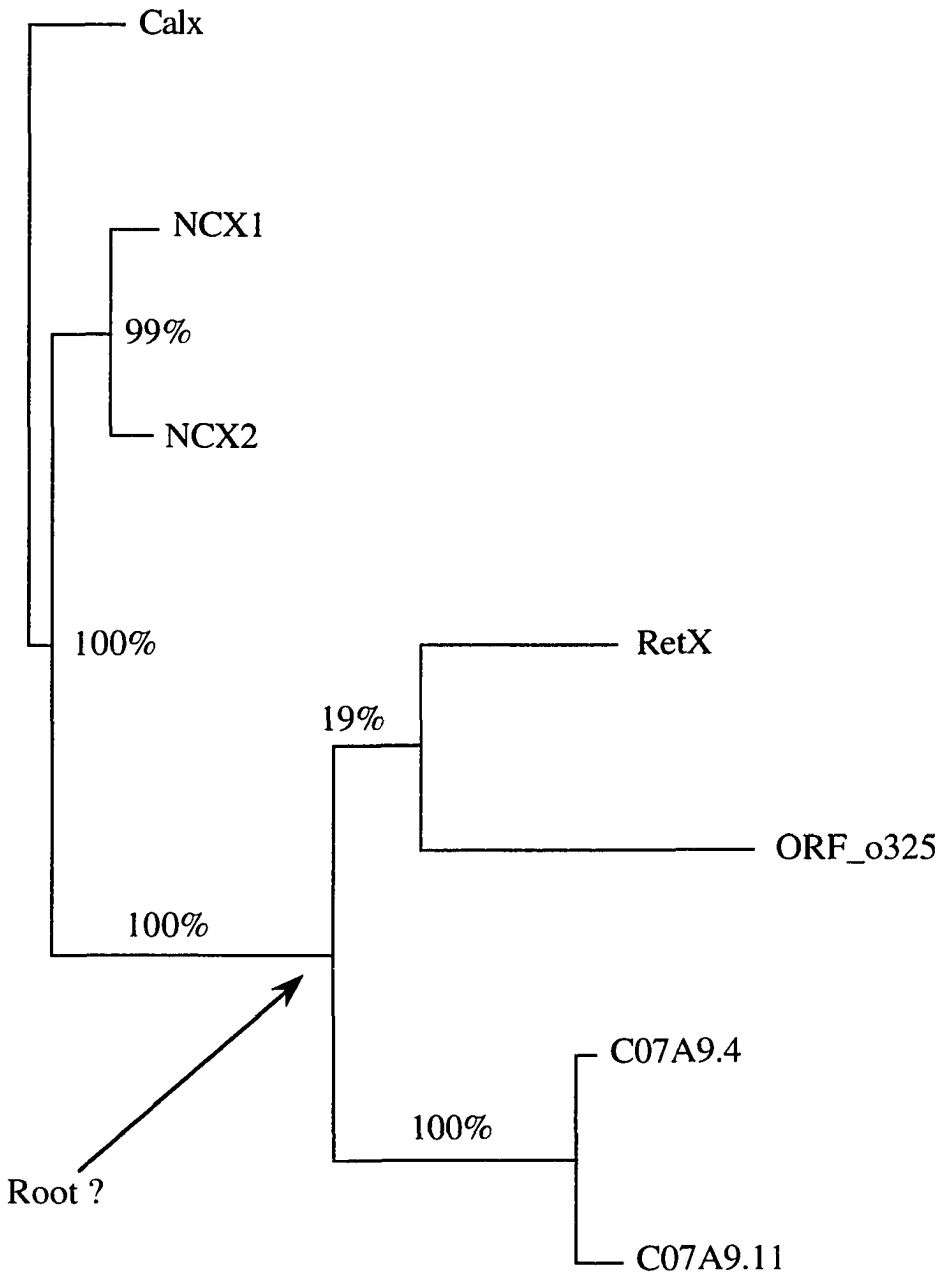

7 taxa, 126 residues

$g_1 = -1.00 < -0.48 = g$ ($P \approx 0.01$)

100 codon changes

Figure 13. Evolutionary tree of *Calx*-α motifs. This tree denotes the evolution of *Calx*-α motifs (Figure 4) rather than of whole Calx homologs. Motif names have the same significance as in Figure 4. Branch lengths, skew values, bootstrap values, and the root have the same significance as in Figure 12. Skew was calculated with the following groupings *subtracted* from calculation of the skew value: (Calx-α1, (NCX1-α1, NCX2-α1)); (C07A9.4-α1, C07A9.11-α1); (Calx-α2, (NCX1-α2, NCX2-α2)); and (C07A9.4-α2, C07A9.11-α2). This constraint was imposed to prove that, even without the contribution of these groupings (which are expected to occur, given the results in Figures 12 and 14), phylogenetic signal remains in the *Calx*-α motif data. In other words, *Calx*-α sequence information has the potential to resolve very ancient phylogenetic events that antedate the divergence of the proteins encoding it.

Figure 13:

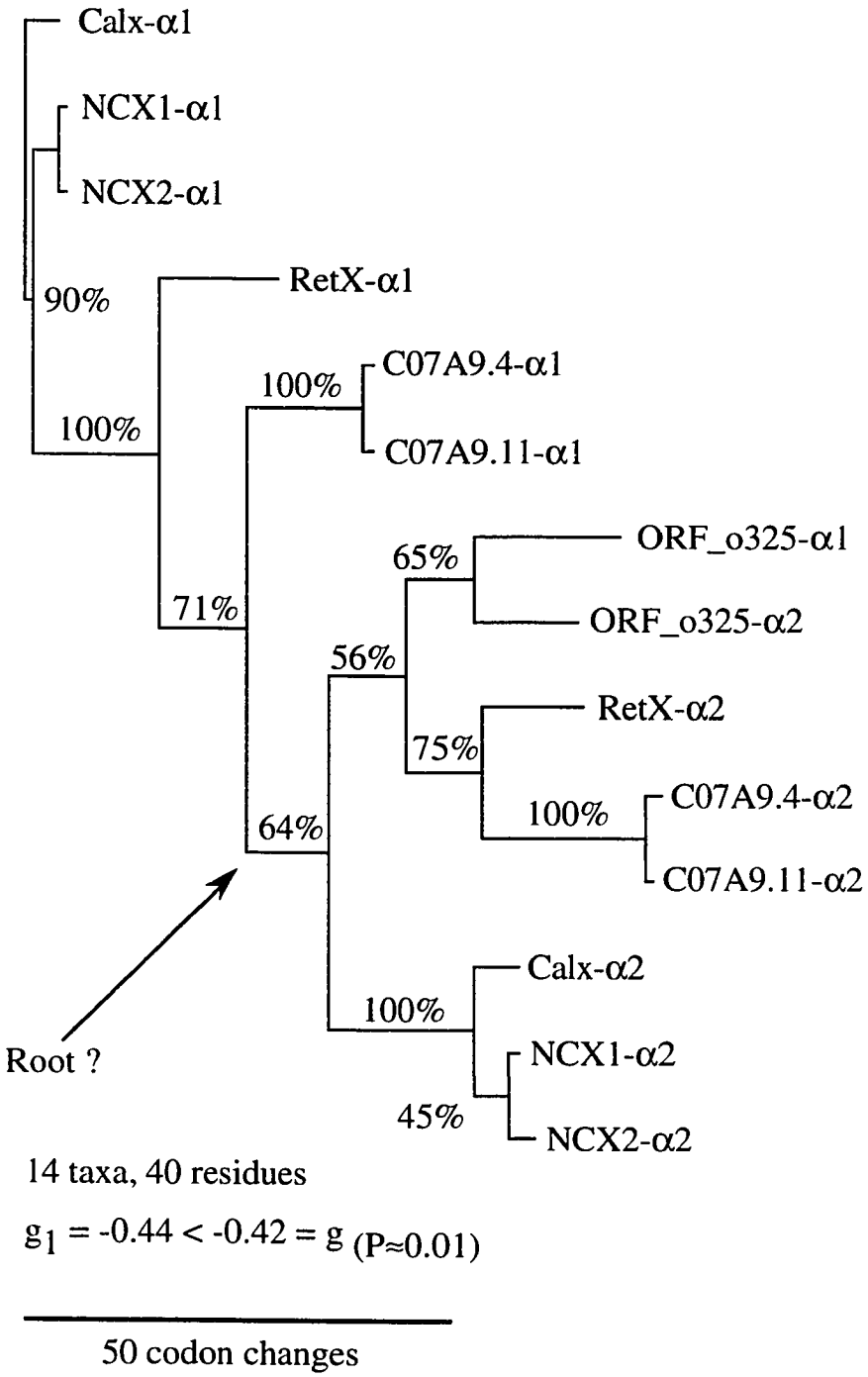
Calx-α1
NCX1-α1
NCX2-α1
90%
RetX-α1
100%
C07A9.4-α1
100%
C07A9.11-α1
65%
ORF_o325-α1
71%
ORF_o325-α2
56%
RetX-α2
75%
100%
C07A9.4-α2
64%
C07A9.11-α2
Calx-α2
100%
Root ?
NCX1-α2
45%
NCX2-α2
14 taxa, 40 residues
g_1 = -0.44 < -0.42 = g (P≈0.01)
50 codon changes

Figure 14. Evolutionary tree of *Calx*-β motifs. This tree denotes *Calx*-β motif (Figure 4) evolution; otherwise, it is like Figures 12-13.

Figure 14:

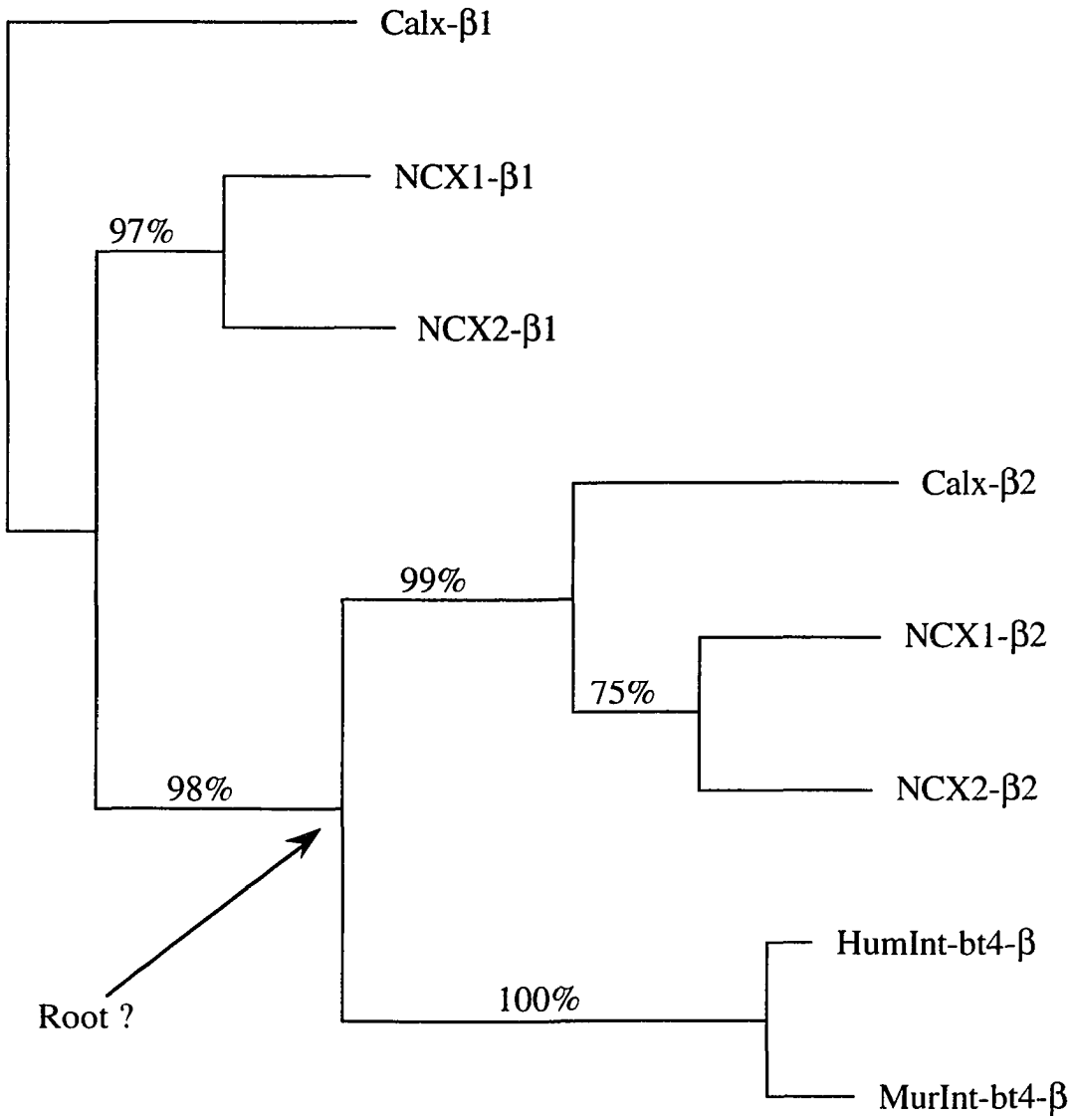

8 taxa, 93 residues

$g_1 = -1.22 < -0.42 = g$ ($P \approx 0.01$)

50 codon changes

References

Aceto, J.F., Condrescu, M., Kroupis, C., Nelson, H., Nelson, N., Nicoll, D., Philipson, K.D., and Reeves, J.P. (1992). Cloning and expression of the bovine cardiac sodium-calcium exchanger. Arch. Biochem. Biophys. *298*, 553-560.

Al-Atia, G.R., Fruscoloni, P., and Jacobs-Lorena, M. (1985). Translational regulation of mRNAs for ribosomal proteins during early *Drosophila* development. Biochemistry *24*, 5798-5803.

Allen, T.J.A. (1991). The exchange in intact squid axons. Ann. N.Y. Acad. Sci. *639*, 71-84.

Altschul, S.F., Boguski, M.S., Gish, W., and Wootton, J.C. (1994). Issues in searching molecular sequence databases. Nature Genet. *6*, 119-129.

Angelichio, M.L., Beck, J.A., Johansen, H., and Iveyhoyle, M. (1991). Comparison of several promoters and polyadenylation signals for use in heterologous gene-expression in cultured *Drosophila* cells. Nucl. Acids Res. *19*, 5037-5043.

Ashburner, M. (1989a). *Drosophila*: a Laboratory Handbook. (CSHL Press: Cold Spring Harbor Laboratory.)

Ashburner, M. (1989b). *Drosophila*: a Laboratory Manual. (CSHL Press: Cold Spring Harbor Laboratory.)

Aslanidis, C., Schmid, K., and Schmitt, R. (1989). Nucleotide sequences and operon structure of plasmid-borne genes mediating uptake and utilization of raffinose in *Escherichia coli*. J. Bacteriol. *171*, 6753-6763.

Bairoch, A. and Bucher, P. (1994). Prosite: recent developments. Nucl. Acids Res. *22*:3583-3589.

Ballinger, D.G. and Benzer, S. (1989). Targeted gene mutations in *Drosophila*. Proc. Natl. Acad. Sci. U.S.A. *86*, 9402-9406.

Barnes, W.M. (1992). The fidelity of *Taq* polymerase catalyzing PCR is improved by an N-terminal deletion. Gene *112*, 29-35.

Barnes, W.M. (1993). PCR amplification of up to 35-kb DNA with high fidelity and high yield from λ bacteriophage templates. Proc. Natl. Acad. Sci. U.S.A. *91*, 2216-2220.

Blakely, R.D., Berson, H.E., Fremeau, R.T., Jr., Caron, M.G., Peek, M.M., Prince, H.K., and Bradley, C.C. (1991). Cloning and expression of a functional serotonin transporter from rat brain. Nature *354*, 66-70.

Blaustein, M.P., Goldman, W.F., Fontana, G., Krueger, B.K., Santiago, E.M., Steele, T.D., Weiss, D.N., and Yarowsky, P.J. (1991). Physiological roles of the sodium-calcium exchanger in nerve and muscle. Ann. N.Y. Acad. Sci. *639*, 254-274.

Bonini, N.M., Leiserson, W.M., and Benzer, S. (1993). The *eyes absent* gene: genetic control of cell survival and differentiation in the developing Drosophila eye. Cell *72*, 379-395.

Carafoli, E. (1987). Intracellular calcium homeostasis. Annu. Rev. Biochem. *56*, 395-433.

Carafoli, E. (1991). The calcium pumping ATPase of the plasma membrane. Annu. Rev. Physiol. *53*, 531-547.

Cavener, D.R. and Ray, S.C. (1991). Eukaryotic start and stop translation sites. Nucl. Acids Res. *19*, 3185-3192.

Cervetto, L., Lagnado, L., Perry, R.J., Robinson, D.W., and McNaughton, P.A. (1989). Extrusion of calcium from rod outer segments is driven by both sodium and potassium gradients. Nature *337*, 740-743.

Choi, D.W. (1992). Excitotoxic cell death. J. Neurobiol. *23*, 1261-1276.

Clark, J.M. (1988). Novel non-templated nucleotide addition reactions catalyzed by procaryotic and eucaryotic DNA polymerases. Nucl. Acids Res. *16*, 9677-9686.

Collins, F.S. and Weissman, S.M. (1984). Directional cloning of DNA fragments at a large distance from an initial probe: a circularization method. Proc. Natl. Acad. Sci. U.S.A. *81*, 6812-6816.

Conway Morris, S. (1993). The fossil record and the early evolution of the Metazoa. Nature *361*, 219-225.

Cooley, L., Berg, C., and Spradling, A. (1988). Controlling P element insertional mutagenesis. Trends Genet. *4*, 254-258.

Cox, D.A. and Matlib, M.A. (1993). A role for the mitochondrial Na^+-Ca^{2+} exchanger in the regulation of oxidative phosphorylation in isolated heart mitochondria. J. Biol. Chem. *268*, 938-947.

Crespo, L.M., Cannell, C.J., and Cannell, M.B. (1990). Kinetics, stoichiometry and role of the Na-Ca exchange mechanism in isolated cardiac myocytes. Nature *345*, 618-621.

Cunningham, K.W. and Fink, G.R. (1994). Calcineurin-dependent growth control in *Saccharomyces cerevisiae* mutants lacking *PMC1*, a homolog of plasma membrane Ca^{2+} ATPases. J. Cell Biol. *124*, 351-363.

Dahan, D., Spanier, R., and Rahamimoff, H. (1991). The modulation of rat brain Na^+-Ca^{2+} exchange by K^+. J. Biol. Chem. *266*, 2067-2075.

Dascal, N. (1987). The use of *Xenopus* oocytes for the study of ion channels. CRC Crit. Rev. Biochem. *22*, 317-387.

Doolittle, W.F. and Brown, J.R. (1994). Tempo, mode, the progenote, and the universal root. Proc. Natl. Acad. Sci. U.S.A. *91*, 6721-6728.

Dunn, J.J. and Studier, F.W. (1981). Nucleotide sequence from the genetic left end of bacteriophage T7 DNA to the beginning of gene *4*. J. Mol. Biol. *148*, 303-330.

Eisenberg, D., Schwarz, E., Komaromy, M., and Wall, R. (1984). Analysis of membrane and surface protein sequences with the hydrophobic moment plot. J. Mol. Biol. *179*, 125-142.

Eisenberg, M., Gathy, K., Vincent, T., and Rawls, J. (1990). Molecular cloning of the UMP synthase gene *rudimentary-like* from *Drosophila melanogaster*. Mol. Gen. Genet. *222*, 1-8.

Felsenstein, J. (1988). Phylogenies from molecular sequences: inference and reliability. Annu. Rev. Genet. *22*, 521-565.

Felsenstein, J. and Kishino, H. (1993). Is there something wrong with the bootstrap on phylogenies? A reply to Hillis and Bull. Syst. Biol. *42*, 193-200.

Fleischmann, R.D., Adams, M.D., White, O., Clayton, R.A., Kirkness, E.F., Kerlavage, A.R., Bult, C.J., Tomb, J.-F., Dougherty, B.A., Merrick, J.M., McKenney, K., Sutton, G., FitzHugh, W., Fields, C., Gocayne, J.D., Scott, J., Shirley, R., Liu, L.-I., Glodek, A., Kelley, J.M., Weidman, J.F., Phillips, C.A., Spriggs, T., Hedblom, E., Cotton, M.D., Utterback, T.R., Hanna, M.C., Nguyen, D.T., Saudek, D.M., Brandon, R.C., Fine, L.D., Fritchman, J.L., Fuhrmann, J.L., Geoghagen, N.S.M., Gnehm, C.L., McDonald, L.A., Small, K.V., Fraser, C.M., Smith, H.O., and Venter, J.C. (1995). Whole-genome random sequencing and assembly of *Haemophilus influenzae* Rd. Science *269*, 496-512.

Francis, G.E., Mulligan, W., and Wormall, A. (1959). Isotopic Tracers: a Theoretical and Practical Manual for Biological Students and Research Workers. (The Athlone Press: University of London), pp. 39-42.

Frank, J.S., Mottino, G., Reid, D., Molday, R.S., and Philipson, K.D. (1992). Distribution of the Na^{+}-Ca^{2+} exchange protein in mammalian cardiac myocytes: an immunofluorescence and immunocolloidal gold-labelling study. J. Cell. Biol. *117*, 337-345.

Furman, I., Cook, O., Kasir, J., and Rahamimoff, H. (1993). Cloning of two isoforms of the rat brain Na-Ca exchanger gene and their functional expression in HeLa cells. FEBS Lett. *319*, 105-109.

Genetics Computer Group (1991). Program Manual for the GCG Package. Version 7, April 1991 (575 Science Drive, Madison, Wisconsin, USA 53711).

Grant, S.G.N., Jessee, J., Bloom, F.R., and Hanahan, D. (1990). Differential plasmid rescue from transgenic mouse DNAs into *Escherichia coli* methylation-restriction

mutants. Proc. Natl. Acad. Sci. U.S.A. *87*, 4645-4649.

Guastella, J.G., Nelson, N., Nelson, H., Czyzyk, L., Keynan, S., Midel, M.C., Davidson, N., Lester, H., and Kanner, B. (1990). Cloning and expression of a rat brain GABA transporter. Science *249*, 1303-1306.

Haase, W., Friese, W., Gordon, R.D., Müller, H., and Cook, N.J. (1990). Immunological characterization and localization of the Na^+/Ca^{2+}-exchanger in bovine retina. J. Neurosci. *10*, 1486-1494.

Hardie, R.C. (1995). Photolysis of caged Ca^{2+} facilitates and inactivates but does not directly excite light-sensitive channels in *Drosophila* photoreceptors. J. Neurosci. *15*:889-902.

Hardie, R.C. and Minke, B. (1993). Novel Ca^{2+} channels underlying transduction in *Drosophila* photoreceptors: implications for phosphoinositide-mediated Ca^{2+} mobilization. Trends Neurosci. *16*, 371-376.

Harlow, E. and Lane, D. (1988). Antibodies: a Laboratory Manual. (CSH Press: Cold Spring Harbor Laboratory.)

Henikoff, S. and Henikoff, J.G. (1992). Amino acid substitution matrices from protein blocks. Proc. Natl. Acad. Sci. U.S.A. *89*, 10915-10919.

Herschuelz, A. and Lebrun, P. (1993). A role for Na/Ca exchange in the pancreatic B cell. Biochem. Pharmacol. *45*, 7-11.

Higgins, C.F. (1992). ABC transporters: from microorganisms to man. Annu. Rev. Cell Biol. *8*, 67-113.

Hilgemann, D.W., Nicoll, D.A., and Philipson, K.D. (1991). Charge movement during Na^+ translocation by native and cloned cardiac Na^+/Ca^{2+} exchanger. Nature *352*, 715-718.

Hille, B. (1992). Ionic Channels of Excitable Membranes. 2cd. ed. (Sinauer Associates Inc.: Sunderland, Massachussetts.)

Hillis, D.M., Allard, M.W., and Miyamoto, M.M. (1993). Analysis of DNA

sequence data: phylogenetic inference. Meth. Enzymol. *224*, 456-487.

Hillis, D.M. and Huelsenbeck, J.P. (1992). Signal, noise, and reliability in molecular phylogenetic analyses. J. Hered. *83*, 189-195.

Hillis, D.M., Huelsenbeck, J.P., and Cunningham, C.W. (1994). Application and accuracy of molecular phylogenies. Science *264*, 671-677.

Hockfield, S., Carlson, S., Evans, C., Levitt, P., Pintar, J., and Silberstein, L. (1993). Selected Methods for Antibody and Nucleic Acid Probes. (CSL Press: Cold Spring Harbor Laboratory).

Hoffman, B.J., Mezey, E., and Brownstein, M.J. (1991). Cloning of a serotonin transporter affected by antidepressants. Science *254*, 579-580.

Holz, R.W. (1979). Polyene antibiotics: nystatin, amphotericin B, and filipin. In Antibiotics: Mechanism of Action of Antieukaryotic and Antiviral Compounds, Vol. V, pt. 2, F.E. Hahn, ed. (Springer-Verlag: New York), pp. 313-340.

Hryshko, L.V., Matsuoka, S., Nicoll, D.A., Weiss, J.N., Schwarz, E.M., Benzer, S., and Philipson, K. (1995). Anomalous regulation of the *Drosophila* Na^{+}-Ca^{2+} exchanger. To be submitted.

Huang, X., Hardison, R.C., and Miller, W. (1990). A space-efficient algorithm for local similarities. CABIOS *6*, 373-381.

Hyde, D.R., Mecklenburg, K.L., Pollock, J.A., Vihtelic, T.S., and Benzer, S. (1990). Twenty *Drosophila* visual system cDNA clones: one is a homolog of human arrestin. Proc. Natl. Acad. Sci. U.S.A. *87*, 1008-1012.

Hynes, R.O. (1992). Integrins: versatility, modulation, and signalling in cell adhesion. Cell *69*, 11-25.

Itoh, N., Salvaterra, P., and Itakura, K. (1985). Construction of an adult Drosophila head cDNA expression library with lambda gt 11. Drosoph. Inf. Serv. *61*, 89.

Jameson, B.A. and Wolf, H. (1988). The antigenic index: a novel algorithm for predicting antigenic determinants. CABIOS *4*, 181-186.

Jobling, S.A. and Gehrke, L. (1987). Enhanced translation of chimaeric messenger RNAs containing a plant viral untranslated leader sequence. Nature *325*, 622-625.

Johnson, B.A., McClain, S.G., Doran, E.R., Tice, G., and Kirsch, M.A. (1990). Rapid purification of synthetic oligonucleotides: a convenient alternative to high-performance liquid chromatography and polyacrylamide gel electrophoresis. Biotechniques *8*, 424-429.

Kaback, H.R. (1992). In and out and up and down with lac permease. Int. Rev. Cytol. *137A*, 97-125.

Karpen, G.H. and Spradling, A.C. (1992). Analysis of subtelomeric heterochromatin in the Drosophila minichromosome *Dp1187* by single *P* element insertional mutagenesis. Genetics *132*, 737-753.

Kaupp, U.B. and Koch, K.-W. (1992). Role of cGMP and Ca^{2+} in vertebrate photoreceptor excitation and adaptation. Annu. Rev. Physiol. *54*, 153-175.

Kennel, S.J., Foote, L.J., Cimino, L., Rizzo, M.G., Chang, L-.Y., and Sacchi, A. (1993). Sequence of a cDNA encoding the β_4 subunit of murine integrin. Gene *130*, 209-216.

Kimura, M., Aviv, A., and Reeves, J.P. (1993). K^+-dependent Na^+/Ca^{2+} exchange in human platelets. J. Biol. Chem. *268*, 6874-6877.

Klingenberg, M. (1981). Membrane protein oligomeric structure and transport function. Nature *290*, 449-454.

Kofuji, P., Lederer, W.J., and Schulze, D.H. (1993). Na/Ca isoforms expressed in kidney. Am. J. Physiol. *265*, F598-F603.

Kozak, M. (1991). An analysis of vertebrate mRNA sequences: intimations of translational control. J. Cell Biol. *115*, 887-903.

Krieger, N.S. (1991). Evidence for sodium-calcium exchange in rodent osteoblasts. Ann. N.Y. Acad. Sci. *639*, 660-662.

Kyte, J. (1981). Molecular considerations relevant to the mechanism of active transport. Nature *292*, 201-204.

Lawrence, C.E., Altschul, S.F., Boguski, M.S., Liu, J.S., Neuwald, A.F., and Wootton, J.C. (1993). Detecting subtle sequence signals: a Gibbs sampling strategy for multiple alignment. Science *262*, 208-213.

Lebovitz, R.M., Takeyasu, K., and Fambrough, D.M. (1989). Molecular characterization and expression of the (Na^+ + K^+)-ATPase alpha-subunit in *Drosophila melanogaster*. EMBO J. *8*, 193-202.

Lee, Y.-J., Dobbs, M.B., Verardi, M.L., and Hyde, D.R. (1990). *dgq*: a Drosophila gene enocding a visual system-specific G_α molecule. Neuron *5*, 889-898.

Lee, S.-L., Yu, A.S.L., and Lytton, J. (1994). Tissue-specific expression of Na^+-Ca^{2+} exchanger isoforms. J. Biol. Chem. *269*, 14849-14852.

Lewis, E.B. (1960). A new standard food medium. Drosoph. Inf. Serv. *34*, 117-118.

Li, W.-H. and Graur, D. (1991). Fundamentals of Molecular Evolution. (Sinauer Associates, Inc.: Sunderland, Massachusetts.)

Li, W., Shariat-Madar, Z., Powers, M., Sun, X., Lane, R.D., and Garlid, K.D. (1992). Reconstitution, identification, purification, and immunological characterization of the 110-kDa Na^+/Ca^{2+} antiporter from beef heart mitochondria. J. Biol. Chem. *267*, 17983-17989.

Li, Z., Burke, E.P., Frank, J.S., Bennett, V., and Philipson, K.D. (1993). The cardiac Na^+-Ca^{2+} exchanger binds to the cytoskeletal protein ankyrin. J. Biol. Chem. *268*, 11489-11491.

Li, Z., Matsuoka, S., Hryshko, L.V., Nicoll, D.A., Berschn, M.M., Burke, E.P., Lifton, R.P., and Philipson, K.D. (1994). Cloning of the NCX2 isoform of the plasma membrane Na^+-Ca^{2+} exchanger. J. Biol. Chem. *269*, 17434-17439.

Li, Z., Nicoll, D.A., Collins, A., Hilgemann, D.W., Filoteo, A.G., Penniston,

J.T., Weiss, J.N., Tomich, J.M., and Philipson, K.D. (1991). Identification of a peptide inhibitor of the cardiac sarcolemmal Na^+-Ca^{2+} exchanger. J. Biol. Chem. *266*, 1014-1020.

Lindsley, D.L. and Zimm, G.G. (1992). The Genome of *Drosophila melanogaster*. (Academic Press, Inc.: San Diego.)

Longoni, S., Coady, M.J., Ikeda, T., and Philipson, K.D. (1988). Expression of cardiac sarcolemmal Na^+-Ca^{2+} exchange activity in *Xenopus laevis* oocytes. Am. J. Physiol. *255*, C870-C873.

Lundin, L.G. (1993). Evolution of the vertebrate genome as reflected in paralogous chromosomal regions in man and the house mouse. Genomics *16*, 1-19.

Luther, P.W., Yip, R.K., Bloch, R.J., Ambesi, A., Lindenmayer, G.E., and Blaustein, M.P. (1992). Presynaptic localization of sodium/calcium exchangers in neuromuscular preparations. J. Neurosci. *12*, 4898-4904.

Maddison, W.P. and Maddison, D.R. (1992). MacClade: Analysis of Phylogeny and Character Evolution. Version 3.0. Sinauer Associates, Sunderland, Massachusetts.

Mager, S., Naeve, J., Quick, M., Labarca, C., Davidson, N., and Lester, H.A. (1993). Steady states, charge movements, and rates for a cloned GABA transporter expressed in *Xenopus* oocytes. Neuron *10*, 177-188.

Maniatis, T., Fritsch, E.F., and Sambrook, J. (1982). Molecular Cloning: a Laboratory Manual. 1st. ed. (CSH Press: Cold Spring Harbor Laboratory.)

Marlier, L.N.J-L., Zheng, T., Tang, J., and Grayson, D.R. (1993). Regional distribution in the rat central nervous system of a mRNA encoding a portion of the cardiac sodium/calcium exchanger isolated from cerebellar granule neurons. Mol. Brain Res. *20*, 21-39.

Matsuoka, S., Nicoll, D.A., Hryshko, L.V., Levitsky, D.O., Weiss, J.N., and Philipson, K.D. (1995). Regulation of the cardiac Na^+-Ca^{2+} exchanger by Ca^{2+}: mutational analysis of the Ca^{2+}-binding domain. J. Gen. Physiol. *105*, 403-420.

Matsuoka, S., Nicoll, D.A., Reilly, R.F., Hilgemann, D.W., and Philipson, K.D. (1993). Initial localization of regulatory regions of the cardiac sarcolemmal Na^+-Ca^{2+} exchanger. Proc. Natl. Acad. Sci. U.S.A. *90*, 3870-3874.

Milanick, M.A. (1992). Ferret red cells: Na/Ca exchange and Na-K-Cl cotransport. Comp. Biochem. Physiol. *102A*, 619-624.

Minke, B. and Armon, E. (1984). Activation of electrogenic Na-Ca exchange by light in fly photoreceptors. Vision Res. *24*, 109-115.

Minke, B. and Tsacopoulos, M. (1986). Light induced sodium dependent accumulation of calcium and potassium in the extracellular space of bee retina. Vision Res. *26*, 679-690.

Moore, E.D.W., Etter, E.F., Philipson, K.D., Carrington, W.A., Fogarty, K.E., Lifshitz, L.M., and Fay, F.S. (1993). Coupling of the Na^+/Ca^{2+} exchanger, Na^+/K^+ pump and sarcoplasmic reticulum in smooth muscle. Nature *365*, 657-660.

Morris, W. (1975). The American Heritage Dictionary of the English Language. (Houghton Mifflin: Boston), p. 188.

Nakatani, K. and Yau, K.-W. (1989). Sodium-dependent calcium extrusion and sensitivity regulation in retinal cones of the salamander. J. Physiol. *409*, 525-548.

Nicoll, D.A., Longoni, S., and Philipson, K.D. (1990). Molecular cloning and functional expression of the cardiac sarcolemmal Na^+-Ca^{2+} exchanger. Science *250*, 562-565.

Nicotera, P., Bellomo, G., and Orrenius, S. (1992). Calcium-mediated mechanisms in chemically induced cell death. Annu. Rev. Pharmacol. Toxicol. *32*, 449-470.

O'Day, P.M., Gray-Keller, M.P., and Lonergan, M. (1991). Physiological roles of Na^+/Ca^{2+} exchange in *Limulus* ventral photoreceptors. J. Gen. Physiol. *97*, 369-391.

OH, S.-K., Scott, M.P., and Sarnow, P. (1992). Homeotic gene *Antennapedia* mRNA contains 5'-noncoding sequences that confer translational initiation by internal

ribosome binding. Genes Dev. *6*, 1643-1653.

Ou, S.K., Huang, J.M., and Patterson, P.H. (1993). A modified method for obtaining large amounts of high titer polyclonal ascites fluid. J. Immunol. Meth. *165*, 75-80.

Pearson, W.R. and Lipman, D.J. (1988). Improved tools for biological sequence comparison. Proc. Natl. Acad. Sci. U.S.A. *85*, 2444-2448.

Perry, R.J. and McNaughton, P.A. (1993). The mechanism of ion transport by the Na^+-Ca^{2+},K^+ exchange in rods isolated from the salamander retina. J. Physiol. *466*, 443-480.

Philipson, K.D. and Nicoll, D.A. (1993). Molecular and kinetic aspects of sodium-calcium exchange. Int. Rev. Cytol. *137C*, 199-227.

Qian, S., Zhang, J.-Y., Kay, M.A., Jacobs-Lorena, M. (1987). Structural analysis of the *Drosophila* rpA1 gene, a member of the eucaryotic 'A' type ribosomal protein family. Nucl. Acids Res. *15*, 987-1003.

Quick, M.W. and Lester, H.A. (1994). Methods for expression of excitability proteins in *Xenopus* oocytes. Meth. Neurosci. *19*, 261-279.

Quick, M.W., Naeve, J., Davidson, N., and Lester, H.A. (1992). Incubation with horse serum increases viability and decreases background neurotransmitter uptake in *Xenopus* oocytes. BioTechniques *13*, 358-362.

Palazzollo, M.J., Hyde, D.R., VijayRaghavan, K., Mecklenburg, K., Benzer, S., and Meyerowitz, E. (1989). Use of a new strategy to isolate and characterize 436 Drosophila cDNA clones corresponding to RNAs detected in adult heads but not in early embryos. Neuron *3*, 527-539.

Ranganathan, R., Bacskai, B.J., Tsien, R.Y., and Zuker, C.S. (1994). Cytosolic calcium transients: spatial localization and role in Drosophila photoreceptor cell function. Neuron *13*, 837-848.

Reeves, J.P. and Hale, C.C. (1984). The stoichiometry of the cardiac sodium-

calcium exchange system. J. Biol. Chem. *259*, 7733-7739.

Reiländer, H., Achilles, A., Friedel, U., Maul, G., Lottspeich, F., and Cook, N.J. (1992). Primary structure and functional expression of the Na/Ca,K-exchanger from bovine rod photoreceptors. EMBO J. *11*, 1689-1695.

Reilly, R.F. and Shugrue, C.A. (1992). cDNA cloning of a renal Na^+-Ca^{2+} exchanger. Am. J. Physiol. *262*, F1105-F1109.

Reilly, R.F., Shugrue, C.A., Lattanzi, D., and Biemesderfer, D. (1993). Immunolocalization of the Na^+/Ca^{2+} exchanger in rabbit kidney. Am. J. Physiol. *265*, F327-F332.

Roberts, D.B. (1987). Basic Drosophila care and techniques. In Drosophila: a Practical Approach, D.B. Roberts, ed. (IRL Press: Washington, D.C.), pp. 1-38.

Rost, B. and Sander, C. (1994). Combining evolutionary information and neural networks to predict protein secondary structure. Proteins *19*, 55-72.

Sachs, A. and Wahle, E. (1993). Poly(A) tail metabolism and function in eucaryotes. J. Biol. Chem. *268*, 22955-22958.

Sambrook, J., Fritsch, E.F., and Maniatis, T. (1989). Molecular Cloning: a Laboratory Manual. 2cd. ed. (CSH Press: Cold Spring Harbor Laboratory.)

Schnetkamp, P.P.M., Basu, D.K., and Szerencsei, R.T. (1989). Na^+-Ca^{2+} exchange in bovine rod outer segments requires and transports K^+. Am. J. Physiol. *257*, C153-C517.

Schubiger, M., Feng, Y., Fambrough, D.M., and Palka, J. (1994). A mutation of the Drosophila sodium pump α subunit gene results in bang-sensitive paralysis. Neuron *12*, 373-381.

Schuler, G.D., Altschul, S.F., and Lipman, D.J. (1991). A workbench for multiple alignment construction and analysis. Proteins *9*, 180-190.

Shieh, B.-H., Xia, Y., Sparkes, R.S., Klisak, I., Lusis, A.J., Nicoll, D.A., and Philipson, K.D. (1992). Mapping of the gene for the cardiac sarcolemmal Na^+-Ca^{2+}

exchanger to human chromosome 2p21-p23. Genomics *12*, 616-617.

Simchowitz, L., Foy, M.A., and Cragoe, E.J., Jr. (1990). A role for Na^+/Ca^{2+} exchange in the generation of superoxide radicals by human neutrophils. J. Biol. Chem. *265*, 13449-13456.

Smith, D.P., Shieh, D.-H., and Zuker, C.S. (1990). Isolation and structure of an arrestin gene from *Drosophila*. Proc. Natl. Acad. Sci. U.S.A. *87*, 1003-1007.

Spinardi, L., Ren, Y.-L., Sanders, R., and Giancotti, F.G. (1993). The β_4 subunit cytoplasmic domain mediates the interaction of $\alpha_6\beta_4$ integrin with the cytoskeleton of hemidesmosomes. Mol. Biol. Cell *4*, 871-884.

States, D.J. and Boguski, M.S. (1991). Similarity and homology. In Sequence Analysis Primer, M. Gribskov and J. Devereux, eds. (Stockton Press: New York), pp. 89-157.

Strathmann, M., Hamilton, B.A., Mayeda, C.A., Simon, M.I., Meyerowitz, E.M., and Palazollo, M.J. (1991). Transposon-facilitated DNA sequencing. Proc. Natl. Acad. Sci. U.S.A. *88*, 1247-1250.

Suzuki, S. and Naitoh, Y. (1990). Amino acid sequence of a novel integrin β_4 subunit and primary expression of the mRNA in epithelial cells. EMBO J. *9*, 757-763.

Swofford, D.L. (1990). PAUP: phylogenetic analysis using parsimony, version 3.0o. Computer program distributed by the Illinois Natural History Survey, Champaign, Illinois.

Syvanen, M. (1994). Horizontal gene transfer: evidence and possible consequences. Annu. Rev. Genet. *28*, 237-261.

Tamkun, J.W., Deuring, R., Scott, M.P., Kissinger, M., Pattatucci, A.M., Kaufman, T.C., and Kennison, J.A. (1992). brahma: a regulator of Drosophila homeotic genes structurally related to the yeast transcriptional activator SNF2/SWI2. Cell *68*, 561-572.

Tautz, D. and Pfeifle, C. (1989). A non-radioactive in situ hybridization method

for the localization of specific RNAs in *Drosophila* embryos reveals translational control of the segmentation gene *hunchback*. Chromosoma *98*, 81-85.

Tsang, S.S., Yin, X., Guzzo-Arkuran, C., Jones, V.S., and Davison, A.J. (1993). Loss of resolution in gel electrophoresis of RNA: a problem associated with the presence of formaldehyde gradients. BioTechniques *14*, 380-381.

Unwin, N. (1993). Nicotinic acetylcholine receptor at 9 Å resolution. J. Mol. Biol. *229*, 1101-1124.

Vidal, F., Aberdam, D., Miquel, C., Christiano, A.M., Pulkkinen, L., Uitto, J., Ortonne, J.-P., and Meneguzzi, G. (1995). Integrin β4 mutations associated with junctional epidermolysis bullosa with pyloric atresia. Nature Genetics *10*, 229-237.

von Heijne, G. (1986). A new method for predicting signal sequence cleavage sites. Nucl. Acids Res. *14*, 4683-4690.

Wilkins, A.S. (1986). Genetic analysis of animal development. (Wiley: New York.)

Wilson, R., Ainscough, R., Anderson, K., Baynes, C., Berks, M., Bonfield, J., Burton, J., Connell, M., Copsey, T., Cooper, J., Coulson, A., Craxton, M., Dear, S., Du, Z., Durbin, R., Favello, A., Fraser, A., Fulton, L., Gardner, A., Green, P., Hawkins, T., Hillier, L., Jier, M., Johnston, L., Jones, M., Kershaw, J., Kirsten, J., Laisster, N., Latreille, P., Lightning, J., Lloyd, C., Mortimore, B., O'Callaghan, M., Parsons, J., Percy, C., Rifken, L., Roopra, A., Saunders, D., Shownkeen, R., Sims, M., Smaldon, N., Smith, A., Smith, M., Sonnhammer, E., Staden, R., Sulston, J., Thierry-Mieg, J., Thomas, K., Vaudin, M., Vaughan, K., Waterston, R., Watson, A., Weinstock, L., Wilkinson-Sproat, J., and Wohldman, P. (1994). 2.2 Mb of contiguous nucleotide sequence from chromosome III of *C. elegans*. Nature *368*, 32-38.

Wilson, C., Pearson, R.K., Bellen, H.J., O'Kane, C.J., Grossniklaus, U., and Gehring, W.J. (1989). P-element-mediated enhancer detection: an efficient method for isolating and characterizing developmentally regulated genes in *Drosophila*. Genes Dev. *3*,

1301-1313.

Windhager, E.E., Frindt, G., and Milovanovic, S. (1991). The role of Na-Ca exchange in renal epithelia: an overview. Ann. N.Y. Acad. Sci. *639*, 577-591.

Zinsmaier, K.E., Hofbauer, A., Heimbeck, G., Pflugfelder, G.O., Buchner, S., and Buchner, E. (1990). A cysteine-string protein is expressed in retina and brain of Drosophila. J. Neurogenetics *7*, 15-29.